HYDROGEN AND OXYGEN ISOTOPIC STUDIES OF SERPENTINIZATION OF ULTRAMAFIC ROCKS

Thesis by

David Bruce Wenner

In Partial Fulfillment of the Requirements
For the Degree of
Doctor of Philosophy

California Institute of Technology
Pasadena, California
1971
(Submitted December 30, 1970)

ACKNOWLEDGEMENTS

I wish to thank Dr. Hugh P. Taylor, Jr. for encouragement and guidance throughout the course of this research.

I am grateful for the valuable discussions I have had with Drs. A. L. Albee, R. G. Coleman, S. Epstein, H. H. Hess, P. Hostetler, L. McKague, S. M. F. Sheppard, L. T. Silver, T. Suzuoki, and all my other collegues at Caltech.

Samples were generously provided by Drs. M. Bass, C. Bowin, R. Coleman, J. Duncan, G. Faust, R. Forester, H. H. Hess, R. Hill, L. Hollister, N. Irvine, D. Lapham, T. McGetchin, L. McKague, W. Melson, E. Moores, N. Page, I. Paterson, L. Rogers, J. Ruckmick, J. Souther, H. Taylor, G. Thompson, and W. Wolfe.

I am indebted to Dr. S. Epstein for the use of his laboratories and mass spectrometer facilities. Assistance with the construction and/or maintenance of the stable isotope facilities was received from Messrs. C. Bauman, E. V. Nenow, and P. Yanagisawa. Mr. A. A. Chodos and Mrs. L. Ray provided assistance with the electron microprobe and Mrs. E. Bingham with the x-ray diffraction equipment.

I would also like to thank Mmes. R. Talovich, J. Scott, E. Nielsen, and Mr. G. Thrall for their help in preparation of this thesis.

I wish especially to express my sincere thanks to my wife, Jennifer, for her encouragement during the duration of this study and for her able assistance in both the typing of the thesis and drafting of the figures.

During part of this research the writer was supported by a Geological Society of America grant. This research was supported by grants from the National Science Foundation Grant No. GA-12945 and Project Agreement #7 under Atomic Energy Commission Contract No. AT(04-3)-767.

ABSTRACT

Lizardite-chrysotile serpentines in alpine ultramafic bodies from North America show latitudinal variations in δD and δO^{18} which indicate that meteoric ground waters were important in their formation. In per mil relative to SMOW they exhibit the following geographic variations in δD and δO^{18}, respectively: British Columbia -205 to -150, 1.9 to 8.2; Washington-Oregon -142 to -107, 4.1 to 8.0; California -108 to -82, 6.6 to 8.8; Caribbean-Central America -97 to -59, 3.3 to 8.7. The δD-latitude correlation is exceedingly good, but the δO^{18}-values appear to be in large part dependent upon the O^{18}/O^{16} of the country rock. This suggests that the waters involved in serpentinization had previously exchanged O^{18} with these country rocks. For example, the Cassiar, British Columbia, serpentinite body has δD = -195 to -162 and δO^{18} = 8.0 to 8.2, whereas the serpentines in zoned ultramafic bodies of SE Alaska have δD = -127 to -140, δO^{18} = -5.0 to -1.6; the former body lies in a terrane of abundant O^{18}-rich limestones, whereas the zoned bodies are surrounded by low-O^{18} igneous rocks.

All antigorites, irrespective of geographic location, have very uniform isotopic compositions (δD = -66 to -39, δO^{18} = 4.7 to 8.8). This is practically identical to the range exhibited by metamorphic chlorites, indicating that a deep-seated or metamorphic type water was involved in antigorite-type serpentinization. This isotopic uniformity further indicates that little or no isotopic exchange has occurred subsequent to formation of the antigorites, because many samples were collected from northerly regions where the ground waters are very low in δD and δO^{18}.

Five lizardite-chrysotile type serpentinites from California, Guatemala and the Dominican Republic show oxygen isotope fractionations of 15.1 to 12.9 per mil between coexisting serpentine and magnetite (δO^{18} magnetite = -7.6 to -4.6 per mil relative to SMOW). Nine antigorites (mainly from Vermont and SE Pennsylvania) show distinctly smaller fractionations of 8.7 to 4.8 per mil (δO^{18} magnetite = -2.6 to +1.7 per mil). Two lizardite and chrysotile serpentinites dredged from the Mid-Atlantic Ridge exhibit fractionations of 10.0 and 12.5 per mil (δO^{18} magnetite = -6.8 and -7.9 per mil, respectively), whereas antigorite from this area shows a value of 8.2 per mil (δO^{18} magnetite = -6.2). These data all clearly indicate that the antigorites formed at higher temperatures than the chrysotile-lizardites. Electron microprobe analyses of magnetites from the above samples show that they are chemically homogeneous and essentially pure Fe_3O_4. A few magnetite samples from serpentinites in near proximity to later granitic intrusions show a wide variation of Cr content, and also give erratic oxygen isotopic results, suggesting non-equilibrium.

A rough serpentine-magnetite geothermometer curve was constructed by extrapolation of (1) observed δO^{18}-values of chlorite and Fe-Ti oxides in low-grade pelitic schists whose isotopic temperatures are known from the quartz-muscovite geothermometer, and (2) estimates of the O^{18} fractionation between chlorite and serpentine (assumed to be zero). This serpentine-magnetite geothermometer suggests approximate equilibrium temperatures as follows: continental lizardite-chrysotile, 85° to 115°C; oceanic lizardite and chrysotile, 130°C and 185°C, respectively; continental antigorites, 220° to 460°C; and oceanic antigorite, 240°C.

The isotopic compositions of the waters involved in serpentinization of various ultramafic rocks have been estimated, utilizing the above "temperatures". These calculations indicate that most lizardite-chrysotile serpentinization probably involved exchanged meteoric waters, and thus must have occurred at relatively shallow levels in the earth's crust, consistent with the proposed isotopic "temperatures". However, this type of serpentinization is clearly not a weathering phenomenon taking place at the earth's surface. Isotopic evidence for such low temperature serpentinization (δO^{18} of +11.8 to +12.5) has been discovered only for several "deweylite" samples from Pennsylvania and Delaware.

Serpentines from the ocean floor (Mid Atlantic Ridge, Puerto Rican trench, and Blanco Fracture zone in the Pacific Ocean) form a unique isotopic grouping, with $\delta D = -68$ to -31, $\delta O^{18} = +0.8$ to $+6.7$. The waters that would have coexisted with these serpentines (at the temperatures inferred from serpentine-magnetite O^{18} fractionations) have calculated isotopic compositions that cluster around SMOW. This strongly suggests that ocean water is the major component of the waters responsible for sub-oceanic serpentinization. A few of the low-δD oceanic serpentines are, however, consistent with formation from magmatic water-ocean water mixtures. No serpentines presently found in continental areas give any isotopic evidence of ever having been serpentinized in oceanic environments. This statement also applies to the serpentines in a typical ophiolite sequence, the Vourinos Complex, Greece. Serpentine from this body is unique, however, in that it exhibits remarkably large

δO^{18} variation, from +2.1 to +12.7. All other bodies that were examined in detail were found to have very uniform isotopic compositions.

TABLE OF CONTENTS

I. INTRODUCTION

1.1 Object of the research

Studies of the variations of hydrogen and oxygen isotopes in rocks and minerals are useful as a tracer for discerning the various kinds of waters involved in the formation of such materials. Such studies are feasible because many of the different kinds of waters that play an important role in geologic processes are isotopically distinct from one another.

In addition, measurements of O^{18}-fractionations in coexisting minerals are useful for ascertaining approximate temperatures of isotopic equilibration. This can be done only if quantitative data are available on experimentally determined or empirically derived mineral fractionation factors as a function of temperature.

The purpose of the present research is to apply the techniques of stable isotope geochemistry to the problems of serpentinization of ultramafic rock. Such studies should be able to more closely define the various kinds of waters involved in the formation of serpentines, as well as possibly delineating the conditions under which the various serpentine "polymorphs" form. In particular, measured O^{18}-fractionations on coexisting serpentine and magnetite in serpentinites should help to define the P-T conditions under which serpentinization occurs.

In this study, the D/H and O^{18}/O^{16} variations in serpentines from many different types of ultramafic bodies are examined. It is important to recognize the magnitude of isotopic variation within a given body, as well as the degree of variation in each separate class of serpentinized ultramafic bodies. It is also important to analyze samples from as wide a geographic distribution as possible.

If systematic 0^{18}-fractionations among coexisting minerals can be established for a given serpentine 'polymorph' type, it may be possible to classify serpentines according to their temperatures of formation. Providing that approximate D/H and $0^{18}/0^{16}$ serpentine-water "geothermometers" can be constructed, it should be possible to estimate the isotopic compositions of waters that may have equilibrated with various serpentines, and thus further delineate the kinds of waters involved in serpentinization. However, in any such treatment, it is absolutely essential to examine the question of whether the measured isotopic compositions of serpentine samples are acquired during formation or as a result of later isotopic exchange.

Finally, it is important to apply these isotopic studies to the general problem of the origin of serpentinites and ultramafic intrusions, and also to the various tectonic theories that have been utilized to explain serpentinization of ultramafic rocks.

1.2 Previous work

In recent years O^{18}/O^{16} data have been accumulated for numerous igneous rocks and minerals. Of particular relevance to the present study, Reuter et al. (1965) and Taylor (1967b, 1968) found that ultramafic rocks from a variety of locations are very uniform in O^{18}/O^{16}, with olivines, pyroxenes, and whole-rock samples all falling in the range $\delta O^{18} = +5.4$ to $+6.6$ per mil.

Seven samples of strongly serpentinized ultramafic rocks analyzed by Epstein (1966) show a somewhat wider variation in δO^{18} from $+2.8$ for serpentinized dunite from SE Alaska to $+6.8$ for serpentines from the Mayaguez Puerto Rico mohole test site and the Bay of Islands, Newfoundland.

From the above results, Taylor (1967b) suggested that much serpentine may form by simple addition of H_2O to the ultramafic body, without appreciable oxygen exchange with adjacent parts of the crust. He also suggested that this H_2O must have an O^{18}/O^{16} ratio not too dissimilar from that of the ultramafic rock itself.

Inasmuch as serpentine is a hydrous mineral that is generally thought to form at relatively low temperatures, it is essential that in the present work one also consider the δD and δO^{18} variations previously obtained on all low-temperature hydrous minerals and rocks.

For example, Savin and Epstein (1970) have shown that clay minerals formed under subaerial conditions are essentially in isotopic equilibrium with their environments. The clay minerals define lines on a δD-δO^{18} plot that are roughly parallel to the meteoric water line of Craig (1961a). Taylor (1968) obtained a similar, poorly defined relationship for "hydrated volcanic glass" for a number of perlites and H_2O-rich obsidians from the Western United States.

Lawrence (1970) studied a large number of soils, weathering zones and clay deposits. He found that Quaternary soils and weathering zones throughout the United States show a systematic correlation with the isotopic values of present-day meteoric waters. However, the D/H and O^{18}/O^{16} ratios of most pre-Quaternary kaolinites, bentonites, and shales are higher than those of clay-rich Quaternary soils in the same geographic areas. The D/H ratios of Lower Paleozoic and Precambrian shales from the United States and Western Canada show no correlation with present-day meteoric waters.

Lawrence (1970) concludes that the isotopic values of most of the pre-Quaternary clay minerals are largely preserved. From the D/H ratios of Tertiary kaolinites formed by weathering processes, he was able to estimate the approximate D/H ratios of some Tertiary meteoric waters.

Certain serpentinites occur in metamorphic terranes, and these must be examined in context with the δD and δO^{18} variations previously obtained on regional metamorphic rocks. A general survey of oxygen isotopic compositions of coexisting minerals of regional metamorphic rocks was made by Garlick and Epstein (1967). They observed a consistent correlation between grades of metamorphism and oxygen isotope fractionations among coexisting minerals. Taylor and Coleman (1968) studied O^{18}/O^{16}

ratios of coexisting minerals in glaucophane-bearing metamorphic rocks, and found that the isotopic fractionations were systematic and larger than those measured in pelitic schists metamorphosed at the grade of biotite zone or higher. In particular, they suggest that the low-temperature, Franciscan-type blueschists formed in a temperature range from 200°C to 325°C.

II. THEORETICAL CONSIDERATIONS

2.1 Terminology and notation

The isotope data in this work are reported in the δ-notation, defined as:

$$\delta O^{18} = \left[\frac{(O^{18}/O^{16})_{\text{sample}} - (O^{18}/O^{16})_{\text{standard}}}{(O^{18}/O^{16})_{\text{standard}}}\right] \times 1000$$

$$\delta D = \left[\frac{(D/H)_{\text{sample}} - (D/H)_{\text{standard}}}{(O^{18}/O^{16})_{\text{standard}}}\right]$$

where $(O^{18}/O^{16})_{\text{standard}}$ and $(D/H)_{\text{standard}}$ represent the isotope ratios in the reference standards. For both oxygen and hydrogen, the standard is Standard Mean Ocean Water (SMOW) defined by Craig (1961b).

The fractionation factors between two compounds or phases containing oxygen or hydrogen are defined by the equations:

$$\alpha_{A-B}^{\text{oxygen}} = \frac{(O^{18}/O^{16})_A}{(O^{18}/O^{16})_B} \qquad \alpha_{A-B}^{\text{hydrogen}} = \frac{(D/H)_A}{(D/H)_B}$$

where A and B denote the compounds or phases. The fractionation factors are related to the δ's by the equations

$$\alpha_{A-B}^{\text{oxygen}} = \frac{1 + \frac{\delta_A O^{18}}{1000}}{1 + \frac{\delta_B O^{18}}{1000}} \quad \text{and} \quad \alpha_{A-B}^{\text{hydrogen}} = \frac{1 + \frac{\delta_A D}{1000}}{1 + \frac{\delta_B D}{1000}}$$

Two approximations which may be derived from the above relationships are

$$\alpha \cong 1 + \frac{\delta_A - \delta_B}{1000}$$

and $\ln \alpha_{A-B} \approx \alpha_{A-B} - 1 = \dfrac{\delta_A - \delta_B}{1000 + \delta_B}$

or $1000 \ln \alpha_{A-B} \approx \delta_A - \delta_B$

Therefore isotope fractionations are conveniently reported as $1000 \ln \alpha_{A-B}$, which in this work will be abbreviated as Δ_{A-B}.

2.2 Isotope fractionation

Isotopic equilibrium can be described in terms of an exchange reaction of the type

$$aA_1 + bB_2 = aA_2 + bB_1$$

where A and B are molecules which have one element as a common constituent and the subscripts 1 and 2 indicate that the molecule contains only the light or heavy isotope respectively. The equilibrium constant for the exchange reaction is:

$$K = \frac{[A_2]^a [B_1]^b}{[A_1]^a [B_2]^b}$$

This equilibrium constant is related to the statistical mechanical partition functions by the relationship

$$K = \left(\frac{Q_{A2}}{Q_{A1}}\right)^a / \left(\frac{Q_{B2}}{Q_{B1}}\right)^b$$

where the Q's are the partition functions of the molecules.

A very useful treatment of isotope equilibrium was developed by Urey (1947) and Bigeleisen and Mayer (1947) for the case of ideal gases of non-interacting particles. This treatment assumes that the only important contributions to the energy of the molecule result from translational, rotational, and vibrational motions, and that the partition functions are expressed as

$$Q = Q_{\text{translational}} \cdot Q_{\text{rotational}} \cdot Q_{\text{vibrational}}$$

The translational portion of the partition function can be treated classically. The rotational partition function can also be approximated classically except for some molecules containing hydrogen. Only the vibrational partition functions have to be used in quantum theory form, and one needs to know only the fundamental frequencies of vibration to calculate the isotope exchange constant.

The following generalizations are a consequence of the theory given above:

(1) At low temperature or high frequencies, $\ln K$ is proportional to $1/T$, where T is given in degrees Kelvin.

(2) At high temperature or low frequencncies, $\ln K$ is proportional to $1/T^2$.

(3) At infinitely high temperatures, $\ln K$ approaches 0.

Urey (1947) was able to calculate the equilibrium constants for a large number of isotopic exchange reactions utilizing experimentally determined vibration frequencies. In instances where these constants have been determined directly from experiment, agreement between the theoretical and experimental results have been good.

Such calculations are exceedingly useful for isotopic exchange involving gases, but are complicated greatly when applied to ionic solids and species in solution. In general the isotopic fractionations among condensed phases must be measured directly by experiment.

The equilibrium constant, K, of an isotopic exchange reaction is essentially a function of temperature alone. Pressure does not appreciably alter the equilibrium isotopic fractionations, because the volume changes accompanying isotopic substitution are very small.

III. EXPERIMENTAL TECHNIQUES

3.1 Sample collections and study

Many of the samples analyzed in this research were collected by the author, and others were supplied by various individuals identified in the Appendix. In the Appendix, each individual sample is described in detail. For most samples x-ray powder diffraction analysis was utilized for identification, particularly of the various serpentine "polymorphs". Petrographic investigation was performed both to identify the various types of serpentine and to ascertain genetic relationships among various minerals in each assemblage.

3.2 X-ray powder diffraction analysis

The x-ray powder diffraction studies were performed with a Phillips x-ray diffractometer with Ni-filtered, Cu radiation, a chart speed for most runs of 1° 2θ per minute, a 1° divergence slit, a 0.006" receiving slit, and a 1° scatter slit. Almost all samples were packed into a standard geometry aluminum holder, though some samples were sedimented on glass slides to enhance basal peaks.

The characterization of serpentine minerals by x-ray diffraction was clarified by Whittaker and Zussman (1956) who proposed the following classification:

$$\text{serpentine} \left\{ \begin{array}{l} \text{chrysotile} \quad \left\{ \begin{array}{l} \text{ortho-chrysotile} \\ \text{clino-chrysotile} \\ \text{para-chrysotile} \end{array} \right. \\ \text{lizardite} \\ \text{antigorite} \end{array} \right.$$

The reflection peaks used for identification of serpentines in the present work are those given by Whittaker and Zussman (1956).

Many of the x-ray determinations were run using CaF_2 as an internal standard. The three major peaks of CaF_2 (ASTM card 4-864, dÅ = 3.153, 1.931, 1.647) are spaced in such a way as not to interfere with any serpentine peaks, yet are scattered roughly equidistantly across the 2θ range (65° to 5°) used for most serpentine analyses.

Antigorite is distinguished from lizardite and chrysotile essentially by the absence of a peak at $2\theta = 19.4^\circ$ to 19.2°, the presence of a major peak at $2\theta = 35.5^\circ$ (16,0,1), and a medium strength peak at $2\theta = 59.0^\circ$ to 59.1° (24,3,0).

Chrysotile and lizardite are distinguished from antigorite by the presence of a peak at $2\theta = 19.4^\circ$ to 19.2° (020), a major peak at $2\theta = 36.0^\circ$ to 35.9° (202), minor peaks at $2\theta = 43.16^\circ$ and 42.07°(204), and a single moderately intense peak at $2\theta = 60.24^\circ$(060).

Chrysotile and lizardite are distinguished from one another by the location of the (204) reflection ($2\theta = 43.16^\circ$ for chrysotile and $2\theta = 42.07^\circ$ for lizardite). Chrysotile may also be distinguished from lizardite by the absence of a small peak at $2\theta = 61.74^\circ$ (208), and occasionally by the positions of the (202) and (206) peaks.

In this work, no attempt was made to distinguish between ortho- and clino-chrysotile. Distinctions may be made on the basis of (202) reflections, but lizardite presents interfering reflections. Most samples of chrysotile in this work contain variable amounts of lizardite which makes distinction of clino-and ortho-chrysotile difficult.

It might be emphasized here that distinctions of various serpentine minerals based on powder diffraction analysis were made utilizing all the above described criteria where possible, though some weaker reflections were not visible for some samples. Slower chart speeds ($\frac{1}{4}^{\circ}$ 2θ/min.) and regrinding and remounting of samples were utilized on those samples which initially gave ambiguous results. The various criteria for polymorph identification are similar to those discussed by Aumento (1970).

The presence of olivine in the samples masks some of the diagnostic peaks that distinguish lizardite and chrysotile (Hostetler et al, 1966). For such samples, olivine was removed in order to make positive identifications. For most of the samples in which mineral separation was not done, the results of the x-ray diffraction study merely indicated the presence of antigorite or lizardite-chrysotile.

Other minerals readily identified by x-ray diffraction techniques include brucite, talc, and chlorite. These minerals show very pronounced basal reflections, especially when sedimented, and are easily identified in small amounts. Hostetler et al. (1966) report that 10 percent or less of brucite in serpentinite produces only a (001) reflection. Hess and Otalora (1964) report that less than 1 percent brucite can easily be detected.

Aumento (1970) reports that as little as 1 weight percent impurity of minerals such as chlorite, biotite, talc, tremolite, brucite, olivine, clinopyroxene orthopyroxene, magnetite, calcite and dolomite are clearly distinguishable by x-ray. In some cases, detection limits extend to considerably less than 1 weight percent of the impurity.

Aumento (1970) has also investigated, by x-ray diffraction techniques, the limits to which various serpentine polymorphs can be identified in mixtures of the other polymorphs. He reports that lizardite can be identified down to as little as 1 weight percent for any two- or three-component mixture. Antigorite can be detected down to 10 percent in either lizardite or chrysotile, whereas chrysotile is difficult to identify at concentrations less than 20 percent in the presence of either of the other polymorphs. The limits of detectability reported by Aumento (1970) for various impurities and serpentine polymorphs are probably a little better than those of the present study, as slightly different sample mounting techniques and chart speeds were employed.

Interpretations of the x-ray diffraction patterns on most samples are given in the appendix. Where more than one serpentine mineral is present, relative abundances are estimated from peak heights for each of the minerals. For example, if the (202) and (204) peak heights for chrysotile and lizardite are similar, then these minerals are assumed to be present in roughly equal proportions. If the (202) and (204) peak heights of chrysotile are greater than for lizardite, then it is inferred that lizardite is a minor constituent. However, if the (202) peak for lizardite is only barely visible above background (204 is generally not seen under these circumstances), it implies that lizardite is a trace constituent.

3.3 Petrographic examination

Most of the samples in this work were studied in thin section and the results are reported in the Appendix. Some of the samples, particularly those in which magnetite was separated and analyzed for O^{18}/O^{16}, were also studied in polished section in order to distinguish magnetite and chromite.

Thin section examination, particularly when supplemented with x-ray diffraction analysis, is exceedingly useful in distinguishing the various serpentine minerals and their textural types, as well as in determining the genetic relationships among the various minerals.

The various serpentine minerals can often be distinguished simply on the basis of texture and optical properties (Chidester, 1962). A summary of the optical properties of various serpentine minerals is given by Deer, Howie and Zussman (1962) and by Page and Coleman (1967). Most of the optical distinctions made in the present study are based largely on textural and morphological criteria. The x-ray diffraction analysis served an integral role in the interpretation of microscopic observations, particularly when several serpentine minerals were present.

Other minerals encountered in this study were generally easily distinguished by microscopic examination, particularly the primary ultramafic minerals such as olivine, enstatite, and clinopyroxene, as well as other minerals associated with serpentinites, such as carbonates, tremolite, talc, and chlorite. Brucite, however, is exceedingly difficult to distinguish optically and the only satisfactory method of detection is by x-ray diffraction analysis. The various textural terms employed in the microscopic description of serpentine minerals are the following:

Mesh-texture serpentine is a latticework of longitudinally divided cross-fibre veins which enclose areas of isotropic or nearly isotropic material (serpophite). This texture is described in detail by Deer, Howie and Zussman (1962). Page (1968) reports that mesh texture serpentine in the Tiburon Peninsula, California area is composed of lizardite and chrysotile. This textural form is probably derived from olivine. Plate 3-1 illustrates the "classical" mesh texture after olivine.

Bastite is the name commonly applied to serpentine pseudomorphs after orthopyroxene in mafic and ultramafic rocks. Generally the cleavage pattern of orthopyroxene is preserved, often despite deformation (see plate 3-2). Bastite is generally composed of lizardite [Whittaker and Zussman (1956), Page (1968)].

Platy lizardite is utilized as a textural term in this study because of its fairly widespread occurrence. Page (1968) used this term to describe large plates of lizardite which have probably developed from the mesh texture serpentine in the Tiburon serpentine body. This serpentine type was observed in the present study to have also developed from bastites. The optic axial angle is commonly small, suggesting that perhaps many textures of this type are composed of lizardite. Several examples are illustrated in plates 3-3 and 3-4.

Cross-fibre veins commonly are found to crosscut various other serpentine textural forms, and are generally late-stage. This type of vein commonly displays a small cross-fibre habit normal to the trend of

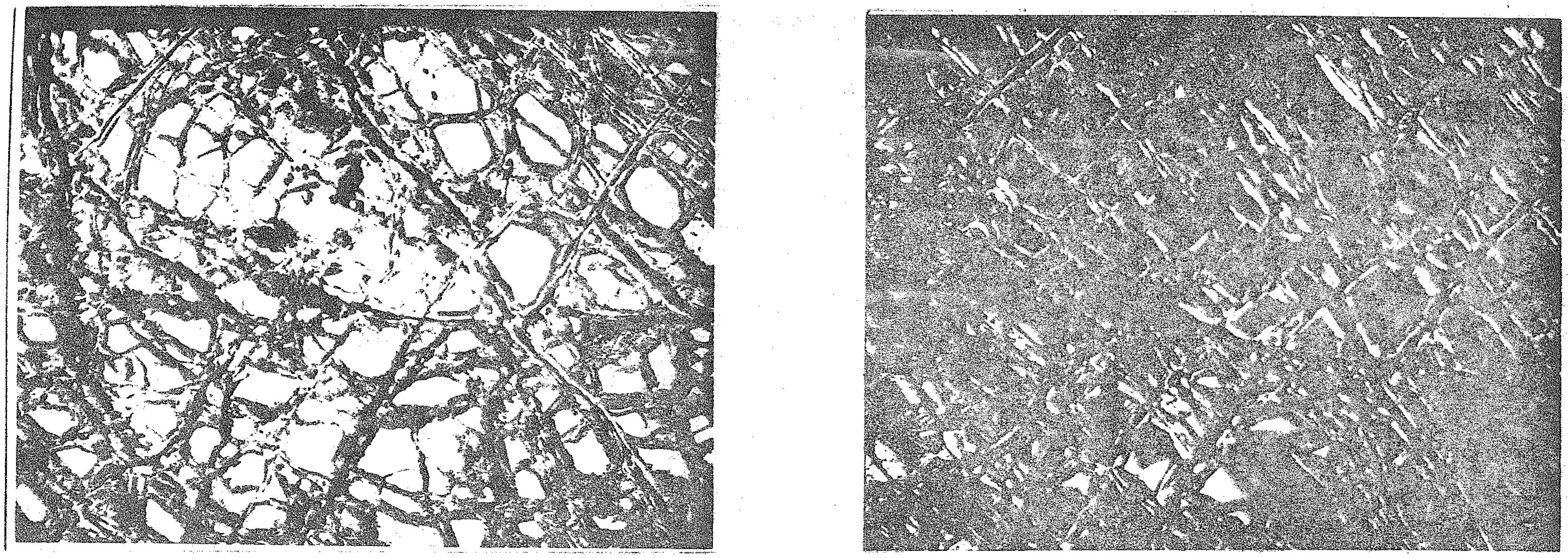

(a) Plane light

(b) Crossed nicols

Plate 3-1

(0.37 x 0.57mm)

Sample 1, Josephine County, Oregon. This illustrates mesh texture serpentine after olivine. Note small veins of magnetite that probably formed along former olivine grain boundaries. The serpentine of this sample has a $\delta 0^{18} = + 5.0$, the magnetite has a $\delta 0^{18} = -5.5$.

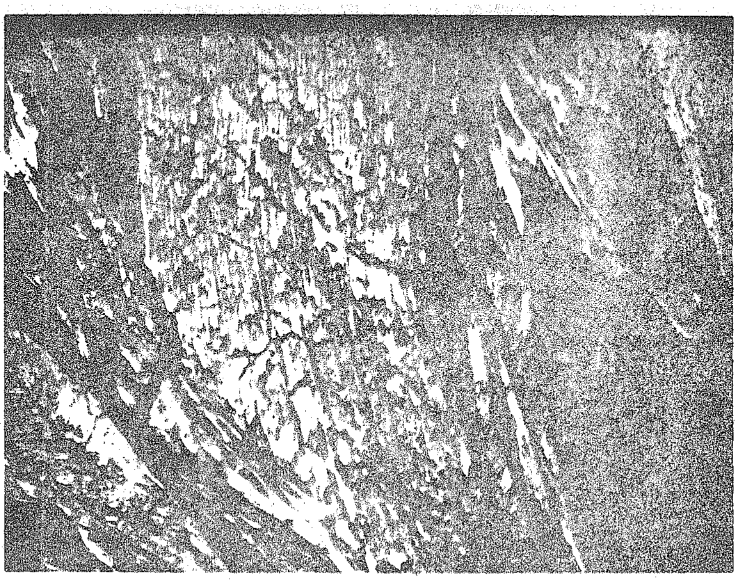

Plate 3-2

(Plane light, 0.37 x 0.57mm)

Sample 1, Guatemala. This shows a typical deformed bastite pseudomorph after enstatite; note the remnant cleavage traces. The bastite has been replaced along the lower edge by a higher birefringent serpentine (Chrysotile?). The bulk serpentine in this sample has a δO^{18} = +8.0, the magnetite has a δO^{18} = -4.6.

Plate 3-3

(Crossed nicols, 0.73 x 1.33mm)

Sample 2, Tiburon Peninsula, California. This illustrates platy lizardite formed from mesh-texture serpentine. The isotropic material is mesh-texture serpentine. A cross-fibre chrysotile vein transects the other two serpentine forms. The serpentine of this sample has a $\delta O^{18} = +8.1$, the magnetite has a $\delta O^{18} = -5.7$.

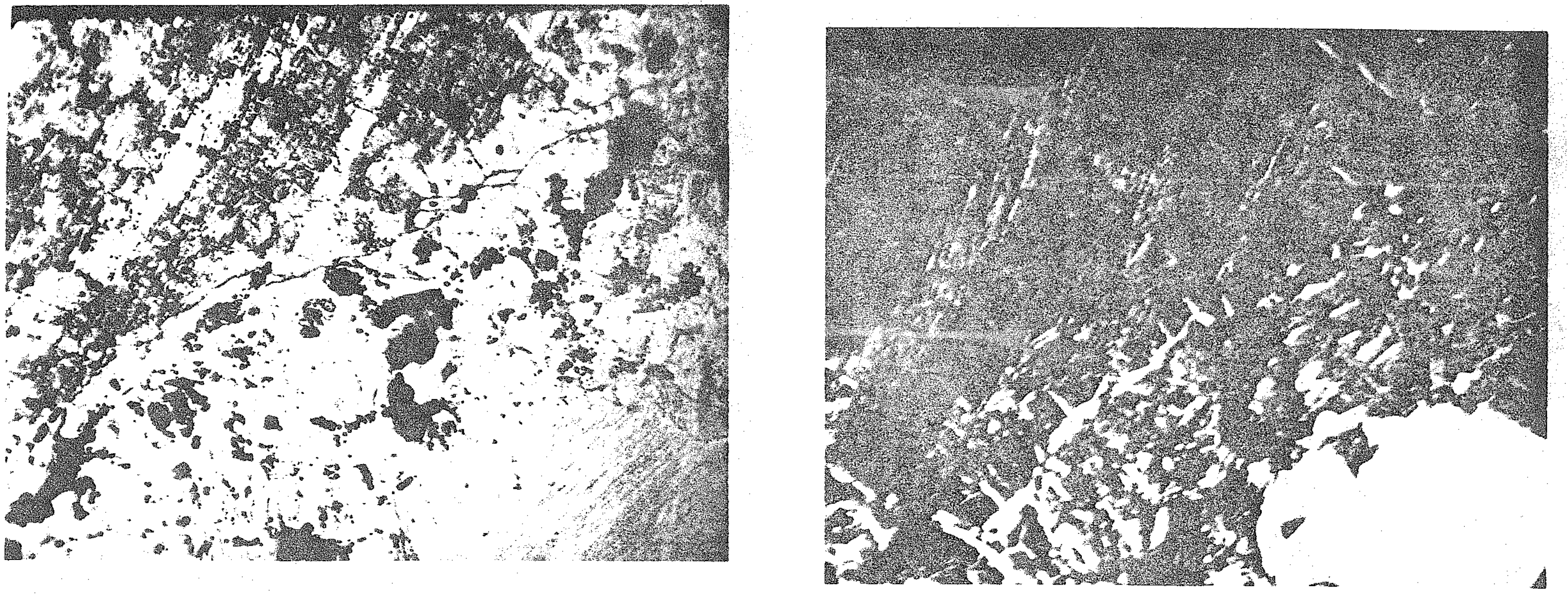

(a) Plane light

(b) Crossed nichols

Plate 3-4

(0.37 x 0.57 mm)

Sample 1, Grand Forks, British Columbia. (a) Platy lizardite (upper right) has replaced mesh-texture serpentine. Bastite (lower left) is highly fractured by chrysotile veins; note the remnant cleavage traces after enstatite. (b) Note the high birefringence of platy lizardite relative to bastite and mesh-texture serpentine.

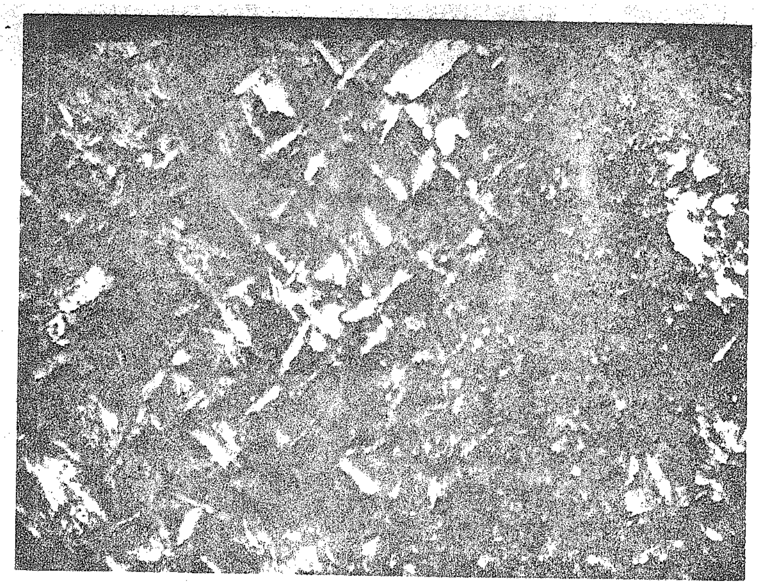

Plate 3-5

(crossed nicols, 0.17 x 0.25 mm)

Sample 10, Skagit, Washington. This illustrates the two major textures exhibited by antigorite. The right side of the photograph shows a pattern resembling that of galvanized iron, whereas the left side displays a felted pattern of bladelike crystals; the latter form is the most abundant textural type observed in antigorite.

the vein. An example of such a vein is displayed in Plate 3-3. This type of vein is probably composed of chrysotile (see Faust and Fahey, 1962); large fibre sizes are often mined for commercial use as asbestos. This textural form is commonly associated with small magnetite veins found either in the central portions or outer edges of the vein.

Galvanized-iron type antigorite can be observed under crossed nicols. This terminology is used by Chidester (1962) in describing antigorites from North-Central Vermont. This pattern was commonly encountered in the present study, and is illustrated by plate 3-5.

Antigorite in a felted pattern of bladelike particles occurs in a fine groundmass of smaller particles. Such a pattern is very commonly described in the literature and is the most abundant textural form of antigorite encountered in the present study (see plate 3-5).

3.4 Electron microprobe investigations

Microprobe studies were made on many of the magnetite separates that were analyzed for $\delta 0^{18}$ in this study. These were done on a three-channel Applied Research Laboratory (EMX) electron microprobe analyzer, using the general technique of Bence and Albee (1968) to calculate compositions. A revised set of interelement correction factors was used for the corrections. All analyses were made at 15kV with constant integrated beam current and pulse height selection. A beam current of 0.05 μA was used with a 1 μ^2 spot size. The Fe was measured relative to a fayalite standard, Cr relative to a chromite standard, and Al relative to a kyanite standard.

Initially, several magnetite grains from four different probe sections were examined by wavelength scanning in order to determine chemical variations. Major variations in Cr were observed in some samples; Mn and Ni were found only in trace amounts (< 0.1%), with no substantial variations observed among different samples.

Portions of the magnetite concentrates prepared for isotopic analysis were placed in an epoxy grain mount and polished until many of the grains exhibited the bright color characteristic of polished magnetite under reflected light. At least one-hundred grains per sample were scanned utilizing a speaker system in conjunction with the channel output. This method proved satisfactory for rough qualitative estimates of relative element variations from grain to grain within a given sample.

The various grain mounts were examined for variations in Cr, Fe, and Al. The extreme range as well as "average" amounts of Cr, Al, and Fe were counted for several grains in each grain mount. Data on the counted grains were then reduced to values of weight percent oxide. The speaker system made it possible to estimate the amounts of chromite impurities by noting the relative amounts of Fe, Cr, and Al; it was also possible to roughly ascertain the extent of serpentine impurities.

Finally, several probe mounts were examined in order to determine the chemical compositions of the different textural forms of magnetite. The element homogeneity within a given grain was examined using E.B.S. techniques.

3.5 Preparation of samples for isotopic analysis

Serpentine. The various textural forms of serpentine were separated by hand-picking, if possible, but most samples were simply ground to a grain size between 100 and 200 mesh. The amount of original material available varied considerably, but at least ten grains of sample were generally used. Magnetite was separated by a hand magnet, and olivine and pyroxene, where separates were utilized, were separated by heavy liquid techniques using bromoform. The remaining serpentine grains were inspected with a binocular microscope in order to determine the extent of impurities. The (001) x-ray reflection of brucite was looked for in all samples. Although the amounts of brucite contaminent were invariably quite small, it is important for hydrogen isotope analysis to determine these quantities as accurately as possible. This is because of the high hydrogen yield of brucite relative to serpentine (17.15 μ moles/mg. for brucite vs 7.22 μ moles/mg. for serpentine). The O^{18}/O^{16} contamination due to brucite impurities was in almost all cases completely negligible.

Magnetite. Magnetite reacts with fluorine to give quantitative oxygen yields only with great difficulty; consequently the magnetite must be ground to a very fine grain size. Most of the initial magnetite concentrates were found to contain impurities of serpentine. Absolutely pure magnetite is very difficult to obtain, because it is typically composed of dust sized particles deeply embedded in a serpentine matrix.

All magnetite samples were therefore ground in an alumina mortar and pestle to minus 200 mesh. The sample was then placed in a beaker with water and the serpentine was floated off; the magnetite was held at the bottom of the beaker by a hand magnet while the mixture was swirled and decanted. The sample was then dried and reground in the mortar and pestle again, and the above procedure repeated several times in order to obtain a reasonable purity of magnetite. Many of the samples still contained serpentine impurities after many repeated washings. Consequently it was very important for most samples to make an isotopic correction for the serpentine impurities in the magnetite.

Other minerals. Many of the other minerals studied in this work were separated by handpicking of individual grains. The talc and "blackwall" minerals were generally in nearly monomineralic zones or were coarse-grained, facilitating easy separation by hand. Other minerals, such as in mica schist, were separated by using a Frantz magnetic separator. This latter technique was found impractical for separating minerals from serpentinites because of the ubiquitous presence of magnetite in all serpentines.

3.6 Oxygen extraction

The extraction of oxygen from silicates and oxides was performed by reacting with F_2 in nickel vessels. This technique has been described in detail by Taylor and Epstein (1962a). The procedures used are essentially those of the above mentioned authors, and will be discussed only where significant variations from the published procedures were used. Mass spectrometric analyses were performed on CO_2 gas obtained from oxygen by combustion with a resistance-heated graphite rod.

The temperatures of the nickel reaction vessels were monitored with chromel-alumel thermocouples in contact with the bottom of each reaction vessel. By this method one could calibrate the variac setting in conjunction with each resistence furnace. The temperature was checked periodically and it was found that little temperature variation occurred during runs. The maximum temperature that could be utilized was determined by placing a small amount of fluorine gas in the vessel and observing the temperature at which the fluorine began to react appreciably with the nickel. Above about 630-640°C, the nickel reaction vessels reacted rapidly with fluorine, though in the range of 600 to 620°C there still existed fluorine gas in the reaction vessel even after several days.

It is particularly important to react the magnetite samples at the maximum possible temperatures; consequently this maximum temperature was determined several times throughout the duration of this study.

Oxygen extraction of serpentine

Pure serpentine separates were reacted with fluorine at various temperatures in order to assess the degree to which reaction temperatures affect the isotopic composition of the liberated oxygen.

Three different samples representing the three serpentine polymorphs were reacted at various temperatures from 250°C to 600°C. Table 3-1 demonstrates that the reaction of serpentine and fluorine is nearly complete above 250°C with a small and consistent fractionation of 0.3°/oo between the low temperature reaction (250°C) and the high temperature (i.e., complete) reaction (600°C). Serpentine in fact reacts

TABLE 3-1

Oxygen yield and δO^{18} data of pure serpentines reacted in the temperature range 600° - 250°C.

Reaction temperatures	Yield $\left(\frac{\mu mole}{mg}\right)$	δO^{18}	No. Runs
Sample 2, Ship Mts., Calif. (lizardite)			
600°C (complete reaction)	15.4 ± 0.2	+ 3.6 ± 0.05	2
500°C	15.2 ± 0.2	+ 3.6 ± 0.1	3
400°C	15.2 ± 0.2	+ 3.3 ± 0.05	2
350°C	15.4	+ 3.3	1
250°C	15.3	+ 3.3	1
Belvedere Mt., Vt. (cross-fibre chrysotile)			
575°C (complete reaction)	15.5	+ 6.5	1
350°C	15.1	+ 6.4	1
250°C	15.1	+ 6.2	1
Sample 9, Skagit, Wash. (antigorite)			
550°C	15.3 ± 0.0	+ 9.1 ± 0.05	2
250°C	15.2 ± 0.05	+ 8.8 ± 0.0	2

δO^{18} in per mil relative to SMOW; the ± indicates average deviation from the mean for samples in which two or more runs were made.

TABLE 3-2

Oxygen yield and δO^{18} data on pure serpentines reacted at 300^{o} - $575^{o}C$, using various mesh sizes

Reaction $T^{o}C$	mesh size	Yield $\left(\frac{\mu moles}{mg}\right)$	δO^{18}	No. Runs
Sample 81, New Caledonia (lizardite and chrysotile)				
300	50 - 80	14.7	+ 8.6	1
300	80 - 120	14.8	+ 8.8	1
300	120 - 170	14.7	+ 8.8	1
300	P 170	14.5	+ 8.8	1
575	80 - 120	15.1	+ 9.0	1
575	P 170	15.1	+ 9.0	1
Sample 4, San Luis Obispo, California (lizardite, minor chrysotile)				
300	60 - 80	15.3	+ 7.6	1
300	80 - 120	15.2	+ 7.7	1
300	120 - 170	15.2 ± 0.05	+ 7.8 ± 0.05	2
300	P 170	15.2	+ 7.9	1

with a small and consistent isotopic fractionation as low as 200°C, but at temperatures lower than 150°C, the yield is substantially smaller and the isotopic fractionation greater.

Also, various grain size distributions of serpentine were studied to determine if different grain sizes result in low yields and/or isotopic fractionation. From the results of Table 3-2, one can see that a mesh size of greater than 80 probably does not result in any substantial isotopic fractionation, even if the reaction takes place at a temperature as low as 250°C.

Low temperature extraction of oxygen from impure serpentines

A series of experiments were done to see if serpentine could be reacted with fluorine selectively without substantially affecting the primary minerals such as olivine and pyroxene. This was done because many serpentines contain primary olivine and pyroxene which are difficult and time consuming to separate. Olivine in partially serpentinized dunites and peridotites typically ranges down to very small grain sizes (< 0.1 mm) which causes difficulties in obtaining pure serpentine separates.

In Table 3-3, samples of partially serpentinized peridotites and dunites are compared to the best serpentine fraction that could be separated by a number of treatmentswith heavy liquids. This fraction, though not pure, shows considerable enrichment of serpentine relative to that in the natural mixture, as can be seen from the increased yields. This table strongly suggests that serpentine selectively reacts with

TABLE 3-3

Reaction of various serpentine-olivine-enstatite mixtures with fluorine at 300°C for 24 hours

Sample No.	Whole Rock Yield $\left(\frac{\mu mole}{mg}\right)$	Whole Rock $\delta 0^{18}$	Heavy Liquid Serpentine Separate Yield $\left(\frac{\mu mole}{mg}\right)$	Heavy Liquid Serpentine Separate $\delta 0^{18}$
5 - Fort St. James, B.C.[1]	11.9	- 2.8	13.9	- 2.6
1 - Yalakom, B.C.[2]	6.6	+ 4.0	12.8	+ 4.0
3 - Fort St. James, B.C.[2]	9.2	+ 2.5	13.2	+ 2.4
36J - Costa Rica[2]	12.6	+ 6.1	14.5	+ 5.9
685a - Vourinos Complex[1]	6.7	+ 2.1	10.5	+ 2.0
1 - Duke Island, Alaska[1]	8.3	- 2.3	12.0	- 2.6

[1] serpentinized dunite

[2] serpentinized peridotite

TABLE 3-4

Reaction of artificial serpentine[1]-olivine[2] mixtures with fluorine at 300°C for 24 hours

	Yield $\left(\frac{\mu\text{moles}}{\text{mg serp}}\right)$	δO^{18}	No. Runs
Serpentine-olivine mix (100-200 mesh olivine)	15.4	+ 3.3	2
Serpentine-olivine mix (minus 200 mesh size for olivine)	19.1	+ 6.9	1

[1] δO^{18} pure lizardite, sample 2 - Ship Mt., Calif. = + 3.3

[2] δO^{18} pure olivine (BC-32E) = + 20.8

fluorine at 300°C without involving any significant oxygen contamination from the primary minerals. The isotopic discrepancy between the natural mixture and the serpentine concentrate is about 0.4°/oo or less, probably depending upon the isotopic composition of the serpentine relative to the primary minerals. For example, sample 5 from Fort St. James, British Columbia and sample 1 from Duke Island, Alaska, show the greatest differences between the untreated and treated samples; these two samples also display the greatest isotopic differences between the serpentine and the coexisting primary minerals.

In Table 3-4, the isotopic composition and yield of artificial mixtures of serpentine and olivine are reported; these mixtures were reacted at 300°C for 24 hours. The olivine (forsterite from a contact metamorphic zone) utilized in this experiment had a δO^{18} value of +20.8‰, whereas the serpentine δO^{18} equals +3.3°/oo; consequently any oxygen contamination from the olivine during reaction would be very obvious. The results demonstrate that if the grain size of the olivine is between 100 and 200 mesh, virtually none of the olivine reacts at 300°C. If one uses a much finer grain size (minus 200 mesh), some of the olivine reacts with fluorine.

Experiments were also carried out to show that pure olivine and enstatite of 100 to 200 mesh size do not react with fluorine at 300°C for 24 hours. Magnetite of very fine grain size (much less than 200 mesh) reacted under similar conditions to the extent of about 5%.

Thus it can be concluded with reasonable certainty, based on the data in Table 3-3 and 3-4, that serpentine can be selectively reacted with fluorine at 300°C for 24 hours, without any substantial contamination of oxygen from olivine and pyroxene. We have, however, seen in Table 3-4 that fine-grained olivine reacts to some extent in the presence of serpentine, resulting in isotopic contamination of the sample oxygen. None of the heavy liquid serpentine separates in Table 3-3 were completely pure, so there exists the possibility that some of the very fine-grained olivine in the serpentine-olivine mixtures reacted to some extent with the fluorine. This also probably holds true for very fine-grained enstatite, although the enstatite in serpentinized peridotites is generally not as fine grained as the olivine.

In any case, for most of the serpentines studied in this work, the δO^{18} values of the serpentine are not too greatly different from that of primary olivine, so that the reported serpentine analyses should all be accurate to $\pm$ 0.2 to $\pm$ 0.3 per mil. In support of the above assertions, it has been shown (Taylor, 1959) that the δO^{18} values of oxygen obtained by fluorination of olivine are not very sensitive to low yields.

Summary of reaction conditions utilized for routine oxygen extraction from serpentine

All pure serpentine samples in the present study were reacted with fluorine in the temperature range of 575° to 600°C for 24 hours. The yields obtained at such temperatures weretypically 15.3 to 15.6 μmoles O_2/mg. whereas the Mg end member should give a theoretical yield of 16.25 μmoles O_2/mg. This apparent discrepancy is probably due in large part to Fe replacement of Mg in the octahedral position of the serpentine. If 10 mole % Fe is present in the serpentine structure, the oxygen yield is 15.7 $\frac{\mu\text{moles}}{\text{mg}}$. Page (1967, 1968) notes that many serpentines contain up to 10% Fe substituted into the octahedral position of serpentine. Also, all serpentine samples contain small amounts of magnetite dust, and this contaminant, which is very difficult to get to react with fluorine, could in part account for the slightly low oxygen yields.

All serpentine samples which contained primary minerals, such as olivine and pyroxene, were first separated by handpicking if possible. By this method one can often separate zones or areas rich in serpentine from those poor in serpentine. Then the serpentine-rich fraction was crushed to between 100 to 200 mesh and reacted at 250° to 300°C for 24 hours. The samples reported in Table 3-3, for example, were treated this way. The δO^{18} value of the serpentine obtained by this method was corrected by +0.3°/oo, the average difference between the low and high temperature reaction, as reported in Tables 3-1 and 3-2.

By the above technique, one can rapidly determine the approximate δO^{18} of serpentine in partially serpentinized ultramafic rocks, without lengthy and sometimes exceedingly difficult mineral separation. For samples in which the accurate δO^{18} determination of serpentine was required, mineral separations were made using heavy liquids.

Oxygen extraction of magnetite

Even though lengthy separation procedures had been applied, most of the magnetite concentrates still contained from 5 to 30 weight percent of serpentine impurities; this, of course, results in sizeable discrepancies between the measured δO^{18} of the magnetite separate and the true value of the pure magnetite. Thus it was absolutely necessary to find a way of correcting for the serpentine impurity.

The technique employed in the present work to correct for serpentine impurities in magnetite is to measure the SiF_4 yield from each reaction. Such a method is described by Taylor and Epstein (1970), who employed this method for correcting the measured isotopic composition of ilmenite for impurities of pyroxene. However, serpentine generates HF as well as SiF_4 in reacting with fluorine; therefore a method had to be devised for separating SiF_4 from HF.

It was necessary to slightly modify the fluorine extraction apparatus in order to collect the SiF_4 and HF. Two stainless steel traps were placed in the metal part of the vacuum system between the KBr furnace and the reaction vessels. A coiled metal trap was used in place of trap B described by Taylor and Epstein (1962), and it is in this trap that the SiF_4 and HF were condensed out at liquid nitrogen temperatures. A simple U-trap was employed between the above described coiled trap and the KBr furnace in order to prevent diffusion of Br_2 back into the coiled trap, thus preventing contamination of the HF and SiF_4.

During a typical extraction procedure, all of the SiF_4 and HF was allowed to condense into the coiled trap for about 10 minutes. Then the remaining O_2 and F_2 were allowed to enter the KBr furnace where all the F_2 reacted. After the O_2 was converted to CO_2 and collected, the coiled trap was isolated from the KBr furnace and opened to the glass

Figure 3-1. Relationship between SiF_4 yield and sample weight for four different serpentine samples.

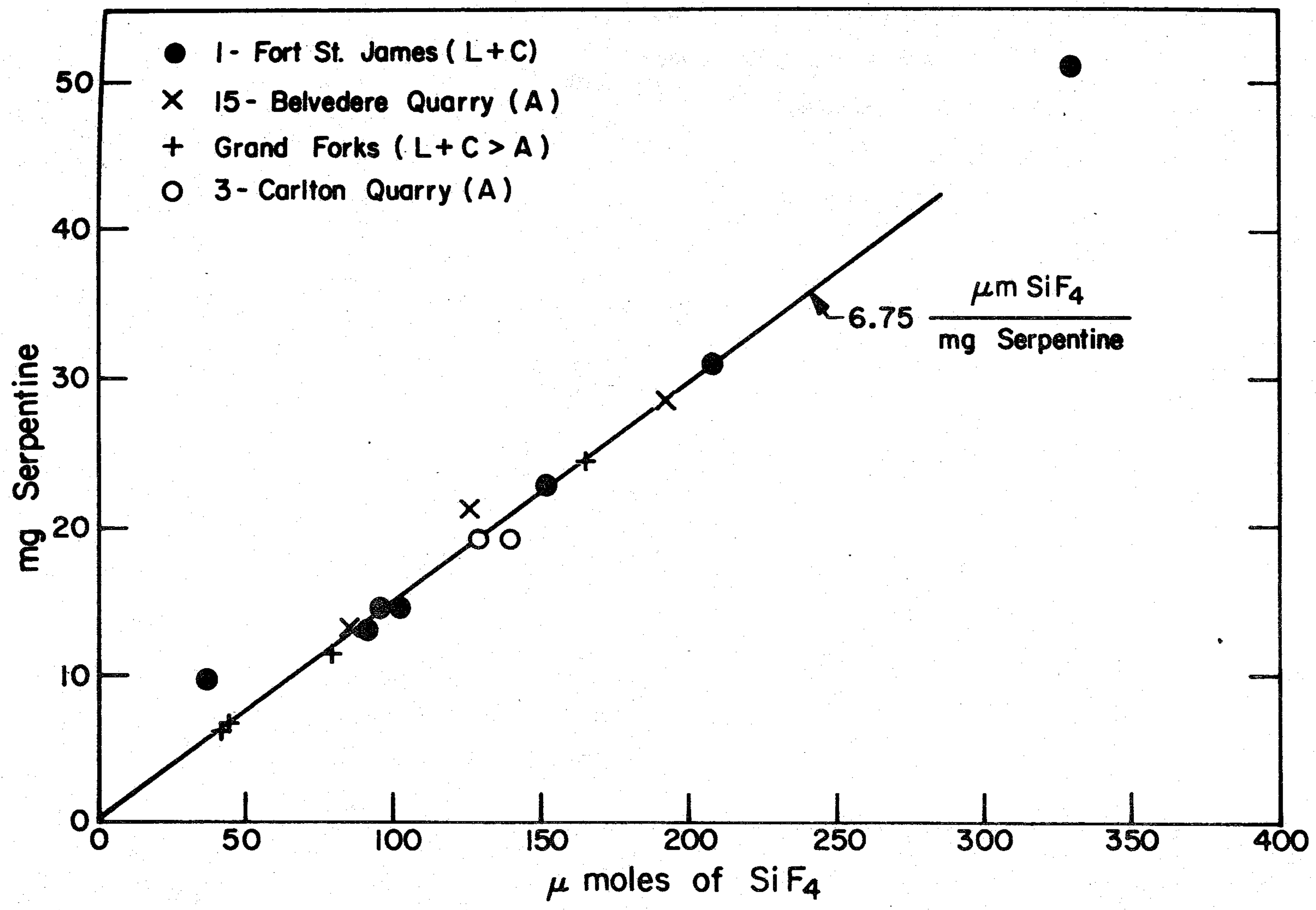
● 1- Fort St. James (L+C)
× 15- Belvedere Quarry (A)
+ Grand Forks (L+C > A)
○ 3- Carlton Quarry (A)
6.75 $\frac{\mu m\ SiF_4}{mg\ Serpentine}$
mg Serpentine
0
10
20
30
40
50
0
50
100
150
200
250
300
350
400
μ moles of SiF_4

Figure 3-1

portion of the vacuum line. The liquid N_2 on the coiled trap was replaced by a vessel filled with a dry ice-organic solvent (M-17) mixture, and the SiF_4 vapor was allowed to condense into a nearby U-trap in the glass portion of the line.

The separation of SiF_4 from HF was accomplished by warming the coiled trap up from liquid N_2 temperatures, where SiF_4 and HF have negligibly low vapor pressures, to the temperature of the dry ice mixture (-78°C), where SiF_4 is completely vaporized and HF has a vapor pressure of about 4.2 mm. (see Simons, 1950). By this technique, the SiF_4 is quickly condensed at liquid N_2 temperatures into the nearby glass U-trap.

It was observed that the amount of material that condensed into the glass U-trap was constant even though the condensation periods varied from 30 to 90 seconds. The nearly pure SiF_4 in the glass U-trap is then transferred to a manometer and its volume measured.

Four different samples representing different types and mixtures of serpentine were tested in order to determine if consistent yields of SiF_4 could be obtained utilizing the above described procedures. In figure 3-1, the measured quantity of SiF_4 liberated is plotted against various sample weights. The yields in terms of μ moles of SiF_4/mg of sample show nearly consistent values with only a few small discrepancies. There is some departure from linearity with large samples, but most of the magnetite samples examined in this work contain very little serpentine impurity. The average measured yield of SiF_4 (6.75 μmoles SiF_4/mg) is smaller than the theoretical Mg end member yield. For example, 10% Fe in the octahedral position of serpentine gives a theoretical yield of 6.98 μmoles SiF_4/mg.

The weight of serpentine impurity in any given magnetite sample is computed by measuring the amount of SiF_4 and using the average yield shown in figure 3-1. The amount of oxygen contributed by the serpentine impurity in the magnetite sample is computed by multiplying the calculated weight of serpentine by 15.6 μmoles O_2/mg, the average oxygen yield for pure serpentine samples. One can then compute the δO^{18} of the pure magnetite utilizing the accurately measured δO^{18} value of the coexisting pure serpentine.

Oxygen extraction of other phases

All other mineral and whole rock samples studied in this work, except serpentine that contains olivine, pyroxene or magnetite, were reacted at 550° to 600°C for 16 hours.

3.7 Hydrogen extraction

The experimental technique for the extraction of hydrogen from OH-bearing minerals is similar to that described by Friedman (1953) and Godfrey (1962). All of the minerals except serpentine were degassed at 100-150°C under high vacuum for about 1 hour, then heated by an induction furnace to a maximum temperature of 1300 to 1500°C to liberate H_2 and H_2O. The H_2O was reduced to H_2 by passing it over hot uranium at about 750°C. The volume of total H_2 evolved was then measured and the gas was ready for mass spectrometric analysis.

It is possible that not all of the adsorbed water is removed during this preliminary outgassing, and even if it is completely removed, it is also possible that isotopic exchange occurs between the adsorbed and structural water at temperatures of 100-150°C.

Some minerals which contain interlayer water, such as montmorillonite, easily exchange this water with their immediate environment (Savin and Epstein, 1970). Savin and Epstein (1970) developed a technique of removing this interlayer water by heating in a vacuum at temperatures of 100-250°C for two hours or more. However, recent work by Lawrence (1970) has shown that because of exchange during outgassing, there are some difficulties with this method.

Serpentine, particularly chrysotile, is known to absorb water from the atmosphere. Hess (1964) has noted this fact while commenting on the anomalous densities measured for the Mayaguez bore hole serpentinites. Pundsack (1956) found that natural chrysotile adsorbed 2.5% water by weight when stored in an environment of 100% humidity at 25°C; this water comes back off at temperatures between 175°C and 200°C. Because of the large amount of adsorbed water in some serpentine samples, a series of experiments were designed to test whether this adsorbed water can be removed without affecting the δD of the OH-structural hydrogen.

Exchange experiment

In order to determine if adsorbed water can be removed by a preliminary outgassing technique, it was essential to determine the amount of exchange occurring at room temperature. It has been determined by Roy and Roy (1957) that less than 0.5% of the OH in kaolin minerals is exchanged at room temperatures, even after a few days of treatment.

To test if all of the adsorbed water in chrysotile can be removed by simple heating at low temperatures, a sample consisting of chrysotile and lizardite (sample 304.7 from the Mayagues site in Puerto Rico) was placed in heavy water ($\delta D = +1870^{\circ}/_{oo}$) for four days. This sample was then dried for 12 hours at 100°C and exposed to air for several hours. Afterwards the sample was placed in a quartz crucible and outgassed at 200°C for 2 hours and finally dehydrated at 1100°C for 3 hours to remove all structural water.

The measured isotopic composition of the sample exposed to the heavy water was $\delta D = -48^{\circ}/_{oo}$ as compared to the identical sample, not exposed to heavy water, where $\delta D = -63^{\circ}/_{oo}$. The exchange is less than 1%, which is similar to that found for kaolin minerals. This suggests that only a very small amount of adsorbed water is retained after the preliminary outgassing. Since the isotopic composition of any reasonable adsorbed water is not nearly as extreme as the heavy water used in this experiment, we conclude that any water which is not lost during the preliminary outgassing procedure has a negligible effect upon the isotopic composition of the true hydroxyl in serpentine.

Procedures related to the extraction of H_2O from serpentine

Throughout the duration of this work, various procedures for the extraction of hydrogen from serpentine were adopted and compared.

Initially all serpentine samples were extracted in the manner described by Godfrey (1962). Samples were placed in a Pt-crucible while exposed to air and then placed into the vacuum system. All air was pumped away and the sample was then dehydrated using an RF generator.

A series of different outgassing procedures were used for a given sample in order to determine the conditions most favorable for removal of adsorbed water. In Table 3-5, different outgassing temperatures and times were employed before the dehydration. It becomes immediately obvious that the measured δD of the structural-OH is insensitive to variations in the outgassing procedure. It appears that adsorbed water is easily removed and does not isotopically contaminate the structural water. Many other samples were also tested using different outgassing temperatures and times, as shown in Tables 3-5 and 3-6.

A second variation of the basic procedure used by Godfrey (1962) was employed for comparison. Suzuoki (personal communication) utilized a method whereby the Pt-crucible is never exposed to air before the sample is loaded. The basic apparatus for hydrogen extraction was modified to conform to his design. In this procedure, the sample is contained in a small glass vial in the vacuum system. The Pt-crucible is then preheated to about 1000°C to remove any possible absorbed water. After the Pt-crucible cools, the sample is loaded into the crucible while under vacuum. By this method, the Pt-crucible is never exposed to air before the outgassing and dehydration sequence. The two different techniques are compared for many samples listed in Table 3-5. As one can see, the results compare favorably with each other, though δD differences between samples employing the above described techniques vary by as much as 5°/oo. The original method suggested by Godfrey

TABLE 3-5

Hydrogen extraction of serpentine utilizing an RF generator

Sample No.	Technique	Outgas Temperature	Outgas Time (hrs.)	$\delta D^{o}/_{oo}$*	No. Runs
303.58 Mayaguez bore hole test site, Puerto Rico	1a	25°C	3/4	- 66	1
	1	200°C	2	- 64 ± 1	2
	1a	200°C	2	- 64	1
	1a	240°C	1/2	- 61	1
	1a	360°C	1/2	- 63 ± 1	2
	1a	360°C	3/4	- 63	1
	1a	420°C	2/3	- 60	1
11a Vaurinos Complex	1	250°C	1	- 99	1
	1a	300°C	1/3	-102	1
2 Guatemala	1	200°C	1	- 97	1
	1a	300°C	1/2	- 91	1
5 Mt. Stewart, Washington	1	230°C	1	-127	1
	1a	200°C	1	-124	1
5 Del Puerto, California	1	200°C	1	-105	1
	1a	200°C	1	-104	1
2 Duke Island, Alaska	1	200°C	1	-130	1
	1a	200°C	1/2	-135	1
1 Josephine County, Oregon	1	200°C	1	-107	1
	1a	300°C	2/3	-112	1

Technique: 1. The sample is placed in a Pt-crucible directly and outgassed for various times at different temperatures (basic method utilized by Godfrey (1962).

1a. Pt-crucible is pre-heated to > 1000°C, then the sample is placed in the cold crucible under vacuum (modified procedure suggested by Suzuoki).

*δD in per mil relative to SMOW; the ± indicate average deviation from the mean for samples in which two analyses were made.

(1962), where the Pt-crucible was momentarily exposed to air during the loading sequence, was employed for most subsequent runs because of simplicity.

A second general technique was employed for the extraction of hydrogen from serpentine. In this method, the vessel, which contains the sample, is closed during dehydration, resulting in a buildup of pressure. The basic problem of dehydration under vacuum, whereby the evolved water is condensed into a nearby trap cooled to liquid N_2 temperatures and the H_2 evolved is collected with a toepler pump, is the problem of gas discharge caused by the RF generator. Experiments have demonstrated that this discharge results in erroneous isotopic compositions, probably due to ionic reactions with the vacuum grease and the walls of the containing vessel. Consequently, during the dehydration process the gas pressure must be kept low enough to avoid this discharge. This results in lengthy dehydration times, of the order of one to two hours. The method of allowing a H_2O pressure buildup during dehydration, suggested by R. L. Armstrong (personal communication), allows complete dehydration after about 15 minutes.

The resulting pressure is high enough to retard gas discharge, except for brief moments during the beginning of each run. After this dehydration, the RF furnace is turned down, and the vessel opened to a trap cooled by liquid N_2 to condense the H_2O. The remaining non-condensable gas (H_2) is then collected by the toepler pump. For several samples, this gas was passed through the U-furnace before being collected by the toepler pump. No differences were observed for samples in which the evolved hydrogen either was or was not passed through the U-furnace before being collected.

After all hydrogen was collected by the toepler pump and the sample chamber was evacuated, the sample was reheated to ensure complete dehydration. After the dehydration was complete, the trap into which the water was condensed was warmed up using a dry ice-M-17 bath and outgassed to high vacuum. By this technique, all material except water was pumped away. This was done because it had been previously observed that if these materials that are noncondensable at dry ice temperatures (presumably CO_2, SO_2, etc.) were allowed to pass through the uranium furnace, they caused a premature contamination or "poisoning" of the uranium metal.

To determine if this discarded non-condensable material contained hydrogen, extractions of several samples were carried out both with and without the dry ice-M-17 bath. In the latter method, all of the material condensed into the trap at liquid N_2 temperatures was passed through the U-furnace and collected. The δD measurements and H_2 yields for several samples were identical within experimental error, indicating that no hydrogen was present in this non-condensable fraction.

The two methods, (1) allowing the H_2O pressure to build up upon dehydration, and (2) the method of Godfrey (1962), where collection is done at low H_2O pressure, are compared in Table 3-6. These two basic methods were studied using both the RF generator and an electrical resistance furnace as a heating source.

TABLE 3-6

Hydrogen extraction of serpentine utilizing various techniques

Sample No.	Technique	Outgas Temperature	Outgas Time (hrs.)	$\delta D^o/_{oo}$	No. Runs
303.58 Mayaguez bore hole test site Puerto Rico	1	200°C	1	- 64	1
	2	230°C.	1/2	- 64	1
	2	200°C	1/2	- 64	1
	3	200°C	2	- 67	1
	3	340°C	3/4	- 65	1
	4	230°C	1	- 64	1
81 New Caledonia	1	350°C	1/2	- 85	1
	3	200°C	2	- 83	1
1 Yalakom, British Columbia	1	200°C	1/2	- 86	1
	3	220°C	2	- 91	1
4 San Luis Obispo California	1	250°C	1	- 88	1
	4	220°C	1	- 86	1

Techniques:

1. RF furnace used for heating sample - sample dehydrated at negligibly low H_2O pressure.
2. RF furnace used for heating sample - sample dehydrated in the presence of H_2O vapor.
3. Electrical resistance furnace used for heating sample - sample dehydrated at negligibly low H_2O pressure.
4. Electrical resistance furnace used for heating sample - sample dehydrated in the presence of H_2O vapor.

When the resistance furnace is used, the sample is placed in a quartz crucible and lowered down into a quartz tube; after preliminary outgassing, the sample is heated to about 1000-1100°C for about four hours. Thus, in Table 3-6 essentially four different techniques are compared. The data indicate almost no variation in δD for the different methods. Therefore it is concluded that the extraction of H_2 and H_2O from serpentine after a simple, preliminary outgassing treatment represents a valid technique for obtaining the D/H ratio of the hydroxyl of the serpentine.

3.8 Mass spectrometry and other corrections

The experimentally determined isotope ratios were all corrected and reported as δ-values relative to S.M.O.W. (Standard Mean Ocean Water). All of the δ-values in this work are reported in per mil.

Oxygen

Mass spectrometric analysis of oxygen isotopes are performed on CO_2 gas. The mass spectrometer used is a 60 degree, single focusing, double-collecting and dual gas-feed instrument of the type described by Nier (1947) with modifications by McKinney *et al.* (1950).

The mass spectrometer measures the ratio of the mass 46 beam to the mass 44 and 45 beams. Due to C^{13} and O^{17} species, the $\frac{46}{44+45}$ is not exactly equal to O^{18}/O^{16}. Craig (1957) has derived a correction factor which applies to this situation. All CO_2 samples have essentially the same carbon isotopic composition, that of the carbon rods used in the conversion of O_2 to CO_2. Since both the sample and the working standard (quartz from the Rose Quartz pegmatite) have the same carbon isotopic composition, the expression derived by Craig (1957) reduces to δO^{18}corr. = 1.01 δO^{18}meas.

Other correction factors one has to apply to the raw data are the background, mixing of standard and sample gas, and leakage through the mass spectrometer switching valves. Since the O^{18}/O^{16} ratio of the mass spectrometer standard gas is about 25 per mil larger than that of ocean water, the raw values based on this standard are lower than the corresponding values based on the ocean water standard. The O^{18}/O^{16} ratio must therefore be multiplied by 1.025.

The background correction is determined by the ratio of the long-lived background ion current probably from such sources as the degassing of adsorbed CO_2 from the source and the feed system. This correction factor is variable, but it is typically 1.02 to 1.04.

The working standard used in this research is quartz from the Rose Quartz pegmatite which has a δO^{18} of +8.43. This value is obtained by comparison with the Potsdam sandstone and St. Peter sandstone standards utilized by Taylor and Epstein (1962) and Garlick and Epstein (1967). The δ-value of a particular sample (X) relative to S.M.O.W. is calculated by the following formula:

$$\delta_{\text{x-smow}} = 1.05\ (\delta_{\text{x}}^{\text{raw}} - \delta_{\text{RQ std.}}^{\text{raw}}) + 8.43$$

The value of 1.05 is an approximate summation of all the multiplicative correction factors. This value is of course variable, principally due to changes in the background correction.

$\delta^{raw}_{RQ\ std.}$ is the mean value of one of the groups of Rose Quartz standard measured against the mass spectrometer reference gas. The groupings are obtained by noting all the different raw values; these are arbitrarily subdivided where significant differences occur. Such differences are due to secular drifts in the mass spectrometer and slight differences in the gas standards used in the mass spectrometer.

Another correction to be applied to all analyses is that for the oxygen contamination in the fluorine. This correction is generally less than 0.2°/oo, but it varies slightly depending upon the amount of fluorine used, the isotopic composition of the sample, and the amount of sample used.

The mass spectrometer precision is about 0.1 per mil, whereas the analytic precision for δO^{18} of minerals is about 0.1 to 0.2 per mil for pure samples. As was mentioned earlier, this analytical error is slightly greater for partially serpentinized samples and for magnetite samples.

Hydrogen

Mass spectrometric analyses of hydrogen isotopes are performed on hydrogen gas using a mass spectrometer similar to the one described by Nier (1947) and McKinney et al. (1950), except that it employs an extra arm containing the mass-2 collector. The ratio of mass-3 to mass-2 is measured. Because the mass-3 beam consists of both HD^+ and H_3^+ ions, a correction factor for the contribution of H_3^+ ions must be made, as described by Friedman (1953). Also, correction factors must be made for background, leakage through the switching valves, and the change of standard, similar to those utilized in O^{18}/O^{16} measurements.

The equation which is used in converting raw numbers to SMOW values is:

$$\delta_{x\text{-smow}} = 0.94052 \quad \delta_{x\text{-std.}} \quad - 68.75$$

where $\delta_{x\text{-std.}}$ is the isotopic composition of the sample relative to the machine standard. This was derived by direct comparison with NBS standard water.

The precision of the hydrogen mass spectrometric analyses is about 0.5 per mil for hydrogen, but the total analytic error for δD in serpentines is about 2 - 3 per mil.

IV. OXYGEN ISOTOPE GEOTHERMOMETRY OF SERPENTINE-MAGNETITE PAIRS

4.1 General statement

Clayton (1961a) observed experimentally that the equilibrium O^{18}/O^{16} fractionation between calcite and H_2O follows an equation of the form

$$\ln K = AT^{-2} - B$$

analogous to the theoretical behavior of ideal gases at high temperatures (see Chapter 2). This relationship appears to hold for many oxygen compounds over a wide range of temperatures, as demonstrated by experimental results on the systems calcite-water (Clayton, 1961b), muscovite-water (O'Neil and Taylor, 1969), quartz-water (O'Neil and Clayton, 1964), and alkali feldspar-water and anorthite-water (O'Neil and Taylor, 1967).

The fundamental basis for making estimates of temperatures of formation for any given mineral assemblage rests on the assumption that there was attainment and retention of isotopic equilibrium. In many naturally-occurring mineral assemblages this is not achieved. Equilibrium is assumed to have been attained if the isotopic fractionations between different mineral pairs from the same assemblage yield the same temperature upon the application of experimentally determined calibration curves. However, much of the experimental data necessary for this evaluation is not yet available; hence, assumptions regarding attainment of isotopic equilibrium rest largely upon observations of systematic isotope variations in minerals. This technique is applicable to many igneous and metamorphic rocks composed of two or more oxygen-bearing minerals.

The applicability of oxygen isotope geothermometry to problems of serpentinization is complicated by the fact that only two phases may be readily utilized, namely serpentine and magnetite. Although a preliminary magnetite-H_2O fractionation curve was published by O'Neil and Clayton (1964), this was later found to be in need of revision (J. R. O'Neil, personal communication); therefore only an approximate calibration is available for magnetite-H_2O. The serpentine-water fractionation has not yet been investigated in the laboratory, but its general behavior can be inferred by various extrapolations of natural and experimental O^{18}/O^{16} data.

4.2 Serpentinization reactions

Various reactions have been proposed for the serpentinization of ultramafic rocks. These can be basically classified according to whether serpentinization occurs at constant volume, as advocated by Thayer (1967a) and Turner and Verhoogen (1960) or occurs with volume expansion, as suggested by Hostetler *et al.* (1966) and Page (1967, 1968).

According to the concept of serpentinization at constant volume, Turner and Verhoogen (1960) give the reaction as:

$$\begin{array}{ccccccccc} 5Mg_2SiO_4 & + & 4H_2O & \rightarrow & 2Mg_3Si_2O_5(OH)_4 & + & 4MgO & + & SiO_2 \\ \text{olivine} & & \text{introduced} & & \text{serpentine} & & (161\text{gm}) & & (60\text{gm}) \\ (700\text{gm}, 219\text{cc}) & & (72\text{gm}) & & (552\text{gm}, 220\text{cc}) & & \multicolumn{3}{c}{\text{removed in}} \\ & & & & & & \multicolumn{3}{c}{\text{solution}} \end{array} \qquad (1)$$

This requires that large amounts of both magnesia and silica must be removed in solution from the ultramafic mass. As a consequence of such a reaction, large volumes of water would have to be available to remove both magnesia and silica. Also, according to Turner and Verhoogen (1960), one would expect to observe significant Mg- metasomatism of the adjoining rocks though there is little evidence for such effects (Turner and Verhoogen, 1960; Coleman, 1965).

If volume expansion occurs during serpentinization, then the following reaction can be written (Turner and Verhoogen, 1960):

$$\begin{array}{ccccc} \mathrm{3Mg_2SiO_4} & + & \mathrm{4H_2O + SiO_2} & \rightarrow & \mathrm{2Mg_3Si_2O_5(OH)_4} \\ \text{olivine} & & \text{introduced} & & \text{serpentine} \\ \text{(420gm; 131cc)} & & & & \text{(522gm; 220cc)} \end{array} \qquad (2)$$

where silica is derived from external aqueous solutions. If the silica is derived instead from pyroxene, then the following reaction may occur (Hostetler *et al.*, 1966):

$$\begin{array}{ccccccc} \mathrm{Mg_2SiO_4} & + & \mathrm{MgSiO_3} & + & \mathrm{2H_2O} & \rightarrow & \mathrm{Mg_3Si_2O_5(OH)_4} \\ \text{olivine} & & \text{pyroxene} & & \text{introduced} & & \text{serpentine} \\ \text{(141gm; 44cc)} & & \text{(100gm; 31.5cc)} & & \text{(36gm)} & & \text{(277gm; 110cc)} \end{array} \qquad (3)$$

which also requires a volume expansion. Thayer (1967a) and Turner and Verhoogen (1960) argue that volume expansion is unlikely because of evidence from microscopic fabric and field relations. However, Hostetler *et al.* (1966) feel that many of the microscopic features which argue against volume expansion are ambiguous. In fact they cite field relationships which support such a volume expansion.

More realistic serpentinization reaction equations can be written to describe the paragenesis of most of the serpentinites encountered in this study. It has been generally observed for most serpentinites that much of the magnetite occurs as small veinlets and scattered dust-sized particles associated with late-stage veins. Similar observations were made by Page (1968), who also observed from microprobe studies that late-stage chrysotile veins in general have lower FeO contents (5 wt. %) than do the earlier formed bastite and mesh texture serpentine ($\leqslant$10wt. %).

These observations suggest that much of the early serpentinization can be represented by the reaction

$$\underset{\text{olivine}}{3(Mg_{.90}Fe_{.10})_2SiO_4} + \underset{\text{introduced}}{SiO_2} + 4H_2O = \underset{\text{serpentine}}{2(Mg_{.90}Fe_{.10})_3Si_2O_5(OH)_4} \qquad (4)$$

which is analogous to (2) above. In this case, SiO_2 is introduced into the ultramafic body from the exterior environment. Such a reaction is suggested by the fact that many country rocks undergo SiO_2 loss to serpentine during the formation of rodingite (Coleman, 1967). If silica is supplied to serpentine from pyroxene, as indicated in (3), then the reaction can be given as:

$$\underset{\text{olivine}}{(Mg_{.90}Fe_{.10})_2SiO_4} + \underset{\text{pyroxene}}{(Mg_{.90}Fe_{.10})SiO_3} + 2H_2O =$$

$$\underset{\text{serpentine}}{(Mg_{.90}Fe_{.10})_3Si_2O_5(OH)_4} \qquad (5)$$

For reactions (4) and (5), essentially all iron contained within the olivine and pyroxene is taken up by the serpentine. However, some oxidation of Fe^{+2} in olivine may occur, since Fe^{+3} appears to be present in lizardite (Page, 1968).

During development of late-stage chrysotile veins, a reaction of the type

$$\underset{\text{olivine}}{1.05(Mg_{.9}Fe_{.1})_2SiO_4} + \underset{\text{pyroxene}}{1.05(Mg_{.9}Fe_{.1})SiO_3} + \underset{\text{introduced}}{2.06H_2O} =$$

$$\underset{\text{serpentine}}{(Mg_{.95}Fe_{.05})_3Si_2O_5(OH)_4} + \underset{\text{magnetite}}{0.06Fe_3O_4} + \underset{\text{expelled}}{0.1\ SiO_2 + 0.06H_2} \qquad (6)$$

may occur in which only part of the Fe is incorporated into serpentine, with the excess Fe expelled to form magnetite. Such a reaction of course implies that reacting fluids become reducing, since part of the ferrous iron becomes oxidized. Such a reaction may account for the highly reduced phases associated with some serpentines (Chamberlain _et al_., 1965; Page, 1967; Gresens, 1969).

Although brucite is reported to be commonly associated with many alpine type serpentinites (Hostetler _et al_., 1966), it was not observed in most of the samples investigated in this study. However, variable amounts of magnetite were encountered in essentially all of the serpentinites, suggesting that the above reactions (4), (5) and (6) probably best describe the serpentinization history of most samples encountered in this work.

The various minerals that comprise the serpentine group all have the approximate composition $Mg_3(Si_2O_5)(OH)_4$, with comparatively little substitution of other ions (Deer et al., 1962). Aumento (1970) shows from over 200 serpentine analyses, that the various serpentine polymorphs exhibit only very small chemical differences; they exhibit diffuse compositional fields when plotted on a SiO_2 - MgO - H_2O ternary diagram.

As noted previously, the small differences in MgO content and oxidation state of iron between chrysotile and lizardite, may, however, suggest that these two serpentine minerals are not polymorphs (Page, 1967).

Since magnetite is the only mineral coexisting with serpentine in most samples, the serpentine-magnetite pair represents the only suitable isotopic geothermometer. However, in order to obtain temperatures of serpentinization, we must decide which (if any) of the analyzed samples were formed in equilibrium. A partial test of chemical equilibrium can be made by investigating the chemical homogeneity of the magnetites.

The chemical variations of magnetite in serpentinite have not been investigated to the same extent as those of serpentine. However, it has been noted that magnetite occurs within serpentinites both in a very fine-grained, disseminated form and as veins associated with late-stage serpentinization. In particular, magnetite commonly occurs in antigorites in a disseminated and scattered aggregrate form (e.g. the Roxbury serpentinites, Jahns, 1967) and as veins in lizardite-chrysotile type serpentinites (e.g. the Tiburon body, Page, 1968). Several other studies related to the chemical variations in magnetite from serpentinites involve discussions of the alteration of chromites.

Lapham (1964) examined the chemical composition of spinels in the Mayaguez Bore hole serpentinites by electron microprobe analyses. He observed zoning in the spinel grains from the peridotite (augite harzburgite) portion of the body. The dunites contain unzoned chromite, whereas the spinels from the peridotite exhibit a core of Mg-Al spinel with an inner shell of Fe(-Cr?) sulfide, and an outer rim of magnetite. It is suggested that the chromite and Mg-Al spinel resulted from primary crystallization of the ultramafic rock, followed by formation of the two marginal zones in the Mg-Al spinel at lower temperatures synchronous with serpentinization.

Thayer (1956), in a review article on the mineralogy of chromite, discusses many observations in which translucent chromites are rimmed by opaque material. This opaque outer rim is regarded as an Fe-rich chromite or magnetite which formed by alteration of the translucent chromite. Thayer (1956) associates this zoning of translucent chromite with hydrothermal activity subsequent to formation of the primary ultramafic rock.

From a study of opaque minerals in a serpentinite body of Archean Age at Puddy Lake, Ontario, Simpson and Chamberlain (1967) observed by electron microprobe analyses that the chromites exhibited a chromium magnetite rim that was thought to have formed in a lower temperature environment, perhaps during serpentinization. Three forms of magnetite were observed within the serpentinites, euhedral crystals, stringers associated with the serpentine, and veins up to several inches thick associated with later granitic intrusions. The euhedral crystals were commonly zoned and are thought to be similar in composition to the chromium magnetite rims of the chromite crystals. The magnetite stringers associated with the serpentine had the highest Fe content of all the magnetites, with no noticeable Cr content and a small quantity of Ni (< 1.2 %). The magnetite veins showed enrichment of Ni.

Simpson and Chamberlain (1967) suggest that the euhedral magnetites were once primary chromite crystals that have been completely altered during serpentinization in a manner similar to the partial alteration of larger zoned chromite crystals. They further suggest that the granitic intrusion was later than serpentinization with the coarse magnetite veins formed by remobilization of the magnetite stringers generated during serpentinization.

4.3 Previous estimates of temperatures of serpentinization

The experimental work of Bowen and Tuttle (1949) established the upper stability limits of chrysotile serpentine in the presence of brucite at about 400°C at P_{H_2O} = 1Kb according to the reaction

$$\underset{\text{chrysotile}}{Mg_3Si_2O_5(OH)_4} + \underset{\text{brucite}}{Mg(OH)_2} = \underset{\text{forsterite}}{2Mg_2SiO_4} + \underset{\text{water}}{3H_2O} \qquad (7)$$

In the absence of brucite, Scarfe and Wyllie (1967) were able to bracket the uppermost stability limit of serpentine at 430°C at 1Kb and 470°C at 3Kb according to the reaction

$$\underset{\text{chrysotile}}{Mg_3Si_2O_5(OH)_4} = \underset{\text{talc}}{Mg_3Si_4O_{10}(OH)_2} + \underset{\text{forsterite}}{6Mg_2SiO_4} + \underset{\text{water}}{9H_2O} \qquad (8)$$

Hostetler et al. (1966) estimate that the stability limit of Mg-rich olivine (Fo_{90}) is about 400°C at P_{H_2O} = 1Kb according to the reaction:

olivine (Fo_{90}) + H_2O + O_2 → clinochrysotile + brucite + magnetite

They furthermore point out that the common presence of brucite in alpine serpentinites suggests that much serpentinization may occur under the pressure-temperature conditions implied by the above reaction.

From the study of rodingites that lie between serpentinites and adjacent country rock, Coleman (1967) concludes that some serpentinization may have taken place at temperatures as low as 240°C and at pressures of approximately 4Kb or higher.

Other estimates of temperatures of serpentinization were made by Aumento (1970), based on cell parameters of serpentine and variations in brucite content in the serpentinite. His estimates, based largely on the conclusions of Hostetler et al. (1966), range from 485°C to 400°C or less.

Many authors have, in general, considered serpentinization to be "hydrothermal" (see Faust and Fahey, 1962, for example), though the specific conditions are generally not described except for the uppermost stability conditions imposed by the experimental work. The experimental work of Bowen and Tuttle (1949) has shown that hydrous magnesian silicate melts can exist only at temperatures above 1000°C; hence there is no likelihood of a "serpentine magma" or a system in which olivine and serpentine are in equilibrium with a hydrous silicate melt, as originally proposed by Hess (1938).

Recently Barnes (1967) proposed that some serpentinization may, in fact, be occurring today in a near-surface environment in some of the West Coast ultramafic bodies. Barnes' evidence for serpentinization is the presence of high-pH calcium hydroxide water issuing from a linear array of springs located along the bottoms of deep canyons that cut fresh or partially serpentinized peridotite bodies. In general, the chemical composition of the water is throught to be due to the selective removal of Ca, largely from pyroxene, during the serpentinization process.

In a more recent paper, Barnes and O'Neil (1969) state that free energy potentials for all these Ca^{+2} - OH^{-1} type spring waters are such that forsterite will dissolve and yield Mg-serpentine and $Mg(OH)_2$. Hydrogen and oxygen isotopic analysis of the Ca^{+2} - OH^{-1} waters, however, indicate normal meteoric water that has suffered no 0^{18} exchange.

Such evidence is consistent only with a very low-temperature reaction. Barnes and O'Neil (1969) also conclude that because of the isotopic composition of the Ca^{+2} - OH^{-1} waters, the volume of such waters must be very large relative to the phases with which it reacted. This "swamping-out" effect could be due to two end-member possibilities: (1) a very small amount of the serpentine in the ultramafics is being formed by this low-temperature process, or (2) a large fraction of the serpentine is being formed in this manner, but at a rate which is very slow compared to the flow of water through the rock.

4.4 Oxygen isotope data on coexisting serpentine and magnetite

The $0^{18}/0^{16}$ fractionations for coexisting serpentine and magnetite from some of the serpentinite bodies examined in this work are given in figure 4-1. The various samples are divided into three classifications, "normal" lizardite-chrysotile, "anomalous" lizardite-chrysotile, and antigorite. These categories are defined on the basis of mineralogic and chemical data, but, as will be shown below, they may also be delineated by means of the isotope data.

Electron microprobe studies were made on several samples in order to better understand the chemical homogeneity and genesis of some of the opaque phases (Table 4-1). The various modes of occurrence of magnetite, along with a visual estimate of the total amount of magnetite in each sample, are also presented in Table 4-1. These estimates were made from petrographic examination of thin sections and polished thin sections.

The microprobe examinations involve an estimate of the $Cr_2 0_3$ content of the various magnetite grains in each magnetic separate, along with a rough estimate of the abundance of chromite grains. For example, in sample 1 from the Tiburon area, where $\delta 0^{18}$ is $-6.1^{o}/oo$, the magnetite concentrate consists of approximately 99% of a low $Cr_2 0_3$(0-0.5 wt. %) magnetite and about 1% of a high $Cr_2 0_3$ (5-10 wt. %) magnetite in addition to about 10% chromite (see Table 4-1). Some of the magnetite in this sample also contains trace amounts of Mn.

The grain mount studies of the magnetite concentrates whose $\delta 0^{18}$ values are given in figure 4-1 are important in understanding how much of the magnetite was formed during serpentinization. They also provide

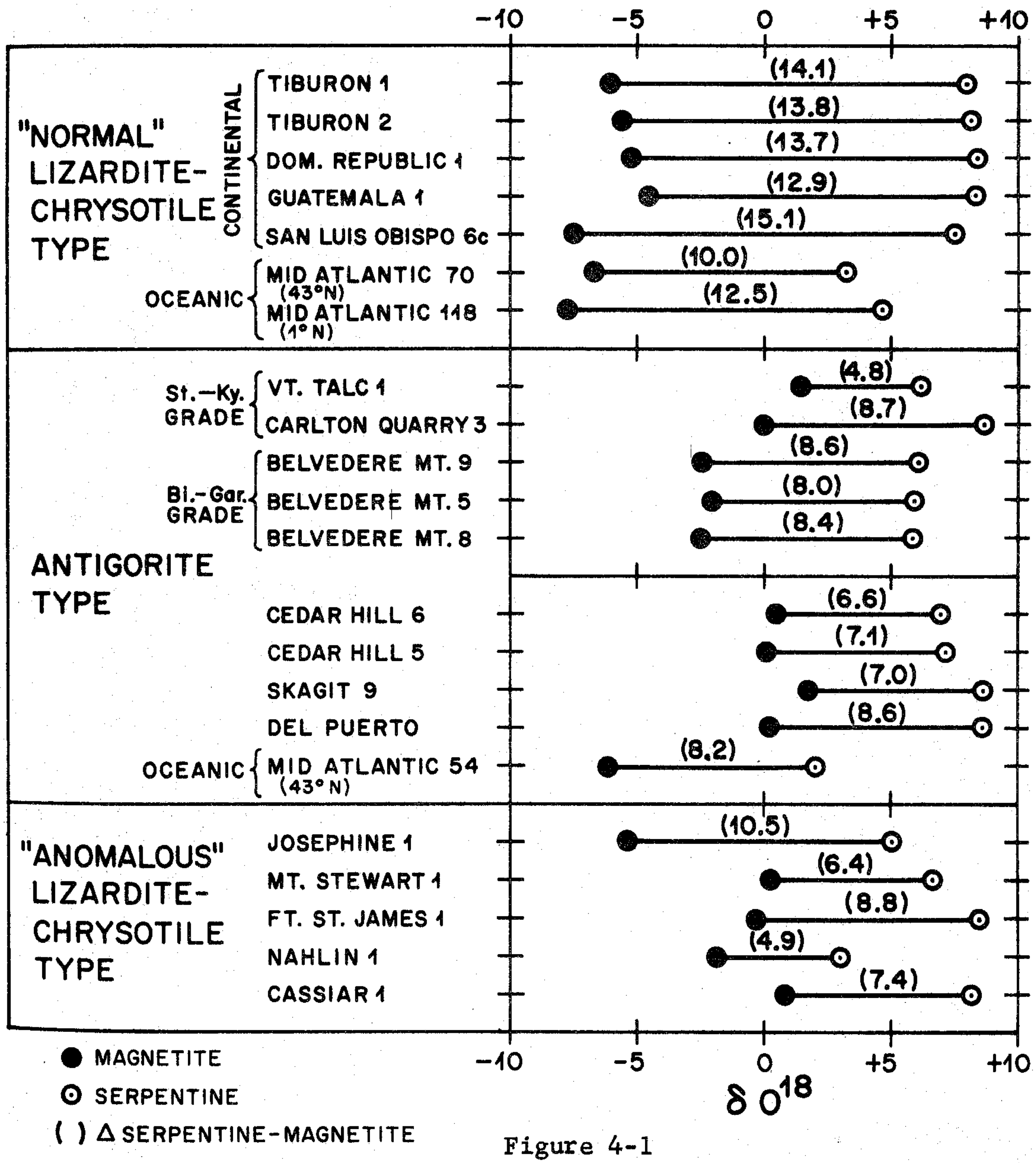

Figure 4-1

Plot of measured δO^{18} values of coexisting serpentine and magnetite for different types of serpentines from a wide variety of localities. The numbers in parentheses represent Δ serpentine-magnetite values. The magnetites of the "anomalous" lizardite-chrysotile type have widely varying chemical compositions, suggesting a lack of chemical equilibrium between serpentine and magnetite. The other serpentine types contain chemically homogeneous magnetites that are essentially stoichiometric Fe_3O_4.

Table 4-1

Summary of petrographic and microprobe observations of magnetite in serpentinites for samples given in figure 4-1.

Sample	petrographic thin-section studies							microprobe studies of grain mounts							microprobe studies of polished thin-sections	
	volume percent magnetite[1]	magnetite mode of occurrence[2]						chromite content (%)[3]	volume % magnetite having particular Cr_2O_3 contents[4]						trace elements present[5]	EBS Studies[6]
		euhedral grains	clots	veinlets	disseminated veinlets	disseminated dust	rims on chromite		0 - 0.5%	0.5 - 1.0%	1.0 - 5.0%	5.0 - 10.0%	10.0 - 15.0%	>15%		
Tiburon 1	-			NE				<10	99			1			Mn	NE
Tiburon 2	1	M			M	m		<10	98						Mn	NE
Dominican Republic 1	1			m	M		M	0	98						Mn, Cu	see plates 4-1 and 4-2
Guatemala 1	< 1	m	M	M				15	90		5	5			NE	NE
San Luis Obispo 6c	< 1				X		m	NE				NE			NE	NE
Mid-Atlantic (1^oN) 118	2		M	m	M	o		0	99						NE	NE
Mid-Atlantic (43^oN) 70	3			m	X	m		< 5	99						Mn	NE
Belvedere Mt. 9	5	M			m			0	95		5				NE	NE
Belvedere Mt. 5 (magnetite vein)	-	X						0				NE			NE	NE
Belvedere Mt. 8 (magnetite vein)	-	X						0				NE			NE	NE

TABLE 4-1 (continued)

Sample	petrographic thin section studies							microprobe studies of grain mounts							microprobe studies of polished thin-sections	
	volume percent magnetite	magnetite mode of occurrence[2]						chromite content (%)[3]	volume % magnetite having particular Cr_2O_3 contents[4]						trace elements present[5]	EBS Studies[6]
		euhedral grains	clots	veinlets	disseminated veinlets	disseminated dust	rims on chromite		0 - 0.5%	0.5 - 1.0%	1.0 - 5.0%	5.0 - 10.0%	10.0 - 15.0%	>15%		
Cedar Hill 5	< 5	M	M			m		NE		NE					NE	NE
Cedar Hill 6	2	M		m	M			<< 5	99						Ni, Mn	see plates 4-7 and 4-8
Skagit 9	1		X		m			< 5	95	5					NE	NE
Del Puerto 2a	< 1	M	M			m		< 5	99			1			Mn	NE
Vt. Talc 1	10		X			m		NE			NE				Mn	NE
Carlton Quarry 3	2	M	M			m		NE			NE				NE	NE
Mid-Atlantic (43^oN) 54	3		X			m		NE			NE				NE	NE
Fort St. James 1	2		X	m	m			0	15				40	45	Mn,Ni, Co,V,Ti	see footnote 7
Nahlin 1	5		X			m		0	5		95				Ni	see plates 4-3, 4-4, and 4-5
Cassiar 1	2		X	m	m			0	2					98		see footnote 7
Josephine Co. 1	3				M	M	m	10	90					10		see footnote 8
Mt. Stewart 1	2								80			20		1		

TABLE 4-1 (continued)

footnotes

1 Estimates of the total amount of magnetite in each serpentinite sample were made from visual observations of thin-sections.

2 Classification as to various magnetite modes of occurrence within each serpentinite sample is based on thin- and polished-section examination. X = >80%; M = 40 - 50%; m = <20%; **o** = trace

3 Estimates of the approximate volume percent chromite in each of the grain mounts examined.

4 A rough estimate is given of the volume percent magnetite in each grain mount, subdivided into fractions having various Cr_2O_3 contents. Such grain mounts represent a portion of the magnetite concentrate whose δO^{18} value is given in figure 4-1. For samples not totaling to 100%, a very small portion of the magnetite contains a high but undetermined Cr_2O_3 content.

5 Trace elements present in some of the magnetite grains in polished thin-sections were noted from wave length scans.

6 EBS examinations of magnetite in polished thin sections are also discussed in the text.

7 Pure Fe_3O_4 occurs as very fine grains; high Cr-magnetite is present as larger grains and clots.

8 Pure Fe_3O_4 occurs as disseminated grains; high Cr-magnetite occurs as rims around chromite.

NE Not examined.

supporting data as to whether or not it is reasonable that the measured serpentine-magnetite fractionations represent isotopic equilibrium.

"Normal" lizardite-chrysotile serpentinites

The serpentinites of this classification are those samples in which essentially all of the magnetite is pure Fe_3O_4, with only trace amounts of other elements. As an example, let us examine in some detail a sample of lizardite-chrysotile type serpentinite from the Dominican Republic (sample 1). The magnetite in this rock exhibits only trace amounts of chemical impurities, principally Mn, in small isolated concentrations within the magnetite. The two principal modes of occurrence of this magnetite are shown in plate 4-1. A chromite is shown in plate 4-2; it contains appreciable quantities of Al and Mg (as ascertained from EBS photographs), and it shows some Fe concentration and Al depletion along its extreme outer edges. The Al also appears to be enriched in the adjacent serpentine along one of the edges, suggesting that Al migrated away from the chromite into the adjacent serpentine, perhaps at the time of serpentinization. Other chrysotile-lizardite samples in Table 4-1 show similar relationships to those described above for sample 1 from the Dominican Republic. It thus appears that essentially pure Fe magnetite is generated during lizardite-chrysotile type serpentinization of ultramafic rocks. Such magnetite occurs in veins and as small disseminated grains dispersed throughout the serpentinite.

The actual δO^{18} values for the magnetites given in figure 4-1 are probably somewhat lighter than the measured analyses because of small

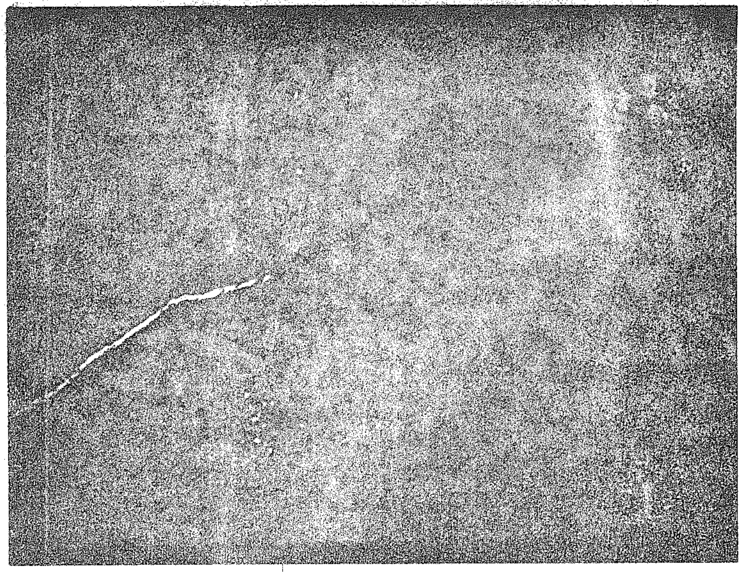

Plate 4-1

(Reflected light, 0.37 x 0.57mm)

Sample 1, Dominican Republic. The bright reflecting material is magnetite, which occurs as veins and as scattered aggregrates of irregular shape. Electron microprobe analysis indicates that it is essentially pure Fe_3O_4 (see Table 4-1). The serpentine of this sample has δO^{18} = + 8.4°/oo, and the coexisting magnetite has δO^{18} = -5.3°/oo.

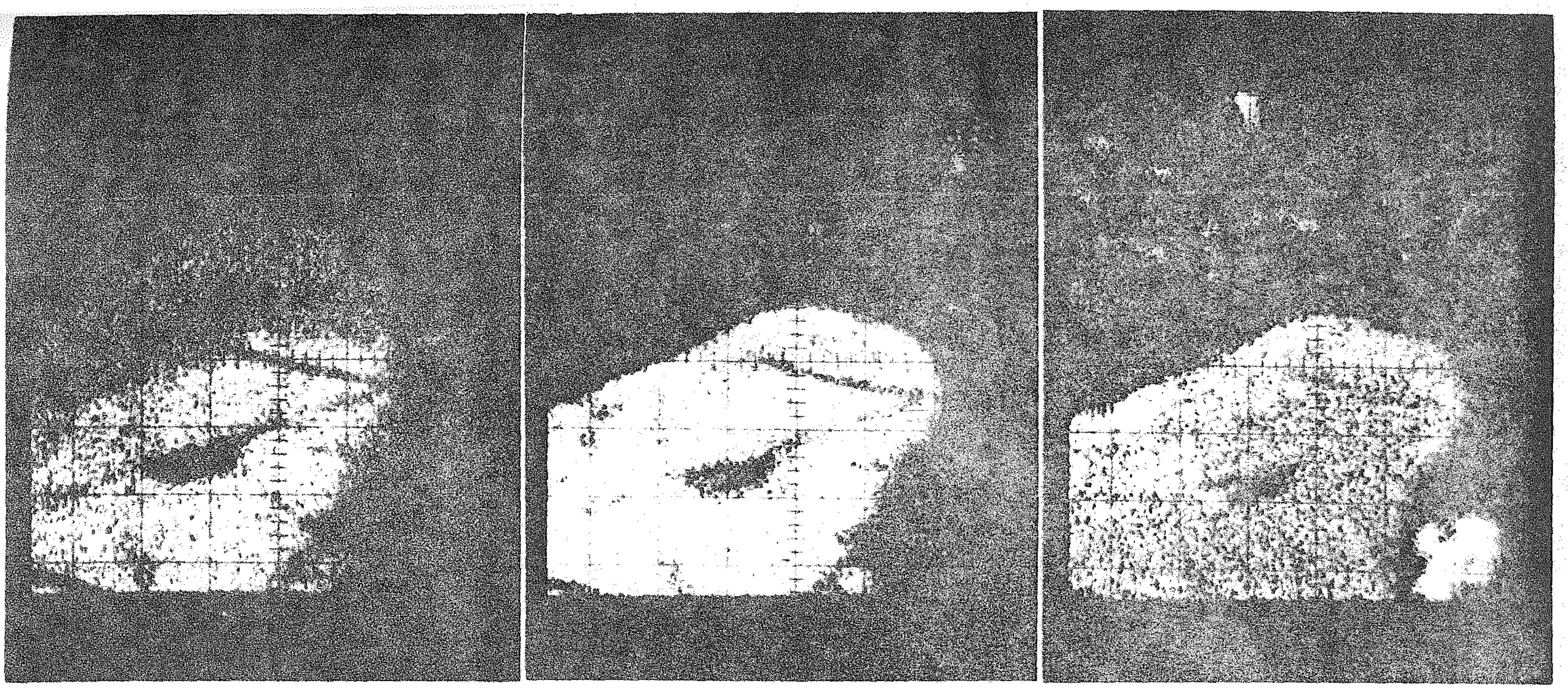

(a) Al (b) Fe (c) Cr

Plate 4-2

Sample 1, Dominican Republic. EBS photographs of chromite grain ($175\mu^2$). Note that in (a) the Al shows depletion along the outer edges (as ascertained by grain edge in (b), (c)) and enrichment in the adjacent serpentine. In (b) there is a suggestion of Fe concentration along the outer edge; note the scattered grains of Fe_3O_4 in proximity to the chromite [e.g., lower right corner of (b)]. The finely disseminated bright spots in (b) outside of the chromite grain are presumed to be due to small amounts of Fe in the serpentine.

amounts of chromite contamination (see Table 4-1). Chromite is relict from the primary ultramafic assemblage, and therefore probably has a δO^{18} of about +3 to +4°/₀₀ (Taylor, 1968). This, however, is a minor effect which would cause at most a 0.3 to 0.4 per mil decrease in the δO^{18} value given in figure 4-1.

Several arguments can be made that the magnetite in these lizardite-chrysotile samples formed essentially in equilibrium: (1) Chemical equilibrium is suggested by the purity and homogeneity of the magnetite grains. (2) Isotopic equilibrium is suggested by the similarity of the O^{18}/O^{16} fractionations exhibited by two different serpentine-magnetite pairs from the Tiburon area, as well as by the general consistency of the O^{18}/O^{16} fractionations exhibited by all the other samples. (3) Low temperatures of equilibration are suggested by the lack of solid solution in the magnetites and by the very large O^{18}/O^{16} fractionations of 12.9 to 15.1 per mil measured for the serpentine-magnetite pairs. Such Δ-values are exceedingly large relative to those observed for analogous mineral pairs in all igneous and metamorphic rocks; this indicates that serpentinization of this type must occur at temperatures significantly lower than those involved in even the lowest grades of regional metamorphism. Such low temperatures are consistent with a hypothesis which will be advanced later, that meteoric ground waters are heavily involved in chrysotile-lizardite serpentinization. Furthermore, the uniformity of the Δ-values suggests that serpentinization of this type occurs over a fairly limited temperature range. The O^{18}/O^{16} fractionations shown in figure 4-1 further suggest that oceanic lizardite-chrysotile serpentines may form at higher temperatures than those of continental origin; the former have Δ values that are 0.4 to 5.1 per mil smaller than the continental lizardite-chrysotiles.

"Anomalous" lizardite-chrysotile serpentinites

The serpentinites of this classification contain magnetites that have varying amounts of Cr_2O_3 in solid solution. The polished grain mounts generally contain a large proportion of high chromian magnetite (see Table 4-1).

For example, in sample #1 from the Fort St. James area of British Columbia, the magnetite exhibits extreme heterogeneity in Cr_2O_3. About 10 to 20% of the magnetite sample is very pure Fe_3O_4 (0 - 0.5 wt. % Cr_2O_3); about 40% of the magnetite contains a moderate amount of Cr_2O_3 (10 - 15 wt. %); and some 40 to 50% of the magnetite has a very high Cr_2O_3 content (> 15 wt. %). In contrast, the magnetite of sample #1 from Cassiar, British Columbia consists of 98% chromian magnetite (> 15% Cr_2O_3) and only 2% of essentially pure Fe_3O_4.

The opaque phases of one sample (sample #1) from the Nahlin Body in British Columbia were studied in polished thin section by microprobe analyses in order to determine grain homogeneity. The principal modes of occurrence of various opaque phases in sample #1 from the Nahlin, British Columbia body are shown in plate 4-3. In plate 4-4, the Fe and Cr distribution of a large grain of chromian magnetite from this sample is observed to be relatively homogeneous. This grain is typical of the other chromian magnetite grains in this sample. Note that small, essentially pure Fe_3O_4 grains occur in proximity to the chromian magnetite mass shown in plate 4-4.

In plate 4-5, the edge of the chromian magnetite grain shown in plate 4-4 is examined at greater resolution. The marginal zone of the grain is composed of pure Fe_3O_4. This feature was observed in all samples

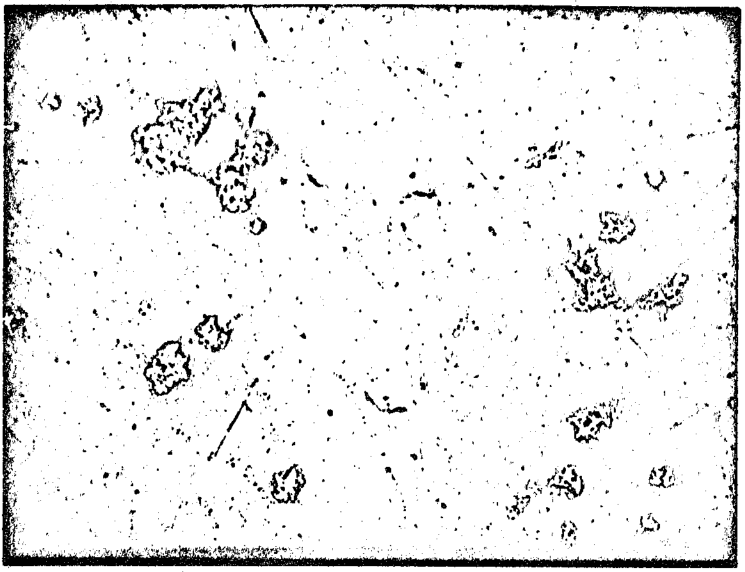

Plate 4-3

(Reflected light, 0.37 x 0.57mm)

Sample 1, Nahlin, British Columbia. The chromian magnetite (~ 5% Cr_2O_3) occurs as large, irregularly shaped masses. Smaller grains of disseminated magnetite are essentially pure Fe_3O_4. The very bright white masses are millerite (NiS). The serpentine has δO^{18} = + 3.0°/oo, and the total magnetite has δO^{18} = -1.9°/oo. The fine-grained magnetite (pure Fe_3O_4), if separated, would probably have a much lighter δO^{18}-value.

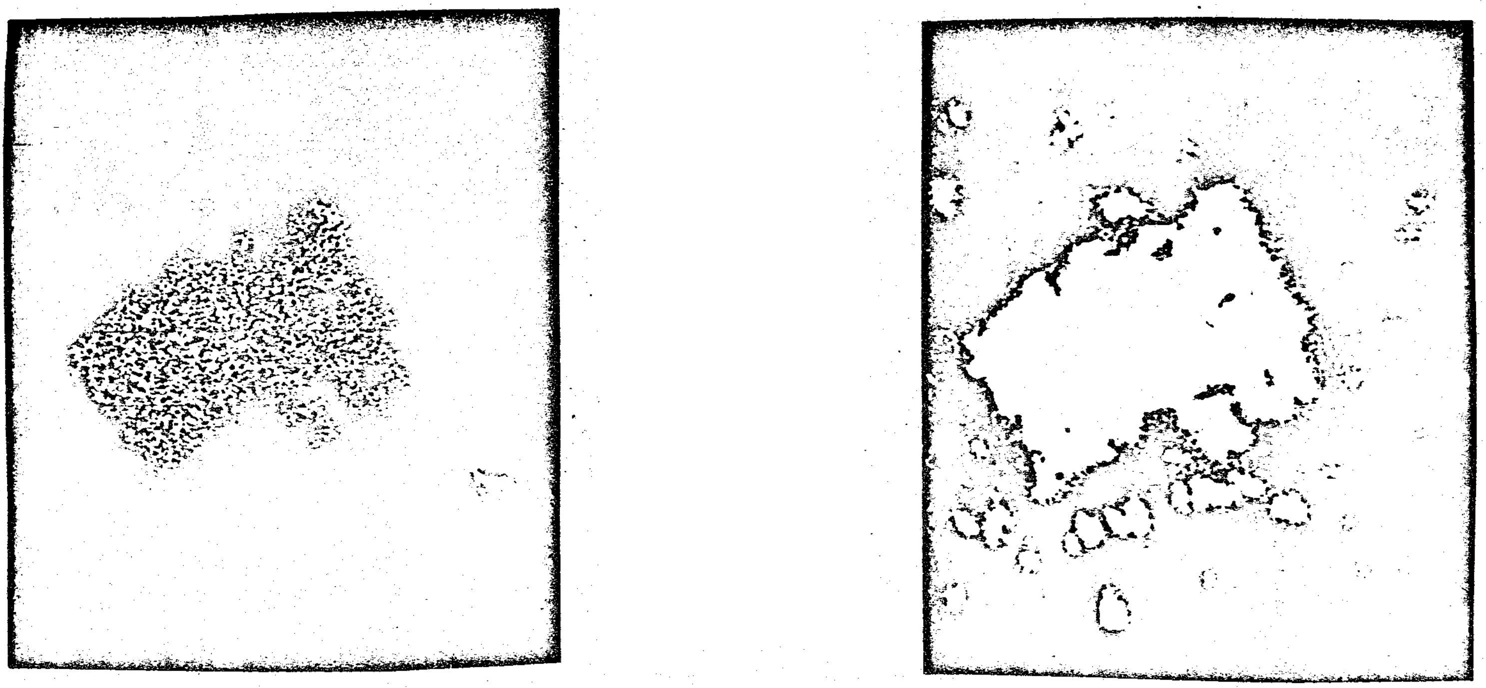
(a) Cr

(b) Fe

Plate 4-4

Sample 1, Nahlin, British Columbia ($350\mu^2$). Electron beam scanning pictures of a chromian magnetite sample shows the Cr distribution in (a) and Fe content in (b). Note in particular the relatively pure Fe_3O_4 grains scattered around the main chromian magnetite grain. The Cr_2O_3 content within the chromian magnetite grain averages 4.9 ± 0.3% as determined from seven point analyses in a scan across the grain. Point analyses of several small relatively pure Fe_3O_4 grains above the large chromian magnetite grain indicate 0.1% Cr_2O_3 in the magnetite.

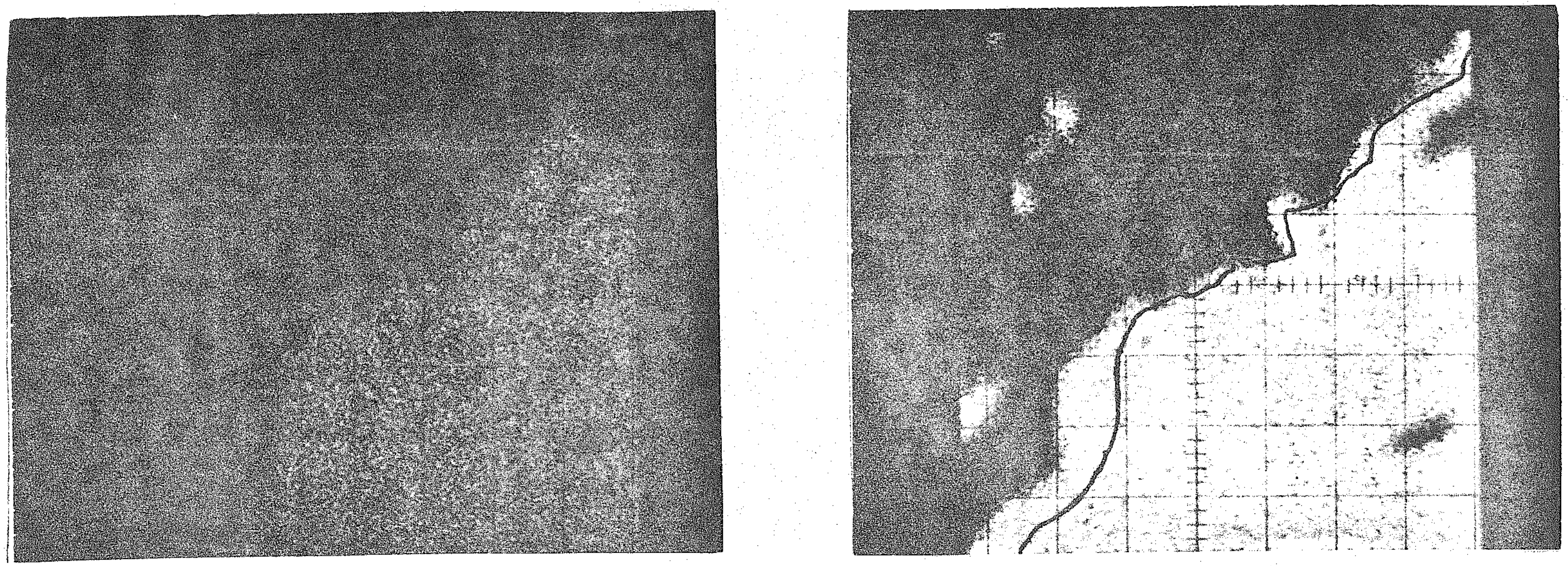

(a) Cr

(b) Fe

Plate 4-5

Sample 1, Nahlin, British Columbia. EBS photograph of a portion of a chromian magnetite grain shown in plate 4-4 ($85\mu^2$). Note in particular the zone of pure Fe_3O_4 which occurs along the outer margin of the chromian magnetite in (b) (indicated by the black line in b).

that contain abundant chromian magnetite (e.g., sample #1 from both the Cassiar body and the Fort St. James area). This strongly suggests that the serpentinization process itself, which is known to commonly generate almost pure Fe_3O_4, also produced these marginal zones. The development of the chromian magnetite therefore must have preceeded the chrysotile lizardite serpentinization episode. This is in disagreement with the conclusions of Simpson and Chamberlain (1967). It is possible that the chromian magnetite formed during a deuteric or higher-temperature hydrothermal event (perhaps accompanying the intrusion of nearby granitic rocks?). The geometric relationships suggest that chrysotile-lizardite serpentinization, perhaps accompanied by recrystallization of pre-existing serpentine, occurred after the postulated hydrothermal event.

All of the serpentinites which contain chromian magnetite lie in close proximity to granitic intrusions, as will be discussed more fully in a later chapter. The O^{18}/O^{16} fractionations for serpentine-magnetite pairs from all these samples are given in the lower portion of figure 4-1. No chromite was observed in three of these samples (sample 1, Fort St. James area, sample 1, Nahlin Body, and sample 1, Cassiar area).

Two of the samples (Josephine Co., Oregon, sample 1; and Mt. Stewart, Washington, sample 1) contain relict chromite and only small amounts of chromian magnetite. The magnetite associated with the veins is essentially pure Fe_3O_4, whereas some of the small grains found in near proximity to chromite are chromian magnetite. EBS photographs of chromite in one of the samples reveals Fe-enrichment and Mg-depletion along outer margins (plate 4-6); no appreciable Al was observed in this

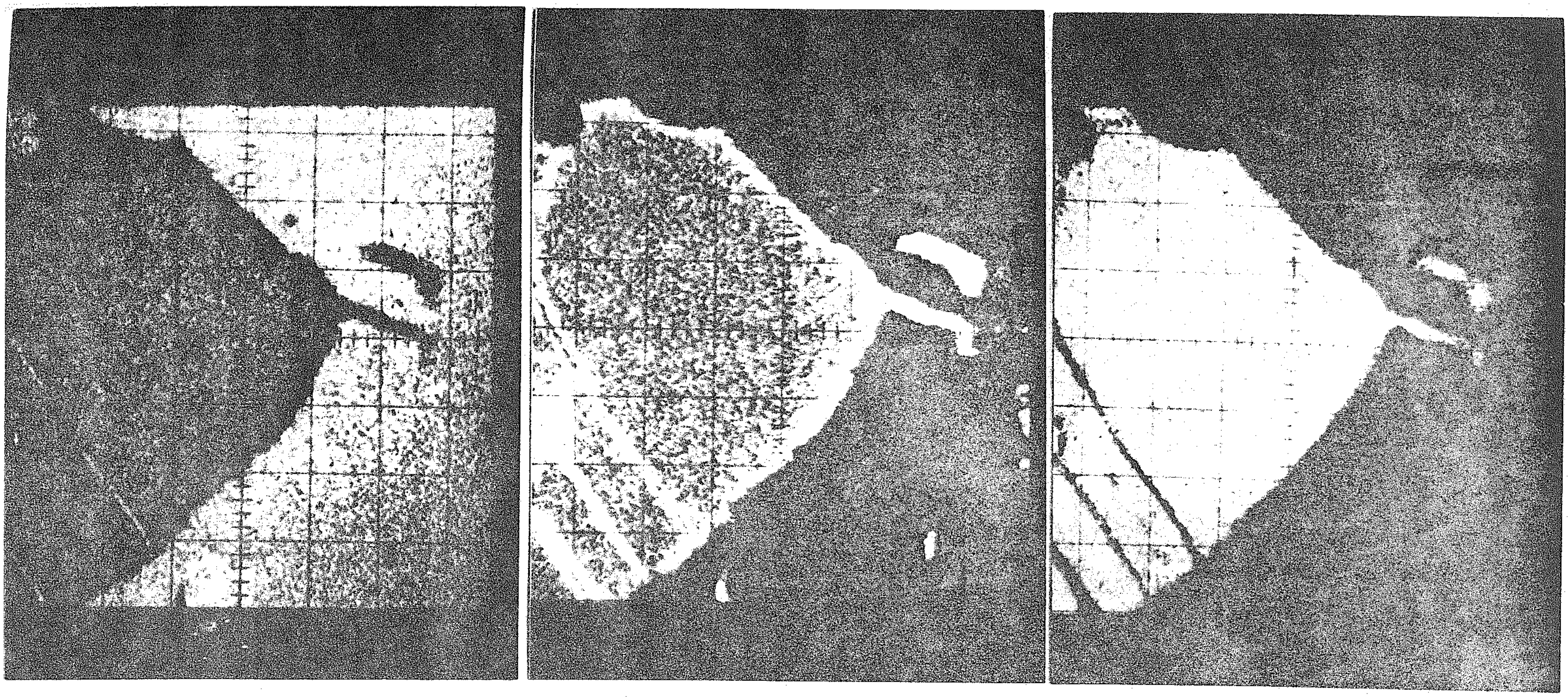

(a) Mg (b) Fe (c) Cr

Plate 4-6

Sample 1, Mt. Stewart, Washington. EBS photograph of chromite grain ($350\mu^2$). Note the Mg-depletion in (a) and Fe-enrichment in (b) along the outer edges and in fracture zones of the chromite grain. The high concentration of Mg is from adjacent serpentine. Also note the small chromian magnetite grain to the right of the chromite. Several grains out in the serpentine are essentially pure Fe_3O_4, (b) and (c). No appreciable Al was detected within the chromite grain.

chromite. EBS photographs of chromite edges at greater resolution ($85\mu^2$) reveal no development of pure Fe_3O_4 along the outer edge of the grain.

If the pure Fe-magnetite could somehow be separated from the above rocks, we might find similar relationships to those found for "normal" lizardite-chrysotile serpentinite. However, this was not possible, and these analyzed magnetites therefore represent mixtures of at least two types of magnetite. Sample 1 from Josephine Co., Oregon contains the largest amount of relatively pure Fe-magnetite (see Table 4-1) and hence should represent the closest approach to isotopic equilibrium of any of the samples containing Cr-magnetite in the lower portion of figure 4-1. It does, in fact, exhibit the largest Δ-value (10.5) among this set of samples, a value not too different from the 12.9 to 15.1 per mil range observed in "normal" lizardite-chrysotile serpentinites.

The wide δO^{18} variations of the magnetites shown on the lower portion of figure 4-1 are explicable if we assume that they contain varying amounts of a chromian magnetite that has a distinctly heavier δO^{18} than the pure Fe-magnetite derived from serpentinization. The δO^{18} of this chromian magnetite is probably at least as high as the $+0.8^{\circ}/_{oo}$ value observed in sample 1 from the Cassiar area, because this particular magnetite concentrate was almost entirely composed of chromian magnetite (see Table 4-1). Thus the isotopic data provide supporting evidence that these chromian magnetites may have formed at temperatures considerably higher than those at which serpentinization occurred. The value of +0.8 is similar to the δ-values observed in fine-grained, disseminated magnetites in the ultramafic complexes of southeastern Alaska. Taylor and Noble (1969) suggested that the latter magnetites attained their δ-values during a deuteric stage of recrystallization, changing from an original magmatic δO^{18} of about +3 to +4°/oo to a value of about +0.6°/oo.

Antigorites

Electron microprobe examination of many magnetites whose δO^{18} values are given in the middle portion of figure 4-1 reveals that the magnetite fraction is quite homogeneous and is composed of relatively pure Fe-magnetite (Table 4-1). All of the magnetite samples from antigorite serpentinites contain at least 95% of a chemically homogeneous magnetite whose Cr_2O_3 content is less than 0.5 wt. %. This suggests that nearly all of the magnetite was formed during the serpentinization reaction, and that there is a good chance that this magnetite formed in isotopic equilibrium with its coexisting antigorite. This magnetite is chemically very similar to the pure Fe-magnetite observed in the "normal" chrysotile-lizardite serpentinites.

In sample 6 from the Cedar Hill Quarry, Pennsylvania (plate 4-7), clots and anhedral masses of magnetite show only slight zonation and isolated concentrations of trace quantities of Cr. A chromite grain from the same polished thin section (see plate 4-8) reveals a distinct and pronounced Fe-rich margin with accompanying Cr depletion; Al and Mg are also clearly depleted in this marginal zone, with concentrations similar to those in an adjacent magnetite grain. Furthermore the EBS photographs in plate 4-8 clearly show that a Fe-rich zone has developed along the outer margins of the chromite, perhaps during serpentinization.

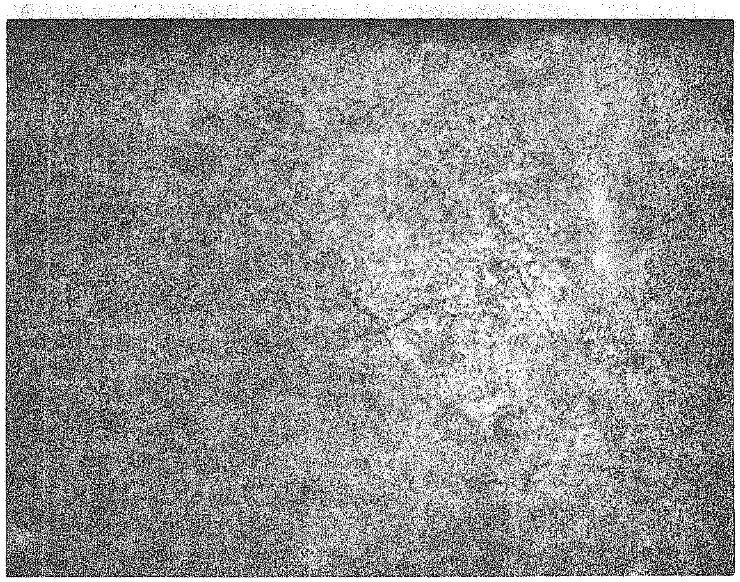

Plate 4-7

(Reflected light, 0.37 x 0.57 mm)

Sample 6, Cedar Hill Quarry, Pennsylvania. The bright reflecting material is magnetite. It is essentially pure Fe_3O_4, and occurs principally as irregularly-shaped masses. The serpentine of this sample has $\delta O^{18} = +7.0^{\circ}/_{oo}$, with the coexisting magnetite $\delta O^{18} = +0.4^{\circ}/_{oo}$.

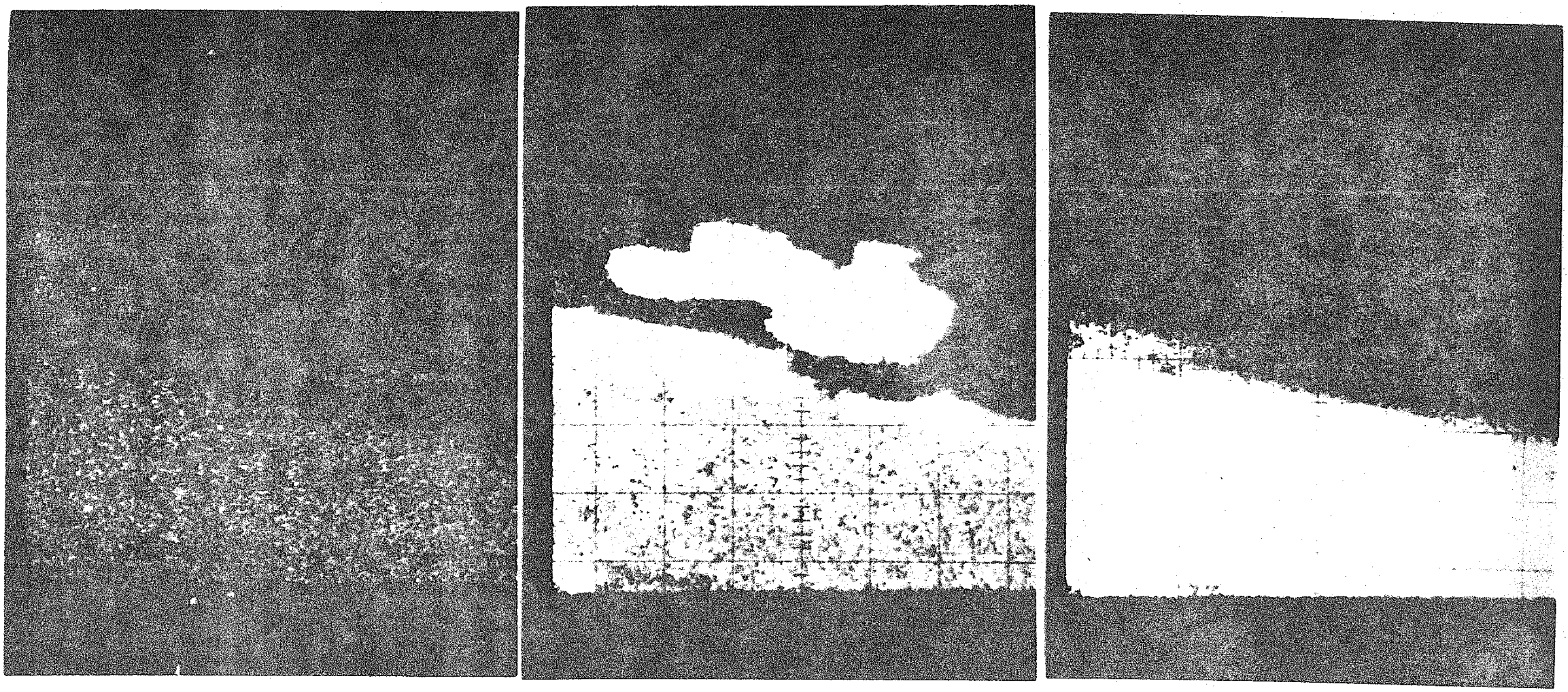

(a) Al (b) Fe (c) Cr

Plate 4-8

Sample 6, Cedar Hill Quarry, Pennsylvania. EBS photographs of a chromite grain ($175\mu^2$). Note the distinct Fe marginal zonation of the chromite in (b) and the corresponding Cr depletion in (c). An adjacent magnetite grain in (b) shows no appreciable Cr content. Al shows a distinct depletion in the Fe rich zone in (a), with accompanying migration into adjacent serpentine.

The general chemical homogeneity and purity of the magnetite samples, in combination with the general isotopic uniformity of the Δ-values (6.6 to 8.7 for nine antigorite samples, with one sample having a value of 4.8) indicate that the O^{18}/O^{16} fractionations given in the middle portion of figure 4-1 probably represent a close approach to isotopic equilibrium. Such equilibrium is further suggested by the similarity of O^{18}/O^{16} fractionations in two different samples from the same body, namely the Cedar Hill, Pennsylvania serpentinite ($\Delta = 6.6$ and 7.1).

There is also a general tendency for the O^{18}/O^{16} fractionations to decrease with increasing metamorphic grade, as would be expected if isotopic equilibrium prevailed.

Sample 1 from the Vermont Talc Quarry, in a staurolite-kyanite grade metamorphic terrane, shows the smallest serpentine-magnetite Δ-value (4.8), whereas the three samples from the Belvedere Mountain Quarry (also in Vermont), which lies in a biotite-garnet grade terrane, have larger Δ-values (8.0, 8.4, 8.6); these data are consistent with a lower temperature of serpentinization than for the staurolite-kyanite zone sample.

However, this picture is not perfectly straightforward, because sample 3 from the Carlton Quarry, Vermont has a Δ-value of 8.7, not consistent with its staurolite-kyanite grade occurrence. Such a relatively large Δ-value could be due to (1) retrogradation of the serpentine and/or the magnetite, or (2) insulation of the phases from the metamorphism which affected the general terrane. The second possibility appears unlikely because of the high H_2O content of the serpentine as well as the general "wetness" of the regional metamorphic environment (see Taylor et al., 1963; Garlick and Epstein, 1967), which would probably readily allow recrystallization of both minerals.

Two coarse-grained magnetite samples (#5 and #8) from the Belvedere Mountain Quarry, Vermont, which occur as massive (≈ 1/8 inch thick) veins in the antigorite, have δO^{18} values very similar to the fine-grained and disseminated magnetite in the nearby antigorite (sample 9). This suggests that both forms of magnetite may have equilibrated at similar temperatures.

The other antigorite samples studied all exhibit Δ-values similar to the Vermont samples from biotite-garnet grade zones, suggesting similar temperatures of isotopic equilibration.

The magnetite δO^{18} values from antigorites are therefore completely distinct (except for the one oceanic sample) from those of the "normal" lizardite-chrysotile serpentinites; they range from $\delta O^{18} = +1.7^{\circ}/_{oo}$ to $-2.6^{\circ}/_{oo}$ (the one oceanic antigorite sample has $\delta O^{18} = -6.2^{\circ}/_{oo}$). In contrast, δO^{18} magnetite from equilibrium lizardite-chrysotile type serpentines ranges from $-4.6^{\circ}/_{oo}$ to $-7.9^{\circ}/_{oo}$. Furthermore, antigorites exhibit Δ-values ranging from 8.7 to 4.8, whereas the equilibrium lizardite-chrysotile serpentinites have Δ-values in the range 10.0 to 15.1. It is therefore practically an absolute certainty that these antigorites formed at distinctly higher temperatures than the "normal" lizardite and chrysotile serpentinites.

Summary of conclusions

(1) Based on the microprobe data of the various samples listed in Table 4-1, it would appear that essentially pure Fe magnetite is generated during serpentinization of ultramafic rocks. Such magnetite occurs both in veins and as small disseminated grains.

(2) In "normal" lizardite-chrysotile type serpentines, chromite shows some depletion of Al and slight enrichment of Fe along its outer margins, possibly as a consequence of low temperature serpentinization.

(3) In antigorite-type serpentines, chromite grains show considerable Fe-enrichment and Al-depletion along their outer margins. These phenomena may be a consequence of a higher temperature serpentinization than that of (2).

(4) In lizardite-chrysotile type serpentinites located in close proximity to later granitic intrusions, chromite grains commonly have lost all Al and they show extensive Fe-enrichment and Mg-depletion along their outer margins. Almost all primary chromites from ultramafic rocks reported in the literature contain appreciable amounts of Al (see Thayer, 1956).

(5) Perhaps as a result of still higher temperatures, some chromites from ultramafic rocks in close proximity to later granitic intrusions may completely recrystallize to form chromian magnetite. In several samples where extensive chromian magnetite is developed, no chromite is present. However, pure Fe_3O_4 develops along the outer edges of the chromian magnetite and in small isolated irregular shaped grains;

serpentinization apparently occurred after development of the chromian magnetite.

The total magnetite separates from such "anomalous" lizardite-chrysotile serpentinites obviously do not represent a system in equilibrium with coexisting serpentine. They, therefore, cannot be expected to give meaningful 0^{18} temperature data. It is important when trying to obtain oxygen isotope temperature information on serpentines to analyze only those magnetites which are essentially pure Fe_3O_4.

(6) The presence of NiS (Millerite) in several of the serpentine samples may be due to the generation of reduced phases during the serpentinization. Such secondary sulfides have been noted by a number of workers (as in the Muskox serpentinites by Chamberlain _et_ _al_., 1965).

(7) As has been argued previously, the isotopic Δ-values for the "normal" lizardite-chrysotile serpentines seem to exhibit a close approach to equilibrium, despite the complex textures observed in any given sample. For example, sample 1 from the Dominican Republic displays several modes of magnetite occurrence (see plate 4-1) within a given thin section. Small disseminated grains of magnetite occur along with late-stage magnetite veins. In a similar manner, serpentine also displays complex textures such as mesh textures and bastites crosscut by chrysotile veins. These textures may have been produced in a manner outlined previously by equations (5) and (6) (section 4.2) in which magnetite is largely produced during a later stage of serpentinization.

In actual fact, much of the magnetite from a sample such as described above may have formed in true equilibrium only with the late-stage chrysotile veins with which it is associated. As will be repeatedly indicated in the following chapters, however, only a small δO^{18} variation exists among samples representing different serpentine textures from the same serpentinite exposure. Consequently, it does not matter that the measured Δ-values in "normal" lizardite-chrysotile serpentinites do not represent complete isotopic equilibrium. True equilibrium serpentine-magnetite Δ-values could only be obtained if somehow one were able to analyze each separate serpentine textural form together with the magnetites formed simultaneously with each form. This is, in general, a next-to-impossible analytical problem.

4.5 Isotopic temperatures of serpentinization

In order to estimate the temperatures of serpentinization from the oxygen isotope data, one must know how the equilibrium Δ serpentine-magnetite value varies with temperature. Inasmuch as a laboratory-calibrated curve does not exist, we can obtain only an approximate curve from (1) measured oxygen isotopic fractionations between chlorite and Fe-Ti oxides in low grade pelitic schists, (2) application of experimental geothermometric curves for quartz-water and muscovite-water to these same pelitic schists, (3) an estimate of the isotopic fractionation between chlorite and serpentine in the temperature range of interest, and (4) the assumption that all these equilibrium Δ-values graph essentially as straight lines when plotted against $1/T^2$.

Measured 0^{18} fractionations between chlorite and Fe-Ti oxides

A series of pelitic schists containing both chlorite and Fe-Ti oxides were studied by Garlick (1969) from various metamorphic grades and different terranes. The isotopic data referred to below are taken from his figure 8-B-28 (p. 26). The data, arranged in sequence of increasing metamorphic grade, show that isotopic fractionations tend to decrease with increasing grade. This effect is most pronounced for the quartz-ilmenite and quartz-magnetite fractionations. Quartz-chlorite Δ-values show irregular behavior, particularly in higher grade metamorphic rocks. This suggests that isotopic re-equilibration of the chlorite sometimes occurs during the declining temperatures of metamorphism (Garlick, personal communication). Thus it is assumed that only those samples from low grade terranes (biotite and lower garnet grade) generally contain primary, unaltered chlorite. For this reason, only such low-grade samples were used in determining a chlorite-ilmenite 0^{18} relationship.

It is useful to plot quartz-chlorite fractionations against quartz-ilmenite fractionations for the low-grade mineral assemblages that contain coexisting quartz, chlorite and ilmenite. Such a plot is shown in figure 4-2. A similar procedure was used by Taylor and Coleman (1968) for determining 0^{18} relationships among several other mineral phases.

A line drawn through the data points and the origin falls reasonably close to most of the data points. Presumably, if true equilibrium was attained in all the assemblages, the data points would lie exactly on a line or a smooth curve through the origin. If all the samples from

Figure 4-2. Relationship between quartz-chlorite and quartz-ilmenite, for quartz-chlorite-ilmenite assemblages in biotite- and lower garnet-grade pelitic schists analyzed by Garlick (1969). The sample numbers are those of Garlick as shown on his figure 8-B-28 (page 26). Rocks with similar mineral assemblages from higher-grade metamorphic zones exhibit a great deal of scatter, suggesting retrograde formation of the chlorite. The diagonal line is drawn through the origin as a least squares fit of the data points.

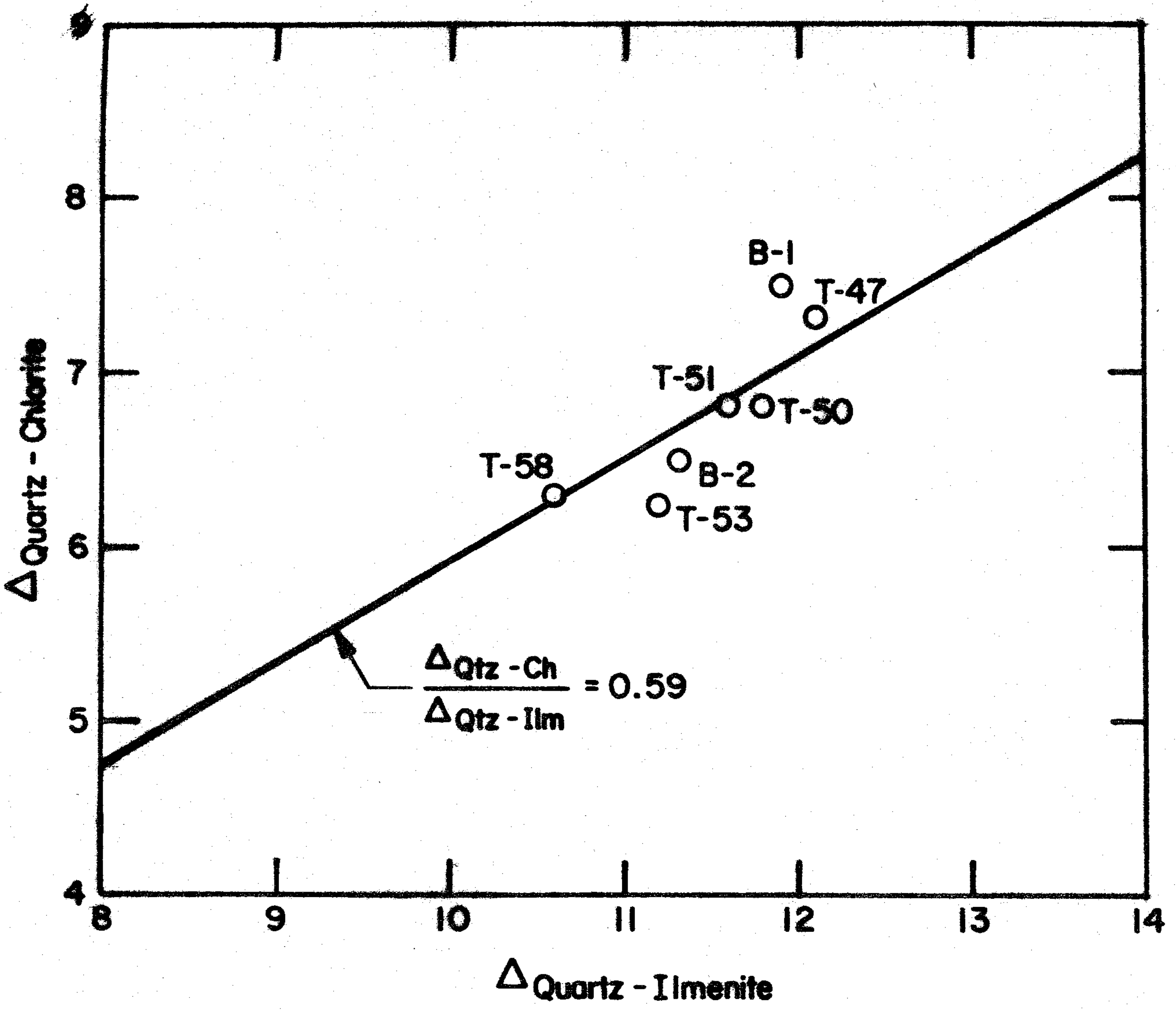

$\Delta_{Quartz - Chlorite}$
4
5
6
7
8
9
8
9
10
11
12
13
14
$\Delta_{Quartz - Ilmenite}$
B-1
T-47
T-51
T-50
T-58
B-2
T-53
$\frac{\Delta_{Qtz - Ch}}{\Delta_{Qtz - Ilm}} = 0.59$

Figure 4-2

Garlick (1969) are plotted, a great deal of scatter is observed, indicating non-equilibrium in many of the assemblages. The linear relationship drawn in figure 4-2 suggests that at equilibrium, Δ quartz-chlorite is equal to 0.59 times Δ quartz-ilmenite.

Calculation of a tentative chlorite-magnetite geothermometer

One can obtain a relationship between Δ quartz-chlorite and temperature by utilizing the following:

(1) $\frac{\Delta \text{quartz-chlorite}}{\Delta \text{quartz-ilmenite}} = 0.59$ (see figure 4-2)

(2) $\frac{\Delta \text{quartz-muscovite}}{\Delta \text{quartz-ilmenite}} = 0.35$ (Taylor and Coleman, 1968)

Also:

$\Delta \text{quartz-water} \approx 3.57\ (10^6/T^2) - 2.73$

(Clayton, O'Neil and Mayeda, personal communication)

$\Delta \text{muscovite-water} = 2.38\ (10^6/T^2) - 3.83$

(O'Neil and Taylor, 1969)

and therefore:

(3) $\Delta \text{quartz-muscovite} \approx 1.19\ (10^6/T^2) + 1.10$

From all the above, we obtain:

(4) $\Delta \text{quartz-chlorite} \approx 2.01\ (10^6/T^2) + 1.85$

and

(5) $\Delta \text{chlorite-water} \approx 1.56\ (10^6/T^2) - 4.56$

An approximate quartz-magnetite fractionation as a function of temperature is obtained by combining

$$(6)\quad \frac{\Delta\,\text{quartz-ilmenite}}{\Delta\,\text{quartz-magnetite}} = 0.92 \text{ (Garlick and Epstein, 1967)}$$

with equations (2) and (3) given above. This leads to

$$(7)\quad \Delta\,\text{quartz-magnetite} \approx 3.70\ (10^6/T^2)\ +\ 3.42$$

The chlorite-magnetite geothermometer curve is then derived by simple combination of (4), and (7) giving,

$$(8)\quad \Delta\,\text{chlorite-magnetite} \approx 1.69\ (10^6/T^2)\ +\ 1.57$$

Oxygen isotope fractionation between chlorite and serpentine

Taylor and Epstein (1962) showed that δ-values could be assigned to various types of bonds associated with oxygen in igneous minerals. Garlick (1965) and O'Neil and Taylor (1967) utilized this same approach for several minerals which have equilibrated over a wide range of temperatures. Fractionation factors between various oxygen bond types and water are obtained from laboratory calibrated mineral-water systems. For example, the Si-O-Si-water fractionation is assumed to be identical to the quartz-water fractionation.

The basic assumption inherent in estimating fractionation factors in systems which contain more than one bond type is that the fractionation factors involving each bond type are essentially independent of the presence of all other bond types in the mineral. By this method, one can estimate fractionation factors for various phases by a linear combination of the various bond types in each mineral. However, such estimates are very uncertain for complex minerals, expecially if one or more of the bond types which compose the mineral are not derived from experimentally measured mineral-water systems. Nevertheless, two similar minerals can be compared relative to one another by this technique, especially when utilized in conjunction with actual 0^{18} measurements of mineral fractionations. Serpentine and chlorite are chemically similar and a considerable amount of 0^{18} data is available for chlorite; this is the principal basis for comparing these two minerals with one another.

The percent of various oxygen bond types for chlorite and serpentine is shown in Table 4-2, whereas the various bond-water fractionations as a function of temperature are indicated in Table 4-3. The values of slope and intercept presented in Table 4-3 are derived from experimentally measured data and from data on natural assemblages by Taylor (unpublished data).

Combining the various oxygen bond type-water fractionations according to the proportion of such bond types for both chlorite and serpentine, one finds the following:

	slope (m)	intercept (b)
chlorite-H_2O	0.70	- 5.27
serpentine-H_2O	0.59	- 5.37

TABLE 4-2

Percent of various oxygen bond types in chlorite and serpentine

	Si-0-Si	Si-0-Al	Si-0-M	Al-0-M	Al-0H-H	M-0-H
Chlorite $Mg_5Al(OH)_8Al\ Si_3O_{10}$*	16.7	16.7	16.7	5.5	11.1	33.3
Serpentine $Mg_6(OH)_8Si_4O_{10}$	33.3		22.2			44.5

* Note that an Al- and Fe^{+3}- free chlorite would be identical to serpentine

TABLE 4-3

Various oxygen bond type - water fractionations assuming a behavior according to:

$$10^3 \ell n\, \alpha = m(\frac{10^6}{T2}) + b$$ (H. P. Taylor, unpublished report)

	Si-0-Si*	Si-0-Al*	Si-0-M	Al-0-M	Al-0-H	M-0-H
Slope (m)	3.57	2.25	1.3	1.2	1.0	-2.0
Intercept (b)	-2.73	-3.90	-4.74	-4.96	-5.01	-7.66

* Experimentally measured data, all other slopes and intercepts are estimated.

The values obtained for chlorite-water may be compared with those based on natural mineral assemblages (equation 5 above). The percentage of various oxygen bond types given in Table 4-2 is based on the chlorite formula $Mg_5Al(AlSi_3O_{10})(OH)_8$. Such a chlorite thus differs chemically from serpentine only with respect to partial substitution of Al for Mg and Si. It is similar to chlorite compositions given by Albee (1968) for the same type of rocks studied by Garlick (1969). A typical formula of this type is

$$(Mg_{2.8}Fe^{+2}_{1.5})(Al_{1.5}Fe^{+3}_{0.2})(Si_{2.6}Al_{1.4})O_{10}(OH)_8.$$

Note that in both these chlorite formulas, Al substitution for Mg is concomitantly balanced by Al substitution for Si. The former should tend to enrich the chlorite in O^{18} relative to coexisting serpentine (at equilibrium) whereas the latter would produce the reverse effect (see discussion of muscovite on page 1745, Taylor and Coleman, 1968).

Thus, because the above effects tend to cancel one another, and because of the uncertainties and small deviations from complete equilibrium exhibited by the chlorite-quartz-ilmenite assemblages on which the geothermometer curves are based, it will be assumed for the purposes of this work that serpentine and chlorite show essentially zero O^{18} fractionation with respect to one another at the temperatures of interest (25° to 500°C). The uncertainties which may exist for such an assumption are thought to be no greater than all of the other variations which are inherent in the construction of this tentative serpentine-magnetite geo-thermometer.

Application of the serpentine-magnetite geothermometer

The approximate serpentine-magnetite geothermometer assumed for the present work is shown in figure 4-3. It is identical to the chlorite-magnetite curve derived previously (equation 8 above). The various coexisting serpentine-magnetite O^{18}/O^{16} fractionations from figure 4-1 are plotted on the geothermometer curve, excluding all the "anomalous" lizardite-chrysotile data. The individual samples shown on this figure will be discussed in a later chapter when considering individual outcrops and exposures of serpentinite. Nevertheless certain general conclusions are worth noting at this time.

(1) Continental lizardite-chrysotile type serpentinites appear to have formed in a temperature range of about 85°C to 115°C.

(2) Antigorites show a much wider temperature variation from about 220°C to 460°C. Most of the antigorite samples, however, fall in the temperature range of about 300°C to 220°C.

(3) Oceanic lizardite-chrysotile type serpentinites appear to form at somewhat higher temperatures than do those of continental origin.

The inferred temperatures for the antigorite samples appear in some instances to be abnormally low. For example, sample 1 from the Vermont Talc Quarry, selected from a staurolite-kyanite grade terrane, gives a temperature which is somewhat low (staurolite-kyanite grade rocks generally fall in the range 510 - 580°C, Epstein and Taylor, 1967). Furthermore, samples from biotite-garnet grade rocks (Belvedere Mt., Vermont) also appear to suggest anomalously low temperatures. This effect could be due to retrogradation among the phases, as was suggested

Figure 4-3. Oxygen isotope "temperatures" for serpentine-magnetite mineral pairs analyzed in this study. The serpentine-magnetite goethermometer is calculated in section 4.5. All serpentine-magnetite mineral pairs in figure 4-1 are included except the anomalous lizardite-chrysotile type. Sample numbers: 1 = 6c - San Luis Obispo; 2 and 3 = 1, 2 - Tiburon, California; 4 = 1 - Dominican Republic; 5 = 1 - Guatemala, 6 = 118 - Mid Atlantic Ridge (1°N); 7 = 70 - Mid Atlantic Ridge (43°N); 8 = 3 - Carlton Quarry, Vermont; 9 = 2a - Del Puerto, California; 10 and 11 = 9, 8 - Belvedere Mountain, Vermont; 12 = 54 - Mid Atlantic Ridge (43°N); 13 = 5 - Belvedere Mountain, Vermont; 14 = 5 - Cedar Hill, Pennsylvania; 15 = 9 - Skagit, Washington; 16 -= 6 - Cedar Hill, Pennsylvania; 17 = 1 - Vermont Talc Quarry, Vermont.

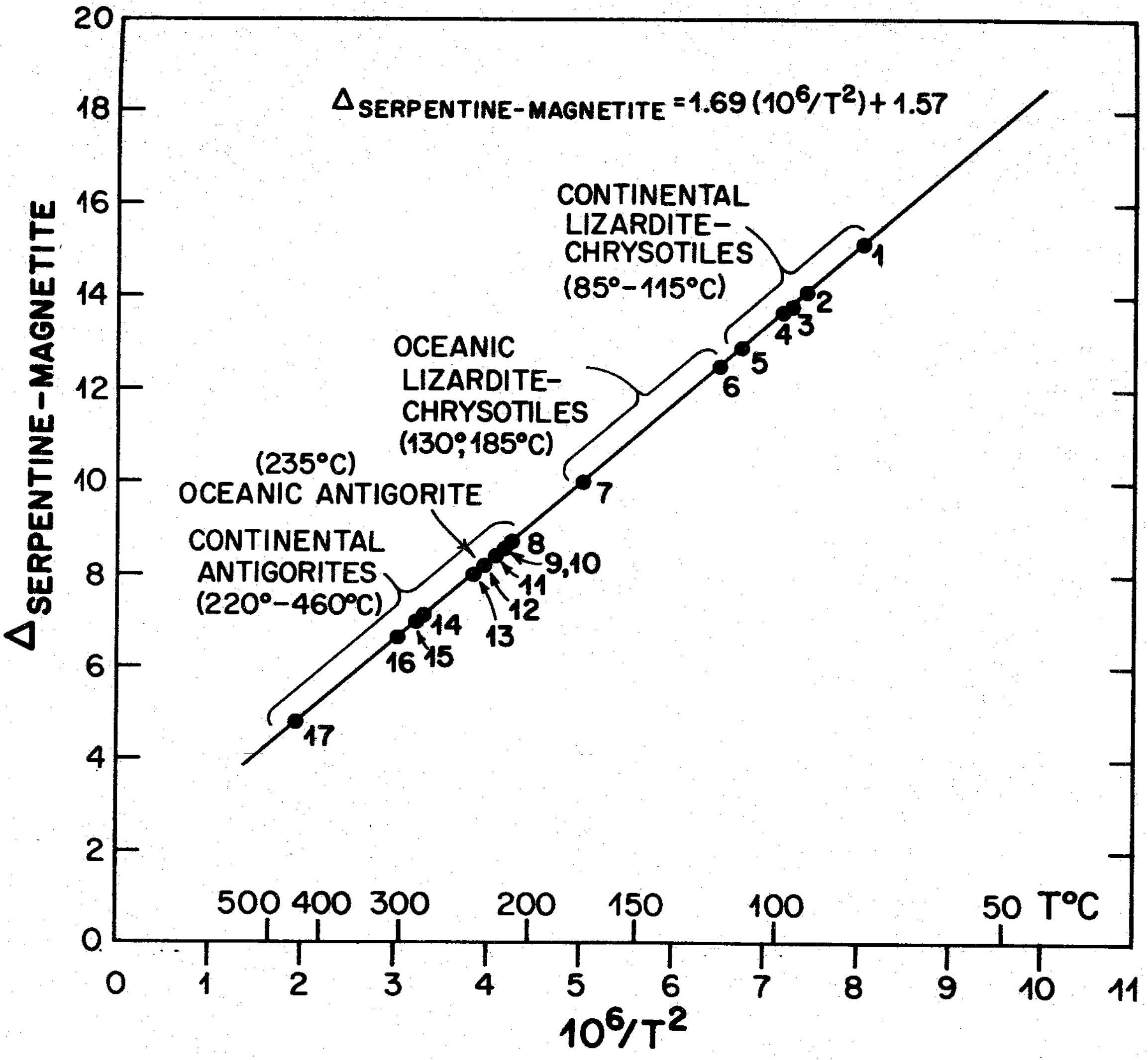
$\Delta_{SERPENTINE-MAGNETITE} = 1.69(10^6/T^2) + 1.57$
CONTINENTAL LIZARDITE-CHRYSOTILES (85°-115°C)
OCEANIC LIZARDITE-CHRYSOTILES (130°,185°C)
(235°C) OCEANIC ANTIGORITE
CONTINENTAL ANTIGORITES (220°-460°C)
1
2
3
4
5
6
7
8
9,10
11
12
13
14
15
16
17
$\Delta_{SERPENTINE-MAGNETITE}$
0
2
4
6
8
10
12
14
16
18
20
500
400
300
200
150
100
50
T°C
0
1
2
3
4
5
6
7
8
9
10
11
$10^6/T^2$

Figure 4-3

previously for sample 3 from the Carlton Quarry, Vermont, or serpentinization may largely occur at the lower temperatures associated with either the early prograde or the waning stages of regional metamorphism.

Because of the general uncertainties involved in the construction of the serpentine-magnetite geothermometer, it is useful to consider some other possible derivations of this geothermometer curve, based on another point of view.

If one assumes that sample 1 from the Vermont Talc Quarry was formed at roughly the same temperatures as the surrounding staurolite-kyanite grade schists (about 510 - 580°C, Epstein and Taylor, 1967), then a plausible serpentine-magnetite geothermometer curve might be that labeled curve 2 in figure 4-4. Curve 2 was drawn parallel to curve 1, but shifted slightly so that the isotopic "temperature" of the serpentine-magnetite pair in this sample is about 525°C. Note that even when this is done, sample 8 from Belvedere Mt., Vermont only shows a small "temperature" shift from around 230°C to 250°C. Within experimental error, the lower temperature lizardite-chrysotile type serpentines would not be affected at all.

If we assume that both sample 1 from the Vermont Talc Quarry and sample 8 from Belvedere Mt. were serpentinized at temperatures consistent with the metamorphic grade of the country rock (staurolite-kyanite grade at around 510 to 580°C and biotite-garnet grade at about 400 - 490°C, respectively), then one could construct geothermometer curve 3 shown in figure 4-4. However, such a curve would have even a greater slope than the quartz-magnetite geothermometer, implying that

Figure 4-4. Calculated serpentine-magnetite geothermometer shown in figure 4-3 compared to other possible constructions. Curve 2 represents a possible serpentine-magnetite geothermometer drawn parallel to curve 1 (shown in figure 4-3), and through the point that assumes Vermont Talc-1 equilibrated at temperatures of staurolite-kyanite grade metamorphism (~ 540°C). Curve 3 is drawn assuming that Vermont Talc - 1 equilibrated at ~ 540°C and Belvedere 8 equilibrated at biotite grade temperatures (~ 450°C). The tentative quartz-magnetite geothermometer (equation 7, page 90) is shown for reference, and clearly indicates that serpentine-magnetite curve 3 is impossible.

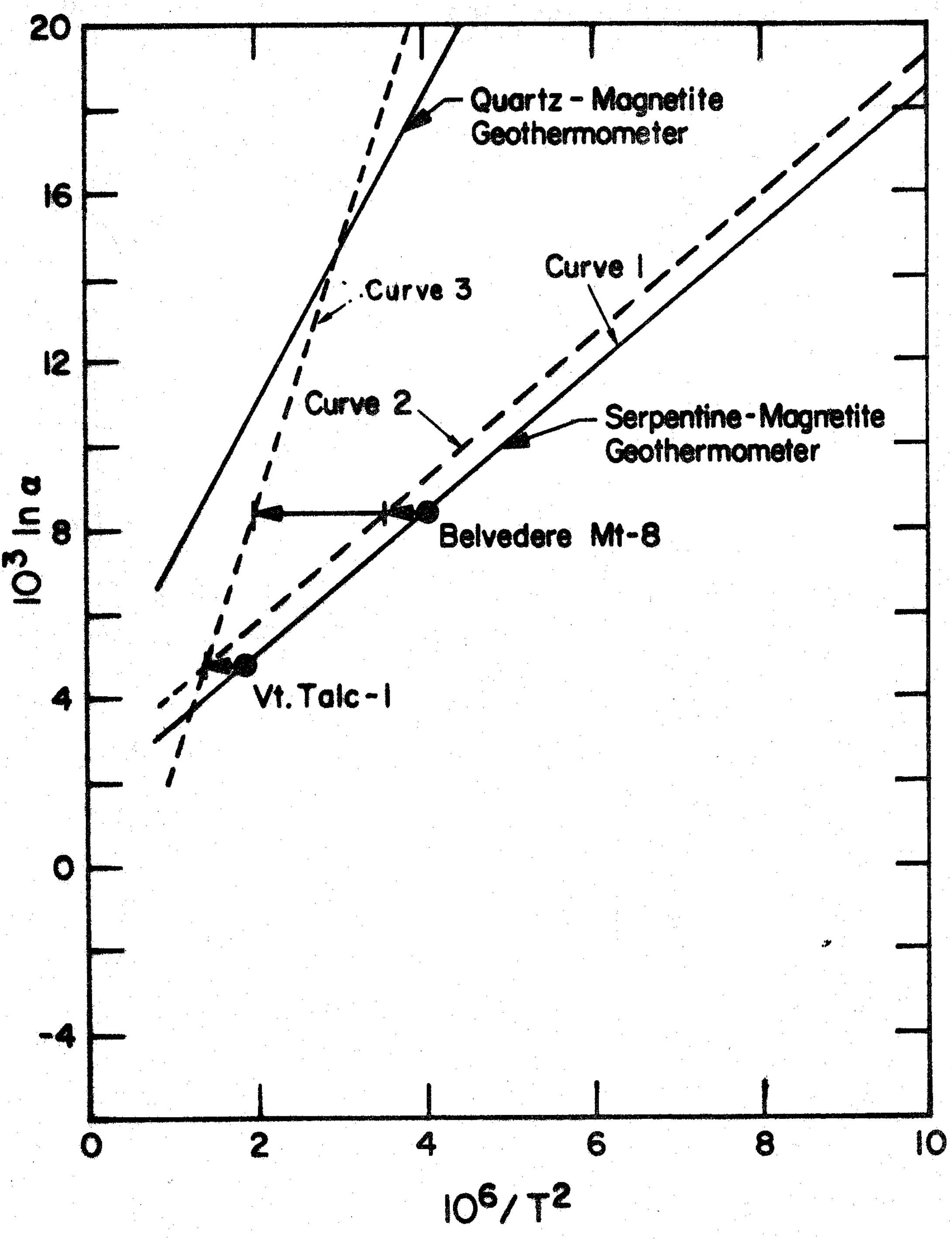

Quartz - Magnetite Geothermometer
Curve 3
Curve 1
Curve 2
Serpentine-Magnetite Geothermometer
Belvedere Mt-8
Vt. Talc-1
$10^3 \ln \alpha$
$10^6/T^2$
20
16
12
8
4
0
-4
0
2
4
6
8
10

Figure 4-4

serpentine would concentrate 0^{18} relative to quartz at lower temperatures. This is an impossible relationship in the light of our present knowledge of the behavior of $0^{18}/0^{16}$ fractionations among minerals. Therefore the serpentine-magnetite geothermometer cannot have a slope even remotely approaching that of curve 3.

The actual slope of the serpentine-magnetite geothermometer curve must therefore be restricted to a value fairly close to the one given in this work on the basis of a variety of considerations. However, the intercept is not firmly fixed, and of course small changes in the slope are perfectly permissible. These arguments indicate that the higher "temperatures" obtained with this tentative isotopic geothermometer could conceivably be in error by perhaps 100°C, but at lower temperatures the errors are much less.

Although accurate oxygen isotopic measurements of silicates can be made to within $\pm$ 0.1 per mil or less, the analytical error associated with the magnetite $\delta 0^{18}$ values in this work is much larger because of the analytical difficulties referred to previously. It is thus probable that the determinations of Δ serpentine-magnetite have an uncertainty of about $\pm 0.4^{\circ}/_{oo}$. Based on this estimated uncertainty, we obtain the errors in isotope "temperatures" shown in Table 4-4. These variations are based purely on the assumed analytical precision and do not, of course, take into account the much larger errors in the tentative geothermometer curve itself. Note that the tabulated errors for antigorites are quite large, but for lizardite-chrysotile they are less than 10°C.

In particular, it is noteworthy that Vermont Talc 1 from the staurolite-kyanite grade terrane exhibits a sufficiently large analytical error that the "temperature" of this sample could essentially coincide with the regional metamorphic temperature estimate. Regardless of the analytical uncertainties, however, the antigorites from lower grade metamorphic terranes give "temperatures" which are consistently lower than the peak metamorphic temperature estimated for the adjacent country rocks. The general consistency of the data suggests that many of these coexisting antigorites and magnetites did in fact equilibrate at these lower temperatures.

Small changes in the tentative serpentine-magnetite geothermometer would not substantially change the isotopic temperatures inferred for the continental lizardite-chrysotile type serpentines. The fractionations given in the upper part of figure 4-1 must represent quite low equilibrium temperatures. It is totally inconceivable, on the basis of any "reasonable" geothermometer curve, that these temperatures could be higher than 200°C.

4.6 Isotopic compositions of waters involved in serpentinization

δO^{18} values of waters

Utilizing the tentative serpentine-water O^{18}/O^{16} fractionation given by equation 5, section 4.5 , we can calculate the δO^{18} of the waters that would have coexisted in equilibrium with all the serpentine-magnetite pairs for which we have obtained isotopic "temperatures". These calculated δO^{18} values are given in Table 4-4.

TABLE 4-4

Calculated waters in equilibrium with the serpentines of figure 4-1.

	Sample	ΔSerp.-Mag.	T°C (± error)	δO^{18} °/oo serp.	δO^{18} °/oo Calc. H_2O	δD °/oo Serp.	δD °/oo Calc. H_2O
lizardite-chrysotile type	Tiburon 1	14.1	95 ± 6	+ 8.0	+ 1.0	- 90	- 44
	Tiburon 2	13.8	100 ± 6	+ 8.1	+ 1.6	- 89	- 43
	Dom. Republic 1	13.7	100 ± 6	+ 8.4	+ 1.9	- 63	- 16
	Guatemala 1	12.9	115 ± 6	+ 8.3	+ 2.5	- 88	- 45
	San Luis Obispo Obispo 6c	15.1	85 ± 6	+ 7.5	- 0.1	- 91	- 45
	Mid Atlantic (43°N) 70	10.0	185 ± 10	+ 3.2	+ 0.3	- 59	- 23
	Mid Atlantic (1°N) 118	12.5	130 ± 7	+ 4.6	- 0.4	- 44	0
antigorite type	Vt. Talc 1	4.8	460 ± 50	+ 6.2	+ 7.8	-	-
	Carlton Quarry 3	8.7	220 ± 15	+ 8.6	+ 6.7	- 57	- 25
	Belvedere Mt. 9	8.6	225 ± 15	+ 6.1	+ 4.4	- 57	- 25
	Belvedere Mt. 5	8.0	240 ± 18	+ 5.9	+ 4.5	-	-
	Belvedere Mt. 8	8.4	230 ± 15	+ 5.8	+ 4.2	-	-
	Cedar Hill 5	7.1	280 ± 22	+ 7.0	+ 6.5	- 66	- 39
	Cedar Hill 6	6.6	310 ± 25	+ 7.1	+ 7.1	- 42	- 17
	Skagit 9	7.0	295 ± 22	+ 8.7	+ 8.4	- 58	- 32
	Del Puerto 2a	8.6	225 ± 15	+ 8.7	+ 7.0	-	-
	Mid Atlantic (43°N) 54	8.2	235 ± 16	+ 2.0	+ 0.5	- 31	0

The $\delta 0^{18}$ values of the waters given in Table 4-4 will be discussed in more detail in later chapters when specific occurrences are considered. We cannot calculate $\delta 0^{18}$ values for most of the analyzed serpentine samples because magnetites have only been analyzed in a few of these samples. The consistency of the "temperatures" obtained for the few continental lizardite-chrysotile serpentinites in Table 4-4 (85° to 115°C) suggests, however, that we might not be far amiss in assuming an average temperature of formation of 100°C for all such serpentinites. Thus, except for the samples in Table 4-4, we shall in succeeding discussions assume a model in which all the continental lizardite-chrysotile samples studied in this work formed at 100°C.

In a similar manner, we will assume that all antigorites studied (except those given in Table 4-4) were formed at about 310°C. This is a little higher than the average antigorite temperature given in Table 4-4, but it allows for a little retrogradation and also makes for ease of calculation, as indicated below.

The models outlined above correspond to the assumptions that (1) $\Delta 0^{18}$ serpentine-water = $+ 6.6^{\circ}/_{oo}$ for the continental lizardite-chrysotile type serpentines, and (2) $\Delta 0^{18}$ serpentine-water = 0 for all antigorite samples.

<u>δD values of waters</u>

The D/H fractionation factors for the serpentine-water pair can be estimated from a combination of available experimental data on certain mineral-water systems and from measurements on hydrous minerals in nature.

Among these fractionation factors adopted for constructing a D/H geothermometer curve for serpentine-water are the following:

(1) The serpentine-water fractionation at low temperatures (i.e., that of a weathering environment) can be estimated from the δD value of deweylite, a serpentine-like mineral structurally similar to antigorite, from southeastern Pennsylvania. The occurrence and structure of deweylite are discussed in detail in a later chapter, but for the present we simply assert that the D/H fractionations between deweylite and water are probably very similar to those of the other serpentine polymorphs and water.

Assuming that the deweylites from S.E. Pennsylvania were formed recently in isotopic equilibrium with local meteoric waters, one can calculate the fractionation at 20 - 30°C as follows:

δD of deweylite 4 (see chapter 11)	≈ -94°/oo
δD of local meteoric water (Susquehanna River at Marietta, Pennsylvania, Friedman, et al., 1964)	-42°/oo
thus giving Δ serpentine water	≈ -56

As will be indicated in more detail in the next chapter, the δD values of meteoric waters during the Tertiary were apparently not too dissimilar from present day waters; this is probably particularly true of a location like S.E. Pennsylvania or of other localities near the east or gulf coasts of the United States (see Savin and Epstein, 1970, Lawrence, 1970). Therefore the values calculated above are not particularly sensitive as to whether the deweylites are of Tertiary or Holocene age.

(2) There is some evidence (given in a later chapter) that antigorite sample 54 from the Mid Atlantic Ridge (43°N) may have formed from ocean water. The hydrogen isotopic fractionations for such an antigorite-water system would then be:

δD of sample 54 $\approx -31^{o}/_{oo}$
and δD of ocean water $\approx 0^{o}/_{oo}$
therefore Δ serpentine-water ≈ -31.5

Furthermore, if it is assumed that the δD value of the antigorite was "frozen in" at nearly the same temperature as the δO^{18}, it can be assumed that this D/H fractionation applies to a temperature of about 240°C (see Table 4-4).

(3) In a similar manner, sample 118 from the Mid-Atlantic Ridge (1°N), composed of lizardite and minor chrysotile, may also have formed from ocean water. The hydrogen isotopic fractionation for such a serpentine-water system would be:

δD of sample 118 $\approx -44^{o}/_{oo}$
δD of ocean water $\approx 0^{o}/_{oo}$
thus Δ serpentine-water ≈ -45

Again, if one assumes a "freezing in" of both the hydrogen and oxygen isotopic compositions at the same temperatures (i.e. about 130°C, Table 4-4), this suggests that the serpentine-water fractionation at that temperature is equal to -45.

(4) From studies of exchange experiments of various mineral-water systems, Suzuoki and Epstein (1970) report that at 400°C, the serpentine-water fractionation is about $-20^{o}/_{oo}$. By analogy with other

mineral-water systems studied by Suzuoki and Epstein, it would appear that the serpentine-water fractionation may be about -10°/$_{oo}$ at around 500°C. Inasmuch as serpentine contains virtually no Al and shows only a small amount of Fe substitution for Mg in the octahedral position, these isotopic fractionations are not complicated by variations in chemical composition (Suzuoki and Epstein, 1970).

From the admittedly tentative estimates of serpentine-water D/H fractionations given above, one can construct an approximate D/H equilibrium fractionation curve as shown by the curve in figure 4-5. Note that the fractionations increase with decreasing temperature; this is theoretically the most likely trend, thus giving general support to the validity of this curve. Based on this curve, calculated δD values for water formed in isotopic equilibrium with various serpentine samples are given in Table 4-4.

In succeeding discussions, we shall make model calculations to obtain the δD values of the waters that would have coexisted with the various serpentine samples studied in this work. For this purpose we shall use the curve figure 4-5 in conjunction with the same temperature assumed in the oxygen isotope model calculations. Thus, the continental lizardite-chrysotile D/H ratios are assumed to have "frozen in" at 100°C and those of the antigorites at 310°C. These correspond to D/H fractionations of -26 per mil for antigorite-water and -48 per mil for lizardite (chrysotile) -water.

Figure 4-5. Estimated D/H serpentine-water geothermometer based on the laboratory calibrated point at 400°C by Suzuoki and Epstein (1970) and the measured δD values of natural samples. The two oceanic samples are assumed to have equilibrated with pure ocean water at the temperatures indicated by their serpentine-magnetite O^{18} fractionation. The deweylite is presumed to have formed in equilibrium with the local meteoric water in S.E. Pennsylvania at about 25°C.

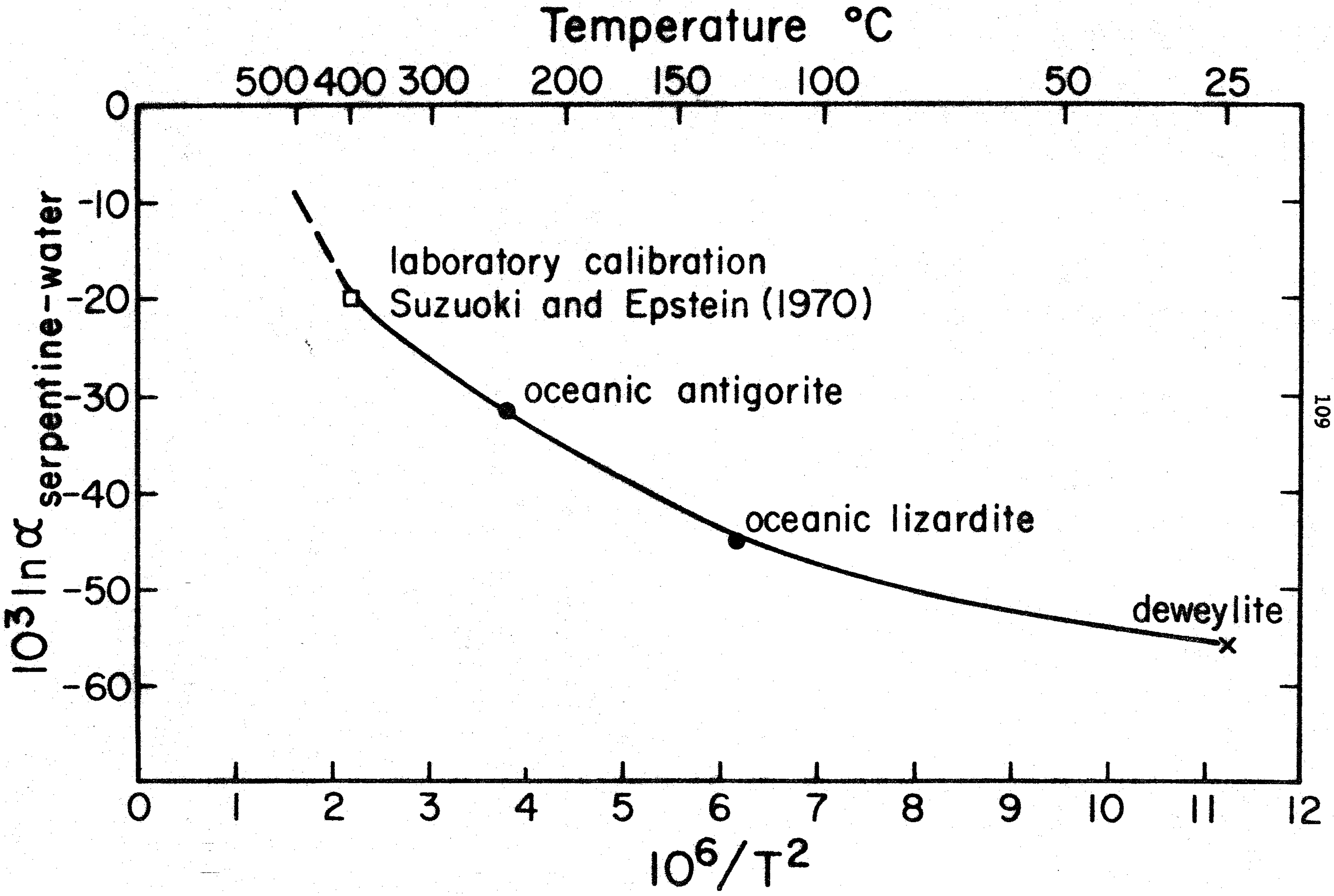
Temperature °C
500
400
300
200
150
100
50
25
0
-10
-20
-30
-40
-50
-60
$10^3 \ln \alpha_{\text{serpentine-water}}$
laboratory calibration
Suzuoki and Epstein (1970)
oceanic antigorite
oceanic lizardite
deweylite
0
1
2
3
4
5
6
7
8
9
10
11
12
$10^6/T^2$

Figure 4-5.

V. ISOTOPE GEOCHEMISTRY OF NATURAL WATERS

The D/H and O^{18}/O^{16} ratios of various types of natural waters involved in geologic processes are discussed in detail by Epstein and Mayeda (1953), Craig (1963), Taylor (1967a), White (1968), and Sheppard _et al_. (1969). Any or all of these waters conceivably could be involved in serpentinization, so it is useful to consider the general isotopic relationships of these different types of waters. These are illustrated on δD-δO^{18} diagrams in figures 5-1 and 5-4, and are discussed below.

Magmatic water is an H_2O-rich solution that has thoroughly exchanged chemically and isotopically with a magma system or igneous rock body at magmatic temperatures. Such water has a well-defined δO^{18} of + 7.0 to 9.5°/oo (Taylor, 1967b), though lower exchange temperatures or a larger quantity of H_2O relative to the igneous body can modify the δO^{18} value. The δD values of magmatic waters are probably quite variable, but they typically seem to range from -60 to -80 per mil, based on the δD of biotite and hornblende from mafic and ultramafic rocks and deep-seated batholithic rocks (Godfrey, 1962; Taylor and Epstein, 1966; Sheppard and Epstein, 1970). However, δD values for some shallow igneous intrusions can be much lower and more variable as a result of interaction with heated meteoric ground waters.

Primary magmatic waters are tentatively defined by Sheppard _et al_. (1969) as those magmatic waters that have δO^{18} = + 7.0 to + 9.5 per mil and δD = -50 to -80 per mil. As they point out, however, water samples of such isotopic compositions do not _have_ to be of deep-seated igneous origin.

Hydrothermal waters are hot aqueous fluids of unspecified origin. Such waters may consist dominantly of any of the other types of waters discussed in this section. In figure 5-1, the general range of calculated hydrothermal waters from various porphyry copper deposits is given (Sheppard et al., 1970). Also shown is the general range of calculated and experimentally measured hydrothermal waters from the Bluebell Mine of British Columbia (Ohmoto and Rye, 1970). The isotopic data suggest that many (if not most) such hydrothermal waters must contain a large component of meteoric ground waters, as evidenced by the general latitudinal correlation (see figure 5-1).

Metamorphic waters are waters that have isotopically equilibrated with metamorphic rocks. Since metamorphic rocks show very large $\delta 0^{18}$ variations, such waters are also isotopically highly variable. However, most metamorphic waters from terranes composed principally of metasedimentary rocks generally have $\delta 0^{18}$ values in the range + 10 to + 14 per mil (Taylor, 1967a). If carbonates are present in abundance, the $\delta 0^{18}$ values of the coexisting $H_2 0$ will typically be + 17 to + 24 per mil. Metamorphic terranes composed of abundant meta-igneous rocks are much lower in $\delta 0^{18}$. For example, at 500°C the $\delta 0^{18}$ of water in equilibrium with a metabasalt or metagabbro might be as low as + 5 to + 6 per mil.

The δD values of deep-seated regional metamorphic waters probably lie in the range given in figure 5-1. For example, muscovites from pelitic schists have δD values in the range -60 to -36 per mil (Taylor and Epstein, 1966). Assuming that the D/H fractionations between muscovite and water at 400°C and 600°C are about $-20^{\circ}/_{oo}$ and $-10^{\circ}/_{oo}$, respectively (Suzuoki

Figure 5-1. Plot of δD versus δO^{18} for various types of natural waters that may conceivably be involved in serpentinization. The data on meteoric waters for various localities considered in this work are from Friedman et al., 1964; Dansgaard, 1964 and Craig, 1963. The hydrothermal waters are calculated from measured isotopic compositions of sericites from porphyry copper deposits by Sheppard et al. (1970). The primary magmatic water region is that designated by Sheppard et al. (1969). Metamorphic waters are based on δO^{18} estimates by Taylor (1967 a); δD values are estimated from the δD values of muscovites from several pelitic schists (Taylor and Epstein, 1966), assuming fractionation factors reported by Suzuoki and Epstein (1970) at 400°-600°C. Also shown are the isotopic compositions of several geothermal waters (Craig, 1963), the measured hydrothermal fluid inclusions from Providencia, Mexico (Rye and O'Neil, 1968), the calculated hydrothermal fluids from Bluebell Mine, British Columbia (Ohmoto and Rye, 1970), and the measured high-pH waters presumed to be involved in present-day serpentinization by Barnes and O'Neil (1969).

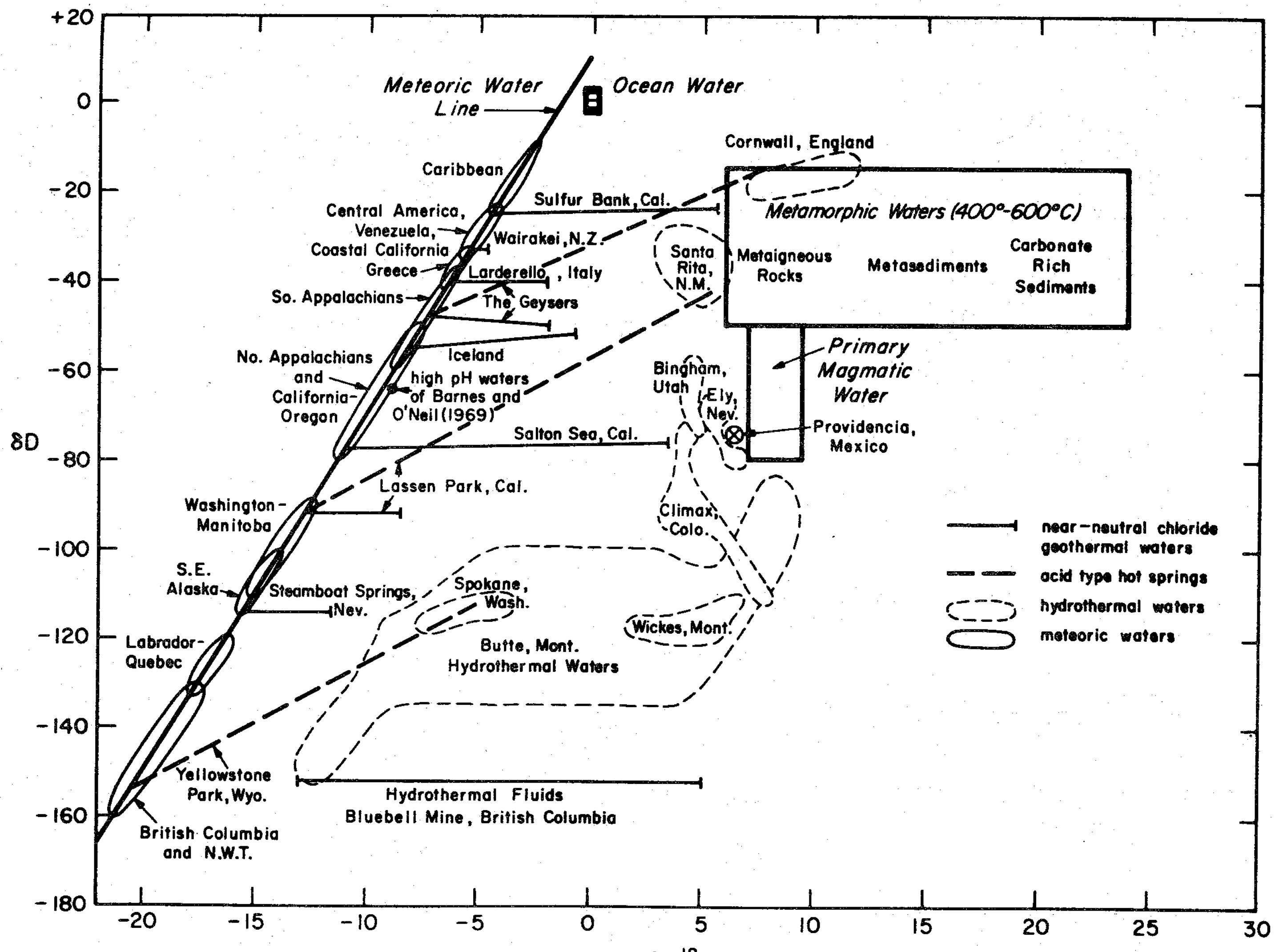
+20
0
-20
-40
-60
-80
-100
-120
-140
-160
-180
δD
-20
-15
-10
-5
0
5
10
15
20
25
30
δO^{18}
Meteoric Water Line
Ocean Water
Cornwall, England
Caribbean
Sulfur Bank, Cal.
Central America, Venezuela, Coastal California
Wairakei, N.Z.
Greece
Larderello, Italy
So. Appalachians
The Geysers
Metamorphic Waters (400°-600°C)
Santa Rita, N.M.
Metaigneous Rocks
Metasediments
Carbonate Rich Sediments
Iceland
No. Appalachians and California-Oregon
high pH waters of Barnes and O'Neil (1969)
Primary Magmatic Water
Bingham, Utah
Ely, Nev.
Providencia, Mexico
Salton Sea, Cal.
Lassen Park, Cal.
Washington-Manitoba
Climax, Colo.
S.E. Alaska
Steamboat Springs, Nev.
Spokane, Wash.
Butte, Mont. Hydrothermal Waters
Wickes, Mont.
Labrador-Quebec
Yellowstone Park, Wyo.
British Columbia and N.W.T.
Hydrothermal Fluids Bluebell Mine, British Columbia
near-neutral chloride geothermal waters
acid type hot springs
hydrothermal waters
meteoric waters

Figure 5-1.

and Epstein, 1970), then the δD values for metamorphic waters in equilibrium with such muscovites would be about -15 to -50°/₀₀ in the temperature range 400° to 600°C.

Ocean waters have a nearly constant isotopic composition, with δD ≈ 0 and $\delta O^{18} \approx 0$, since our standard is Standard Mean Ocean Water. The principal deep-water masses of the ocean differ from SMOW by only 0.3 per mil for δO^{18} and about 3 per mil for δD(Craig and Gordon, 1965). For the surface marine waters that exhibit a wide range of salt contents, δO^{18} varies over a range of approximately 6 per mil; the lowest O^{18}/O^{16} ratios are observed in ocean waters contaminated with meltwater from ice fields (Epstein and Mayeda, 1953).

Connate waters initially have D/H and O^{18}/O^{16} ratios near zero since they are ocean waters trapped in the marine sediments at the time of burial. The isotopic values can, of course, become enriched in O^{18} due to exchange with silicates and carbonates as these waters migrate through a sedimentary-rock section. This is particularly true if carbonates are abundant because they exchange and recrystallize easily, even at low temperatures. The δD values may also become lighter if mixing with meteoric ground water occurs.

Meteoric waters are surface fresh waters derived from rain or melted snow. Sheppard *et al*. (1969) use this term to apply specifically to all ground waters or geothermal waters that have been ultimately derived in large part from such fresh waters, even though their chemical composition may have been drastically changed.

Craig (1961) has shown that the δD and δO^{18} values of all meteoric waters that have not undergone excessive evaporation or exchange processes display a very well-defined linear correlation, with $\delta D = 8\ \delta O^{18} + 10$ (both δ values in per mil).

The isotopic compositions of present-day meteoric surface waters throughout North America have been tabulated by Friedman et al. (1964); Craig (1963); and Dansgaard (1964) and are presented in figure 5-2 where contours are used to indicate roughly how the D/H and O^{18}/O^{16} ratios of meteoric lake, stream, river and spring waters vary over the land surface. The general range of isotopic compositions for the various areas examined in this work is shown in figure 5-1. In general, the isotopic compositions of meteoric waters are lighter at high latitudes and altitudes as indicated in figure 5-2. The altitude effect is particularly pronounced in western North America due to the presence of high mountain ranges.

The isotopic compositions of meteoric waters during the Tertiary have been estimated by Lawrence (1970) from studies of kaolinite deposits; these data are presented in figure 5-3 as contours of D/H for the United States. The distribution of isotopic data can represent conditions during the Tertiary only in a generalized way, since no specific subdivisions within the Tertiary were attempted. As can be observed when comparing the distributions of D/H for present day waters (figure 5-2) with those for the Tertiary (figure 5-3), the meteoric waters for the two periods are isotopically somewhat different. The contour patterns during the Tertiary are grossly similar to those of present day waters, but the gradients are less extreme. Lawrence (1970) suggests that the more gentle gradients during the Tertiary can probably be explained as being

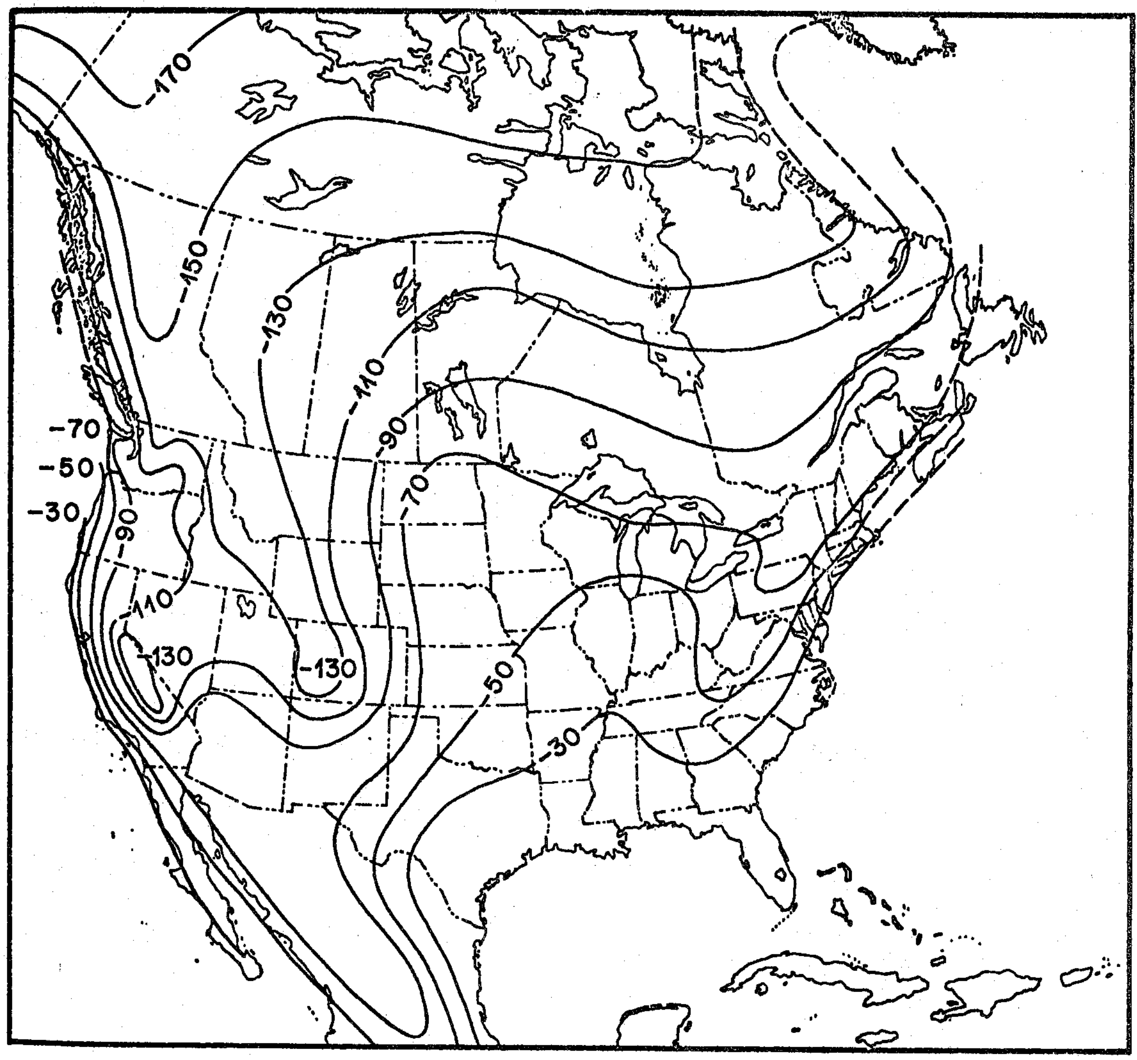

Figure 5-2

Map of North America showing δD-contours of meteoric lake, stream, river and spring waters over the land surface (generalized from data by Friedman _et al._, 1964; Craig, 1963; Dansgaard, 1964).

Figure 5-3. A map of the United States, showing the δD values of kaolinites of Tertiary age (after Lawrence, 1970). Numbers encircled are calculated δD values of meteoric waters of Tertiary age, assuming $\alpha^{hy}_{kaolinite-H_2O} = 0.970$. Rough contours have been drawn showing the calculated distribution of δD in Tertiary meteoric waters.

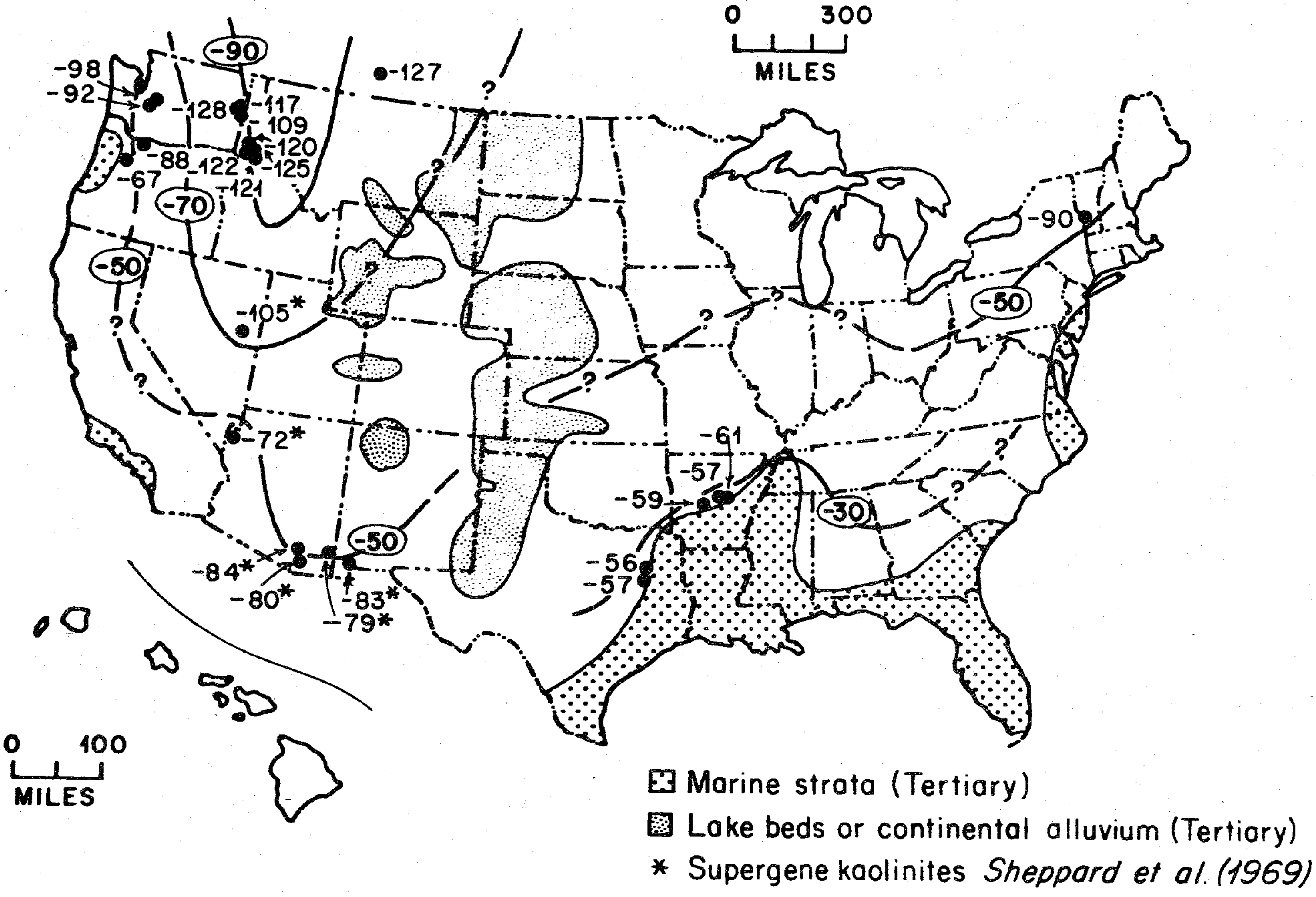
0 300
MILES
0 400
MILES
-98
-92
-128
-117
-109
-120
-125
-122
-121
-88
-67
-127
-90
-70
-50
-105*
-72*
-84*
-80*
-83*
-79*
-50
-61
-57
-59
-56
-57
-30
-90
-50
?
Marine strata (Tertiary)
Lake beds or continental alluvium (Tertiary)
* Supergene kaolinites Sheppard et al. (1969)

Figure 5-3

due to less extreme climatic differences between the coastal and inland regions.

From studies of kaolinites and illites of Cretaceous and Pennsylvanian ages in the United States by Lawrence (1970) and from Mesozoic clay minerals of hydrothermal origin from British Columbia and Alaska by Sheppard *et al*.(1969), it can be inferred that the isotopic compositions of meteoric waters of those ages may have been much heavier than present day meteoric waters.

Exchanged meteoric ground waters are those meteoric surface waters that percolate down into permeable rocks and suffer changes in their isotopic compositions, either because they are heated and/or because they come into contact with easily exchangeable rocks (e.g., limestones). Inasmuch as the rocks are a great reservoir of oxygen but contain little hydrogen, these waters generally undergo only an "oxygen shift" (Craig, 1963). This "oxygen shift" almost always involves an enrichment in δO^{18} in the waters because meteoric waters are invariably much lower in O^{18} than the rocks through which they circulate.

All known geothermal waters from hot springs and geysers show an "oxygen shift" as illustrated in figure 5-1 for near-neutral, chloride-type geothermal solutions (Craig, 1963). In all such geothermal areas, the D/H ratios of the hot waters or steam are essentially identical to the local meteoric water (assuming that little evaporation has occurred). In acid-type hot springs there is commonly a slight enrichment in δD, presumably as a result of evaporation (Craig, 1963) (see figure 5-1).

A study of the Salton Sea geothermal area by Craig (1966) indicates that about 80 percent of the total 0^{18} shift occurs at temperatures below 100°C, and that at about 340°C, the $\delta 0^{18}$ value of water closely approaches that characteristic of magmatic waters. Therefore any meteoric water whose δD happens to be similar to that of magmatic water may be almost indistinguishable from true magmatic water if it has undergone a sizable 0^{18} shift. Consequently it is important to study rocks located in areas of high latitudes or altitudes in order to be able to clearly distinguish waters of meteoric origin from those of deep-seated origin.

Recently, much evidence has accumulated that exchanged meteoric water plays a significant role in determining the isotopic compositions of shallow stocks and even of portions of epizonal batholiths (Taylor and Epstein, 1968 , Taylor and Forester, 1970 , Sheppard and Taylor, 1970). Such rocks commonly have abnormally low D/H ratios, particularly if they were intruded in high-latitude localities where the meteoric ground waters are known to be isotopically light.

These heated meteoric ground waters apparently can circulate to great depths, given favorable situations. For example, in studies of the Skaergaard Intrusion, Taylor (1968) concludes that abundant meteoric water percolated down through at least 15,000 feet of jointed lavas, and exchanged with the marginal parts of the intrusion. Sheppard et al. (1969) argue that the massive clay and sericite alteration of "porphyry copper" stocks has for the most part been produced by recycled meteoric waters rather than by deep-seated primary magmatic waters. Extensive evidence thus exists to suggest that meteoric ground waters are involved in deep circulation patterns within the earth, particularly in the neighborhood of thermal anomalies where convection cells are set up.

Mixed connate and meteoric waters are very difficult to distinguish isotopically from exchanged meteoric waters. For example, the saline formation waters from different sedimentary basins in North America have been interpreted both as a mixture of meteoric and connate waters and as exchanged meteoric waters that have dissolved appreciable quantities of salts from neighboring evaporite fields.

In a study of oil-field saline formation waters of the mid-continental region of the United States, Clayton et al. (1966) conclude that these waters are predominantly of exchanged meteoric origin. Data from the Illinois Basin, Gulf Coast Basin, and Michigan Basin are illustrated in figure 5-4; they indicate that whereas the deuterium content has not been greatly altered by exchange or fractionation processes, the oxygen isotopic composition shows an 0^{18} shift similar to that observed for hot springs and geysers (see figure 5-1). Clayton et al. (1966) thus conclude that the original marine waters in these depositional basins have been almost totally lost during compaction and subsequent flushing by circulating ground waters.

Hitchon and Friedman (1969) have observed a similar trend for saline formation waters of the western Canada sedimentary basin (see figure 5-4). They conclude, however, that these formation waters originate by mixing of surface waters with marine connate waters present in the rocks, and that this could also explain the isotopic relationships in other areas, as for example the Illinois Basin waters shown in figure 5-4.

Figure 5-4. δD-δO^{18} plot for saline formational waters analyzed by Clayton *et al*. (1966), with additional data for the Alberta basin from Hitchon and Friedman (1969). The primary magmatic and metamorphic waters are discussed in figure 5-1.

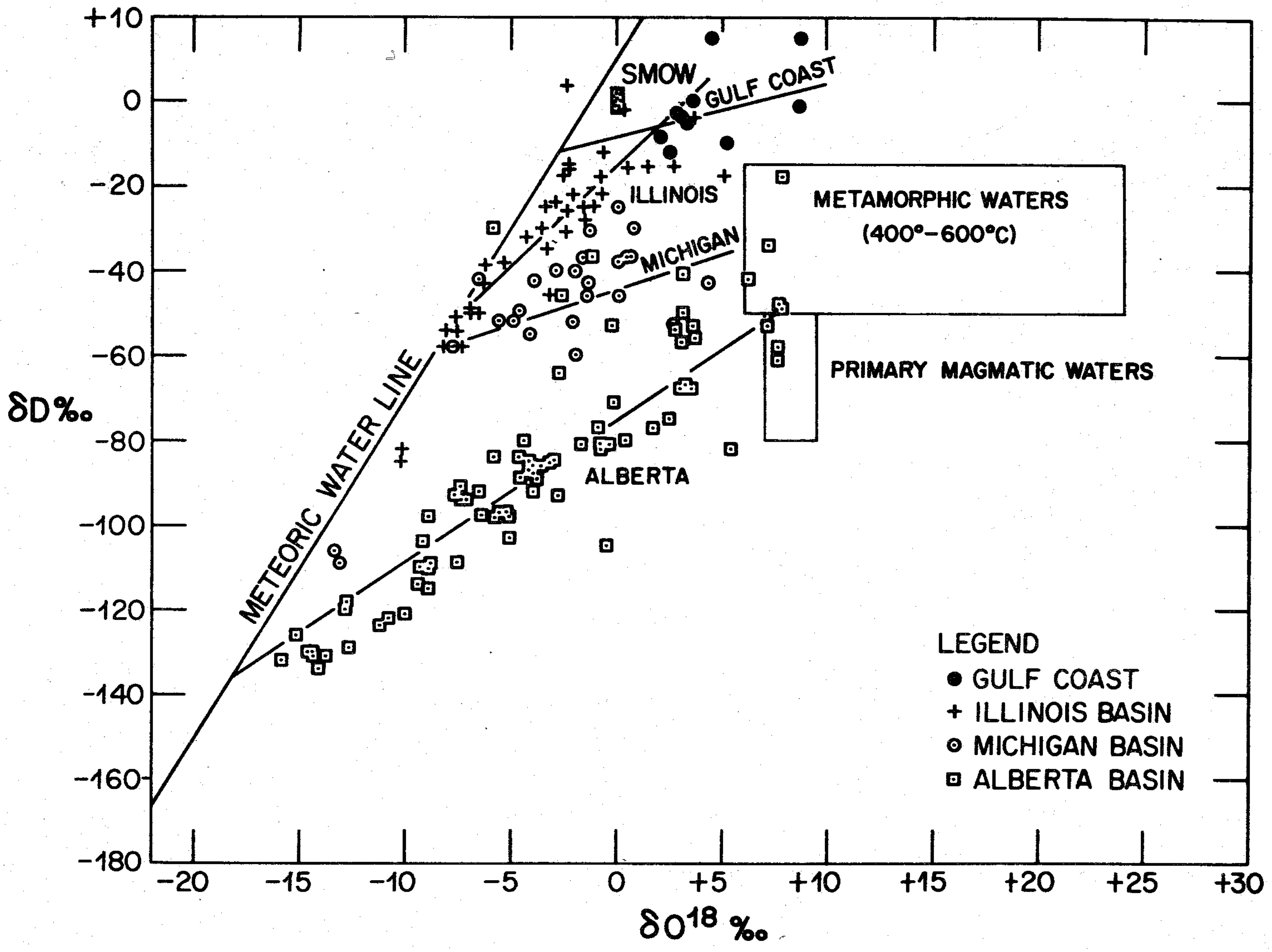
δD‰
+10
0
-20
-40
-60
-80
-100
-120
-140
-160
-180
-20
-15
-10
-5
0
+5
+10
+15
+20
+25
+30
δO18 ‰
SMOW
GULF COAST
ILLINOIS
MICHIGAN
ALBERTA
METEORIC WATER LINE
METAMORPHIC WATERS
(400°-600°C)
PRIMARY MAGMATIC WATERS
LEGEND
● GULF COAST
+ ILLINOIS BASIN
⊙ MICHIGAN BASIN
⊡ ALBERTA BASIN

Figure 5-4.

This mixing process is accompanied by an O^{18} shift due to exchange with carbonates of the basin, and some variations in δD also apparently occur because of exchange with H_2S and as a result of passage of water through micropores in shales.

It is particularly noteworthy that very sizable isotopic variations can occur in these formation waters (see figure 5-4). The Alberta basin waters, for example, vary in δD from about -135 to -20 per mil, and in δO^{18} from -16 to + 8 per mil. This means that some formational waters, even in high-latitude localities, can coincide isotopically with waters of presumed primary magmatic origin.

The studies described above clearly demonstrate that meteoric waters are involved in geologic processes in sedimentary basins over large areas and to great depths. In an analogous study of the Red Sea brines, Craig (1969) argues that these brines apparently were derived from ocean waters originating some 1000km to the south. Such waters are presumed to flow along fissures in basalts of the central Red Sea rift during a time period of the order of a few thousand years. The absence of any O^{18} shift implies, however, that temperatures were probably no higher than 100°C.

In the subsequent discussions of δD and δO^{18} in serpentines, it will be necessary to refer to figures 5-1 and 5-4 repeatedly, because all of above described types of waters that occur in the lithosphere, namely magmatic waters, primary magmatic waters, metamorphic waters, connate waters, meteoric ground waters, exchanged meteoric ground waters, mixed meteoric-connate waters, and unaltered ocean water, have to be considered as possible agents of serpentinization. The main thrust of the following discussion will be to utilize the measured δD and δO^{18} of the serpentine minerals to characterize the isotopic compositions (and hence the origin) of the waters responsible for serpentinization of ultramafic rocks.

VI. OCEANIC SERPENTINES

6.1 General statement

Serpentines and partially serpentinized ultramafic rocks have been dredged from oceanic fracture zones and trenches in many different locations throughout the world. A general list of such localities is given by Phillips et al. (1969).

In the present study, δD and δO^{18} values were measured on ten different serpentine samples from oceanic dredge-hauls at four separate sites. It is important to see whether the waters involved in serpentinization in sub-oceanic environments are isotopically different from those associated with continental serpentinites.

6.2 Previous studies

Except for a single determination (δD = -39 δO^{18}= 6.3) on a serpentine sample from St. Paul's Rocks (Sheppard and Epstein, 1970; polymorph type not reported), no previous isotopic studies have been made of oceanic serpentinites; however, certain other types of studies are pertinent to the present investigation.

Aumento (1970) made a detailed study of serpentinites dredged from an elongated, block-faulted seamount on the Mid-Atlantic Ridge at 45° N. Latitude. The geologic environment is thought to be similar to serpentine occurrences in oceanic fracture zones, where peridotite is exposed beneath an overlying basalt layer. Highly serpentinized peridotites with well-preserved relict structures, along with amphibole-bearing peridotites, are abundant in these dredge hauls. Lizardite is the most abundant serpentine polymorph, and it exhibits relatively small a- and b-cell parameters compared to most of the continental lizardites investigated. This observation led Aumento (1970) to suggest that the serpentines of oceanic origin were formed at higher temperatures than those of continental origin. He also concluded that the amount of brucite present in the serpentinite may characterize the temperature of reaction, with the absence of brucite indicating a higher temperature. Using these data in conjunction with experimentally determined serpentine dehydration reactions, Aumento (1970) concluded that the Mid-Atlantic Ridge serpentinites, which contain only small amounts of brucite, formed at about 485°C. They seem to have formed at higher temperatures than samples from the Mt. Albert intrusion in the Gaspe Peninsula, Quebec, which contain abundant brucite and which are estimated to have formed at about 400°C.

Thompson and Melson (1970), by measuring the boron contents of oceanic serpentinites and metabasalts, observed that the serpentinites were enriched in boron relative to unaltered peridotite, whereas metabasalts showed no such enrichment relative to fresh basalts. They suggest that at 300° to 500°C, boron may be preferentially partitioned into the aqueous phase. It is concluded that if sea water is involved in serpentinization, then the reaction occurred below about 200°C. Additionally it was observed that both the lithium and boron contents of basalts increase during submarine weathering, but the peridotites do not show this relationship. The serpentinized varieties are as low in lithium as the fresh peridotites.

Hess (1964), in commencing on the measured Sr^{87}/Sr^{86} values from serpentine samples from the Puerto Rican trench and St. Paul's Rocks, notes that the values show a rather wide scatter, but are higher than in modern basalt and lower than in sea water. The results suggest that the serpentine samples may have been contaminated by Sr from sea water.

Vdovykin and Dmitriyev (1968) examined the organic matter in unaltered to completely serpentinized peridotites dredged from the Mid-Indian Ridge. They observed no soluble organic material in unserpentinized peridotites and in lizardite-chrysotile type serpentinites, but did observe some in samples representing a secondary serpentinization (described as antigorite, but unsupported by x-ray diffraction analyses). They conclude that this organic matter is derived from sea water, which was responsible for the secondary serpentinization. The lizardite-chrysotile is thought to involve only juvenile waters.

6.3 Sample localities

Puerto Rican Trench

Samples of serpentine and serpentinized peridotite, together with talc, sedimentary rocks of Cretaceous and Tertiary age, and minor basalts were dredged from the north wall of the Puerto Rican trench by Bowen _et al_. (1966). From the location of the various dredge sites, they were able to construct a plausible stratigraphic sequence consisting of a basement of serpentinized peridotite and altered basalt overlain by Upper Cretaceous sedimentary rocks, which in turn are overlain by Lower Tertiary sedimentary rocks and minor basalt. Among the ultramafic rocks three types were distinguished. One type (represented by sample Ch 19 D 10-2) was collected from the contact between serpentinized peridotite and Upper Cretaceous sedimentary rocks. This serpentinite is entirely chrysotile and lizardite, and exhibits normal bastite-and mesh-textures.

A second type (represented by sample Ch 19 D 2-2) was dredged from a deeper level in the serpentinized peridotite zone. This serpentinite has an uncommon texture consisting of small anhedral isolated grains; it is composed largely of chrysotile with monor antigorite. This type of serpentinite is commonly associated with talc, and both minerals are thought by Bowen et al. (1966) to have replaced a finely granulated olivine.

A third type of sample dredged from the bottom of the main scarp is mostly antigorite and talc; however, this type was not examined in the present work.

Mid Atlantic Ridge (43°N.)

Serpentine samples dredged from the Mid-Atlantic Ridge near 43°N latitude are described by Phillips et al. (1969). Serpentinized peridotite was dredged from the flanks of the deepest depression in the vicinity of an apparent fracture zone that intersects the north-trending ridge.

To the south of 43°N, normal ridge structures are observed with a median valley, relatively low heat flow, and simple linear magnetic and topographic trends. Olivine basalts are the principal rocks dredged from the sides of this central valley. The area north of the apparent fracture zone displays a relatively high heat flow, but does not exhibit obvious magnetic symmetry elements and has no central rift. Dredge hauls in this area have revealed much serpentinized peridotite (antigorite and chrysotile with associated amphibole and talc).

Four serpentinite samples were analyzed from the northern area. They are from a 200 kg dredge haul made up only of serpentinized peridotite. Three of the samples are largely chrysotile, but one sample (A II 32-8-54) is pure antigorite.

Mid Atlantic Ridge (St. Paul's Rocks)

Serpentine samples were dredged in the vicinity of St. Paul's Rocks, a series of small islands located near the axis of the Mid Atlantic Ridge. The material exposed above the surface is composed of spinel-peridotite mylonite and hornblende mylonite which may be part of a high temperature intrusion derived from the mantle (Melson *et al.*, 1967a). According to Melson *et al.* (1967b), the ultramafic intrusion extends beneath the sea along a ridge elongated in a E. N. E. direction.

Of the two analyzed serpentinite samples, one is a completely serpentinized peridotite with normal, relatively undeformed texture (A II 20-48-1), while the other (A II 20-26-118) is a banded serpentinite-peridotite mylonite. Lizardite is the predominant serpentine polymorph in both samples, although the two samples have totally different textures and presumably different petrologic histories.

Blanco Fracture Zone

Two small serpentinite pebbles were selected for isotopic analysis from the Blanco Fracture Zone, an east-trending lineament located in the Pacific Ocean two hundred miles off the coast of Oregon. The samples are from a depth of 3600 m, and are largely made up of lizardite. However, one sample contains a significant amount of chrysotile.

6.4 Discussion of the isotope data

The isotope data for the various oceanic serpentine samples are given in figure 6-1 on a δD vs. δO^{18} plot and in the appendix section. From these data, one can note the following:

(1) As will become clear in subsequent discussion, the δD and δO^{18} values of the oceanic serpentinites form a grouping which is totally distinct from serpentines of continental origin. The δD values, in particular, are very heavy and fairly restricted ($\delta D = -31$ to -68), and the δO^{18} values are, in general, lighter than most continental serpentinites.

(2) The various textural and polymorphic types of serpentine tend to have distinctly different δO^{18} and δD values. This feature is very unlike the situation observed in most continental serpentines, where samples representative of various different genetic sequences usually have very similar isotopic compositions (compare with Franciscan samples in next section, in particular). For example, in sample A II 20-48-1, the bastites (lizardite) are 2.3 per mil heavier in δO^{18} than is the mesh-texture fractionation (lizardite, minor chrysotile), although both have similar δD values. In sample A II 32-8-22, the mesh-texture material and a cross-cutting vein (both chrysotile) have identical δO^{18} values, but differ in δD by 8 per mil.

(3) There is no correlation between the isotopic compositions and geographic locations. Four samples from a single dredge haul from

Figure 6-1. Isotopic compositions of all oceanic serpentine samples examined in this study. Tie lines connect separately analyzed textural components of the same specimen.

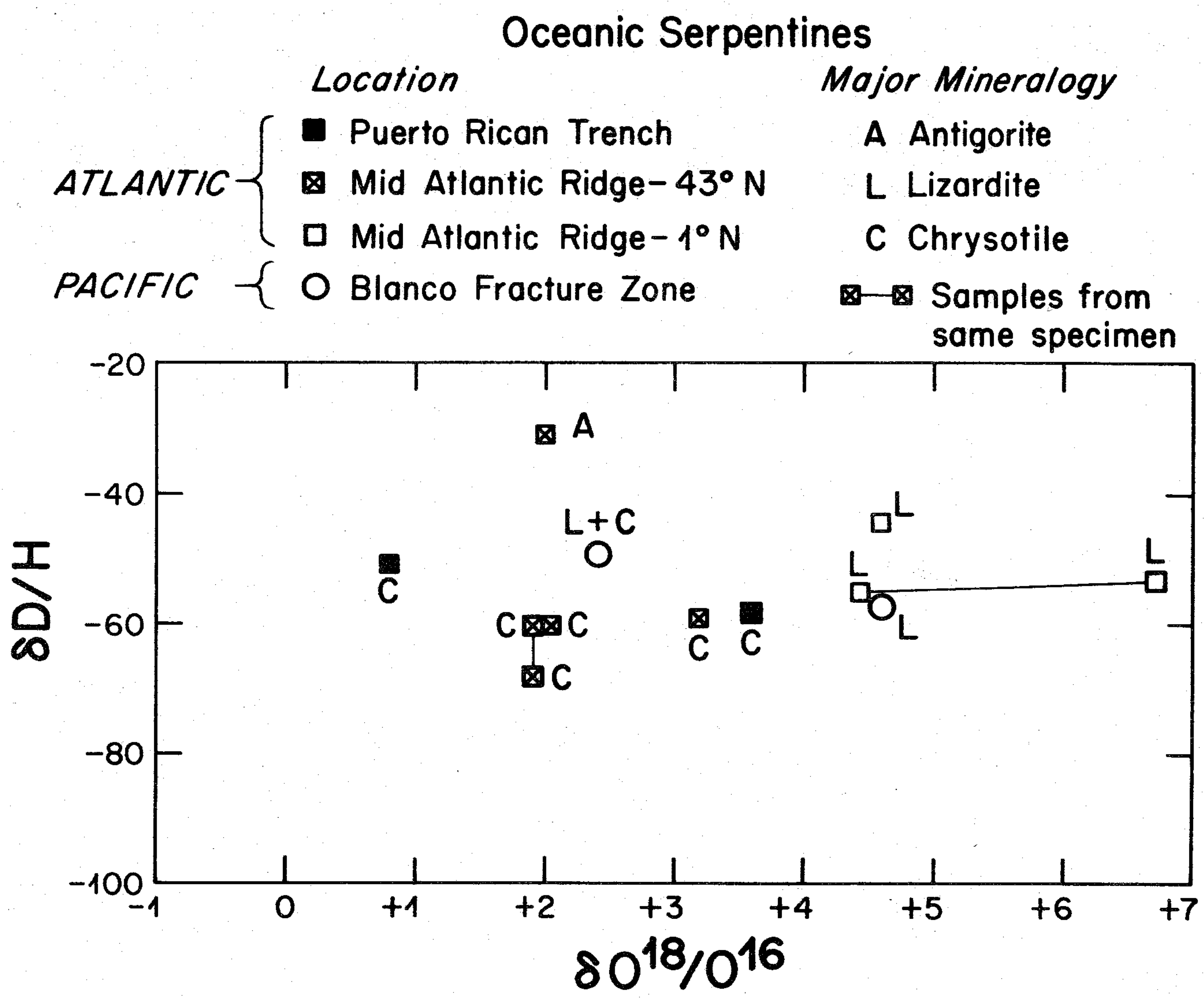
Oceanic Serpentines
Location
ATLANTIC
■ Puerto Rican Trench
⊠ Mid Atlantic Ridge-43° N
□ Mid Atlantic Ridge-1° N
PACIFIC
○ Blanco Fracture Zone
Major Mineralogy
A Antigorite
L Lizardite
C Chrysotile
⊠—⊠ Samples from same specimen
δD/H
-20
-40
-60
-80
-100
-1
0
+1
+2
+3
+4
+5
+6
+7
δO18/O16
A
L+C
C
C
C
C
C
C
L
L
L
L

Figure 6-1.

the Mid Atlantic Ridge (43°N) exhibit wide variations both in mineralogy and isotopic composition.

(4) A sample of pure antigorite (A II 32-8-54) is distinct in its hydrogen isotopic composition ($\delta D = -31$ per mil) from all the other oceanic serpentine samples as well as all continental samples. The other oceanic serpentinites are largely composed of chrysotile and lizardite, and they themselves form a very distinct grouping ($\delta D = -44$ to -68 per mil).

(5) As can be seen in figure 6-1, the $\delta 0^{18}$ values range from +0.8 to +6.8 per mil, and it appears that most of the chrysotile-rich samples are 0^{18}-depleted relative to the lizardite-rich samples.

(6) 0^{18} fractionations were measured on three samples of coexisting serpentine and magnetite (see figure 4-1). A pure antigorite sample (54) from the Mid-Atlantic Ridge (43°N) has a Δ-value of 8.2, whereas a chrysotile sample (70) from the same locality has a larger Δ-value of 10.0. Sample 118 from the Mid-Atlantic Rdige (1°N), composed of lizardite with minor chrysotile, has the largest Δ-value of 12.5.

The pure Fe compositions of magnetites from two of the samples (70 and 118, see Table 4.1), indicate that these magnetites were both probably formed during serpentinization; hence they may have attained chemical and isotopic equilibrium with their coexisting serpentine. Isotopic temperature estimates for these three samples are 235°, 185°, and 130°C, respectively (see Table 4-4). Whereas the antigorite sample gives an 0^{18} temperature (235°C) in the range for many continental antigorites (see Table 4-4), the chrysotile sample (#70) has a temperature (185°C) that is greater than all the "normal" continental lizardite-chrysotile samples (85^{o} to $115^{o}C$). The lizardite sample (#118), however, has a temperature nearly within the latter range. Estimates of the isotopic composition of water which equilibrated with the serpentines at these temperatures are: δO^{18} = +0.5, +0.3, and -0.4 per mil, respectively, and δD = 0, -23, and 0 (see Table 4-4). Considering the errors and assumptions of the calculations, these values are all essentially identical to those of ocean waters. These data are plotted in figure 6-2. The δO^{18} values of these three samples (+2.0, +3.2, and +4.6 per mil) are quite varied, yet each apparently equilibrated with a water whose isotopic composition closely approaches that of ocean water.

If we assume that _all_ other serpentine samples, for which no isotopic temperatures were obtained, also formed at temperatures suggested by the three measured samples (i.e., antigorite ~$235^{o}C$, chrysotile ~$185^{o}C$, lizardite ~$130^{o}C$), then one can estimate the isotopic compositions of waters that formed in equilibrium with these serpentines as well. This is done in figure 6-2. Essentially all of these calculated waters have δO^{18} values in the range -1 to $+1^{o}/_{oo}$, although their δD values show a greater variation from 0 to $-34^{o}/_{oo}$.

Variable water/rock ratios

Estimates of the isotopic compositions of waters initially entering the ultramafic body (δ_{wi}) can be made by means of a closed-system model that will be discussed in detail in section 7.6. This model indicates that essentially 'infinite' water/rock ratios (y/x) are required if δ_{wi} is to be identical to the δO^{18} values of waters calculated in figure 6-2. However, by choosing different water/rock ratios, other values of δ_{wi} will also be able to produce the observed serpentine δO^{18} values.

Figure 6-2. δD - δO^{18} diagram of the oceanic samples shown in figure 6-1 together with their respective calculated waters. Solid tie lines connecting the serpentines and the calculated waters are for samples whose temperatures are derived from measured serpentine-magnetite fractionations; the dashed tie lines are based on assumed temperatures of 185°C for chrysotile, 130°C for lizardite, and 155°C for lizardite + chrysotile. Note how closely the calculated waters cluster around SMOW (ocean water).

Figure 6-3. Calculated waters associated with the oceanic serpentinites assuming three different values of y/x, the water/rock ratio. The calculated ($y/x = \infty$) waters are identical to those shown in figure 6-2.

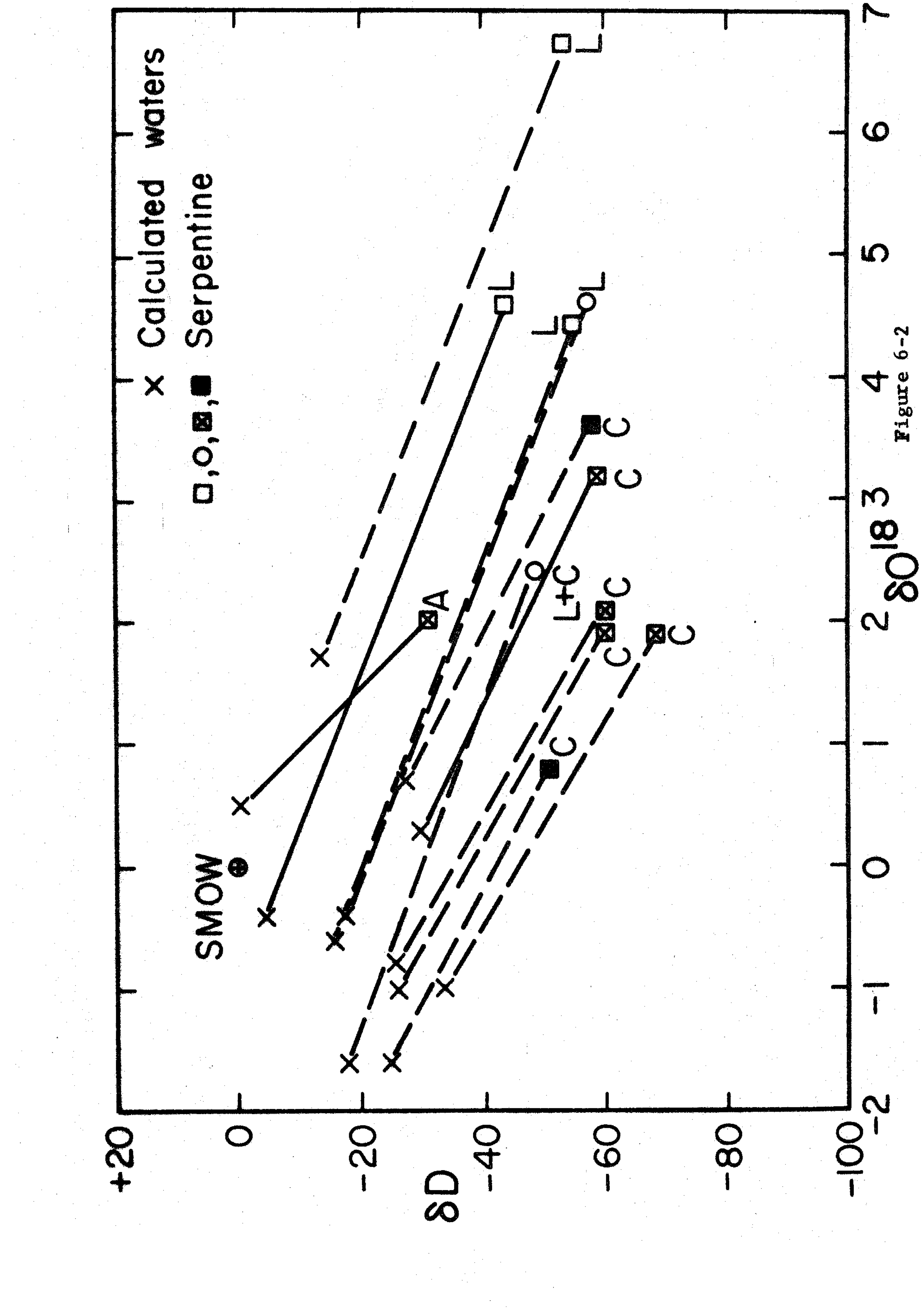
× Calculated waters
□,○,⊠,■ Serpentine
SMOW
δD
+20
0
-20
-40
-60
-80
-100
δO18
-2
-1
0
1
2
3
4
5
6
7
A
L
L
L
○L
L+C
C
C
C
C
C
C

Figure 6-2

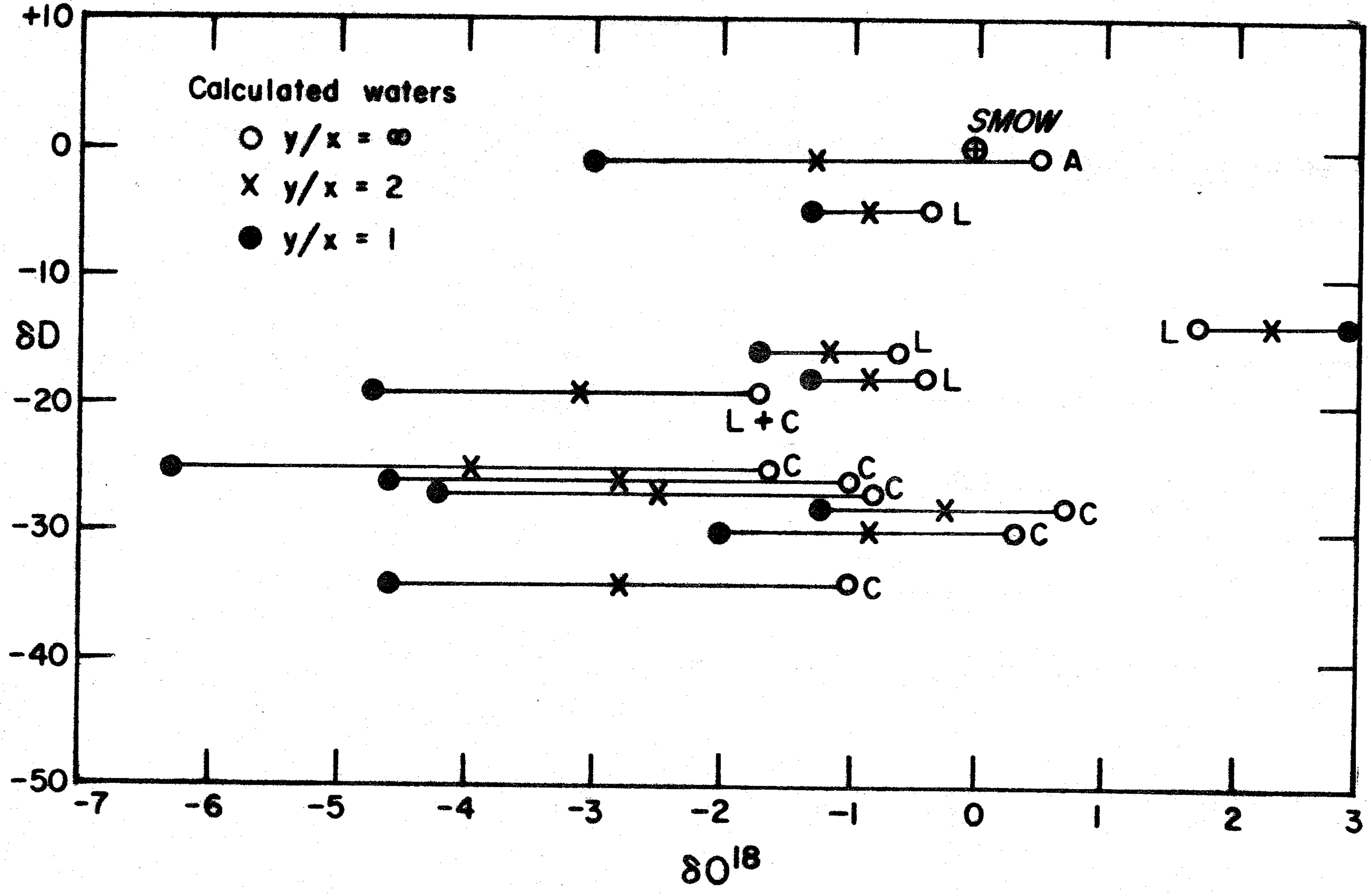
Calculated waters
○ y/x = ∞
X y/x = 2
● y/x = 1
SMOW
A
L
L
L
L
L + C
C
C
C
C
C
C
δD
+10
0
-10
-20
-30
-40
-50
δO^{18}
-7
-6
-5
-4
-3
-2
-1
0
1
2
3

Figure 6-3

In figure 6-3, the calculated ($y/x = \infty$) waters of figure 6-2 are compared with those calculated for smaller y/x ratios. This figure rather convincingly demonstrates that the water/rock ratio for most of the oceanic serpentinites must be greater than unity; many of the calculated ($y/x = 1$) waters are clearly much too O^{18} depleted to be considered as reasonable in an oceanic environment. Many of the waters between $y/x = 2$ and $y/x = \infty$, however, are within a general range suggestive of ocean water, indicating that the actual water/rock ratio may typically be greater than 2 during sub-oceanic serpentinization.

<u>Role of ocean water</u>

The narrow range of estimated δO^{18} values for the calculated ($y/x = \infty$) waters in figure 6-2 almost certainly indicates that ocean water is a major component of the water involved in sub-oceanic serpentinization, because ocean water is the only common water known to have such isotopic compositions. The small variation that does exist among these estimated δO^{18} values can also in part be explained by the fact that the actual temperatures of serpentinization may be slightly different than those assumed in figure 6-2. For example, the bastite fraction of sample 1 from the Mid Atlantic Ridge has a $\delta O^{18} = +6.7^{o}/_{oo}$. We can force the δO^{18} value of the water in equilibrium with this serpentine to exactly coincide with that of ocean water (instead of the +1.7 value in figure 6-2) by assuming that serpentinization occurred at 100°C rather than 130°C.

As was mentioned previously, the chrysotile samples are in general depleted in O^{18} relative to many of the lizardite samples, although there is some scatter in both groupings. If the serpentines all have isotopically equilibrated with a water whose major component is sea water, the chrysotile samples must have formed at significantly higher temperatures than the lizardite samples. Figure 6-1 shows that many of the chrysotile samples have $\delta 0^{18}$ values similar to the antigorite sample (54, Mid Atlantic Ridge, 43°N). This implies that the oceanic chrysotiles may form at temperatures almost as high as the oceanic antigorites, providing of course, that all samples equilibrated with ocean water.

If we assume that both the $0^{18}/0^{16}$ ratio and the D/H ratio of an oceanic serpentine are "frozen in" at the same temperature and neither are subsequently altered, one might expect <u>all</u> serpentine samples to lie along a single curve (illustrated in the δD - $\delta 0^{18}$ plot in figure 6-4) which defines the approximate δD- and $\delta 0^{18}$ -values of serpentine that have equilibrated with sea water in the temperature range 500° to 100°C. However, only two samples lie on this curve, the antigorite (sample 54) and one lizardite (sample 118). Furthermore both of these samples were selected in originally constructing the D/H fractionation curve in figure 4-4. All other serpentines lie below this curve to varying degrees.

The low δD values for many of the oceanic serpentinites suggest the possibility that most of the samples have only preserved their $\delta 0^{18}$-values, and that they may have continued to re-equilibrate their D/H values down to lower temperatures. This conclusion is based on the fact that most of the serpentine samples lie below the D/H - $0^{18}/0^{16}$ "equilibrium curve". Such samples may have formed at temperatures indicated by their $\delta 0^{18}$-values; the δD-values, however, may have continued to become lighter

Figure 6-4. $\delta D - \delta O^{18}$ diagram showing the hypothetical isotopic compositions of serpentines equilibrated with various waters that conceivably could be involved in sub-oceanic serpentinization. All calculated serpentines are shown with either a solid or shaded pattern. The possible waters under consideration are only magmatic waters and ocean water; these define an open triangular shaped band. Most actually analyzed oceanic serpentines lie relatively close to the fields of those calculated serpentines that either equilibrated with pure ocean water or with a 75% ocean water - 25% magmatic water mixture. It appears that none of the analyzed oceanic serpentines could have formed from pure magmatic waters. Note that the magmatic waters considered in this figure include slightly more O^{18}-depleted waters than the primary magmatic water discussed in chapter 5 (see discussion in text).

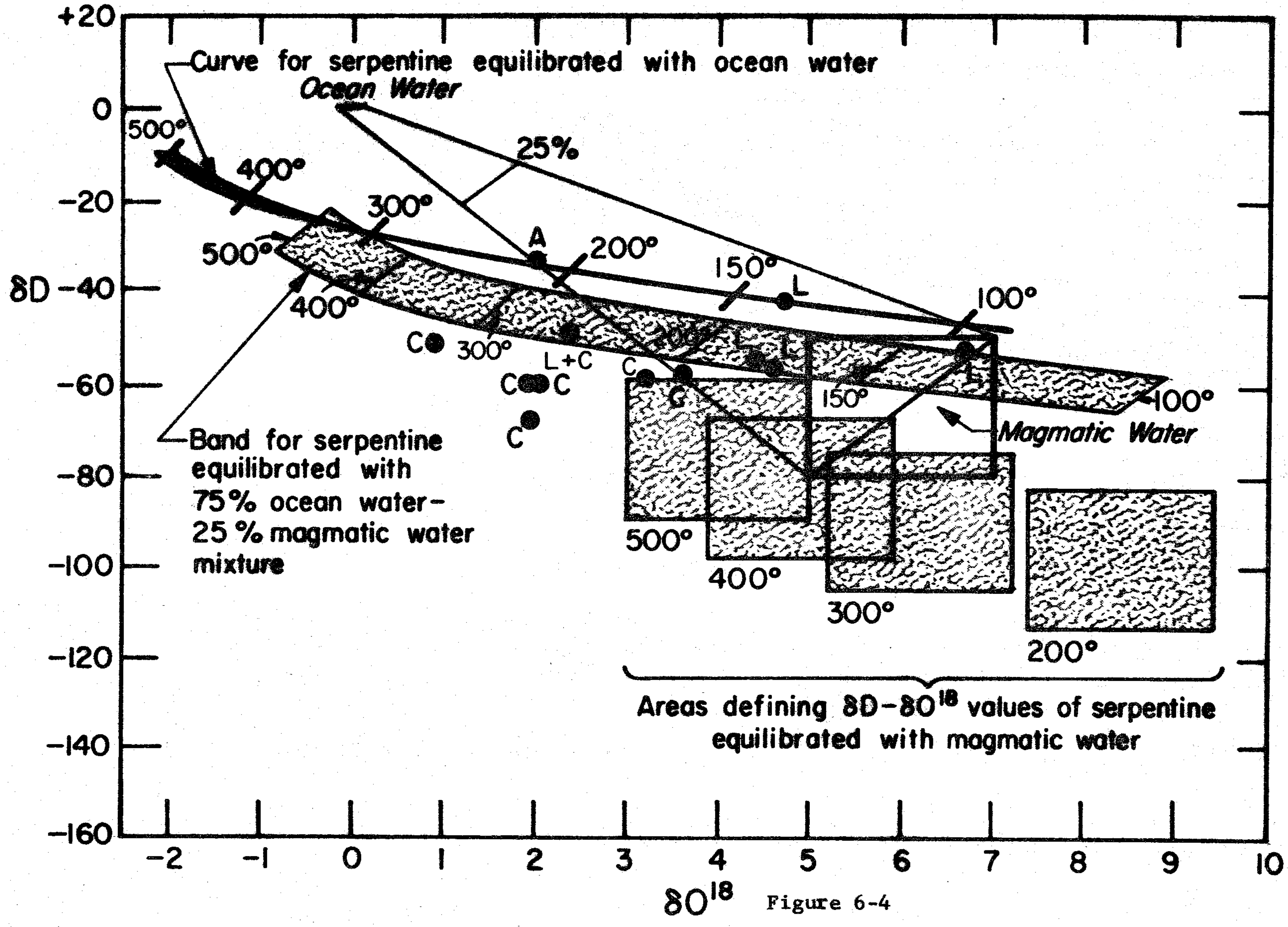
Curve for serpentine equilibrated with ocean water
Ocean Water
25%
500°
400°
300°
200°
150°
100°
A
L
500°
400°
300°
C
L+C
C C
C
C
G
L
150°
100°
Magmatic Water
Band for serpentine equilibrated with 75% ocean water– 25 % magmatic water mixture
500°
400°
300°
200°
Areas defining δD–δO18 values of serpentine equilibrated with magmatic water
δD
+20
0
–20
–40
–60
–80
–100
–120
–140
–160
δO18
–2
–1
0
1
2
3
4
5
6
7
8
9
10

Figure 6-4

through exchange at lower temperatures, moving vertically downward from the "equilibrium curve" to their present positions. This D/H - re-equilibration may have occurred to varying degrees in the different serpentine samples, since they display a spread in δD values. For example, the antigorite sample appears to have essentially "frozen in" its D/H ratio at high temperatures (ca. 235°C) in equilibrium with sea water, whereas most of the chrysotile samples may not have done so. However, for a variety of reasons that will be discussed in detail in chapter 12, D/H retrogradation down to very low temperatures appears to be unlikely.

Role of magmatic water

If the low δD-values of the calculated waters in figure 6-2 are not due to retrograde D/H exchange, these serpentines must not have formed solely from ocean water. This suggests the possibility of mixing of ocean water with water of a lower D/H ratio, such as a deep-seated magmatic- or metamorphic water. The general range of calculated isotopic compositions of serpentines formed in equilibrium both with pure magmatic water and with a mixture of 25% magmatic water and 75% ocean water is illustrated in figure 6-4. The range of pure magmatic waters given in this figure extends to lower δO^{18} values than the range shown in figures 5-1 and 5-4. This extended range includes waters that might be in equilibrium with ultramafic rocks at very high temperatures; the δO^{18} values of such waters cannot yet be exactly calculated, but they probably would lie in the range + 5 to + 6 per mil, because the δO^{18} fractionation between H_2O and olivine is probably negligible at 1200°C.

If magmatic water were the sole source of water involved in serpentinization, then the serpentines would all lie within the various areas indicated in figure 6-4; these areas indicate the isotopic compositions of serpentine in equilibrium with primary magmatic water at 200°-500°C. Only two of the oceanic serpentines examined in this study, however, lie along the outer edges of the areas indicated in figure 6-4, implying that magmatic water probably cannot be the sole constituent of any of the aqueous solutions involved in sub-oceanic serpentinization.

If serpentine were originally formed from pure primary magmatic water and later exchanged with sea water, one would expect these serpentines primarily to display heavier δD-values, since hydroxyl exchange would probably predominate. In effect, such serpentines would be expected to move nearly vertically upward from the areas indicated in figure 6-4. Such a sequence, however, does not seem likely as a general mechanism, since many of the serpentines are O^{18}-depleted relative to any serpentine equilibrated with primary magmatic water.

Several of the oceanic serpentines lie within the calculated serpentine band in figure 6-4, which is based on equilibration with a mixture of 25% magmatic water and 75% ocean water. In particular all of the lizardites and the antigorite, as well as some of the chrysotiles, either lie on the pure ocean water curve or within or very near the calculated (25%-75%) serpentine band; some of the chrysotiles, however, fall significantly below this band. It is particularly interesting that chrysotile sample 70 ($\delta D = -59$, $\delta O^{18} = +3.2$), with a calculated serpentine-magnetite temperature of 185°C, lies in near proximity to the 200°C contour on the band shown in figure 6-4. All of the lizardite samples and chrysotile samples that lie close to the band also lie at the low-temperature end of the band (< 250°C).

Several 'anomalous' chrysotiles that lie well below the calculated serpentine band would lie in near proximity to a calculated serpentine-band based on equilibration with a mixture of 50% ocean water and 50% magmatic water; however, the indicated temperatures in these cases lie above 350°C (one sample about 450°C). Inasmuch as the temperature estimates made in the present study suggest considerably lower temperatures for chrysotile, it seems unlikely that these samples formed at such high temperatures. Furthermore, for reasonable water/rock ratios ($y/x \approx 2$), the calculated waters associated with these samples have unusually low $\delta 0^{18}$ values (see figure 6-3).

The above statement, combined with the observed 0^{18}-heterogeneity of different textural components within several of these chrysotile samples, suggest the possibility that isotopic equilibrium was not attained during their formation. In particular note that two of the 'anomalous' chrysotiles in figure 6-4 are from the same hand specimen. Furthermore, one 'anomalous' chrysotile (sample Ch 19 D2-2, $\delta D = -51$, $\delta 0^{18} = +0.8$) has a truly unusual texture that is distinct from almost all other known oceanic serpentines (see Bowin *et al.*, 1966).

Possible role of metamorphic waters

If primary magmatic waters equilibrated with submarine basalts at fairly low temperatures before being involved in serpentinization (such a water, in effect, would be classified as a metamorphic-type water), then δO^{18} values might fall within the range of the calculated waters in figure 6-2. For example, a juvenile or primary magmatic water of +6.5 equilibrating with basalt at around 200°C would have a $\delta O^{18} \cong -1.2^{o}/_{oo}$, assuming that Δbasalt-water $\approx$ Δplagioclase-water $\cong +7.3$ at 200°C (extrapolation of data of O'Neil and Taylor, 1967) and that δO^{18} basalt = +6.1 (Taylor, 1968). The δD of such a water would, however, probably retain its original primary δD value (-50 to -80 per mil) upon exchanging with basalts, since these rocks generally contain little or no water. Furthermore, any primary magmatic water which would equilibrate with basalt would <u>have</u> to exchange with the basalts at temperatures very close to 200°C in order to attain a δO^{18} value similar to that of sea water; this is because mineral-water fractionations are very temperature sensitive in this general range. It is likely, therefore, that exchanged magmatic waters would show a very wide range in δO^{18}, making them unlikely candidates for sub-oceanic serpentinization.

VII. LOW-GRADE ALPINE SERPENTINE BODIES

7.1 General statement

The low-grade alpine ultramafic rock occurrences in North America and the Caribbean area are shown in figure 7-1. Alpine ultramafic intrusions are typically found along two parallel lineaments about 120 miles apart, on either side of the central axis of an orogenic belt. According to Hess (1955), ultramafic rocks are probably intruded during the first great deformation in an orogenic belt and can be used both to date and to discern the positions of ancient orogenies.

Alpine ultramafic rocks can be classified according to their associated rock types. They are divided into low- and high-temperature associations, as outlined by Wyllie (1967).

Low-grade serpentinites include bodies of peridotite-serpentinite that range in size up to several thousand square miles in area. They usually occur in conjunction with gabbros or mafic volcanic rocks. The associated country rocks are commonly greenschists, glaucophane schists, and unmetamorphosed graywackes and volcanics. Many of the serpentinite bodies are highly elongate and have contacts that are spatially related to major fault zones. Contacts of the highly sheared serpentinites generally show no evidence whatsoever of high-temperature thermal metamorphism; this suggests emplacement as relatively cold, largely solid intrusions. In some areas, well-developed metasomatic rodingite reaction zones are found along the outer contacts and at the margins of foreign inclusions; the mineral assemblages in rodingites are, however, also characteristic of relatively low temperatures (Coleman, 1967). Many of

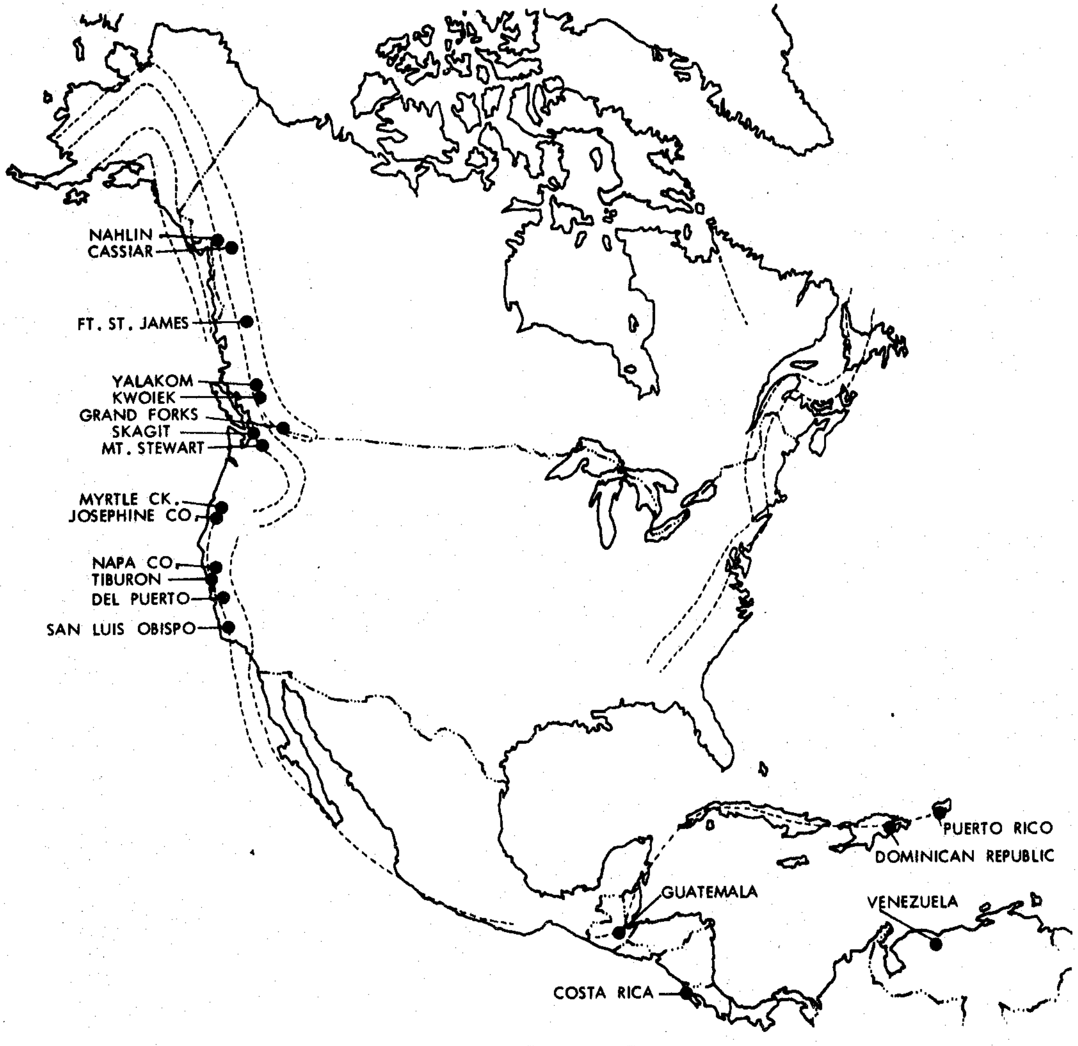

Figure 7-1.

Map of North, Central and South America showing sample localities of all serpentines discussed in chapter 7. Serpentines from low-grade terranes occur along west coast of North America and in Caribbean island arc alpine belt (modified after Hess, 1955).

the large ultramafic masses are only serpentinized along their outer borders, but most of the thinner bodies are completely serpentinized.

Examples of low-grade alpine serpentinites studied in the present work (see figure 7-1) include localities in the Franciscan formation of California; the Klamath Mountains, Oregon; Mt. Stewart, Washington; several areas in British Columbia; and scattered examples in the Caribbean island arc area and in Central America.

The higher grade metamorphic terranes from which serpentinites were studied are mainly from the Appalachian region (see the following chapter), but also from the Skagit area of Washington and from several occurrences in British Columbia.

7.2 Ultramafic bodies of the Caribbean-Central America Region

Within many island arc systems in the world, serpentinized peridotites outcrop over very large areas. For example, well-studied serpentinized ultramafic rocks occur around the perimeter of the Eastern Caribbean area in the Greater Antilles, Venezuela, and Central America (see figure 7-1).

Venezuela

Two serpentinite samples, about 2 km apart, were selected from a 4 km long body located in the Central Aragua region of Venezuela at an elevation of about 700 meters. This body occurs within a major fault zone, and probably was intruded during a period of mid-Cretaceous deformation, although post-intrusive tectonism may also have occurred (Shagam, 1960). Both samples are composed of lizardite and chrysotile, and have the same δD values (-79 and -78) within experimental error.

Costa Rica

Serpentinite and partially serpentinized peridotite samples were collected from areas along the coast of the Santa Elena Peninsula in Costa Rica (figure 7-2). These samples represent debris either from a serpentinite conglomerate, which is part of a limestone-conglomerate unit of Upper Cretaceous age (Harrison, 1949), or they are fragments directly transported from an ultramafic body that outcrops further inland.

Figure 7-2. Geologic map of the northern part of Central America (after King, 1969), showing the sample localities and the distribution of ultramafic intrusions (solid black, elongate bodies). The isotope data for the Guatemalan and Costa Rican samples are also shown.

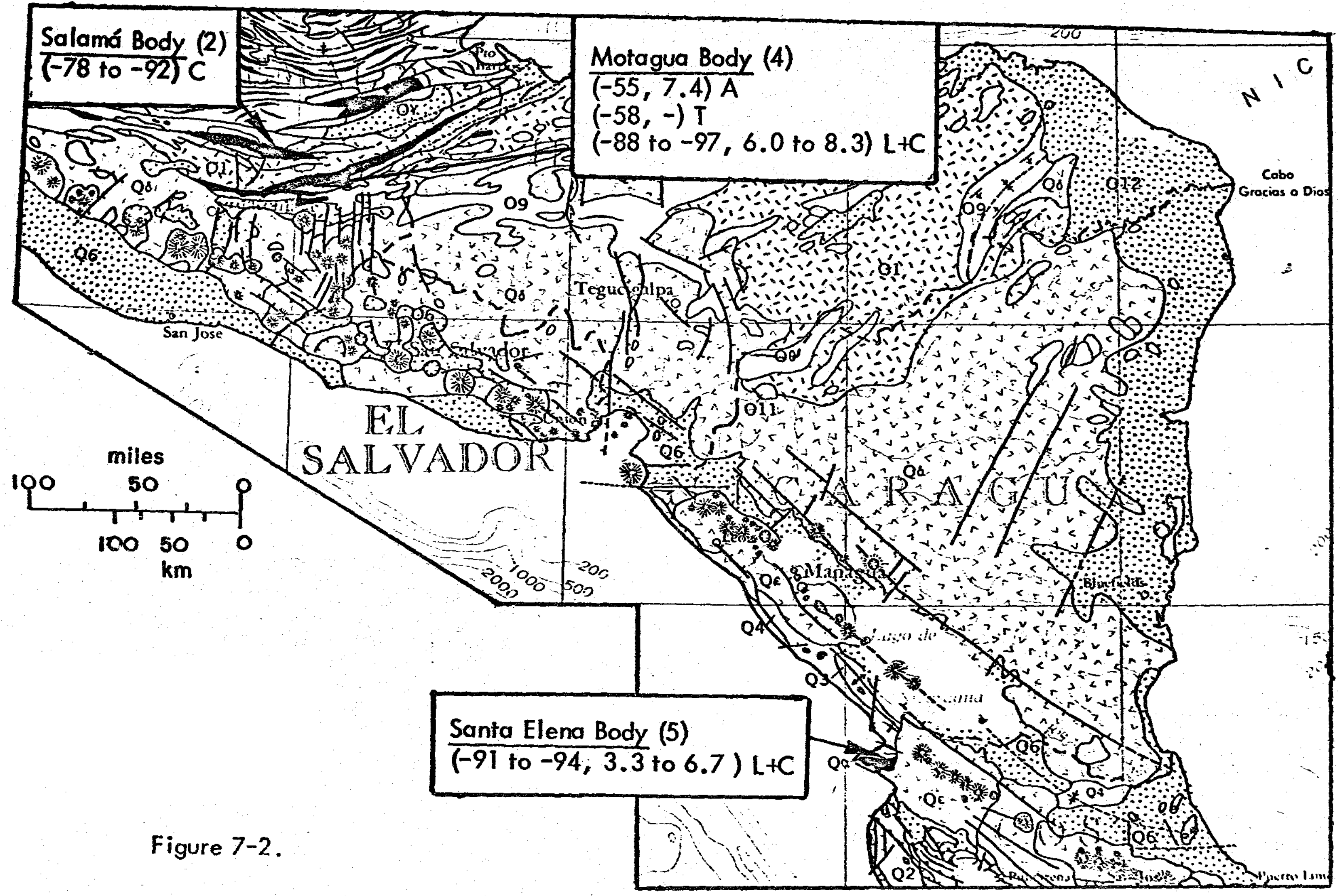
Salamá Body (2)
(-78 to -92) C
Motagua Body (4)
(-55, 7.4) A
(-58, -) T
(-88 to -97, 6.0 to 8.3) L+C
Santa Elena Body (5)
(-91 to -94, 3.3 to 6.7) L+C
N I C
Cabo Gracias a Dios
Tegucigalpa
San Salvador
San Jose
EL SALVADOR
CARAGUA
Managua
Bluefields
Lago de
miles
100
50
0
100
50
0
km

Figure 7-2.

This ultramafic mass trends E -W, in contrast to the general NW - SE regional structures in Central America. The Santa Elena peridotite mass may have been emplaced during the early stages of deformation of the Nicoya Complex (Dengo, 1962), a series of graywackes, cherts, limestones and volcanic rocks that outcrop south of the peridotite. At a later period, gabbroic dikes were intruded throughout both areas.

The mineralogical and isotopic data on these samples are given in figure 7-2 and Table 7-1. Without knowing the specific outcrops from which each sample was derived, it is difficult to interpret the δO^{18} differences. Although all the δD-values are identical within experimental error, two samples of serpentinite ($\delta O^{18} = +3.3$ and $+3.7$) are lower in δO^{18} than the serpentine in three partially serpentinized peridotites ($\delta O^{18} = +6.7$ $+6.3$ and $+5.8$).

Guatemala

The isotopic data on serpentinites in Guatemala are given in figure 7-2 and Table 7-1. Four samples were studied from a serpentinite body that occurs along the Motagua fault zone. This fault zone extends some 130 km in an easterly direction, and forms the south side of a Cordilleran system that extends towards the broad arc of the Caribbean Antilles. According to McBirney (1963), the northern margin of this serpentinite belt is a well-defined fault zone of considerable displacement, but the southern contact is obscured by younger sedimentary and volcanic rocks. In general, the ultramafic rocks of the Motagua fault zone are highly sheared and almost completely serpentinized. Samples 1 and 2 are from this sheared serpentinite zone. Sample 5 is a small

Table 7-1. Isotope data of samples from the Caribbean area.

Sample	Mineralogy*	% serp.	δD_S	δO^{18}_S	δO^{18}_M	T°C	Calculated H_2O§			Est. Pres. Day H_2O	δO^{18} H_2O
							δD	δO^{18} (y/x=∞)	δO^{18} (y/x=1)	δD†	Shift‡
Venezuela											
1	L + C	100	- 79	-	-	100	-33	-	-	-30^2	-
2	L + C	100	- 78	-	-	100	-32	-	-		-
Costa Rica											
1	L + C	70P	-	6.7	-	100	-	0.1	1.3	-30 to -40?	-
19b	L	100	- 93	3.3	-	100	-48	-3.3	-5.5		3.9
19e	L	100	-	3.7	-	100	-	-2.9	-4.7		-
36J	C > L	30P	- 91	6.3	-	100	-46	-0.3	0.5		6.7
36R	C + L	80P	- 94	5.8	-	100	-49	-0.8	-0.5		6.6
Guatemala											
1	C > L	100	- 88	8.3	-4.6	115^+	-45	2.5	5.3	-40 to -50?	9.4
2	L > C	100	- 97	6.0	-	100	-53	-0.6	-0.1		7.3
4	A	100	- 55	7.4	-	310	-24	7.4	9.3		-
5	T	-	- 58	-	-						
15	C > L	90P	- 92	-	-	100	-47	-	-		-
21	C	50P	- 78	-	-	100	-32	-	-		-

Table 7-1 (continued)

Sample	Mineralogy*	% serp.	δD_S	δO^{18}_S	δO^{18}_M	T^oC	Calculated H_2O§			Est. Pres. Day H_2O δD†	δO^{18} H_2O Shift‡
							δD	δO^{18} $(y/x=\infty)$	δO^{18} $(y/x=1)$		
Dominican Republic											
1	L + C	100	- 63	8.4	-5.3	100⁺	-16	1.8	4.7	-10	5.0
1 (x-vein)	C (x - f)	100	- 59	-	-	100	-12	-	-		-
2	L > C	100	- 71	7.7	-	100	-24	1.1	3.3		5.3
Puerto Rico											
1	L > C	100	- 66	6.7	-	100	-19	0.1	1.3	-10	3.7
2	C > L	50P	- 63	7.8	-	100	-16	1.2	3.5		4.4
3	L > C	100	- 59	8.7	-	100	-12	2.1	5.3		5.1
4	L + C	90P	- 64	8.4	-	100	-17	1.8	4.7		5.2
4 (x-vein)	C (x - f)	100	- 60	-	-	100	-13	-	-		-
5	L ≥ C	80P	- 67	7.2	-	100	-20	0.6	2.3		4.4

FOOTNOTES

Footnotes used in Tables 7-1, 7-2, 7-3, 7-4, 8-1, 8-2, 8-3, 8-4, 8-5, 9-1, 10-1, 10-2, 11-1, 11-2:

* Notation: L = lizardite, C = chrysotile, A = antigorite, C(x-f) = cross fibre chrysotile, T = talc, Tr = tremolite, Ch = chlorite, B = brucite, D = serpentinized dunite, P = serpentinized peridotite, S = silicate, M = magnetite, tr.= trace

\+ Deduced from measured serpentine-magnetite fractionations and equation 8, section 4.5. All other temperatures are assumed using the model outlined in chapter 4. ∅ = temperatures assumed identical to those of other samples from the same body.

§ Calculated waters for $y/x = \infty$ and $y/x = 1$ assuming closed-system model discussed in section 7.6.

† All δD values estimated from figure 5-2 except those from (1) Dansgaard (1964) and (2) Friedman <u>et al</u>. (1964).

‡ Magnitude of O^{18} shift that meteoric water had to undergo before entering ultramafic body - calculated by using δD value of H_2O in equilibrium with serpentine in conjunction with meteoric water equation ($\delta D = 8\delta O^{18} + 10$) to arrive at δO^{18} of pristine meteoric water. The O^{18} shift is the difference between this δO^{18} value and the calculated ($y/x = \infty$) δO^{18} of water in equilibrium with serpentine.

} denotes all samples from the same hand specimen.

talc inclusion in serpentinite collected near the Fault zone. Sample 4 was selected from a serpentinite body contained within metamorphic schist and amphibolite units north of the Motagua fault zone. This serpentinite unit is reported to be largely antigorite (McBirney, 1963).

Sample 15 and 21 are partially serpentinized peridotites from the massive Salama body lying some 15 miles north of the Motagua fault (see figure 7-2).

The samples show a wide range of δD values (-97 to $-55^{o}/oo$), but the lizardite-chrysotile samples (-97 to $-78^{o}/oo$) are clearly delineated from the antigorite and talc (-55 and -58, respectively). The general purity of magnetite obtained from one of these lizardite-chrysotile serpentines (sample 1, see Table 4-1) suggests that this magnetite was derived entirely from serpentinization, and hence was probably formed in near equilibrium with the adjacent serpentine.

Dominican Republic

Two samples located some 15 km apart were studied from the Loma Caribe serpentinized peridotite mass, a body in the Dominican Republic (figure 7-3) some 5 km wide, and about 100 km long. According to Bowin (1966), this ultramafic body was intruded into volcanic country rocks before Cretaceous times; subsequently, Lower and Upper Cretaceous volcanic rocks, limestones, and tuffaceous material were deposited upon this mass. During the Eocene, the whole area underwent faulting and minor intrusion of tonalites.

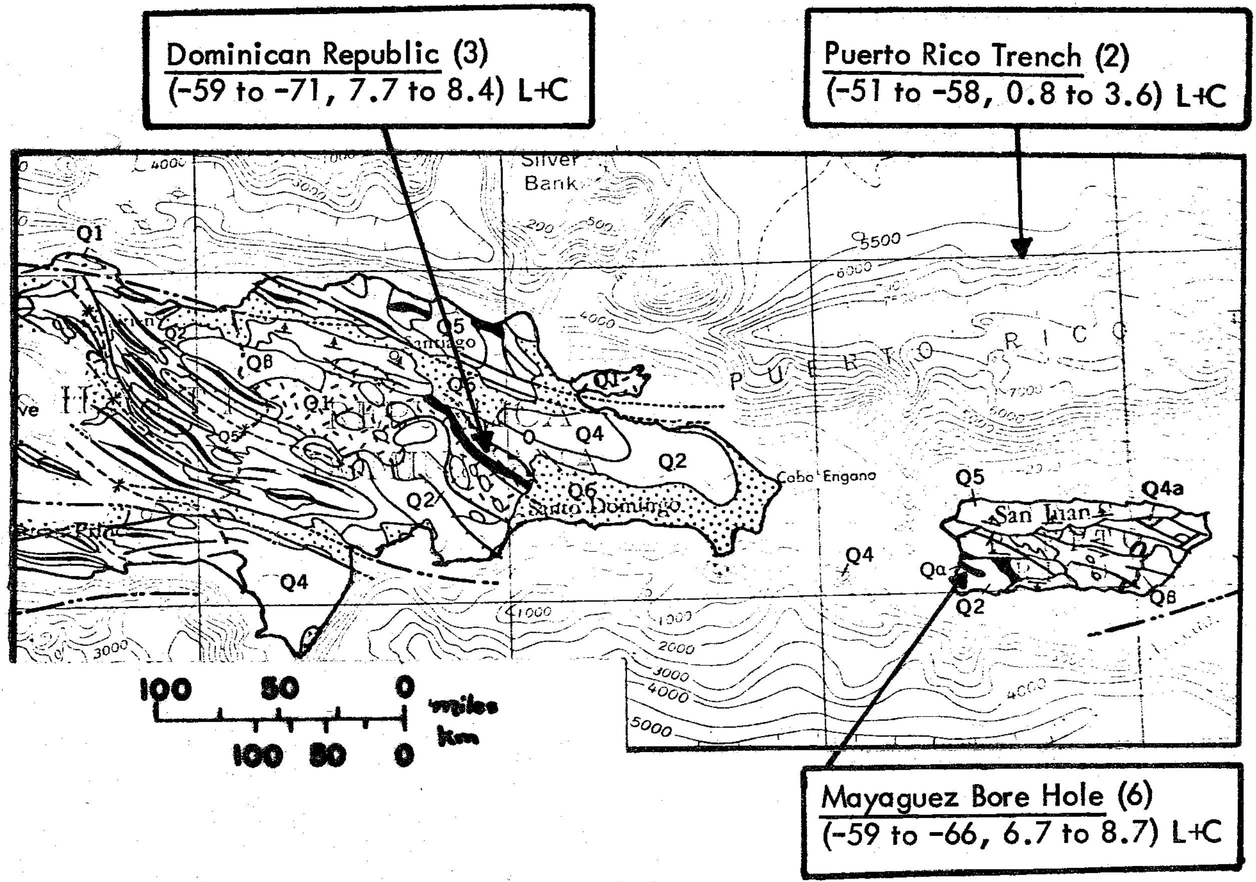

Figure 7-3.

Geologic map of the Dominican Republic and Puerto Rico (after King, 1969) showing the sample localities, isotope data, and distribution of ultramafic intrusions (solid black, elongate bodies).

The isotope data are given in figure 7-3 and Table 7-1. The two samples show only a small difference in δD (-59 to -71$^{o}/_{oo}$). It is particularly noteworthy that in one sample the δD value of a cross-fibre chrysotile vein (-59) is almost the same as that of the matrix lizardite-chrysotile (-63). The general homogeneity and purity of magnetite separated from sample 1 is strongly suggestive that equilibrium was approximately established between the serpentine and magnetite.

Puerto Rico

The Mayaguez bore hole was drilled to a depth of 305 meters in serpentinized dunite and peridotite exposed along the crest of an anticline in southwestern Puerto Rico (figure 7-3). Serpentinite, along with chert and hornblende-feldspar gneiss make up the basement section, termed the Bermeja Complex by Mattson (1960). Lying unconformably upon the complex are Upper Cretaceous sedimentary and volcanic rocks.

The ultramafic mass is 90 per cent serpentinized, consisting of about 60 per cent serpentinized peridotite (specifically diopside harzburgite) and about 35 per cent serpentinized dunite (Mattson, 1964).

The isotopic data for the bore hole samples are given in figure 7-3 and Table 7-1. The total variation in δD is exceedingly small (only 8$^{o}/_{oo}$). The δ0^{18} variation, however, is appreciable (2$^{o}/_{oo}$). The lightest serpentine δ0^{18} is from an altered dunite (10.67 meters, +6.7$^{o}/_{oo}$); the other samples are altered peridotites. The δD and δ0^{18} variations are remarkably small, considering the differences in textures, serpentine polymorph content, and primary mineral content; two samples (10.7 and 204.5 meters) are completely serpentinized, whereas three others (195.6, 303.6, and 304.7 meters) contain relict pyroxene and olivine.

Discussion of the Caribbean-Central America serpentines

From a summary of the isotopic data in Table 7-1, we see that serpentine from the Caribbean-Central America region shows a total variation in δD of -55 to -97 and in δO^{18} of +3.3 to +8.7. The δD values of lizardite-chrysotile samples from Venezuela (-78 to -79), Costa Rica (-91 to -94), and Guatemala (-78 to -97) are definitely lighter than those from the Dominican Republic and Puerto Rico (-59 to -71).

The calculated isotopic compositions of waters which may have coexisted in equilibrium with these lizardite-chrysotile type serpentines show a similar pattern. The calculated waters for the Puerto Rico and Dominican Republic samples (δD = -12 to -24, δO^{18} = +0.1 to +2.1) are consistently isotopically heavier than those for the Guatemala, Costa Rica, and Venezuela samples (δD = -32 to -53, δO^{18} = +0.1 to -3.3, with one value of +2.5).

These isotopic variations are consistent with the presumed isotopic pattern in meteoric waters throughout these regions, since the two former localities are both tropical islands. Such islands (e.g. Hawaii, see Dansgaard, 1964) typically have rainfall with δD = -5 to -20. The calculated waters are in all cases considerably richer in deuterium and depleted in O^{18} relative to typical magmatic waters.

Differences in δD values among individual samples from the same locality, as for example samples 1 and 2 from the Rio Motagua area of Guatemala, suggest, however, that if only meteoric ground waters were involved, then serpentinization probably occurred during different time periods or during a period when the isotopic compositions of the local meteoric ground waters were changing (e.g., by changes in climate and/or elevation). The two low-0^{18} lizardites from Costa Rica (19b and 19e), for example, _must_ have formed either from abnormally low-0^{18} waters (practically unexchanged meteoric waters?) or at considerably higher temperatures than the assumed 100°C.

The δD values of samples from Dominican Republic and Puerto Rico are very similar to the lizardite-chrysotile serpentines dredged from deep-oceanic environments (see chapter 6), but the $\delta 0^{18}$ values are generally somewhat heavier. The calculated waters associated with the Caribbean island samples (+0.2 to +2.2) are, however, almost identical to ocean water. Such waters, therefore, may be either of exchanged meteoric origin or of ocean water origin, or perhaps a mixture of both types, inasmuch as the isotopic compositions of the two kinds of waters are not markedly different in tropical island areas. In either case, the waters appear to have undergone some exchange with rocks of the immediate environment before being involved in serpentinization.

Assuming that only meteoric waters were present in the fluids involved in serpentinization of the Caribbean-Central America serpentines, these waters must have undergone an 0^{18} shift of about 3.7 to 9.4 per mil. The calculated 0^{18}-shift for the Puerto Rico and Dominican Republic samples (3.7 to 5.3) is more uniform and smaller than that observed for Costa Rica (3.9 to 6.7) and Guatemala (7.3 to 9.4). The narrow variation displayed by waters from Puerto Rico is consistent with the fact that these samples are located within a single body.

The estimated isotopic composition of water assumed to be in equilibrium with antigorite sample 4 from Guatemala is distinct from all others ($\delta D = -24$, $\delta O^{18} = +7.4$); this isotopic composition, as well as that of the water from which the talc of sample 5 crystallized, is suggestive of a deep-seated metamorphic origin. For example, it is almost identical to the calculated water involved in the blueschist metamorphism of Franciscan rocks in California (see next section). This sample may therefore have formed during the regional metamorphism which affected the general terrane north of the Motagua fault zone. In any case, the serpentinization of this body would appear to be unrelated to the lizardite-chrysotile type serpentinization of the ultramafic rocks in the Motagua fault zone immediately to the south.

7.3 Franciscan serpentines

The Franciscan formation (Bailey, 1964) consists of a heterogeneous assemblage of eugeosynclinal rocks located in the Coast Ranges of California. The predominant rock type is graywacke, but shale, altered mafic volcanic rock (greenstone), chert, and minor limestone form a part of the stratigraphic sequence. Also included are metamorphic rocks of the zeolite, blueschist, and ecologite facies.. Ultramafic rocks, largely serpentinized, are intruded into most of the above rock types.

Most of the Franciscan ultramafic bodies were originally intruded during or subsequent to the deposition of the Franciscan formation, but prior to the Upper Cretaceous (Bailey et al., 1964).

San Luis Obispo Serpentinite

Several samples were collected for isotopic analysis from a small roadcut exposure that transects the SW contact of an 8 mile by 1½ mile body of serpentinite, just north of San Luis Obispo (see figure 7-4). The samples do not contain any relict olivine or orthopyroxene, but they do contain small percentages of chromite. The sheared portions of the serpentinite are finely granulated and probably developed from the blocky serpentinite during faulting. The contacts of the blocky serpentinite consist of numerous slickensided surfaces, and the contact between the serpentinite and the highly sheared volcanic country rocks is sharp. This serpentinite body is fairly typical of the numerous highly sheared masses which occur throughout the Franciscan Formation.

The different serpentine mineralogies and textural forms in this roadcut presumably represent many different events. Nevertheless, the total range of δO^{18} is only 1.3°/oo, and that of δD is only 9°/oo, even though the samples represent both the blocky and sheared serpentinite and include a wide range in the proportions of lizardite and chrysotile.

Sample 4 (figure 7-4), for example, consists of mesh-texture serpentine and bastite, where about half of the mesh-texture serpentine has been replaced by late-stage chrysotile veins; the bastite contains only minor quantities of late-stage veins. Even so, the bastite is identical in δD and is only 0.5°/oo heavier in δO^{18} than this mesh-texture serpentine.

Thus, despite the obvious differences in serpentinization history represented by the different samples shown in figure 7-4, the isotopic

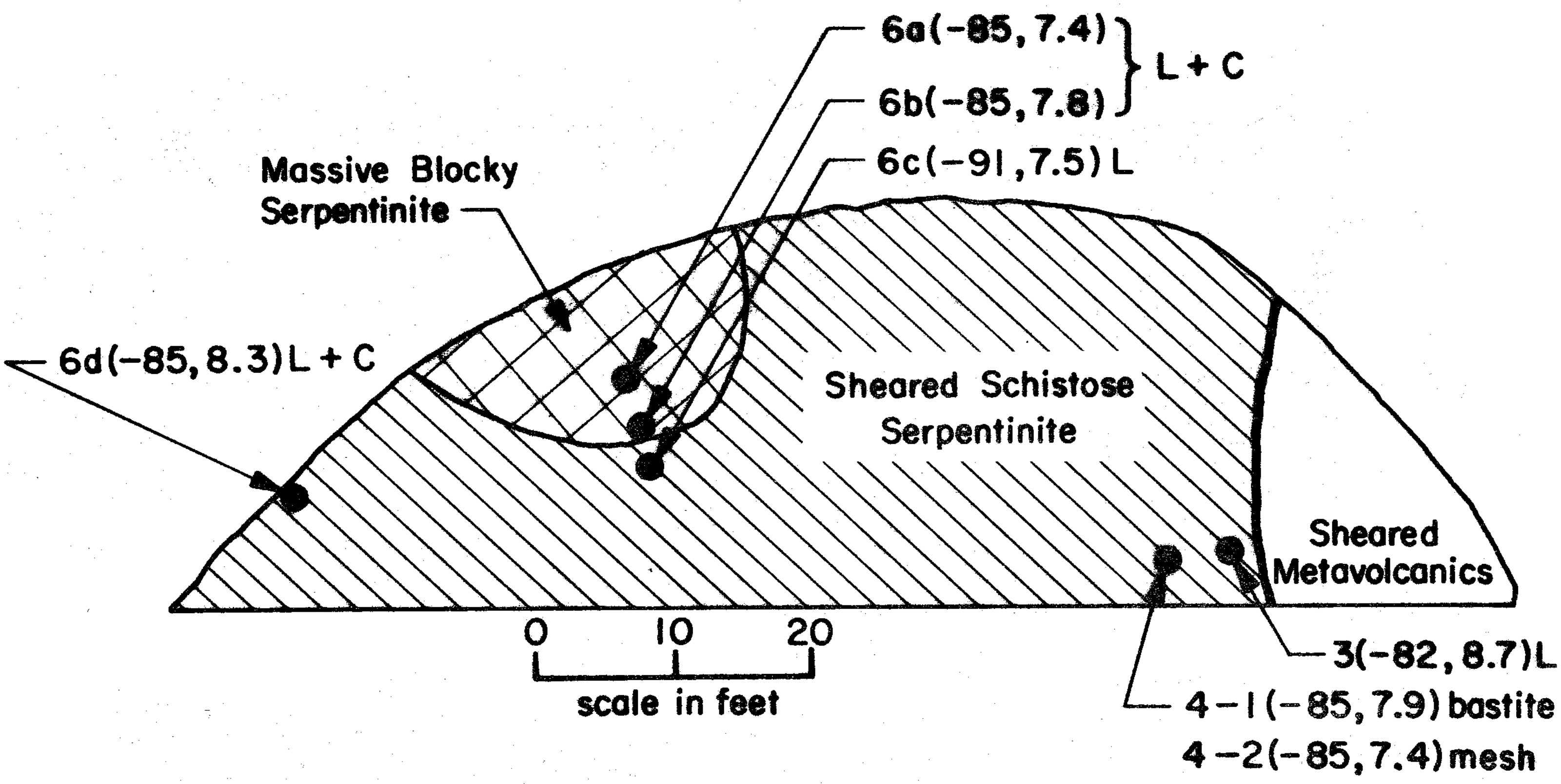

Figure 7-4.

Field sketch (vertical) of a SE-facing roadcut exposure of serpentinite just north of city limits of San Luis Obispo, California on U.S. highway 101 (35° 20' latitude, 120° 40' longitude). Also included are the isotope data for each analyzed sample.

compositions of the varous samples are quite uniform. However, it does appear that both the weathered serpentinite and the serpentinite next to the outer contact (samples 6d and 3) are systematically about 0.5 to $1.0^{o}/_{oo}$ heavier in δO^{18} than samples from the interior portion of the body, perhaps due to small amounts of deweylite (see section 11.3). The general chemical purity of the magnetite in sample 6 suggests that the magnetite and serpentine in this sample may have formed in near equilibrium.

Del Puerto Ultramafic Body

Various serpentinites and partially serpentinized peridotites and dunites were studied from the Del Puerto Ultramafic Body. This body at present lies in the eastern side of the California Coast Ranges at an altitude ranging from about 1400 to 3600 feet. The geologic setting of this body is discussed by Maddock (1964), and summarized by Saad (1969).

It is a slab-shaped body emplaced in the center of a large syncline roughly parallel to the strike of the adjoining Franciscan sediments. The intrusion is bounded on the E by the Tesla-Ortigalita fault, and the other sides of the body are also believed to be fault contacts.

Contact metamorphism is slight to non-existent. Dunite, about 85% serpentinized, occurs in the eastern part of the intrusion, while the rest of the intrusion is serpentinized peridotite. Various other serpentinite bodies also occur throughout the general area.

From studies of partially serpentinized rocks, Saad (1969) was able to demonstrate that a chemical remanent magnetism was acquired during serpentinization. Furthermore, he was able to conclude, from a study of the stable directions of magnetization, that serpentinization occurred after final emplacement of the ultramafic rocks, but prior to folding.

From the apparent polar locations of three different sites, Saad (1969) also concluded that serpentinization occurred in the sequence (1) body margins, (2) peridotites, (3) dunites, and (4) pyroxenites. This serpentinization sequence may possibly have extended from post-Franciscan to the Eocene (Saad, 1969, p. 6577). The samples shown in figure 7-5 represent the first three of the four types of samples studied by Saad. However, Saad (1969) made no distinction concerning the various polymorphic forms of serpentine. His data probably refer only to lizardite-chrysotile serpentinization.

The isotopic data and locations of the various samples studied are given in figure 7-5. The δO^{18} and δD variations in the serpentine are much greater than at the single roadcut exposure near San Luis Obispo. The total variation for hydrogen is $46^{o}/_{oo}$ and that for oxygen is $2.2^{o}/_{oo}$.

The bulk of the serpentinite from the major ultramafic body is largely lizardite and chrysotile with a uniform δD of -108 to $-93^{o}/_{oo}$. However, the small outlying serpentinite body (location 2, figure 7-5) is almost entirely antigorite with $\delta D = -62$. The general chemical purity and homogeneity of the magnetite from this latter sample suggests that the serpentine and magnetite may have formed together in equilibrium.

Sample 8, composed of a mixture of antigorite and lizardite, has a δD value (-74) intermediate between that of the pure antigorite and

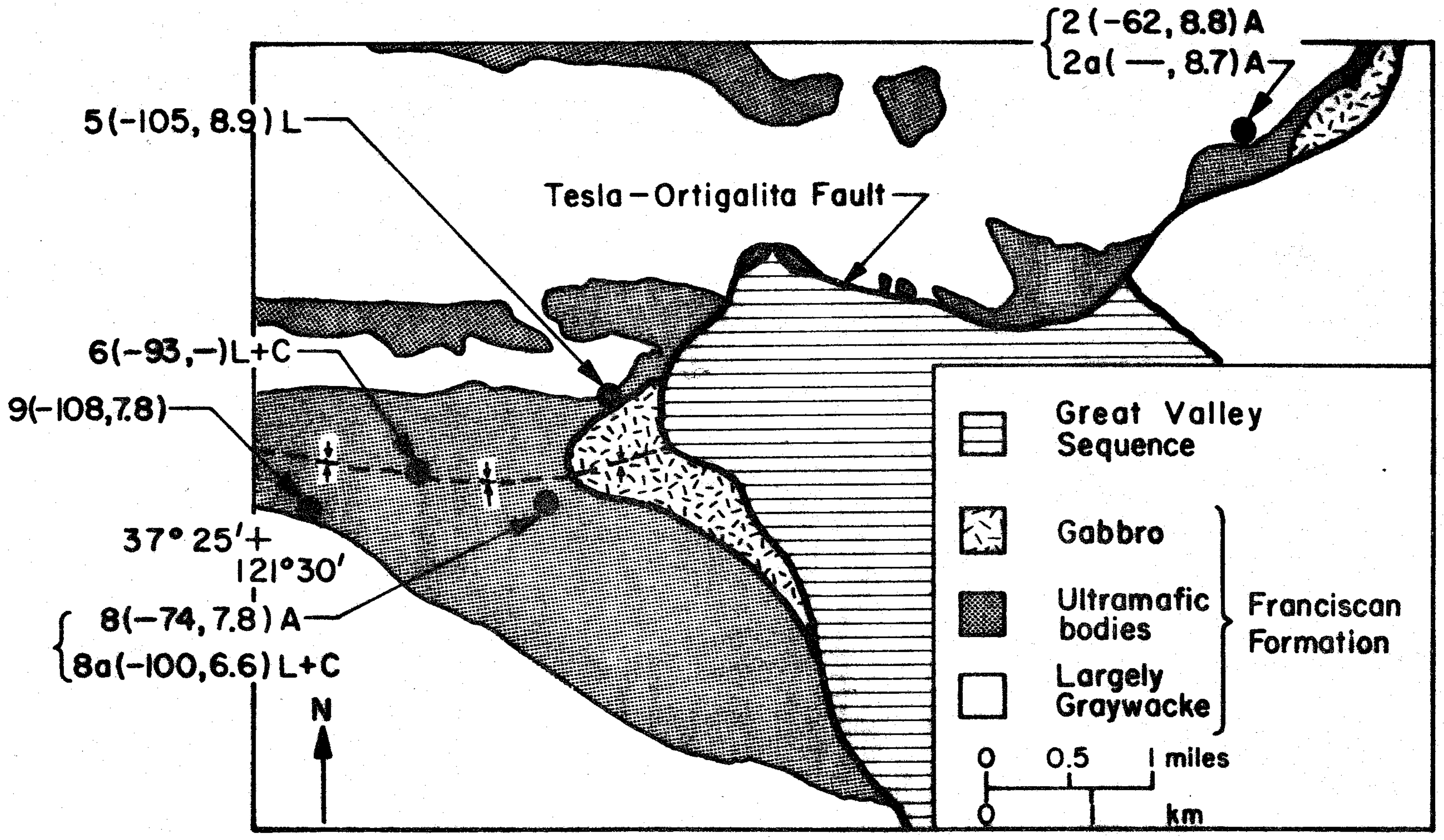

Figure 7-5.

Geologic map of Del Puerto ultramafic body and vicinity, California (after *Maddock*, 1964), showing sample localities and isotope data.

pure lizardite-chrysotile. This suggests that we may be simply dealing with two isotopic end-members, an antigorite with $\delta D \approx -60$ and a chrysotile with $\delta D \approx -100$.

The δO^{18} values of the various serpentine samples are much more uniform than the δD values, although there appear to be several discrete groupings, with the serpentine derived from dunites being lighter ($+6.6^{o}/_{oo}$) than that from peridotite ($+7.8^{o}/_{oo}$). This effect conceivably could be due in part to original oxygen isotope differences in the parent materials, because pyroxene is invariably richer in O^{18} than coexisting olivine (Taylor and Epstein, 1962).

On the other hand, the δO^{18} variations may be principally a function of position of the sample within the ultramafic body. The lowest-O^{18} samples occur in the interior portions of the main ultramafic body. The serpentines from the outer margins of the main body and from the small outlying mass are 1.0 to 3.3 per mil heavier. These differences might have been brought about in part by a larger volume of water circulating through the outer margins of the ultramafic body. As the water/rock ratio increases, the δO^{18} values are determined more by the δO^{18} of the extraneous H_2O than by that of the parent ultramafic body.

Tiburon Peninsula

A small, well-exposed, sheared serpentinite lens on the Tiburon Peninsula was studied in detail by Page (1968). Three samples were analyzed from this body (figure 7-6). This sheared serpentinite lens is similar in general appearance to the exposure at San Luis Obispo.

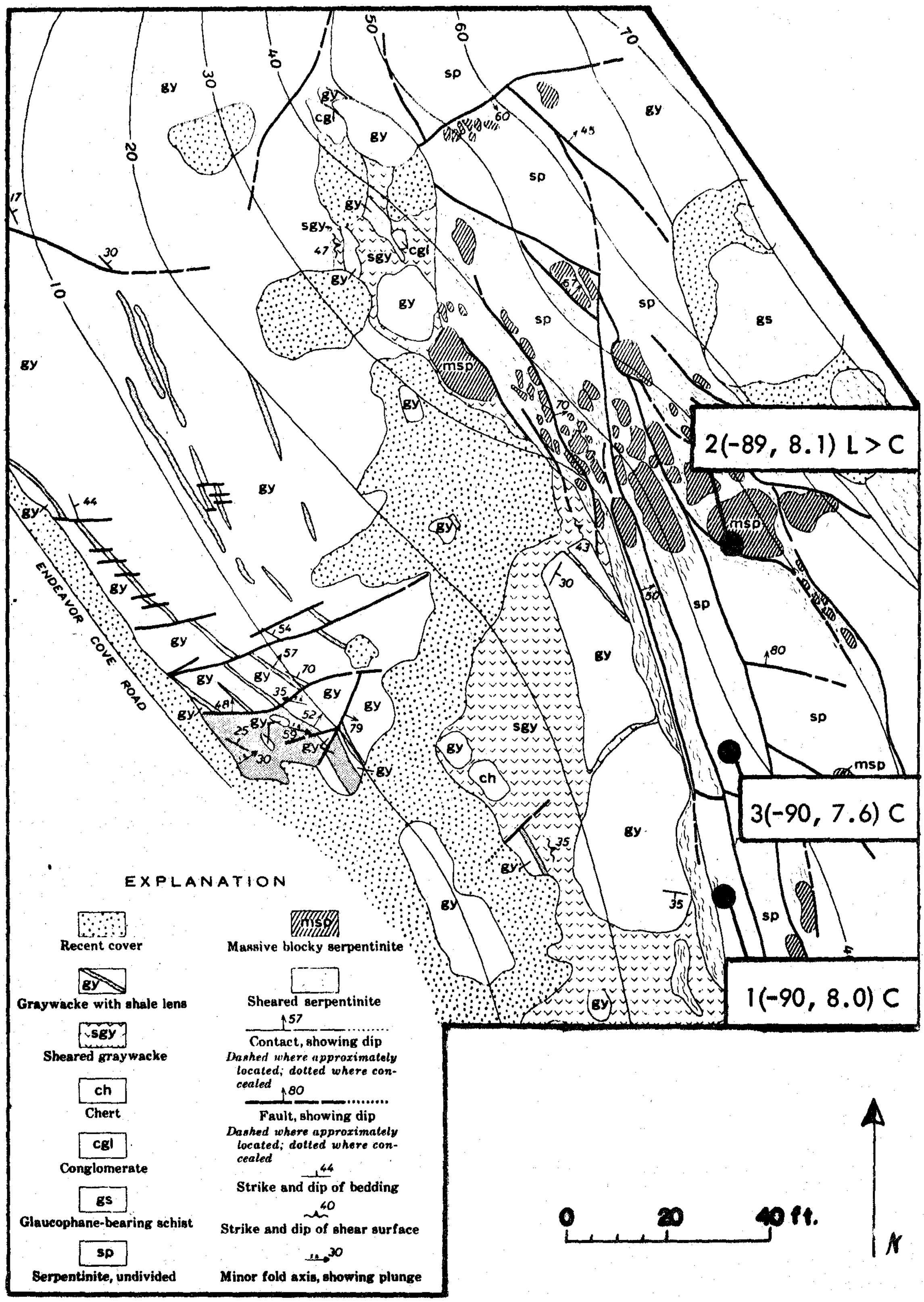

Figure 7-6.

Geologic map of a sheared serpentinite lens on the Tiburon Peninsula, California (after Page, 1968), showing sample locations and isotope data (122° 30' longitude, 37° 55' latitude).

From textural relations, Page (1968) deciphers the following genetic sequence of serpentine types:

(1) bastite and mesh-texture serpentine form simultaneously at various early stages of the serpentinization process;

(2) chrysotile veins begin to form and this continues through many later stages;

(3) platelets of lizardite replace mesh-texture serpentine and bastites;

(4) late chrysotile and lizardite veins cut the above rock types.

From the δD and δO^{18} data presented in figure 7-6, it is apparent that the isotopic compositions of the three samples are exceedingly uniform. This isotopic uniformity contrasts with the heterogeneity of the textural forms of serpentine. For example, sample 2 contains about 25% platy lizardite (stage 3 above) set in a mesh-texture and bastite matrix (stage 1, see Plate 3-3), whereas sample 1 is blocky chrysotile and sample 3 is fine-grained, highly sheared chrysotile (stage 2?). Furthermore, the general chemical homogeneity of the magnetite from samples 1 and 2 and the similarity of the serpentine-magnetite fractionations all suggest that a close approach to isotopic equilibrium has been achieved.

Napa County

A sample of serpentinite, composed of lizardite and minor chrysotile, was collected 10 feet from the contact between a highly sheared serpentinite body and a volcanic unit in Napa County. The isotopic composition ($\delta D = -93$, $\delta O^{18} = +7.3$ per mil) is almost identical to that of the sheared serpentinite body of the Tiburon Peninsula.

Discussion of Franciscan isotope data

The isotopic data for all the California samples are summarized in Table 7-2. The three Franciscan serpentinite bodies from San Luis Obispo, Tiburon, and Napa County are all remarkably uniform in δO^{18} and δD, despite the fact that each has undergone a complex history of serpentinization. The δD-values show a slight decrease as one moves north, but all lie in the range -82 to -93. Also, the δO^{18} values vary only from +7.3 to +8.7, and the average δO^{18} difference between the three bodies is less than the measured variation in the single body at San Luis Obispo.

Most of the serpentinization of these three bodies must therefore have been brought about by waters that had a narrow range of isotopic compositions. This implies either that serpentinization occurred in a fairly restricted environment or that all the early serpentine was completely recrystallized and exchanged during the later episodes, thus destroying any isotopic records of a different environment.

The calculated δD values of waters assumed to have coexisted in equilibrium with these serpentines range from -36 to -48 (see Table 7-2). These values are somewhat heavier than those of the present-day meteoric waters in these areas, except perhaps for the single sample from Napa County. They are also, however, heavier than typical magmatic waters. The isotopic data are compatible with meteoric ground waters having been involved in the serpentinization if (1) there was some mixing with more D-rich marine connate waters or if (2) more ancient meteoric waters (Tertiary?) were involved, perhaps derived during a warmer climatic period.

Table 7-2. Isotope data of samples from the California Franciscan formation.

							Calculated $H_2O^§$			Est. Pres. Day H_2O	δO^{18}
Sample	Mineralogy*	% serp.	δD_S	δO^{18}_S	δO^{18}_M	T°C	δD	δO^{18} ($y/x=\infty$)	δO^{18} ($y/x=1$)	δD†	H_2O Shift‡
San Luis Obispo											
3	L	100	- 82	8.7	-	100	-36	2.1	5.3	-55	7.9
4 (total)	L + C	100	- 85	7.5	-	100	-39	0.9	2.9		7.0
4a (bastite)	L	100	- 85	7.9	-	100	-39	1.3	3.7		7.4
4b (mesh texture)	L + C	100	- 85	7.4	-	100	-39	0.8	2.7		6.9
6a	L + C	100	- 85	7.4	-	100	-39	0.8	2.7		6.9
6b	L + C	100	- 85	7.8	-	100	-39	1.2	3.5		7.3
6c	L > C	100	- 91	7.5	-7.6	85^+	-45	-0.2	1.8		6.7
6d	L + C	100	- 85	8.3	-	100	-39	1.7	4.5		7.8
Del Puerto											
2	A	100	- 62	8.8	-	225	-30	7.0	10.3	-70	-
2a	A	100	-	8.7	0.1	225^+	-	6.9	10.1		-
5	L > C	100	-105	8.9	-	100	-60	2.3	5.7		11.1
6	C > L	50D	- 93	-	-	-	-48	-	-		-
8	A > L	100	- 74	6.8	-	-	-	0.2	1.5		-
8a	L + C	70D	-100	6.6	-	100	-55	0.0	1.1		8.1
9	L + C	30P	-108	7.8	-	100	-63	1.2	3.5		10.3

Table 7-2 (continued)

Sample	Mineralogy*	% serp.	δD_S	δO^{18}_S	δO^{18}_M	T°C	Calculated H_2O§ δD	Calculated H_2O§ δO^{18} (y/x=∞)	Calculated H_2O§ δO^{18} (y/x=1)	Est. Pres. Day H_2O δD†	δO^{18} H_2O Shift‡
Tiburon											
1	C	100	- 90	8.0	-6.1	95+	-45	1.0	3.5	-35	7.9
2	L > C	100	- 89	8.1	-5.7	100+	-44	1.5	4.1		8.3
3	C	100	- 90	7.6	-	100	-45	1.0	3.1		7.9
Napa County	L > C	100	- 93	7.3	-	100	-48	0.7	2.5	-50	7.9

From the isotopic equation for unexchanged meteoric waters ($\delta D = 8\ \delta 0^{18} + 10$), we calculate that the original $\delta 0^{18}$ of this ancient "meteoric water" could have been about -5.8 to -7.2. An 0^{18} shift of about 7 °/oo towards heavier $\delta 0^{18}$ values therefore would have had to occur in these waters; this, however, is not at all unusual for geothermal waters (Craig, 1963). Also this $\delta 0^{18}$ shift would have to have been relatively uniform at 6.7 to 8.3 in all these bodies; this is conceivable if the temperatures of serpentinization were very uniform, because all these serpentine bodies occur within the same type of terrane. As was noted in Chapter 4, two samples from the Tiburon body and one from San Luis Obispo suggest serpentinization temperatures of 85° to 100°C.

The Del Puerto body is isotopically distinct from the other three Franciscan serpentinite bodies. Its chrysotile-lizardite is definitely more depleted in δD by about 10 to 20 per mil, and it shows a larger $\delta 0^{18}$ variation than all of the other three bodies put together. In addition, this body contains antigorite-rich zones which are isotopically unique, with a much higher δD than any of the chrysotile-lizardite samples from California.

The calculated isotopic compositions of waters assumed to have coexisted in equilibrium with these Del Puerto serpentines show a wide variation. For the lizardite-chrysotile samples, these waters exhibit isotopic values ($\delta D = -48$ to -63, $\delta 0^{18} = 0$ to $+2.3$) that are distinct from those associated with the antigorites ($\delta D = -30$, $\delta 0^{18} = +6.9$ to $+7.0$). The antigorites must therefore, have formed from different types of waters and/or under much different P-T conditions than the lizardite-chrysotile.

The antigorite both within the main body and in the small, outlying body, may have been formed at depth before these bodies were brought closer to the surface through tectonic movements. The above data suggest that: (1) meteoric waters (exchanged towards heavier values from an original $\delta O^{18} \approx -7.5$ to -9) were abundantly involved in the serpentinization process during the formation of the chrysotile and lizardite, and (2) a deep-seated (metamorphic?) water was involved in the formation of the antigorite.

The relatively narrow range of δD and δO^{18} calculated for the waters assumed to have coexisted with the lizardite-chrysotile samples from the Del Puerto body suggest that these meteoric waters were isotopically very uniform throughout the various episodes. These calculated δD values furthermore appear to be consistently heavier than the present-day values, suggesting that serpentinization here may also have occurred during a period when the isotopic compositions of meteoric waters were different than today's waters. Since these meteoric waters display a relatively narrow range in δD, the sequence established by Saad (1969) would be in agreement with the isotope data in this work, providing that the isotopic compositions of meteoric waters were very uniform during all periods of serpentinization. This is, however, unlikely if the four periods of serpentinization suggested by Saad actually do range from post-Franciscan through the early Tertiary.

The isotope data on the lizardite-chrysotile samples from the California Franciscan formation are thus all consistent with these serpentines having formed from waters containing an appreciable meteoric-water component. However, the Del Puerto waters were apparently lower in δD than the others. This could have come about in several ways. The surface area from which these waters were derived may have been at a higher elevation than for the other three bodies, as is the case at present. Serpentinization in fact, may have occurred during a period much later than the Franciscan, although the youngest age of serpentinization appears limited by the age of geosynclinal folding. Alternatively, however, we must consider the possibility that lizardite-chrysotile serpentinization at Del Puerto may have occurred during a cooler climatic period (more recent?) than at the other three localities.

The lower δD values of calculated meteoric waters at Del Puerto could also be due to less mixing of the meteoric waters with high D connate waters. This seems less likely because if mixing of waters were common in the Franciscan terrane, it is difficult to see how such remarkable uniformity in δD could be attained in the other three widely separated serpentinite bodies.

Another feature which may be a common isotopic phenomenon in the Franciscan serpentine bodies is a small but consistent O^{18} enrichment of serpentine at the margins of the ultramafic bodies. This feature is observed at both San Luis Obispo (where the δO^{18} value of the marginal serpentine is about 1 per mil heavier) and at the Del Puerto body (with the margin enriched about 1.8 per mil).

This feature seems likely to be due to either of two end-member possibilities, such as (1) a somewhat lower temperature of serpentinization along the outer margins of the ultramafic body (resulting in an increased

Δ serpentine-H_2O, and hence a heavier δO^{18} value of serpentine for the same δO^{18} water), or (2) a larger water/rock ratio at the margins than in the interior part of the body.

If we consider the initial δO^{18} of waters that entered and exchanged with the ultramafic body assuming 1:1 water/rock ratios as shown in Table 7-2 (calculated using a closed-system model discussed in detail in section 7.6), then we observe that the δO^{18} values of these waters are quite dissimilar (+5.7 for the exterior serpentinite, + 1.1 for the interior partially serpentinized peridotite. However, we can generate the observed serpentine δO^{18} values from the same water at identical temperatures by assuming that the exterior serpentinization involved water/rock ratios of around 3:1 whereas the interior samples had water/rock ratios of < 0.6:1. Since the outer parts of the ultramafic body consist of highly sheared serpentinite developed along fault zones, whereas the interior is relatively unfractured and unserpentinized, it does not seem too unlikely that the exterior may have had roughly five times as much water circulating through and exchanging with the serpentine as did the interior.

Lizardite-chrysotile serpentinization within the Franciscan shows no isotopic evidence of ever having occurred within an oceanic environment. The isotopic compositions of the Franciscan serpentines (δD = -82 to -108, δO^{18} = +6.6 to +8.9) are completely distinct from those of oceanic environments (δD = -44 to -68, δO^{18} = +0.8 to +6.7). Furthermore, it seems quite unlikely that any oceanic serpentine could have simply undergone δD exchange only, since most of the oceanic serpentines are depleted in O^{18}. Any remnant oceanic serpentines that may have existed within this terrane must have had their original isotopic compositions totally obliterated.

Estimates of the isotopic compositions of metamorphic-type waters involved in the Franciscan blueschist metamorphism can be made from the average isotopic compositions of muscovites in glaucophane schists from the Cazadero area ($\delta D \cong -40$, Taylor, unpublished data; $\delta O^{18} \cong +10.9$, Taylor and Coleman, 1968). From the assumed equilibrium muscovite - H_2O fractionations at 300°C of 3.4 for O^{18}/O^{16} (O'Neil and Taylor, 1969) and of -30 for D/H (estimated by linear extrapolation of the laboratory calibrated muscovite-H_2O system of Suzuoki and Epstein, 1970), one calculates an isotopic composition for these waters of approximately δD = -10 and δO^{18} = +7.5. Such a metamorphic water is not too dissimilar from that assumed to have been in equilibrium with the antigorites from the Del Puerto body (δD = -30, δO^{18} = +7.0).

7.4 Ultramafic bodies in Oregon and Washington

Myrtle Creek, Oregon

A serpentinite body in the Myrtle Creek area in the Klamath Mountains, Oregon is discussed by Coleman (1967); its emplacement is considered by Irwin (1964) to have been synchronous with the intrusion of the Franciscan ultramafic bodies.

Several serpentinite samples were selected in sequence from zero to about 50 feet away from the contact of a large tabular mass of dacite within the serpentine (see figure 7-7). The dacite, considered by Coleman (1967) to be a tectonic inclusion, is bordered by a three foot-wide rodingite reaction zone. This rodingite is a metasomatic reaction zone consisting of white calc-silicate material containing such minerals as hydrogarnet, diopside, idocrase, and chlorite presumed to have formed at the time of serpentinization (Coleman, 1967). Such metasomatic alterations involve loss of silica to the serpentinite and a concomitant enrichment of Ca and Mg within the reaction zone.

A sketch of the geological relationships, sample locations, mineralogy, and isotopic data for each of the samples is given in figure 7-7. The abundances of metasomatic minerals in the serpentinite decrease away from the reaction zone contact.

The samples in the serpentinite zone contain lizardite and chrysotile, with minor diopside. The δO^{18} values represent whole rock analyses (reacted with F_2 at 575°C). The variation of δD is within experimental error and the variation of δO^{18} is only 1.3 per mil. The samples, however, do show a progressive decrease in O^{18} away from the rodingite contact, which is explicable if the diopside has a

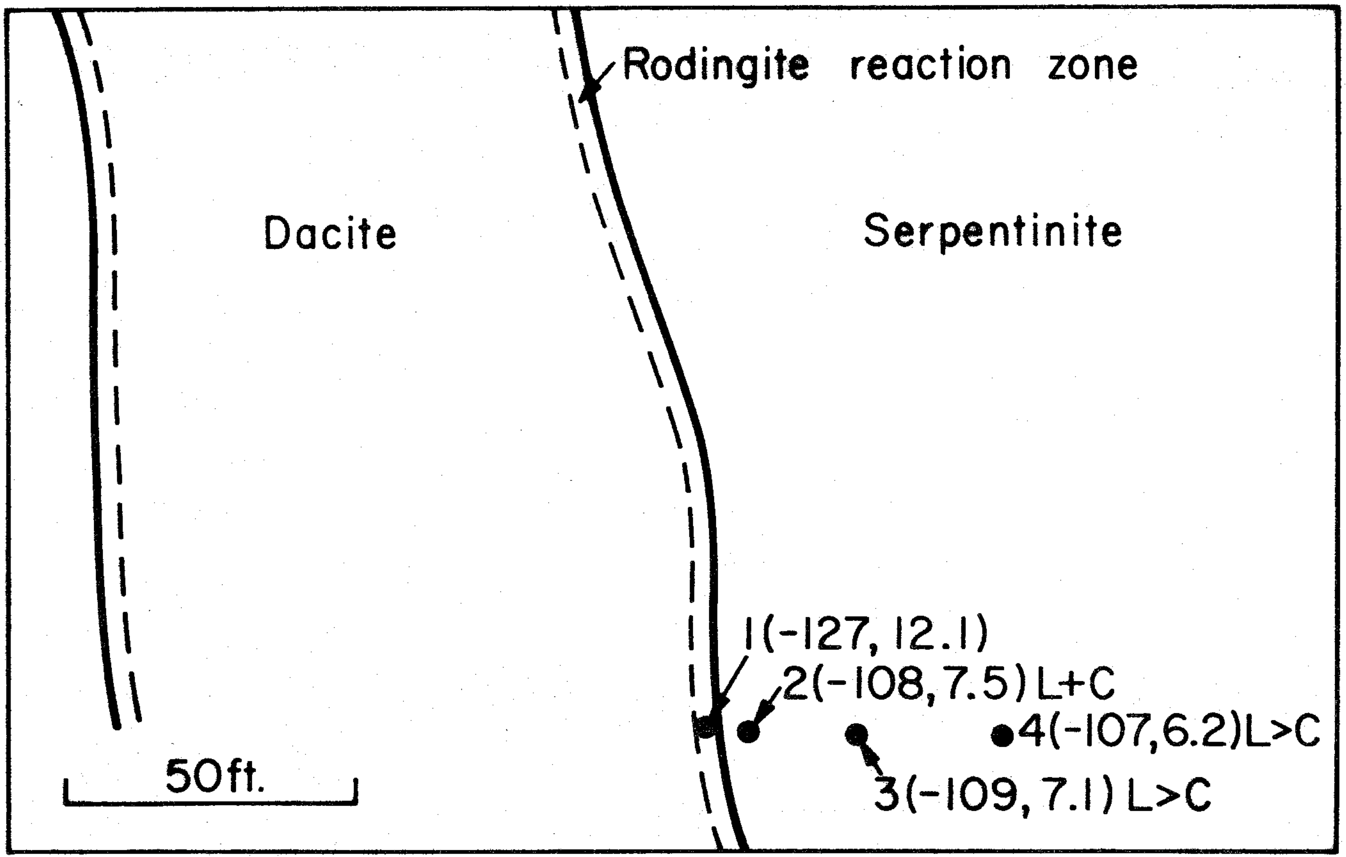

Figure 7-7.

Field sketch (vertical section) of locality at Myrtle Creek, Oregon (generalized from Coleman, 1967) showing location and isotopic analyses of samples. Samples 2 and 3 contain small amounts of diopside. Rodingite sample 1 contains mostly hydrogarnet and xonotlite (43° 02' latitude, 123° 19' longitude).

heavy $\delta 0^{18}$ value relative to the serpentine. The serpentinites at Myrtle Creek are thus isotopically very similar to the chrysotile-lizardite of the Del Puerto body in California, and their δD values are notably lighter than in the other California serpentinite bodies (San Luis Obispo, Tiburon, Napa County).

The analyzed rodingite sample (#1, figure 7-7) is made up of various minerals, predominantly hydrogarnet and xonotlite. Its $\delta 0^{18}$ value is considerably higher than that of the original parent material (unaltered dacites have $\delta 0^{18} = +7.0$ to $+8.5$, Taylor, 1968). This enrichment in $\delta 0^{18}$ is undoubtedly a consequence of the low temperature origin of such rocks (perhaps suggesting even lower temperatures than the 250°-500°C range estimated by Coleman, 1967).

Josephine County, Oregon

In contrast to the serpentinites at Myrtle Creek, the ultramafic bodies in the Illinois River area of Josephine County are associated with the subjacent rocks of the Klamath Mountains (Irwin, 1964). The major orogeny of the Klamath Mountains is late Jurassic in age. A second major orogeny, probably of Late Cretaceous age, greatly affected the Franciscan formation of the Coast Ranges, but was much less important than the Nevadan Orogeny in the Klamath Mountains area.

The ultramafic rocks in the subjacent block of the Klamath Mountains are intruded by Nevadan granitic rocks. Irwin (1964) suggests that these ultramafic rocks, most of which are only partially serpentinized, were emplaced as sheets along a major thrust fault.

The serpentine samples were collected from a 100 foot-wide exposure at the edge of a massive peridotite body. The locations and isotope data are given in figure 7-8. The outer edge of the serpentinite is highly sheared (represented by sample 2), whereas further in toward the peridotite zone it occurs in a massive blocky form (represented by samples 1 and 3). A small, 3-inch wide, elongated rodingite inclusion (sample 4) was collected adjacent to sample 3.

From the isotopic data given in figure 7-8, we again note that the δO^{18} values of these chrysotile-lizardite samples are very uniform, despite variations in serpentine mineralogy and morphological form. The δO^{18} values of the serpentinite, however, are depleted by about 2 to 3 per mil compared to all other continental serpentinites discussed in previous sections, except two anomalously low-O^{18} lizardites from Costa Rica. The magnetite separate from sample 1 contains a small quantity of high Cr-magnetite, suggesting that these serpentinites may have had a complicated petrologic history. The δD value of one of the serpentinites (sample 1) is identical to that of the serpentinites at Myrtle Creek.

The isotopic composition of the rodingite (sample 4) is clearly distinct from a similar rock type at Myrtle Creek. This rodingite sample is composed largely of hydrogarnet with minor chlorite. The δO^{18} value probably largely represents the isotopic composition of the hydrogarnet, whereas the δD value is probably derived about equally from the OH in hydrogarnet and in chlorite. Though less abundant than the hydrogarnet in this sample, chlorite contains a greater quantity of H_2O (typically

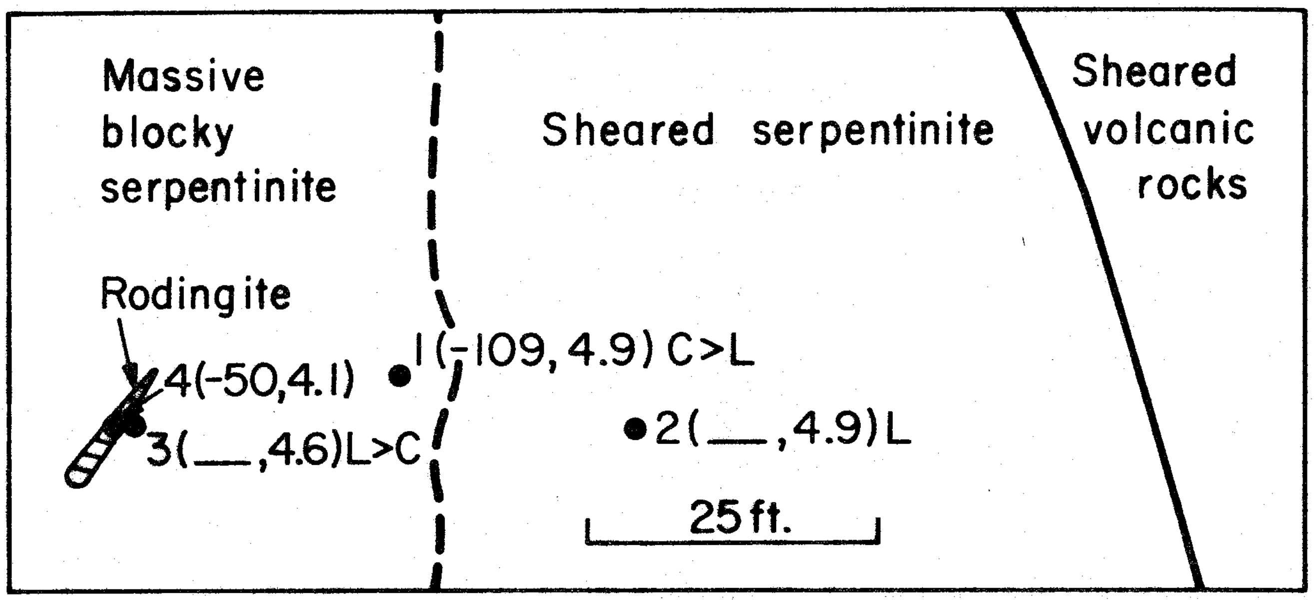

Figure 7-8.

Field sketch (vertical section) of locality along the Illinois River in Josephine County, Oregon, showing sample locations and isotopic analyses. Rodingite sample 4 contains mostly hydrogarnet and chlorite (42° 20' latitude, 123° 46' longitude).

10 to 12 wt. % in chlorite and 1 to 4.5 wt. % in hydrogarnet). Note in particular that the δD of this rodingite is similar to the δD of the Del Puerto, California antigorite samples.

Mt. Stewart, Washington

Smith (1904) described a highly serpentinized peridotite body surrounding a large granodiorite pluton of probable Cretaceous age in the Mt. Stewart area of the central part of the Cascade Mountains. The exact age of this ultramafic intrusion is inknown, but it intrudes upper Paleozoic metasedimentary rocks, and in turn is overlain by sediments of Late Cretaceous and Paleocene age. The ultramafic rocks have been intruded by numerous porphyritic granodiorite dikes and by a gabbro of probable Eocene age.

Two serpentine samples were collected from roadcuts two miles apart along highway U.S. 97, in close proximity to Upper Paleozoic slates and grits (see figure 7-9). The two samples show appreciable, but systematic, differences in both δD and δO^{18}. Sample 1 shows a systematic isotopic depletion (δD = -142, $\delta O^{18} = +6.6$) relative to sample 2 (δD = -127, $\delta O^{18} = +8.0$).

Examination of the magnetite in sample 1 reveals that it is very heterogeneous in chemical composition, suggesting that some of this magnetite may not have been derived from serpentinization. As was mentioned in Chapter 4, the high Cr-magnetite in this sample may have originated at high temperatures during intrusion of nearby granodiorite plutons.

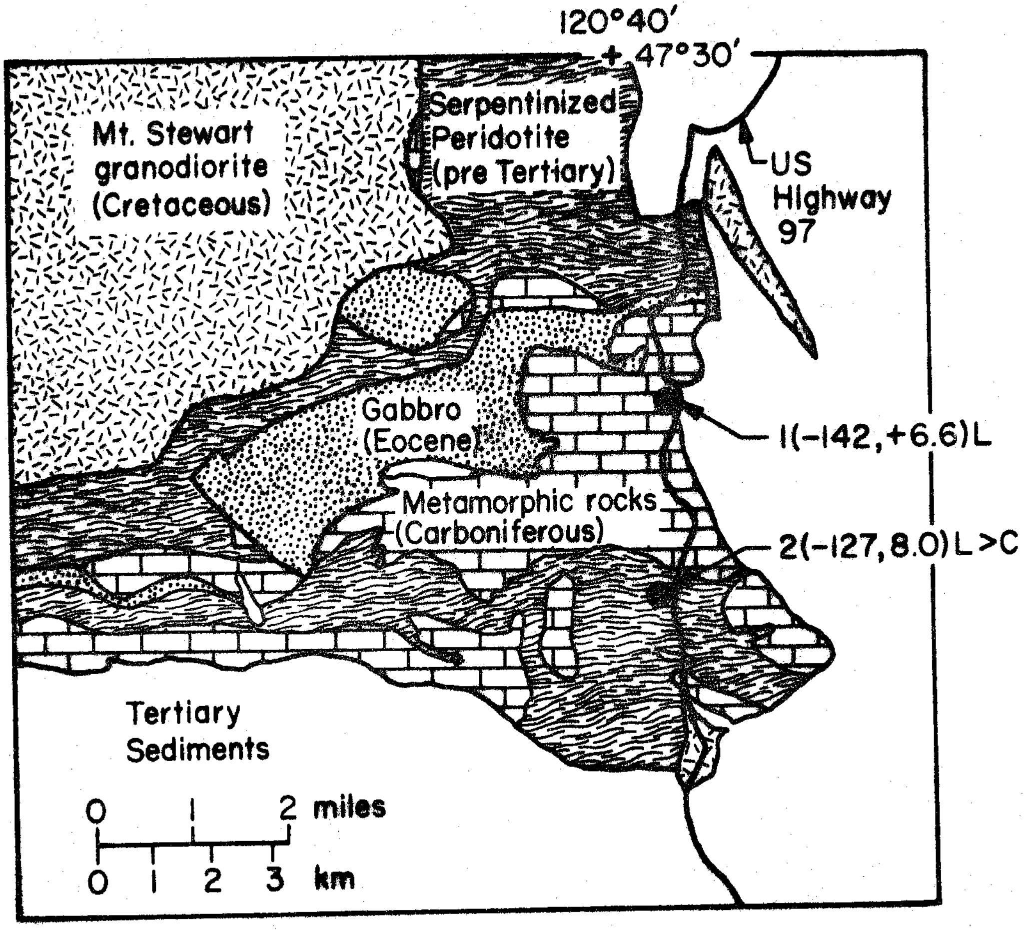

Figure 7-9.

Geologic map in the vicinity of Mt. Stewart, Washington (after Smith, 1904) showing sample locations and isotopic data.

Skagit Region, Washington

The general geology of the Skagit Region of the Northern Cascades is outlined by Misch (1966). Three serpentinite samples were collected from a small body about 3 miles SE of Marblemont, Washington. This ultramafic body intrudes the Cascade River schist, and it has been subjected to a late Permian to early Mesozoic metamorphism (Misch, 1966). The talc sample (#1) was collected from a small (10 foot long) inclusion in the Cascade River schist, 6 miles east of Marblemont.

The serpentine is predominantly antigorite with $\delta D = -58$, $\delta O^{18} = +8.7$ for the pure antigorite (sample 9); the δD value of the pure antigorite is very similar to that of the talc sample (-68). Sample 10, however, contains some chrysotile and has a somewhat lighter δD value (-85). The chemical homogeneity of magnetite from sample 9 (see Table 4-1) suggests that the magnetite and serpentine were probably formed in chemical equilibrium.

Summary of Oregon-Washington Occurrences

The lizardite-chrysotile serpentines from Oregon and Washington have distinctly lighter δD values than those from California. Furthermore, the δD values of the samples from Oregon (-107 to -109) are heavier than those from Washington (-127 to -142). In contrast, the antigorite and talc samples from the Skagit area of Washington are quite distinct ($\delta D = -58$ and -68, respectively).

Estimates have been made of the isotopic compositions of waters that would have coexisted in equilibrium with these samples at the temperatures indicated in Table 7-3. These values indicate, as was

Table 7-3. Isotope data of samples from Oregon and Washington.

Sample	Mineralogy*	% serp.	δD_S	δO^{18}_S	δO^{18}_M	T°C	Calculated H_2O§			Est. Pres. Day H_2O δD†	δO^{18} H_2O Shift‡
							δD	δO^{18} (y/x=∞)	δO^{18} (y/x=1)		
Myrtle Creek, Oregon											
1	Rodingite	-	-127	12.1	-	-	-	-	-	-70	-
2	L + C (+ diopside)	90	-108	7.5	-	100	-63	-	-		-
3	L > C (tr. diopside)	95	-109	7.1	-	100	-64	-	-		-
4	L > C	100	-107	6.2	-	100	-62	-0.4	0.3		8.6
Josephine Co., Oregon											
1	C > L	100	-109	4.9	-	100	-64	-1.7	-2.3	-70	7.5
2	L, tr.C	100	-	4.9	-	100	-	-1.7	-2.3		-
3	L > C	100	-	4.6	-	100	-	-2.0	-2.9		-
4	Rodingite	-	- 50	4.1	-	-	-	-	-		-
Mt. Stewart, Washington											
1	L	100	-142	6.6	-	100	-98	0.0	1.1	-120	13.5
2	L > C	100	-127	8.0	-	100	-83	1.4	3.9		13.5
Skagit, Washington											
1	T		- 68	-	-					-100	
9	A	100	- 58	8.7	1.7	295+	-32	8.4	11.6		-
10	A > C	100	- 85	8.7	-	-	-	-	-		-

inferred for the previously discussed continental lizardite-chrysotile serpentines, that meteoric ground waters must have been involved in the formation of the lizardite-chrysotile type serpentines from Oregon and Washington. A deep-seated (metamorphic?) type water was apparently responsible for the formation of the antigorite and talc. This latter conclusion is consistent with the geological observation that the antigorite and talc bodies have undergone a relatively deep-seated regional metamorphism.

The calculated δD values of waters assumed to have been in equilibrium with the lizardite-chrysotile samples at the time of their formation show a pattern grossly similar to that exhibited by the present-day meteoric waters in this area (see Table 7-3). However, the calculated waters appear to be somewhat heavier for the southern Oregon localities, and distinctly heavier in the Mt. Stewart area. Furthermore, the two samples from the latter locality are themselves different, suggesting, perhaps, that there may have been two (or more) separate periods of serpentinization. For example, sample 2 may have been serpentinized during an initial serpentinization period concomitant with the main Mt. Stewart granodiorite intrusion, whereas sample 1, which is located near a later gabbroic intrusion (see figure 7-9), conceivably could have been further serpentinized during a later period.

The isotopic compositions of the two rodingite samples from different localities in southern Oregon are clearly distinct. The low δD value (-127) of the sample from Myrtle Creek suggests that meteoric water was probably involved in the formation or later exchange of this hydrogarnet. Furthermore, if the rodingite was formed at the same time as the serpentine, the data suggest that the equilibrium water-hydrogarnet hydrogen isotope fractionation is probably larger than the water-serpentine fractionation.

The δD value of the rodingite (-50) from the Illinois River locality in Josephine County is much heavier than the adjacent serpentine, suggesting that although meteoric water probably was involved in the serpentinization process, it was probably not of major importance in the metasomatic reactions which formed this particular rodingite sample. A deep-seated or metamorphic-type water was probably involved in the formation of the chlorite and hydrogarnet in this rodingite.

The δO^{18} value (+4.1) is compatible with the above hypothesis, as it is considerably different from the low-temperature value obtained on the rodingite at Myrtle Creek (+12.1). Thus, whereas the Myrtle Creek rodingite may have formed concomitantly with the lizardite-chrysotile serpentinization of the adjacent ultramafic rocks, the Josephine County rodingite suggests a much different origin. Perhaps this latter sample is a higher-grade tectonic inclusion within the serpentinite.

All waters involved in the lizardite-chrysotile type serpentinization appear to have undergone O^{18} exchange with the adjacent country rock. If one assumes that only meteoric waters were involved, then the approximate amount of O^{18} shift that these waters had to have undergone is shown in Table 7-3. This O^{18} shift for the Oregon localities is generally similar to those suggested for the California serpentinites (see Table 7-2). However, the two samples from the Mt. Stewart area of Washington suggest a considerably greater amount of exchange. It is also noteworthy that the waters involved in serpentinization of the Mt. Stewart serpentinites appear to have undergone similar degrees of exchange despite relatively large δD differences.

The oxygen isotopic differences between the Illinois River (Josephine County) and Franciscan serpentinites may in part be explicable on the basis of their differing geological environments. The Myrtle Creek area and the Franciscan formation are part of the superjacent series, whereas the Illinois River exposure is part of the subjacent series associated with the Klamath Mountain block (Irwin, 1964). The latter is associated with numerous granitic intrusions that have intruded the ultramafic sheet during the Nevadan orogeny. In contrast, granitic bodies are absent from the superjacent rocks of the Franciscan formation.

If serpentinization of the peridotites in the Illinois River area occurred during or after the intrusion of the granitic plutons, one might expect that more water may have been cycled through this serpentinite body than through the Franciscan serpentinites, thus producing the lower δO^{18} values (+4.9 vs. +7.1 to +8.9 for the Franciscan serpentinites). Various workers (see Sheppard et al., 1969; Taylor, 1970) have proposed that an epizonal igneous pluton emplaced into cooler country rocks induces convective circulation of meteoric ground waters in the vicinity of the pluton.

The Illinois River (Josephine County) samples were collected about three miles from the contact of a large granitic intrusion, and thus may have been affected by circulating geothermal waters.

The major difficulty in relating the serpentinization to the granitic intrusions in the subjacent unit is the near identity of the D/H ratios in both the Illinois River serpentinites and those at Myrtle Creek. If one assumes that serpentinization of the Klamath Mountain block occurred during the Nevadan orogeny, and serpentinization of the Franciscan ultramafics occurred during the Upper Cretaceous, then one is required to assert that the local meteoric ground waters were nearly identical during both episodes of serpentinization. This may suggest that the δD values of the Josephine County samples were in fact imprinted (by later retrograde exchange?) during the Late Cretaceous orogeny.

7.5 Ultramafic bodies in British Columbia

Serpentinites and associated rock types were sampled from various localities in British Columbia in order to more fully assess the contribution of meteoric ground waters to the various fluids involved in serpentinization. The British Columbia area is one in which the present-day meteoric waters are isotopically most dissimilar from "deep-seated" or plutonic waters. There is reason to believe that these isotopic differences existed throughout the Tertiary and even into the Late Cretaceous (Taylor, 1968; Sheppard et al., 1969; Lawrence, 1970). The sample localities are discussed in detail below and are shown in figure 7-1.

Most of the ultramafic bodies in British Columbia are from the western Cordilleran region, where the major orogeny occurred during the Mesozoic. In the southern Cordilleran region, the ultramafic rocks have commonly been considered to be an early phase of the Mesozoic intrusive episode, and thus to be of Jurassic or early Cretaceous age. Some of the ultramafic bodies of the northern Cordilleran area appear to be older, but most are of unknown age (White, 1966). The country rocks into which the ultramafic rocks were intruded were later folded and intruded by granitic bodies at different times, mainly during the Upper Jurassic and the Cretaceous.

Grand Forks Area

One serpentinite sample composed of lizardite, chrysotile and minor antigorite was obtained from the Grand Forks area, British Columbia, just north of the United States border (118.5° longitude, 49° latitude, see figure 7-1). Although the exact location of this sample is unknown, it is from one of the small (< 1 km) serpentinite bodies that lie about 5 - 10 km west of Grand Forks in a terrane composed dominantly of graywacke and volcanic rocks. The isotopic composition is $\delta D = -154$, $\delta O^{18} = +8.0$.

Kwoiek Area

The Kwoiek area is a roof pendant of metamorphic rocks within the Coast Range batholith. A major sill-like mass of serpentinite some 15 miles long extends across the map area (see figure 7-10). Also, many small serpentinite masses less than a few hundred feet across are common throughout the roof pendant. The serpentinite bodies are commonly altered to talc, carbonate and tremolite (Duffell and McTaggart, 1951). Hollister (1966) has mapped various metamorphic isograds in the roof pendant, noting that the highest metamorphic grades occur along the southern batholith contact. The grade generally decreases away from the contact to the northeast, except locally in proximity to the plutonic igneous rocks.

The locations and isotopic compositions of the various samples studied in this work are shown in figure 7-10; they were selected from areas ranging from high to relatively low metamorphic grade.

All of the pure talc, chlorite and antigorite samples have δD values in the range -70 to -56. There is no appreciable δD distinction between the pure talc (-61) and the pure chlorite (-56 and -62); the antigorite-rich sample (-70) is only slightly lighter. Samples 187a and 371a, selected from sillimanite-grade metamorphic rocks, contain olivine which shows a partial retrograde alteration to a mesh-texture serpentine.

Figure 7-10. Geologic map of the Kwoiek area, British Columbia showing sample localities and isotope data. Also shown are the metamorphic isograds indicated by coexisting assemblages in high-Ca rocks. The isograd sequence B → C → D indicates increasing metamorphic grade, ranging from greenschist to almandine-amphibolite facies. Highest metamorphic grades are found near the southern batholith contact (after Hollister, 1966).

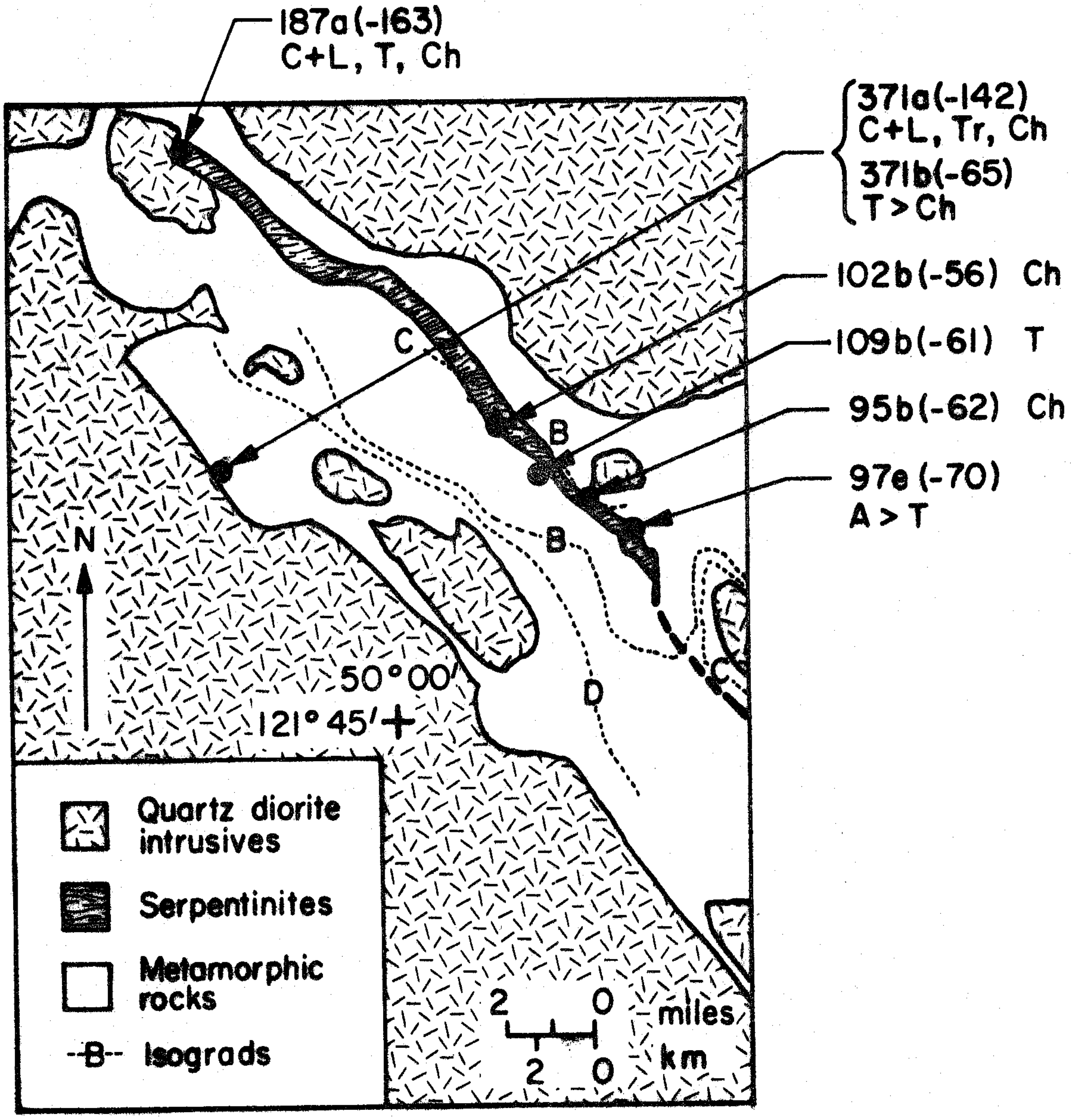
187a(-163)
C+L, T, Ch
371a(-142)
C+L, Tr, Ch
371b(-65)
T>Ch
102b(-56) Ch
109b(-61) T
95b(-62) Ch
97e(-70)
A>T
C
B
B
D
C
N
50°00'
121°45'
Quartz diorite intrusives
Serpentinites
Metamorphic rocks
--B-- Isograds
2 0 miles
2 0 km

Figure 7-10.

This olivine may have formed by dehydration of an original serpentine (Hollister, 1966), and then been rehydrated at a much lower temperature. The very low δD values of these samples (-163 and -142) indicate that the lizardite-chrysotile-type serpentine in the Kwoiek area is strongly depleted in D/H compared to the higher grade minerals (talc, antigorite, tremolite, and chlorite).

Yalakom Area

The Yalakom ultramafic body is an elongate mass some 18 miles long and 8 miles wide located in the southern Cordilleran section of British Columbia. The N and S contacts of the body are bordered by the Yalakom fault system which is part of the northern extension of the Fraser River fault system. The lizardite-chrysotile from a sample of partially serpentinized peridotite (exact location within the body is unknown) has $\delta D = -150$, $\delta O^{18} = +4.4$.

Fort St. James Area

The analyzed serpentine samples from the Ft. St. James area are from four different bodies located in two different geologic terranes (see figure 7-11). The two easternmost ultramafic intrusions, Murray Ridge and Pinchi Mountain, are stocks of partially serpentinized pyroxenite and peridotite that have intruded mid-Mesozoic eugeosynclinal sediments and volcanic flows of the Takla Group. The terrane to the west, across the 200 mile long Pinchi-Omineca Fault, consists of Paleozoic limestones and argillaceous sediments of the Cache Creek Group.

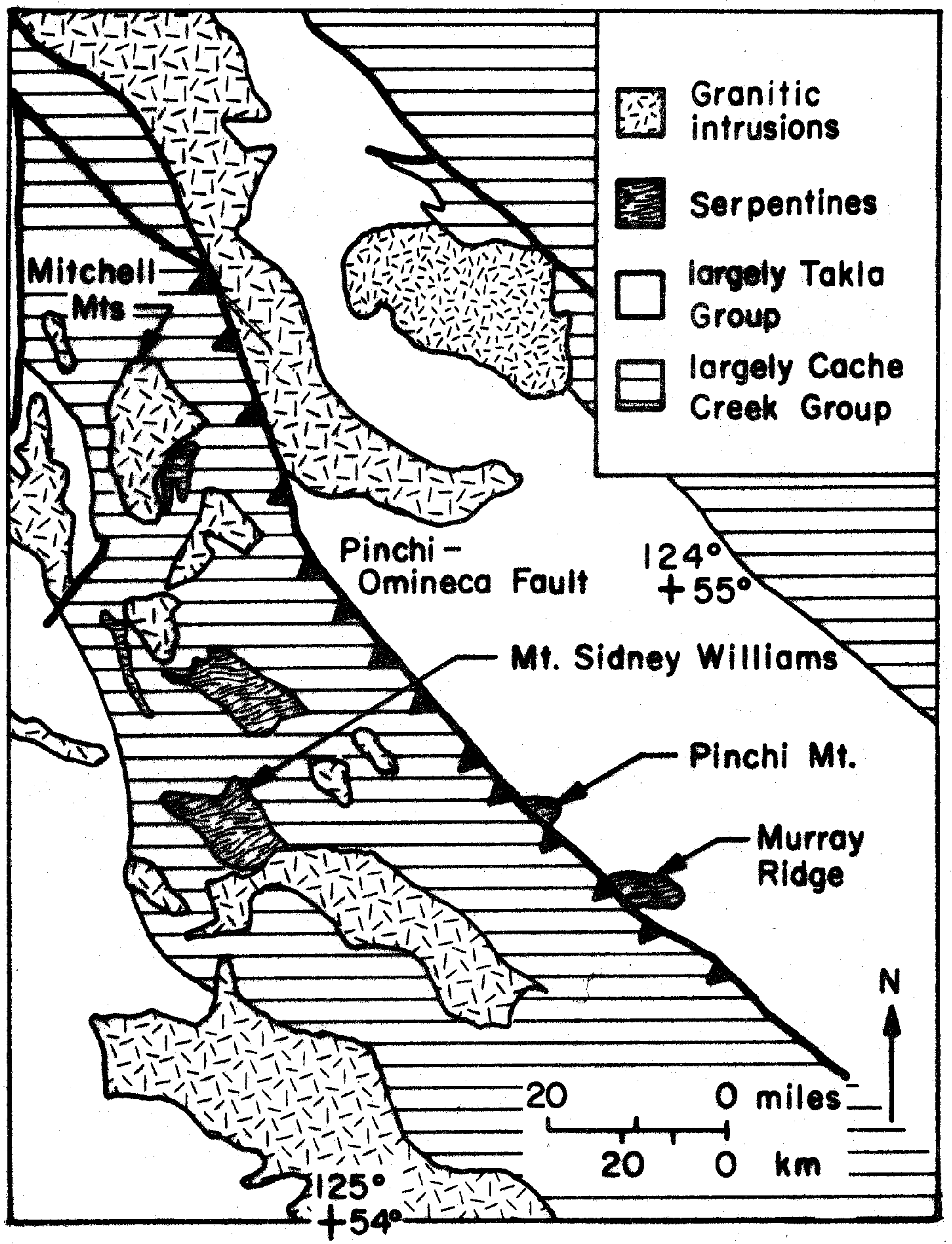

Figure 7-11.

Geologic map of the Fort St. James area, British Columbia (after Little, 1962), showing the sample localities studied in this work.

The ultramafic rocks at Mt. Sidney Williams and the Mitchell Mountains are intrusive into these Cache Creek rocks; they were subsequently intruded by the Omineca intrusions of Lower Cretaceous age. Throughout much of the general area to the west of the Pinchi-Omineca Fault, the ultramafic rocks are altered to talc-carbonate and in some cases to actinolite (Armstrong, 1949).

The high-angle Pinchi-Omineca Fault is thought to have undergone large dip-slip movement during the Mesozoic, with renewed movement in the Tertiary (White, 1966). Along this fault, serpentine at Pinchi Mountain has undergone extensive fracturing and carbonatization, the serpentine being replaced by quartz, chalcedony, and ankeritic carbonate.

The isotope data for samples from these localities, given in figure 7-11, can be divided into two groups. Samples composed solely of lizardite-chrysotile type serpentine, lying to the east of the Pinchi-Omineca fault, have δD values in the range -167 to -190, with δO^{18} values of +2.1 to +4.4. In contrast, samples to the west are composed of both lizardite-chrysotile and antigorite and have δD values in the range -84 to -128 with δO^{18} values of +8.5 to +9.1. The δD values of the various samples can best be explained, as outlined previously, by assuming that all lizardite-chrysotile serpentine in these areas is very low in D/H (e.g., samples 3 and 4 which have $\delta D = -174$ and -167), whereas all antigorite is isotopically much heavier. Consequently, samples that are mixtures of both polymorphs should have intermediate δD values, as for example, samples 1 and 2 ($\delta D = -84$ and -128).

Cassiar Area

The regional geology of the Cassiar region is discussed by Gabrielse (1963). Most of the samples investigated from this locality are from the Cassiar Asbestos mines on the northwest flank of Mount McDame. Near the mine, the country rocks consist of chert, argillite, argillaceous quartzite, greenstone, and graywacke of the Paleozoic Sylvester Group.

According to Gabrielse (1963), the pervasive serpentinization of the ultramafic rocks generally produced mesh-texture serpentine and bastite in areas remote from the Cassiar batholith. However, the Cassiar serpentinite body has been highly fractured, much more so than any other ultramafic body in the area, and it exhibits strong development of fibrous asbestos veins. Gabrielse further suggests that the intrusion of the Cassiar batholith may have facilitated the movement and circulation of water at temperatures sufficient to promote serpentinization. He has proposed that the following combination of conditions led to the localization of the fibrous chrysotile asbestos:

1. Pervasive serpentinization of an ultramafic body resulting in mesh-texture serpentinite and bastite. (This type of serpentine has been analyzed for δO^{18} and δD from the nearby Blue River ultramafic body, see below).

2. Development of abundant fractures in the serpentinite body.

3. Recrystallization of the serpentinite during low-grade metamorphism, perhaps equivalent to the greenschist facies, produced by intrusion of the Cassiar batholith.

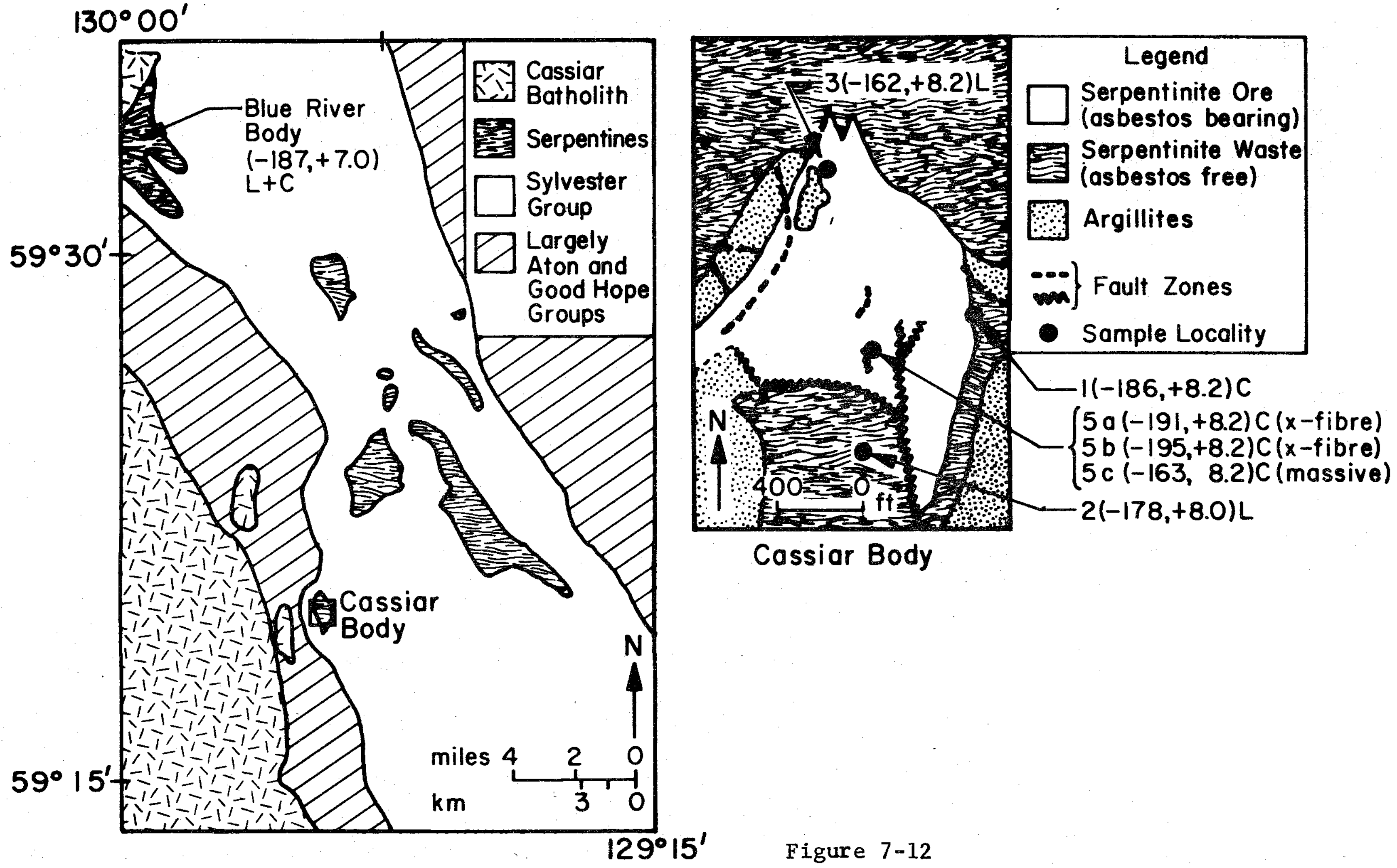

Figure 7-12

Geologic map of Cassiar area, British Columbia (after Little, 1962), showing sample localities and isotopic analyses. The detailed geologic map and sample locations within the Cassiar body were supplied by Cassiar Asbestos Corporation Limited.

From the map of the McDame area in figure 7-12, one can see that a 1000 foot-thick sequence of limestone, dolomite and quartzite (Atan Group) lies very close to the Cassiar serpentinite body, and is in direct contact with the Cassiar batholith about 0.8 miles to the west. The Atan Group has been metamorphosed to crystalline marble, skarn, and hornfels in this area. Some 10 miles to the east of the Cassiar serpentinite unit, many thousands of feet of unmetamorphosed carbonate units of the Atan and Good Hope groups are also exposed.

The Blue River ultramafic body has been intruded by the Cassiar batholith in a region some 20 miles north of the Cassiar serpentinite body (see figure 7-12). In the vicinity of the granitic batholith, various metamorphic reactions occurred, including regeneration of olivine from serpentine and the formation of tremolite and talc (Wolfe, 1965). In this area, no carbonate units are in contact with the Cassiar batholith, although scattered outcrops of carbonates of the Atan group occur some 10 miles to the east.

The isotopic data for the various serpentine samples within the Cassiar area are presented in figure 7-12. The δD values for the samples are all relatively light, but show a wide variation even within a small area. For example, two parallel fibrous chrysotile veins (samples 5a and 5b) within the same hand specimen have very similar δD values (-191 and -195 per mil), but the massive, greasy, fine-grained chrysotile (5c) adjacent to these fibrous veins is considerably heavier ($-163^{o}/_{oo}$). This fine-grained chrysotile is identical in δD to lizardite sample 3. Two other samples (1 and 2) of chrysotile and lizardite have intermediate δD

values (-186, -178). It is also noteworthy that the lizardite-chrysotile sample from the Blue River area has a $\delta D = -187^{o}/_{oo}$, within the range exhibited by the Cassiar serpentinite body.

The serpentines from the Cassiar body, although exhibiting a wide variation in δD-values, are exceedingly uniform in $\delta 0^{18}$. Furthermore, the $\delta 0^{18}$-values are much heavier ($\approx +8.1^{o}/_{oo}$) than most of the other serpentinites studied from British Columbia. The Blue River sample, collected in an area remote from the thermal influence of the Cassiar batholith (Wolfe, personal communication), has a lighter $\delta 0^{18}$-value ($+7.0^{o}/_{oo}$).

Nahlin Area

Four samples (exact location unknown) were studied from the large Nahlin ultramafic body (see figure 7-13). The NW extension of the Nahlin body is referred to by Aitken (1959) as the Mount O'Keefe body. The Nahlin-Mt. O'Keefe body was emplaced along the Nahlin fault zone, which separates massive volcanic graywacke of the Jurassic Leberge Group to the south from the Cache Creek Group to the north.

The degree of serpentinization of the Nahlin body is quite variable (Souther, personal communication), being most intense along the outer contacts and in sheared and brecciated zones. Even though serpentine and carbonatized serpentinite appear to be related to faulting at the outer edges of the body, minerals indicative of higher grades of metamorphism occur within the ultramafic rocks in proximity to a later granitic body emplaced during the Jurassic or Cretaceous (Aitken, 1959).

The isotopic data given in figure 7-13 are again consistent with the fact that chrysotile-lizardite appears to have a relatively light

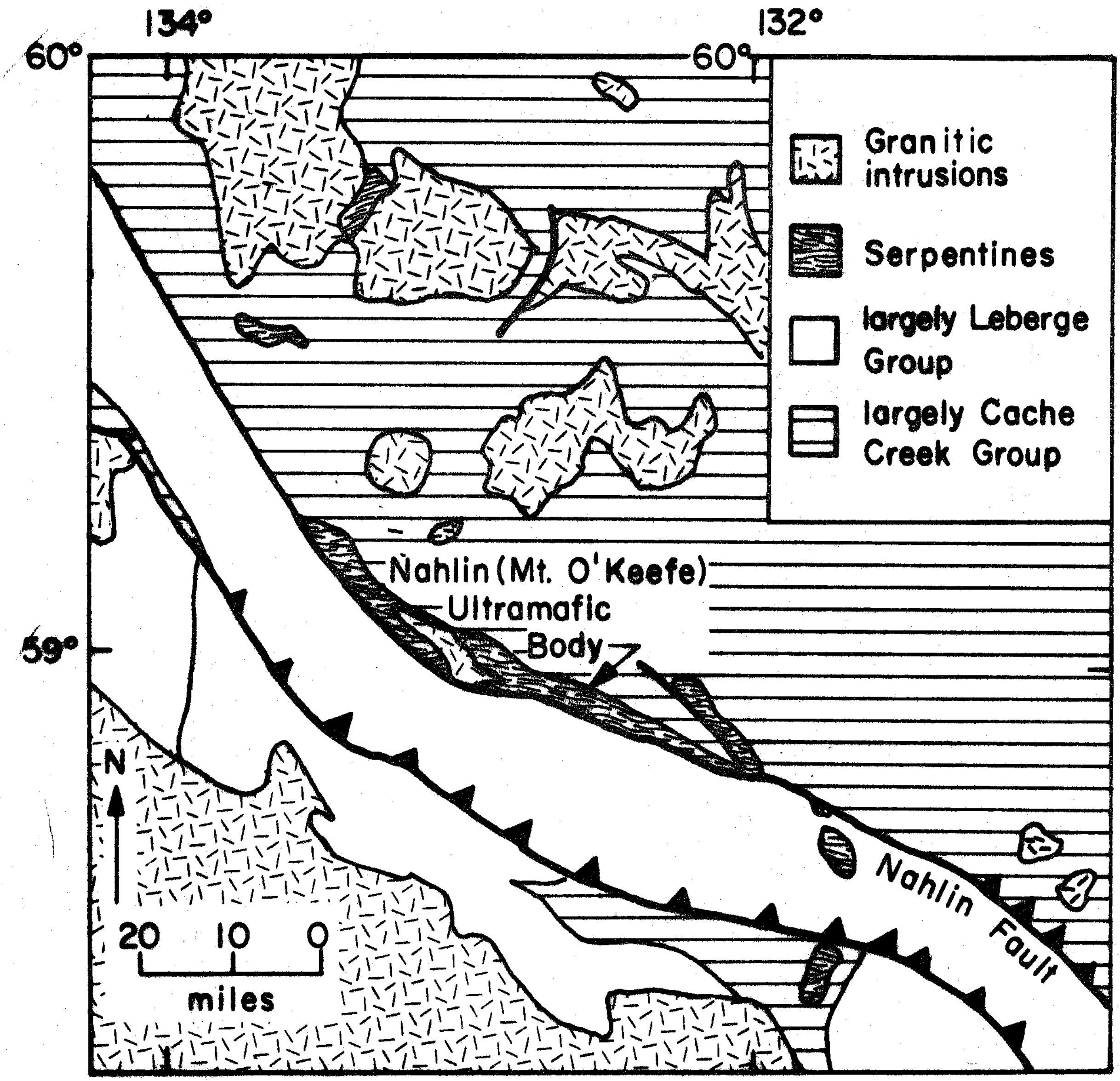

Figure 7-13.

Geologic map of the Nahlin ultramafic body and vicinity (generalized after Little, 1962).

δD value (-198 to -205) whereas the higher grade minerals such as talc, tremolite, and antigorite are isotopically much heavier. Thus samples 3 and 4, which contain mixtures of the higher-grade minerals and lizardite-chrysotile serpentine, have intermediate δD values (-143 and -174, respectively). The δO^{18} values (+1.9 to +3.0) are very much lower than those of the Cassiar serpentinite body, but are similar to those at Pinchi Mountain and Murray Ridge in the Fort St. James area.

Discussion of Isotopic Data from British Columbia Occurrences

The serpentine occurrences in British Columbia may be conveniently divided into three categories based purely on geographic location. These are: (1) the northern bodies in the Nahlin and Cassiar area; (2) the central bodies in the Fort St. James area; (3) the southern bodies at Yalakom, Kwoiek, and Grand Forks.

These serpentines show some remarkable systematics in their isotopic compositions. The relatively pure chrysotile-lizardite samples exhibit a progressive decrease in D/H ratio in going from the southern bodies (average δD = -156, 3 samples) to the central bodies (average δD = -175, 3 samples) to the northern bodies (average δD = -185, 9 samples).

On the other hand, every sample from British Columbia that contains significant amounts of antigorite, talc, chlorite, or tremolite has considerably higher δD values, ranging from -143 to -84. The samples that are essentially free of chrysotile or lizardite have δD = -70 to -56. The only conceivable explanation of these data is that meteoric ground waters are definitely responsible for the lizardite-chrysotile δD values, but that they cannot be involved in any significant fashion with the formation of antigorite, talc, tremolite, or chlorite. These higher grade minerals were most probably formed from a deep-seated (metamorphic?) type of water.

Estimates of the δD of waters assumed to have coexisted in equilibrium with the lizardite-chrysotile serpentines (Table 7-4) also show a very good correspondence with present-day meteoric waters in these areas. The calculated δD-values seem to be almost coincident with present-day waters for the Nahlin and Murray Ridge bodies, although perhaps somewhat heavier for the Cassiar and Yalakom bodies.

The δO^{18} values of the lizardite-chrysotile serpentines do not, however, fit a simple geographic pattern (although the lowest δO^{18} value, +1.9, does come from the most northernly body, the Nahlin occurrence). Instead, the higher δO^{18} values seem to be more closely linked to the type of country rock that surrounds the ultramafic bodies. The serpentines from the Cassiar area and from west of the Pinchi-Omineca fault in the Fort St. James area occur in terranes of abundant limestones. Thus one might _a priori_ suspect that the waters involved in serpentinization may have previously undergone a more significant degree of O^{18}-enrichment through exchange with these O^{18}-rich sediments (limestones and dolomites generally have δO^{18} values in the range +20 to +27 and they readily exchange and recrystallize in the presence of geothermal waters).

In contrast, the δO^{18} values of serpentines from the Yalakom and Nahlin bodies, and from regions east of the Pinchi-Omineca fault (Murray Ridge and Pinchi Mountain), are smaller, ranging from +1.9 to +4.4. These bodies all lie in terranes containing abundant volcanics. Such rocks

Table 7-4. Isotopic data of samples from British Columbia.

Sample	Mineralogy*	% serp.	δD_S	δO^{18}_S	δO^{18}_M	T°C	Calculated H_2O§			Est. Pres. Day H_2O δD†	δO^{18} H_2O Shift‡
							δD	δO^{18} (y/x=∞)	δO^{18} (y/x=1)		
Grand Forks 1	L + C > A	100	-154	8.0	-	-	-	-	-	-130	-
Kwoiek					-						
95b	Ch	-	- 62	-	-					-135?	
97e	A > T	-	- 70	-	-						
102b	Ch	-	- 56	-	-						
109b	T	-	- 61	-	-						
187a	(L + C) > T > A	80D	-163	-	-	-	-	-	-		-
371a	(L + C) > Tr + Ch	40D	-142	-	-	-	-	-	-		-
371b	T > Ch	-	- 65	-	-						
Yalakom	L + C	40P	-150	4.4	-	100	-109	-2.2	-3.3	-135	12.7
Pinchi Mt.											
3	L + C	40P	-174	2.1	-	100	-132	-4.5	-7.9	-150?	13.3
4	C	70P	-167	-	-	100	-125	-	-		-
Murray Ridge 5	L + C	70P	-190	2.9	-	100	-149	-3.7	-6.3	-160?	16.2
Mt. Sidney Williams 2	A > C	100	- 84	9.1	-	-	-	-	-	-160?	-

Table 7-4 (continued)

Sample	Mineralogy*	% serp.	δD_S	δO^{18}_S	δO^{18}_M	T^oC	Calculated H_2O§			Est. Pres. Day H_2O δD†	δO^{18} H_2O Shift‡
							δD	δO^{18} $(y/x=\infty)$	δO^{18} $(y/x=1)$		
Mitchell Mts. 1	L + C tr.A	100	-128	8.5	-	-	-	-	-	-160?	-
Cassiar											
1	C	100	-186	8.2	-	100	-145	1.6	4.3	-160	21.0
2	L > C	100	-178	8.0	-	100	-137	1.4	3.9		19.8
3	L, tr. C	100	-162	8.2	-	100	-119	1.6	4.3		17.7
5a(x - f)	C	100	-191	8.2	-	100	-150	1.6	4.3		21.6
5b(x - f)	C	100	-195	8.2	-	100	-154	1.6	4.3		22.1
5c	C	100	-163	8.1	-	100	-120	1.5	4.1		17.7
Blue River 1	L + C	100	-187	7.0	-	100	-148	0.4	1.9	-160	20.2
Nahlin											
1	L > C	100	-205	3.0	-	100	-166	3.6	-6.1	-160	18.4
2	L + C	100	-198	1.9	-	100	-159	4.7	-8.3		16.4
3	C > T, Tr	100	-143	6.3	-	-	-	-	-		-
4	L > A, T, Tr	100	-174	-	-	-	-	-	-		-

typically have $\delta 0^{18}$ values of +5 to +10 (Taylor, 1968), so even if oxygen isotopic communication existed between these rocks and the waters involved in serpentinization one would not expect very heavy $\delta 0^{18}$ values.

If it is assumed that only meteoric waters were involved in the lizardite-chrysotile serpentinization, these waters would have had to undergo the 0^{18} shifts listed in Table 7-4. These 0^{18} shifts are in general considerably larger than those estimated previously for more southerly localities. The greatest calculated 0^{18} shift is observed in the Cassiar area (17.7 to 22.1 per mil), where the original, unexchanged meteoric ground waters would have had $\delta 0^{18}$ = -16 to -20.5 per mil. The tabulation of "0^{18} shifts" in Table 7-4 reaffirms the statements made above that waters in limestone-rich terranes such as the Cassiar area underwent greater 0^{18} enrichment than those in regions rich in volcanics.

If the $\delta 0^{18}$ values observed in the serpentines were imprinted during the Cretaceous, it is possible that part of the 0^{18}-rich fluid may have been derived from $C0_2$ liberated during metamorphic decarbonation of limestones. In the Cassiar area, for example, major batholithic intrusion occurred in near proximity to the serpentinite bodies during the Cretaceous. Shieh and Taylor (1969a) observed that such $C0_2$ is enriched in 0^{18} relative to the carbonates. However, it is more likely that the major serpentinization occurred somewhat later. For example, the chemical heterogeneity and chromian content in magnetites from three samples located in near proximity to granitic intrusions (samples 1 from Cassiar body, Nahlin body, and Mitchell Mountains in the Fort St. James area) all suggest that the high chromian magnetite was produced at high temperatures (associated with granitic intrusion?) whereas the pure Fe-magnetite formed as the result of a later episode of serpentinization.

The large variation in δD that is observed within the single small Cassiar serpentinite body suggests that there was a complex history of serpentinization and/or that the fluids responsible for serpentinization had a variable D/H ratio. Strong isotopic variations are particularly likely in these very light meteoric waters because even small amounts of mixing with isotopically heavy waters can produce appreciable changes in δD. The meteoric ground waters, for example, could have mixed with deep-seated metamorphic or igneous waters, or with trapped connate waters; all such waters have much higher D/H ratios than fresh, meteoric waters in the British Columbia area. Rather than mixing of waters, however, the observed isotopic relationships might well have been produced by superposition of a major ground-water serpentinization event on a body previously serpentinized by other types of waters.

7.6 Summary of isotopic data on low-grade alpine serpentines

The major conclusions of the D/H and O^{18}/O^{16} studies of low-grade alpine serpentines can be summarized as follows.

δD-latitude correlation

There is an excellent correlation between latitude and δD values for chrysotile-lizardite serpentines, as is illustrated in figure 7-14. The δD values range from -58 in Central America to -205 in northern British Columbia. In contrast, samples composed of antigorite, talc and chlorite show no such correlation, having δD-values in the range -55 to -70 irrespective of geographic location. Samples which contain mixtures of lizardite-chrysotile on the one hand and higher-grade minerals (antigorite, talc, and chlorite) on the other generally have intermediate δD values.

These data indicate that meteoric waters were involved in lizardite-chrysotile type serpentinization whereas deep-seated (igneous? or metamorphic?) type waters were responsible for the formation of antigorite, talc, and chlorite. These conclusions, along with our isotopic temperature estimates for serpentinization (85° to 115°C for lizardite-chrysotile and 220° to 460°C for antigorite) strongly suggest that whereas lizardite-chrysotile forms in a relatively shallow PT environment, antigorite (and also talc and chlorite) appear to form under deeper-seated conditions.

It conceivably could be argued that the latitudinal correlation of δD values of lizardite-chrysotile serpentines might be a result of later low-temperature D/H exchange between these serpentines and surface-

Figure 7-14. δD-latitude plot of all analyzed samples from the low-grade alpine serpentine belts of western North America and the Caribbean. For talc and chlorite, only pure samples are shown; for antigorite and lizardite-chrysotile, mixed samples are also indicated. The degree of filling within the data-points indicates approximate proportions of antigorite and lizardite-chrysotile. Tie lines connect all samples from the same locality.

Figure 7-15. Plot of δD versus δO^{18} showing calculated isotopic compositions of waters that are assumed to have coexisted in equilibrium with relatively pure lizardite-chrysotiles from low-grade alpine serpentinite terranes. Equilibration temperatures are either calculated from measured serpentine-magnetite fractionations or are assumed to be 100°C. The meteoric water line, kaolinite line (Savin and Epstein, 1970), and the Salton Sea geothermal water line (Craig, 1963) are shown for reference.

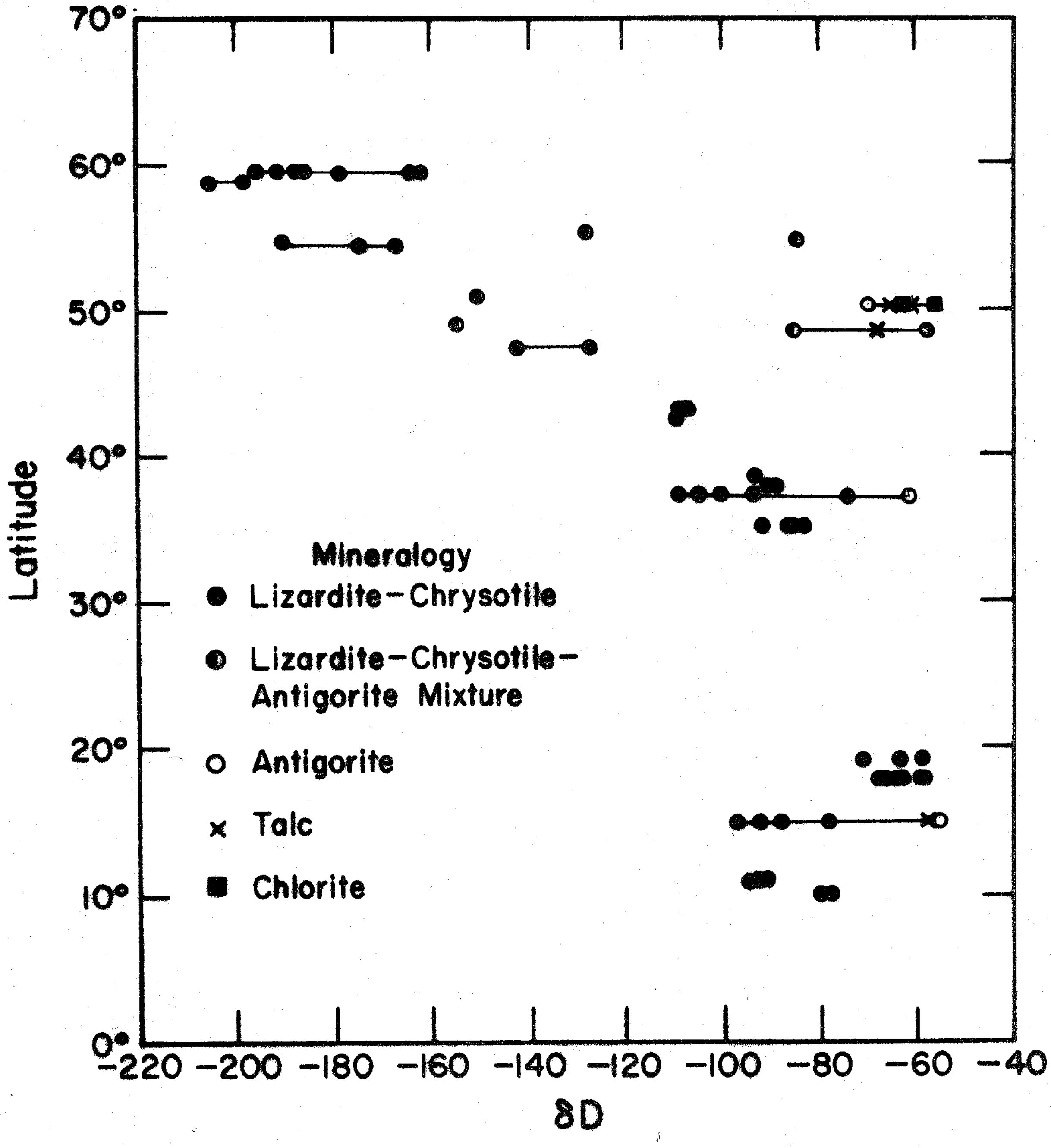

70°
60°
50°
40°
30°
20°
10°
0°
Latitude
−220
−200
−180
−160
−140
−120
−100
−80
−60
−40
δD
Mineralogy
● Lizardite−Chrysotile
◐ Lizardite−Chrysotile−Antigorite Mixture
○ Antigorite
× Talc
■ Chlorite

Figure 7-14.

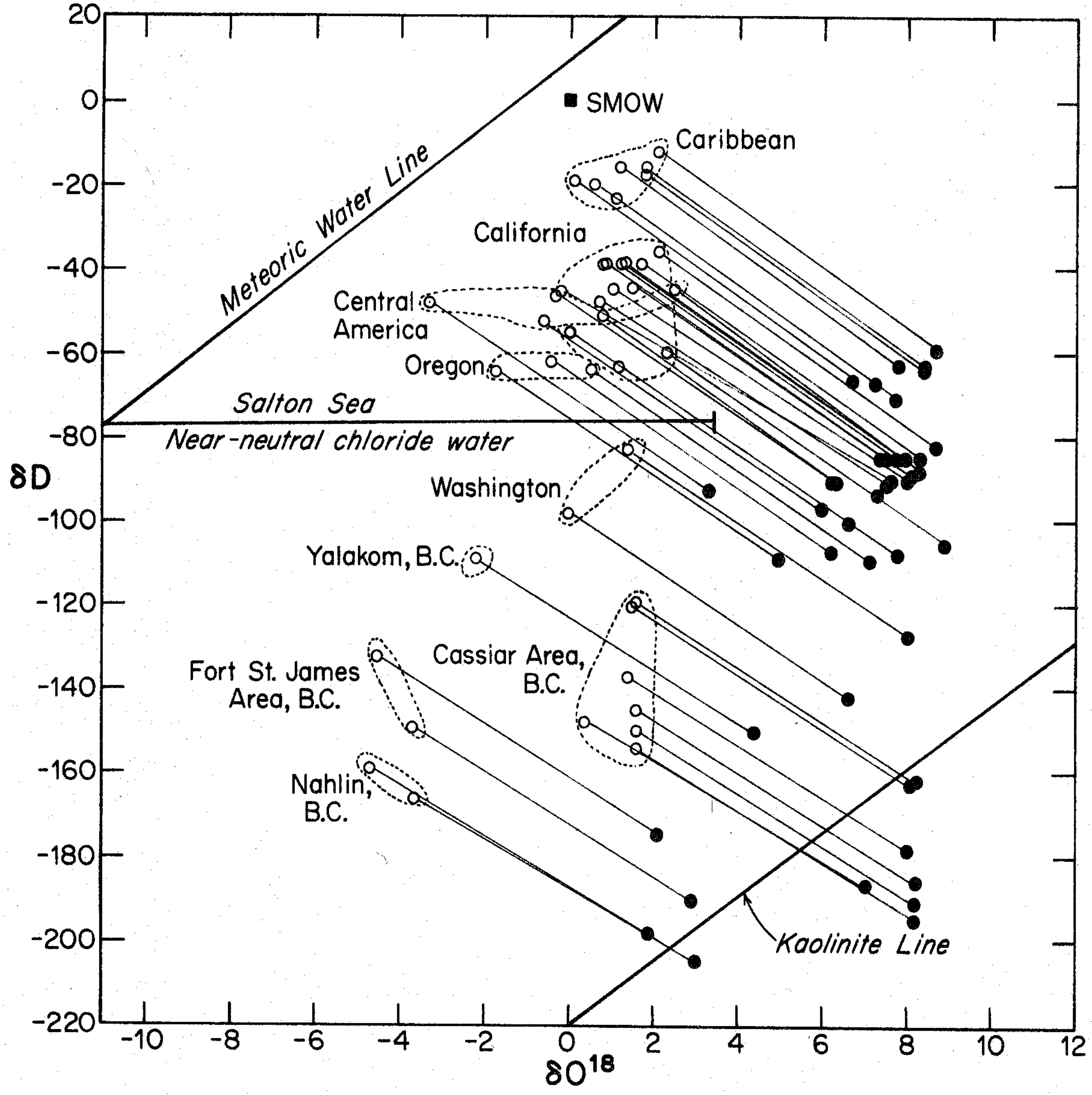
Meteoric Water Line
SMOW
Caribbean
California
Central America
Oregon
Salton Sea
Near-neutral chloride water
Washington
Yalakom, B.C.
Cassiar Area, B.C.
Fort St. James Area, B.C.
Nahlin, B.C.
Kaolinite Line
δD
δO18
20
0
-20
-40
-60
-80
-100
-120
-140
-160
-180
-200
-220
-10
-8
-6
-4
-2
0
2
4
6
8
10
12

Figure 7-15.

meteoric ground waters. However, for a variety of reasons that will be outlined in detail in a subsequent chapter, it can be shown that these D/H values very likely represent the original isotopic imprint at the time the serpentine was formed or recrystallized.

Calculated isotopic compositions of waters coexisting with serpentine

In Table 7-1 to 7-4, we show the calculated isotopic compositions of waters that would have coexisted in equilibrium with the various lizardite-chrysotile samples studied in this work. The equilibration temperatures were either derived from measured serpentine-magnetite fractionations (see Table 4-4) or simply assumed to be approximately 100°C according to the model outlined in Chapter 4. These waters, illustrated graphically on the δD - δO^{18} diagram in figure 7-15, exhibit the same type of δD-latitudinal correlation mentioned above. Furthermore, there also appears to be a general correlation between δO^{18} and latitude, as well.

The waters plotted on figure 7-15 must contain a significant meteoric water component. They conceivably could be composed entirely of meteoric ground waters that have undergone a significant O^{18} shift prior to being involved in serpentinization. This O^{18} shift, arising as a result of exchange with the surrounding country rocks, is well shown in figure 7-15; the magnitude of the shift is indicated by the degree to which these calculated waters are enriched in O^{18} relative to the pristine meteoric water of the same δD value.

These calculated waters indicate that the magnitude of the O^{18} shift is approximately proportional to the δD value (and hence latitude of sample locality). Thus, for example, exchanged meteoric waters assumed to be in equilibrium with the lizardite-chrysotile serpentines show a progressive increase in 0^{18} shift from an average of 6.7 per mil for the Caribbean and California localities, to 10.1 in Oregon and Washington, to an average of 17.4 for all British Columbia samples.

The nature of the surrounding terrane in each of the above localities may be important. Much of the country rock into which ultramafic rocks are intruded consists of graywacke sandstones and altered volcanic rocks, which commonly have $\delta 0^{18} = 9$ to $13^{\circ}/_{oo}$ (see Taylor, 1968; Taylor and Coleman, 1968). Such localities include the Caribbean, Central American, and Franciscan occurrences, along with many of the British Columbia localities such as at Yalakom, Fort St. James, and Nahlin. However, in several areas of British Columbia, such as at Cassiar and Fort St. James (west of Pinchi-Omineca Fault), the sedimentary country rocks are presumably much more 0^{18}-rich, because the $\delta 0^{18}$ values of shales and limestones are ordinarily +14 to + 19 and +18 to +26, respectively.

One would expect that aqueous fluids migrating through and exchanging with the country rocks would become more 0^{18}-enriched in the carbonate-rich terranes than in regions composed only of graywackes and volcanic rocks. As is illustrated in figure 7-15, the calculated waters assumed to have coexisted with the serpentines in the Cassiar area are enriched in $\delta 0^{18}$ by about 6 per mil over analogous waters (with similar δD values) from the Nahlin and Fort St. James areas.

Because the country rocks into which low-grade alpine ultramafic bodies have been intruded are similar in many localities (graywacke- and volcanic-type rocks predominate), it is plausible that waters migrating through such terranes would undergo similar percentage O^{18}-enrichments (see figure 7-16).

If the migrating waters undergo complete equilibration with a very large reservoir of surrounding country rocks, the waters would all acquire some constant δO^{18} value, irrespective of latitude. However, it is very unlikely that the equilibration is so complete or that the water/rock ratios are so small that the original low-O^{18} values of the waters would be completely wiped out. It is more likely that, given similar terranes and similar physical conditions, all such waters would show the same percentage shift toward the "complete exchange-large reservoir" value. It is arbitrarily assumed in figure 7-16 that the latter value would be about + 5^{o}/oo; this is the value that the water would have after exchanging with an oligoclase having a $\delta O^{18} = +14$ at about 200°C (O'Neil and Taylor, 1967). In figure 7-16, most of the calculated waters for the volcanic-and graywacke-rich terranes lie within the 60 to 70 percent exchange band.

Variations in water/rock ratios

Both the initial δO^{18} value of the water and the amount of water which circulates through an ultramafic body during serpentinization are of significance in determining the final δO^{18} value of the serpentine. As the water/rock ratio increases, the serpentine takes on a δO^{18} value controlled more by the δO^{18} of the water than by the original mineral assemblage.

Figure 7-16. δD-δO^{18} diagram showing the calculated waters illustrated in figure 7-15. A δO^{18}-value of +5 (vertical line) is assumed for all waters undergoing complete (i.e. 100 %) equilibration with a very large reservoir of surrounding country rock at 200°C (see text). The series of straight lines lying between this vertical line and the meteoric water line represent lines of constant percent exchange away from the meteoric water line (for 50 %, 60 %, 65 %, 70 %, and 80 %). Location symbols: C = Caribbean; CA = Central America; Ca = California; O = Oregon; W = Washington; Y = Yalakom, B.C.; Cs = Cassiar, B.C.; F = Fort St. James, B.C.; N = Nahlin, B.C. Note in particular that most serpentinites occurring in volcanic- and graywacke-rich terranes (C, CA, Ca, O, Y, F, N) lie within the 60 to 70 percent exchange band.

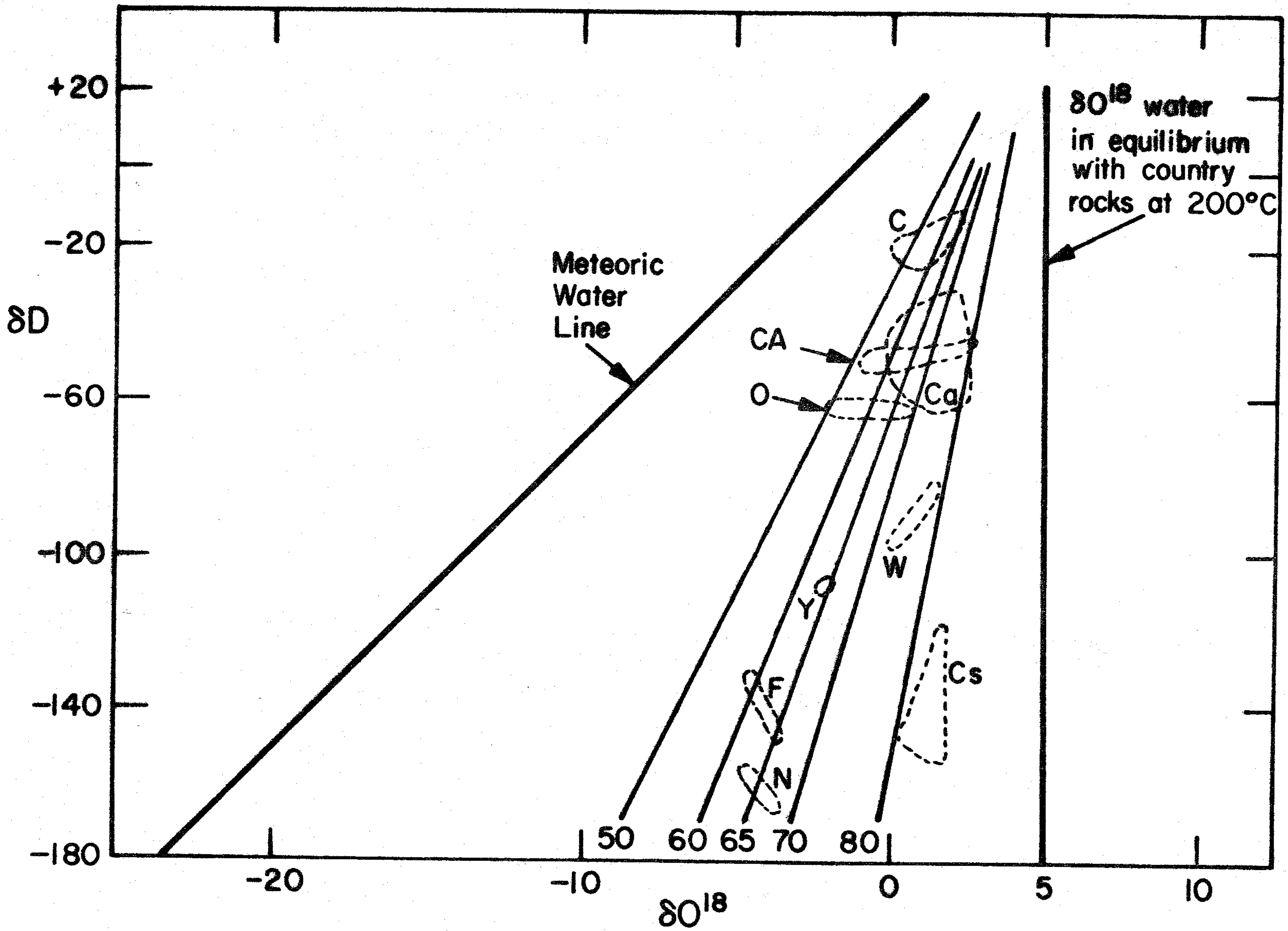
+20
-20
-60
-100
-140
-180
δD
-20
-10
0
5
10
δO18
Meteoric Water Line
δO18 water in equilibrium with country rocks at 200°C
50
60
65
70
80
C
CA
O
Ca
W
Y
F
N
Cs

Figure 7-16.

The relative proportions of exchanging meteoric water to exchanging silicate can be estimated using a closed-system model of the type employed by Sheppard et al. (1969). This model considers a system initially composed of x atom percent of exchangeable silicate oxygen and y atom percent of meteoric water oxygen. Thus, to a close approximation, we have:

Initially: $x\ \delta_{si} + y\ \delta_{wi} = Z$

Finally: $x\ \delta_{sf} + y\ \delta_{wf} = Z$

where δ_{si} = initial isotopic composition of silicates

δ_{sf} = final

δ_{wi} = initial isotopic composition of water

δ_{wf} = final

Z = constant for the system

Then

$$\frac{\delta_{si} - \delta_{sf}}{\delta_{wf} - \delta_{wi}} = \frac{y}{x} .$$

Such a model can be used to set a minimum limit on the relative proportions of fluid to exchanged silicate. In this model, the percent 0^{18} shift is calculated relative to δ_{wf}, the calculated $\delta 0^{18}$ value of water presumed to have been in equilibrium with the serpentine in question. For any sample in which P = 100%, $\delta_{wi} = \delta_{wf}$ (see Table 7-5). In reality, however, the $\delta 0^{18}$ of the water entering the ultramafic system is not necessarily constrained to any given value, hence P may be greater than 100%.

In this model, it is assumed that only olivine with a $\delta 0^{18}$ = + 5 $^{o}/_{oo}$ undergoes serpentinization and is a part of the exchangeable silicate. Also, equilibrium is assumed to be maintained between water and serpentine at a temperature of 100°C.

Although in practice such a serpentinization system is open, the above closed-system model probably gives values of y/x on the right order of magnitude if equilibrium is maintained.

In order to explore the applicability of this model in relation to the calculated waters (illustrated in figures 7-15 and 7-16), we will examine two samples whose $\delta 0^{18}$ values are greatly different. In Table 7-5, one sample from the Nahlin body of British Columbia and one from the San Luis Obispo body of California are compared.

If the $\delta 0^{18}$ value of the exchanged meteoric water entering the ultramafic body (δ_{wi}) is essentially the same as that (δ_{wf}) calculated to be in equilibium with the serpentine using the assumed serpentine-water fractionation factor discussed in chapter 4, then an "infinite" water/rock ratio is required (i.e., probably 5:1 or higher). This means that all of the calculated waters illustrated in figures 7-15 and 7-16 are for an "infinite" water/rock ratio only.

For the Nahlin sample, as the $\delta 0^{18}$ value of the water entering the ultramafic body (δ_{wi}) becomes lighter than $\delta_{wf}(P < 100\%)$, the ratio of water to exchangeable silicate (y/x) decreases. However, a δ_{wi} heavier than δ_{wf} cannot produce a serpentine of this $\delta 0^{18}$ value (+ 1.9$^{o}/_{oo}$) or any other value less than that of the initial silicate, since y/x becomes negative. In contrast, the San Luis Obispo sample requires that

Table 7-5

Sample No.	δ_{si}	δ_{sf}	δ_{wi}	δ_{wf}	P(%)	y/x
2-Nahlin	5.5	1.9	-21.2	-4.7	0	0.21
	5.5	1.9	-13.0	-4.7	50	0.44
	5.5	1.9	- 8.8	-4.7	75	0.88
	5.5	1.9	- 6.4	-4.7	90	2.1
	5.5	1.9	- 5.5	-4.7	95	4.5
	5.5	1.9	- 4.9	-4.7	99	18.0
	5.5	1.9	- 4.7	-4.7	100	∞
SLO - 6b	5.5	7.8	+ 1.2	+1.2	100	∞
	5.5	7.8	+ 1.6	+1.2	105	5.8
	5.5	7.8	+ 1.9	+1.2	110	3.3
	5.5	7.8	+ 4.9	+1.2	150	0.62
	5.5	7.8	+ 8.5	+1.2	200	0.31

P is the percent O^{18} shift away from the meteoric water line relative to δ_{wf}. Values of δ_{wi} at P = 0 are obtained from (1) the calculated δD values of the waters that equilibrated with these samples and (2) application of the meteoric water equation, $\delta D = 8\ \delta O^{18} + 10$. The final oxygen isotopic fractionation between serpentine and water, $\delta_{sf} - \delta_{wf}$, is assumed to be 6.6°/oo at 100°C (see chapter 4).

δ_{wi} be heavier than δ_{wf} in order to produce the observed serpentine δO^{18} value.

The lower limit of y/x in a serpentinite is obviously controlled by the stoichiometric content of H_2O in serpentine, because at least this much water had to enter the system. For the ideal serpentine composition, $y/x = 2/7 = 0.285$.

In figure 7-17, we have calculated the isotopic compositions of waters assuming a water/rock ratio = 1 (about 3 times the minimum stoichiometric amount of water required). These are compared to those in figure 7-16, where the water/rock ratio was assumed to be "infinite". This figure vividly illustrates the same feature discussed previously for the two samples of Table 7-5, namely that δ_{wi} must be greater than δ_{wf} for the O^{18}-rich serpentines and less than δ_{wi} for the low-O^{18} (high latitude) serpentines. Specifically, this model demands that $\delta_{wi} > \delta_{wf}$ when the δO^{18} value of the serpentine is heavier than the initial primary silicate (i.e., $\delta_{sf} > +5.5$), and vice versa.

For cases where $\delta_{sf} = +5.5$, or where the serpentine has the same δO^{18} value as the primary assemblage, this closed-system model is not valid since $y/x = 0$ or is indeterminate. Nevertheless, this model serves as a useful method of estimating the general range of isotopic compositions of waters involved in serpentinization of ultramafic rocks. Since the water/rock ratios very likely lie between 1 and ∞ in most cases of serpentinization, the waters illustrated in figure 7-17 probably represent the extreme range of values to be considered. It is thought, though, that water/rock

Figure 7-17. δD-δO^{18} diagram for calculated waters associated with lizardite-chrysotile in low-grade alpine serpentinite zones, assuming $y/x = \infty$ and $y/x = 1$. The $y/x = \infty$ areas are identical to the areas shown in figure 7-16 (except that all Central America samples are excluded). Note that the calculated ($y/x = 1$) waters (δwi) for serpentines in graywacke- and volcanic-rich terranes define a band distinct from the constant percentage-exchange band in figure 7-16. For two samples, 2-Nahlin and SL06b, listed in table 7-5, δwi-values are shown for a variety of different y/x ratios; note that δwi moves in opposite directions with decreasing y/x for these two samples. Also note that δwi nearly coincides with δwf for $y/x > 3$. The location symbols are identical to those given in figure 7-16.

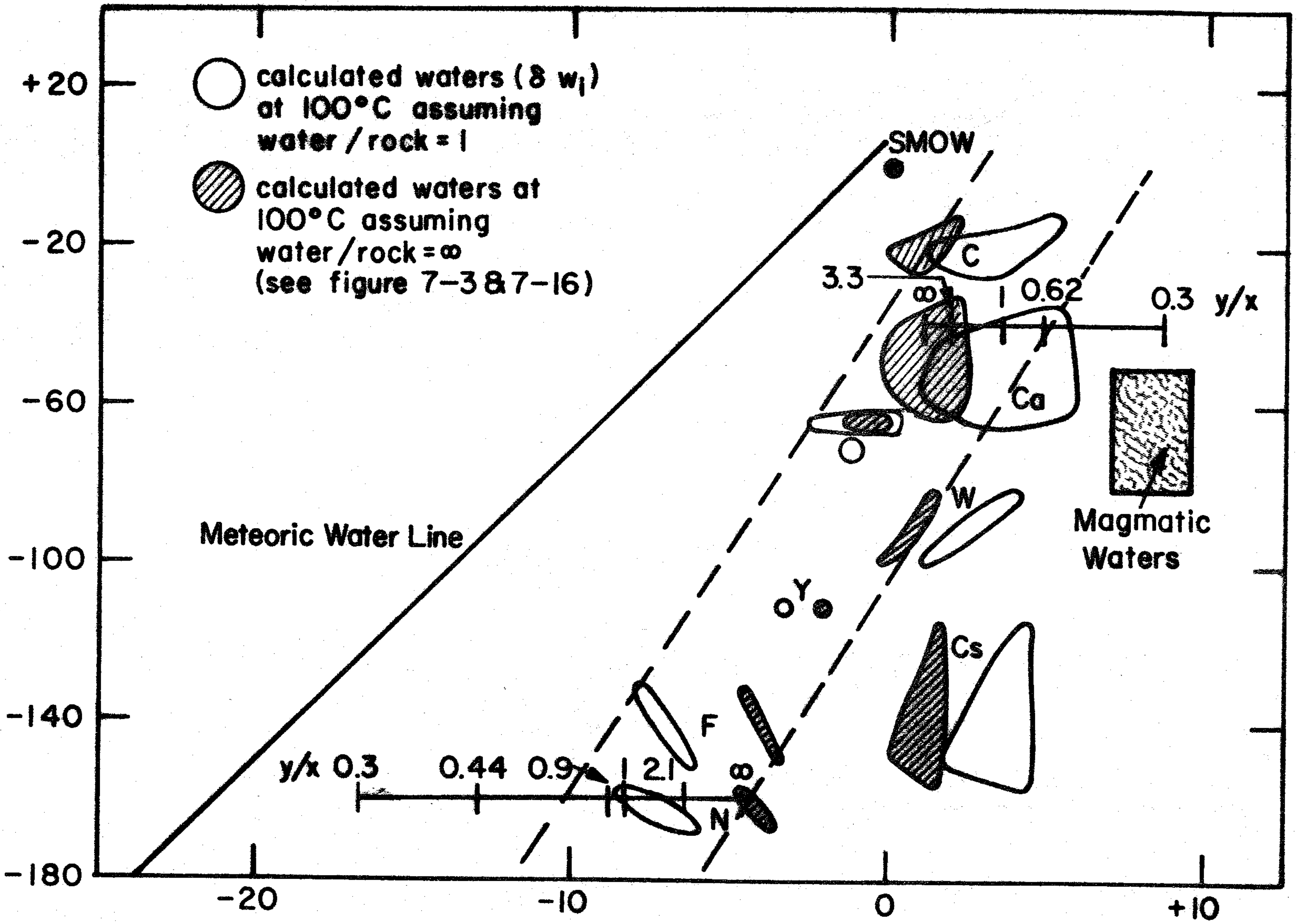
calculated waters (δ w$_i$) at 100°C assuming water / rock = 1
calculated waters at 100°C assuming water/rock = ∞ (see figure 7–3 & 7–16)
SMOW
Meteoric Water Line
Magmatic Waters
C
Ca
O
W
Y
Cs
F
N
3.3
∞
1
0.62
0.3
y/x
y/x 0.3
0.44
0.9
1
2.1
∞
+20
-20
-60
-100
-140
-180
-20
-10
0
+10

Figure 7-17.

ratios approximately equal to one are probably very realistic during serpentinization of low-grade alpine ultramafic rocks.

The general trend of calculated waters for water/rock = 1 is distinct from that illustrated in figure 7-16 for water/rock = ∞; the former waters lie along a trend more nearly parallel to the meteoric water line. Their isotopic compositons cannot be explained by a simple, uniform percentage "0^{18}-shift" relative to some constant $\delta 0^{18}$ value as was done in figure 7-16. This diagram, however, does emphasize even more strongly the contribution of meteoric waters in determining the $\delta 0^{18}$ values of low-grade alpine serpentinites.

The 'band' of calculated waters (for y/x = 1) illustrated in figure 7-17 probably represents the overall isotopic variation of waters responsible for most lizardite-chrysotile type serpentinization of alpine ultramafic rocks in volcanic- and graywacke-rich terranes. The calculated waters for the Washington and Cassiar, British Columbia samples in figure 7-17 lie outside this 'band', probably because these localities are made up of more 0^{18}-rich country rocks. One such calculated water for a serpentinite sample from Del Puerto, California lies outside of this band. This 'anomalously' heavy water may simply be due to an incorrect choice of y/x = 1 for this sample. If a larger water/rock ratio were chosen this point would lie within the above band.

Our choice of y/x = 1 for most of the calculated waters seems reasonable considering the overall trend of the 'band' illustrated in figure 7-17. If a smaller y/x ratio is selected, this band will become parallel or even intersect the meteoric water line at low δD values (e.g., if y/x = 0.3, see figure 7-17). Such a trend is impossible, since it requires progressively greater amounts of 0^{18} exchange for meteoric waters in low-latitude localities. Therefore, we can conclude that water/rock ratios well in excess of stoichiometric requirements (i.e., y/x > 0.3) are required for the development of most low-grade alpine serpentines.

Mixing with magmatic waters

Some of the calculated (y/x = 1) waters illustrated in figure 7-17 conceivably could be interpreted as mixtures of magmatic-meteoric or magmatic-oceanic waters. Contours for specific percentages of magmatic water in a simple magmatic-meteoric water mixture would lie parallel to the meteoric water line (see Craig, 1963); these would represent the maximum amounts of primary magmatic water in any such mixture. The band of calculated waters in figure 7-17, however, cannot wholly just represent simple meteoric-magmatic water mixtures.

Let us consider a few examples from figure 7-17 for purposes of discussion. The Oregon and California serpentinites could have formed from about a 1:1 mixture of unexchanged meteoric and primary magmatic waters. The Caribbean serpentines could result from about a 2/3 - 1/3 mixture of ocean water and primary magmatic water. However, for the British Columbia samples, simple mixing of unexchanged meteoric water with magmatic water requires meteoric waters that are unreasonably low in δD, even for such northerly localities. Conceivably, a mixture of about 2/3 magmatic water with 1/3 unexchanged meteoric water of $\delta D \approx -160$ could produce the calculated (y/x = 1) water for the Yalakom serpentine. However, the more northerly occurrences in British Columbia, in particular the Cassiar serpentinite, clearly cannot be explained by such a mechanism. If a magmatic water component existed in the fluids involved in serpentinization of these British Columbia bodies, it must have been relatively minor.

No single mixing mechanism involving magmatic water can possibly explain all the isotopic data. It is reasonable that the California and Caribbean serpentines were formed by the same types of processes as the British Columbia serpentines; hence, since we can rule out any important contribution of magmatic water in the British Columbia samples it is reasonable to rule it out for all of them.

VIII. ALPINE SERPENTINITES FROM HIGHER-GRADE METAMORPHIC TERRANES

8.1 General statement

Alpine serpentinite bodies emplaced in regionally metamorphosed Paleozoic eugeosynclinal rocks (greenschist to amphibolite facies) are found along the Appalachian ultramafic belt from Alabama to Newfoundland (see figure 8-1). The ultramafic intrusions are of probable Ordovician age, but many of them were subsequently subjected to an early Devonian regional metamorphism, notably those in Vermont (Jahns, 1967), and Quebec and Newfoundland (Stockwell, 1963).

Most of the Appalachian ultramafic rocks are partly to completely serpentinized (dominantly antigorite), and many show well-developed metasomatic mineral zones of talc (steatite), carbonate, and "blackwall" minerals (biotite, chlorite, and actinolite) at their outer contacts. Some bodies are only slightly altered, but others are completely steatitized. In many of the serpentinites of this type, chrysotile also is present as a minor constituent, commonly as cross-cutting veins of fibrous asbestos.

In the present study, detailed sampling was carried out on several bodies in Vermont and SE Pennsylvania together with a few samples from other bodies scattered along the Appalachian ultramafic belt. The localities are shown on the map in figures 8-1 and 8-2.

Figure 8-1. Map of North America showing sample localities discussed in chapters 8, 10, 11, together with the alpine serpentinite belts delineated by Hess (1955). In particular, the alpine serpentinite bodies from high-grade metamorphic terranes (discussed in chapter 8) occur in the Appalachian ultramafic belt, whereas other localities shown represent kimberlites (Moses Rock), Precambrian serpentines, and the zoned ultramafic bodies of SE Alaska. The latter lie within the west coast alpine belt, but are not typical alpine ultramafic bodies. The isotope data are indicated for two of the Appalachian serpentinite localities.

Figure 8-2. Geologic map of Vermont showing distribution of ultramafic bodies (after Chidester; Jahns, 1967). The isotope data and locations of all analyzed serpentine and talc samples are also shown. For Belvedere Mountain, only the range of isotopic compositions is indicated for each mineral type.

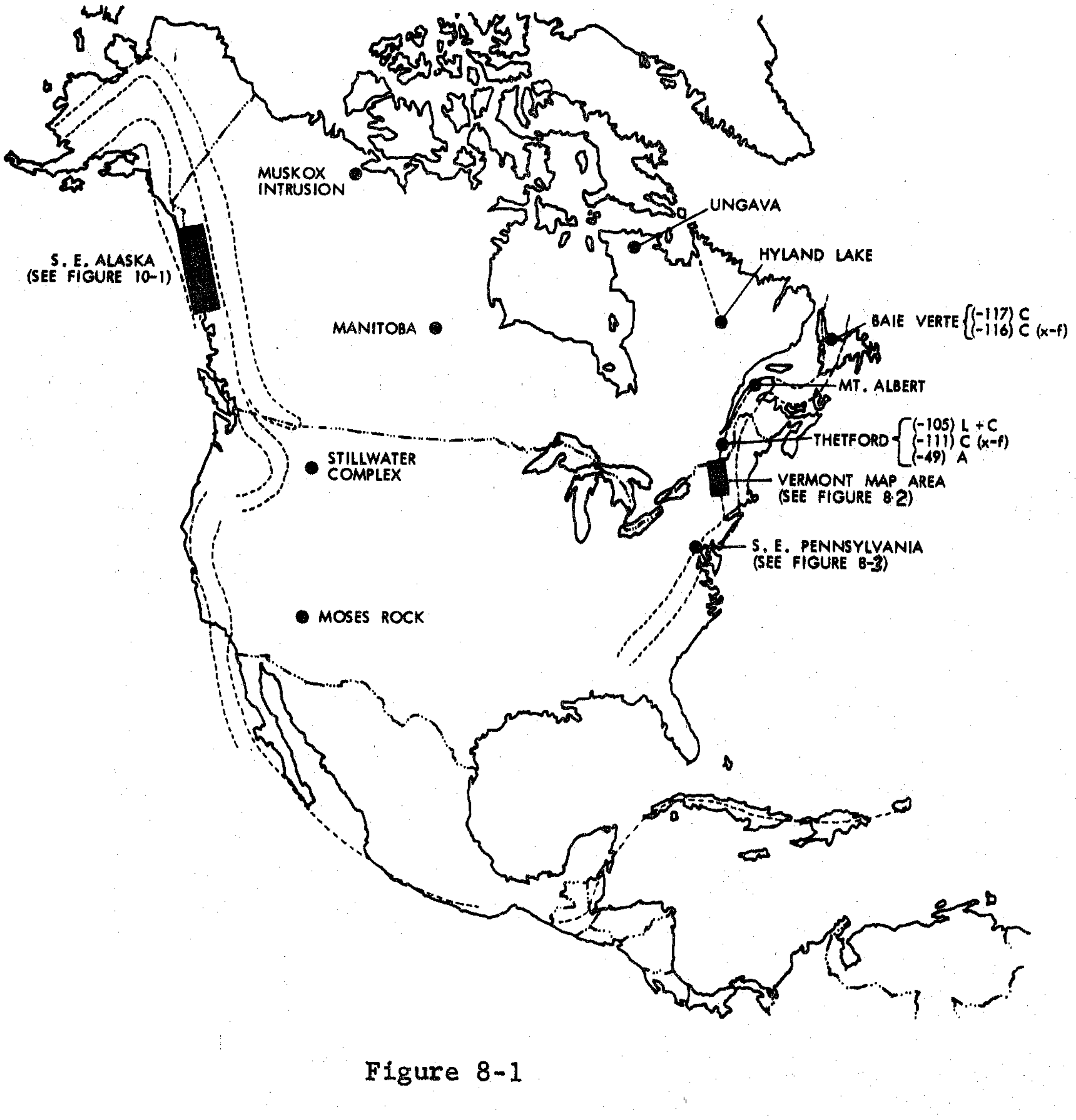
MUSKOX INTRUSION
UNGAVA
HYLAND LAKE
S. E. ALASKA (SEE FIGURE 10-1)
MANITOBA
BAIE VERTE {(-117) C (-116) C (x-f)
MT. ALBERT
THETFORD {(-105) L + C (-111) C (x-f) (-49) A
STILLWATER COMPLEX
VERMONT MAP AREA (SEE FIGURE 8-2)
S. E. PENNSYLVANIA (SEE FIGURE 8-3)
MOSES ROCK

Figure 8-1

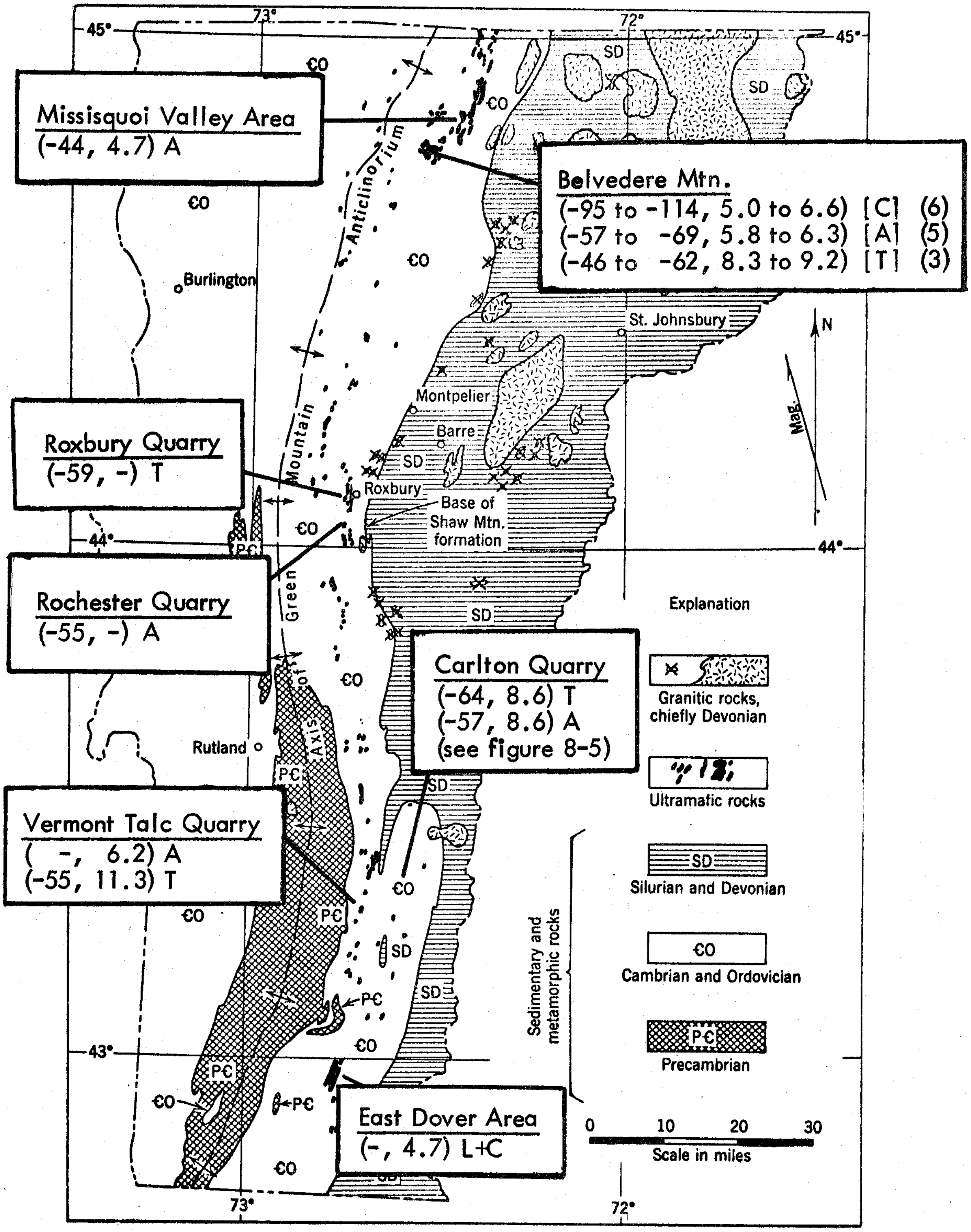

73°
72°
45°
44°
43°
Missisquoi Valley Area
(-44, 4.7) A
Belvedere Mtn.
(-95 to -114, 5.0 to 6.6) [C] (6)
(-57 to -69, 5.8 to 6.3) [A] (5)
(-46 to -62, 8.3 to 9.2) [T] (3)
Roxbury Quarry
(-59, -) T
Rochester Quarry
(-55, -) A
Carlton Quarry
(-64, 8.6) T
(-57, 8.6) A
(see figure 8-5)
Vermont Talc Quarry
(-, 6.2) A
(-55, 11.3) T
East Dover Area
(-, 4.7) L+C
Burlington
St. Johnsbury
Montpelier
Barre
Roxbury
Rutland
Base of Shaw Mtn. formation
Green Mountain Anticlinorium
Axis of
SD
ꞒO
PꞒ
N
Mag.
Explanation
Granitic rocks, chiefly Devonian
Ultramafic rocks
Silurian and Devonian
Cambrian and Ordovician
Precambrian
Sedimentary and metamorphic rocks
0 10 20 30
Scale in miles

Figure 8-2

8.2 Southeast Pennsylvania Ultramafic Bodies

In the southeastern part of Pennsylvania, ultramafic bodies have been intruded into a eugeosynclinal sequence and later subjected to Paleozoic (Acadian) metamorphism (Lapham, 1967).

The large, southernmost serpentinite body in figure 8-3 is intruded into the Peters Creek Formation on the north (dominantly metagraywackes in this region), and a complex zone of metagabbro and metanorite to the south. North of the New Texas serpentinite, the Peters Creek Formation consists largely of mica schist and quartzite. Carbonate units appear to be absent from the surrounding terrane. Furthermore, there appears to be little reported magnesite associated with these serpentinite bodies, except as late-stage fillings in fracture zones (Lapham and Geyer, 1965).

By means of structural studies Lapham and McKague (1964) have been able to correlate some of the deformational patterns in the serpentinite with the regional deformational history. The northern serpentinite belt shows a parallelism with the dominant regional pattern, suggesting re-intrusion, whereas the southern body appears to have partially retained its original orientation.

Lapham and McKague (1964) suggest the following sequence of serpentinization:

Stage 1. An initial chrysotile serpentinization occurred at the time the Cedar Hill body was subjected to a regional deformation.

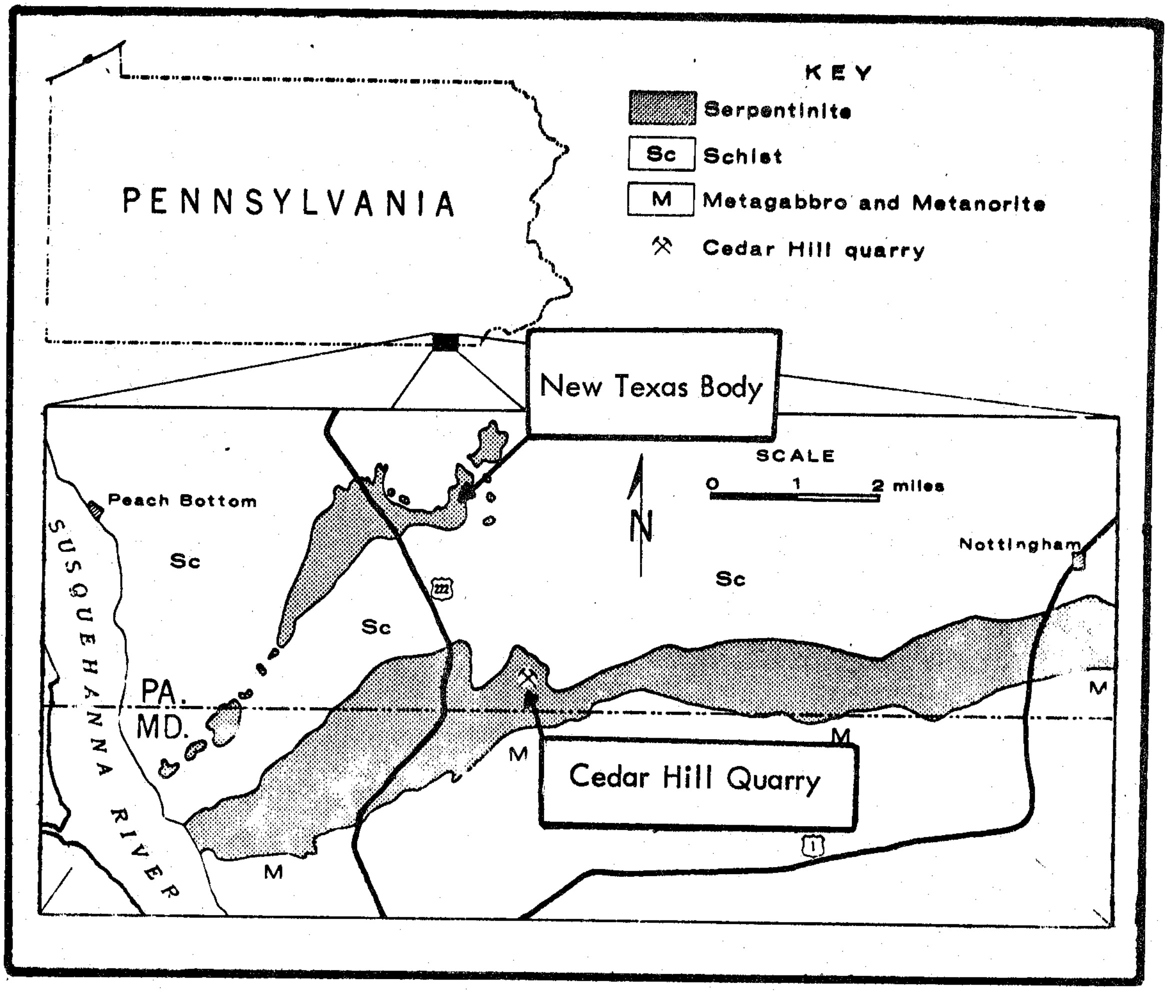

Figure 8-3

Generalized geologic map of a serpentinite area in Pennsylvania and Maryland (after Lapham, 1967). The two localities examined in this study are indicated.

Stage 2. Continuing deformation produced antigorite and/or lizardite. Many of the isotopically analyzed antigorite samples probably formed at this time.

Stage 3. Finally gash fractures containing chrysotile were produced. These are younger than antigorite veinlets of the same orientation.

A series of samples were selected for isotope study from many different physical settings within the Cedar Hill Quarry. The isotope data for these samples are given in Table 8-1. Sample 9 is a dunite partially altered to chrysotile (representing Stage 1 of Lapham and McKague), with later superimposed antigorite (Stage 2) and cross-fibre chrysotile (Stage 3) in minor amounts. Samples 5 and 6 are dominantly antigorite, probably representative of Stage 2. Samples 1, 2, and 7, composed predominantly of antigorite, are all associated with still later faulting. Lapham (personal communication) believes that sample 1 has been recrystallized due to faulting. Brucite sample 8 occurs as large crystalline flakes on fracture surfaces, hence it formed later than at least some of the serpentinization.

The two samples from the New Texas pluton are composed largely of antigorite, but sample 4 is massive and probably represents the bulk of the pluton, whereas the highly sheared sample 2 occurs within a fault zone.

Most of the samples from SE Pennsylvania, which are dominantly antigorite, show a fairly uniform $\delta D = -66$ to -39 and $\delta O^{18} = +6.6$ to $+7.9$. One brucite sample has a δD-value of -66, within the range displayed by

Table 8-1. Isotope data of samples from S. E. Pennsylvania.

Sample	Mineralogy*	% serp.	δD_S	δO^{18}_S	δO^{18}_M	T°C	Calculated H_2O§			Est. Pres. Day H_2O δD†	δO^{18} H_2O Shift‡
							δD	δO^{18} $(y/x=\infty)$	δO^{18} $(y/x=1)$		
Cedar Hill Quarry											
1	A, tr. L	100	-39	7.0	-	310	-14	7.0	8.5	-42	-
2	A	100	-46	6.9	-	310	-21	6.9	8.3		-
5	A	100	-66	7.1	0.0	280+	-39	6.5	8.1		-
6	A, tr. C	100	-42	7.0	0.4	310+	-17	7.1	8.6		-
7	A, tr. C	100	-57	7.6	-	310	-32	7.6	9.7		-
8	brucite	-	-66	-	-						
9	C, tr. A, tr. brucite	60D	-89	-	-	100	-44	-	-		-
New Texas Pluton											
2	A	100	-45	7.9	-	310	-20	7.9	10.3	-42	-
4	A > C	100	-53	6.6	-	-	-	-	-		-

the antigorites. Sample 9, composed largely of Stage 1 chrysotile, is appreciably different with δD = -89. This is distinctly lower than in any antigorite from this area. If the sequence established by Lapham and McKague is correct, this chrysotile must have survived the metamorphic event which produced antigorite. Its δD value thus may reflect a prior event; it is in any case unlikely that the δD value of this chrysotile was acquired from the same fluids that produced the antigorite.

Alternatively, the sequence established by Lapham and McKague may be erroneous, in which case this sample could represent a late stage of serpentinization.

8.3 Carlton Quarry, Vermont

Mineralogical relationships

The Carlton Quarry, described by Chidester *et al*. (1951) and by Phillips and Hess (1936), lies in a terrane of staurolite-kyanite grade schists in the Chester Dome area. Serpentinite is present in the core of the body, and along the outer contact monomineralic metamorphic differentiation zones of talc, actinolite and biotite (blackwall) have been formed. A schematic cross-section of the contact zone is given in figure 8-4, which is a typical example of the higher-temperature type of metamorphic differentiation described by Phillips and Hess (1936).

According to Chidester (1962) and Jahns (1967), who have described similar phenomena in other ultramafic bodies, steatitization was later than serpentinization and the two processes are unrelated. However, the development of the talc-carbonate and steatite apparently occurred simultaneously.

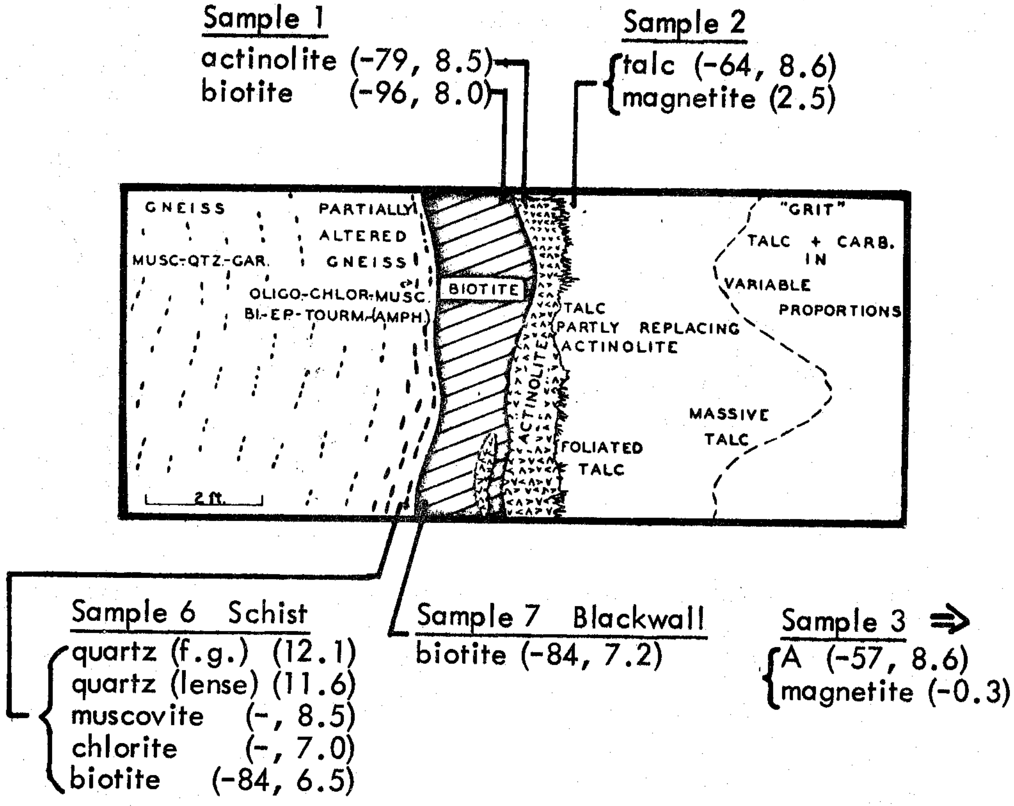

Figure 8-4.

Sketch of the contact metasomatic zonal sequence at the Carlton Quarry, Vermont (after Phillips and Hess, 1936) showing sample positions and isotope data. Samples 1 and 2 are from adjacent positions across the blackwall-actinolite-steatite zones. Samples 6 and 7 were also selected from adjacent positions, but from a different part of the body. Sample 3 was collected from the serpentinite zone in the interior part of the body, 200 feet inward from samples 1 and 2. The δO^{18} values of the various minerals in the schist are nearly identical to determinations made on several other schists from the Moretown formation analyzed by Garlick and Epstein (1967). This indicates that sample 6 above may in fact be typical of the country rock schists and need not have suffered O^{18} depletion as a result of exchange with the ultramafic body.

Both Jahns and Chidester concluded that the blackwall rocks clearly formed by replacement of the country rock. Many of the country rock minerals are preserved within the blackwall zone. The steatite has replaced serpentinite, blackwall rocks, talc-carbonates and country rock. Partial and complete pseudomorphs of talc after chrysotile and antigorite are observed. The talc-carbonate rock apparently formed at the expense of serpentinite, as evidenced by widespread remnants of antigorite and chrysotile and by numerous pseudomorphs of talc and carbonate after these minerals.

Both Chidester (1962)and Jahns (1967) conclude that steatitization occurred during regional metamorphism at essentially the temperature of the country rock at or near the peak of metamorphism. Chidester (1962) suggests that the alteration of serpentine to talc-carbonate rock simply required a gain of CO_2 and loss of H_2O. During the formation of steatite and the blackwall, however, Mg migrated from the serpentine into the blackwall, and Si migrated from the schist into the steatite zone. Other chemical changes are for the most part minor or negligible.

The various samples from the Carlton Quarry studied in this work are shown in figure 8-4. Samples 6 and 7 (schist and blackwall) were taken from adjacent positions; likewise samples 1 and 2 were selected next to each other, but from a different part of the body than 6 and 7.

Discussion of the isotope data

The δO^{18} values of serpentine, actinolite, and talc are similar and show essentially no change from the ultramafic rock outward across the contact zones. Two samples of blackwall biotite, however, have lower δO^{18} values, and they differ among themselves by 0.8 per mil in O^{18}/O^{16} and 12 per mil in D/H. One blackwall biotite sample is 0.7 per mil heavier than biotite in the immediately adjacent schist, even though both biotites have identical δD values of -84. The δD values systematically increase inward from -96 (biotite) to -79 (actinolite) to -64 (talc) to -57 (serpentine). This enrichment in δD is probably due to progressively increasing Mg/Fe ratios in the minerals as one moves inward; it almost certainly does not indicate a changing isotopic composition of the aqueous fluids. It is known that Mg-rich minerals concentrate D relative to their Fe-rich counterparts (Suzuoki and Epstein, 1970).

Isotopic homogenization has occurred locally, as evidenced by the general consistency of isotopic values for samples 1, 2, and 3. However, the isotopic differences between two blackwall biotites (δD = -84 and -96, δO^{18} = +7.2 and +8.0 for samples 7 and 1) from different regions of the same body preclude isotopic equilibration over large distances parallel to the contact.

The isotopic compositions of the various phases from a single schist sample (#6) adjacent to the blackwall zone are given in figure 8-4 and Table 8-2. These data suggest non-attainment of isotopic equilibrium for the following reasons. (1) The relative δO^{18} values of chlorite

Table 8-2. Isotope data of samples from the Carlton Quarry, Vermont.

Sample	Mineralogy*	% serp.	δD_S	δO^{18}_S	δO^{18}_M	T°C	Calculated H_2O§			Est. Pres. Day H_2O δD†	δO^{18} H_2O Shift‡
							δD	δO^{18} ($y/x=\infty$)	δO^{18} ($y/x=1$)		
1 Blackwall zone	biotite		-96	8.0						-70	
	actinolite		-79	8.5							
2 Steatite zone	T		-64	8.6	2.5						
3 Serpentine	A	100	-57	8.6	-0.3	220^+	-25	6.7	9.8		-
6 Schist	quartz (fine grained)			12.1							
	quartz (segregation)			11.6							
	muscovite			8.5							
	biotite		-84	6.5							
	chlorite (minor biotite)			7.0							
7 Blackwall zone	biotite		-84	7.2							

and biotite are opposite to what is observed in most equilibrated samples (see Garlick, 1969). (2) The δO^{18} of the fine-grained quartz is 0.5 per mil higher than in the quartz segregations. (3) There is a larger Δ quartz-muscovite (3.6 per mil) than is normally observed in most staurolite-kyanite grade rocks (Taylor, 1967b). (4) Petrographic evidence indicates that the chlorite formed later than the biotite. All of the above-mentioned features are compatible with extensive retrograde metamorphism.

Serpentinization

The measured serpentine-magnetite O^{18}-fractionation in sample 3 (8.7) suggests an isotopic "temperature" of about 220°C. This is entirely too low compared to the temperatures estimated for kyanite-staurolite grade metamorphism (510° to 580°C, Epstein and Taylor, 1967). However, for a variety of reasons that will be discussed in a later section, it is believed that this sample represents a close approach to equilibrium. Several different possibilities can be suggested to explain this anomalously low "isotopic temperature".

Serpentine and magnetite conceivably could have formed during the early stages of prograde metamorphism, at which time their δO^{18} values were essentially "frozen in", and preserved during the higher temperature stages of regional metamorphism. This, however, seems unlikely if the serpentine body was intimately exposed to the high-temperature fluids prevalent within the adjoining pelitic schists. Under such conditions, one would expect that oxygen-isotope exchange would continue to occur. Perhaps even the serpentine itself would break down at the relatively high temperatures of kyanite-staurolite grade metamorphism.

Serpentine has a very limited stability in the presence of any significant quantity of CO_2, as is illustrated in figure 8-5. According to this diagram, serpentine as well as brucite is stable only in essentially pure H_2O below 400°C. Between 425° and 500°C, a narrow wedge-shaped field of stability of serpentine exists, but it extends only to about 10 mole percent CO_2. However, it must be noted that this diagram is applicable only to the extent that chrysotile and antigorite are similar in their thermodynamic properties. The thermodynamic data used to calculate the serpentine stability fields are for chrysotile, but antigorite is the polymorph of interest in these rocks.

Some carbon dioxide certainly must have been present in the fluid phase of the country rock in order to produce the abundant magnesite observed within this type of body (see Phillips and Hess, 1936; Chidester, 1962; Jahns, 1967). Thus, if the serpentine body was exposed to CO_2-rich fluids ($\geqslant 0.10$ mole fraction) during the peak metamorphism, then serpentine could not have been stable and the ultramafic body would have been completely converted to talc-magnesite. Even if the CO_2 content of the fluid was small but not negligible, then serpentine could still conceivably form in the wedge-shaped serpentine stability field indicated in figure 8-5. However, any serpentine thus formed would tend to disappear and be replaced by talc-magnesite at lower temperatures, if communication with the external CO_2-bearing fluids was maintained.

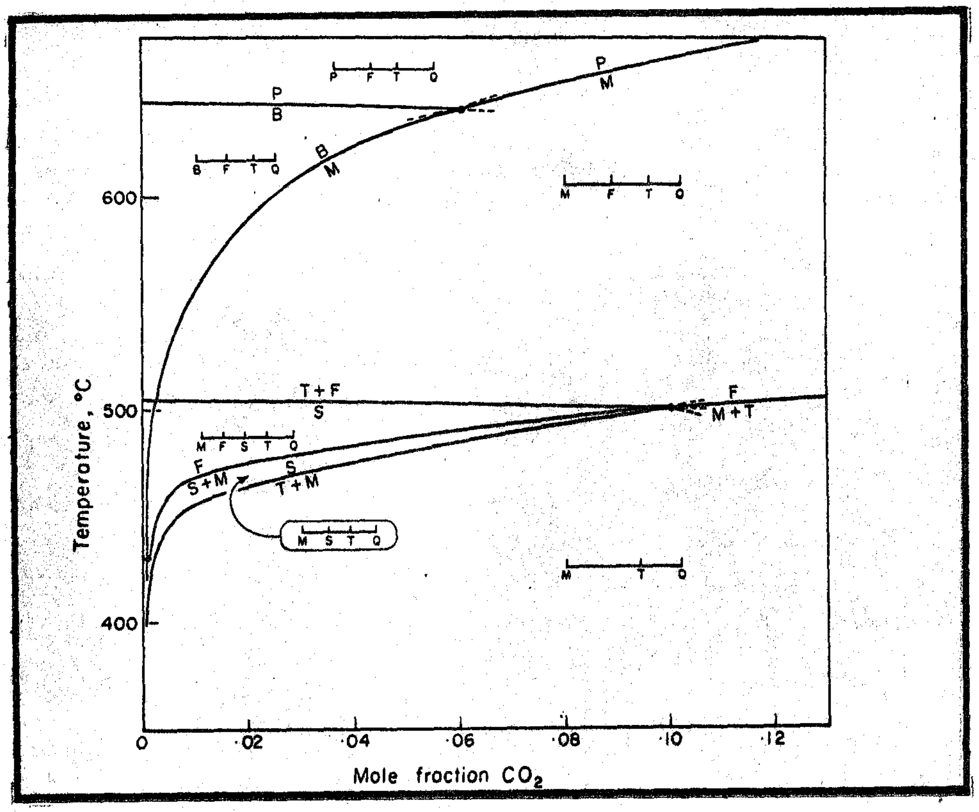

Figure 8-5

Calculated equilibrium curves for the H_2O-rich side of the 2000 bar T-x section in the system $MgO-SiO_2-H_2O-CO_2$. Temperature is plotted along the ordinate and composition of the gas phase along the abscissa. The phase assemblages that occur in each field are represented as points projected on the $MgO-SiO_2$ join. Solid circles represent isobaric invariant points. Symbols: M = magnesite, F = forsterite, S = serpentine, T = talc, Q = quartz, P = periclase, B = brucite (after Greenwood, 1967).

Consequently, if there was complete and easy communication between the serpentinite and the outside environment, the ultramafic body probably would be entirely composed of talc-magnesite in areas where the metamorphic pore fluids contained CO_2. The fact that talc-carbonate is generally confined to the outer contact of the body can thus be taken as evidence that metamorphic fluids did not have ready and complete access to the central portions of the body.

Many examples exist to demonstrate that certain rock types are relatively impervious to oxygen isotopic communication with an external fluid phase. For example, a quartz-rich pod enclosed in a marble unit in Dutchess County, New York (Garlick and Epstein, 1966) has an abnormally large δO^{18} value, suggesting that little O^{18} exchange occurred between the marble and surrounding pelitic schists even during high-rank metamorphism. Relatively plastic, easily deformed rock types like marble and serpentine might tend to be impermeable to metamorphic pore fluids, because fracture openings either do not form, or if they do form, they are quickly sealed by plastic flowage or recrystallization.

In addition to the very limited stability of serpentine in the presence of any significant amount of CO_2, the stability field of serpentine can be greatly reduced even in the presence of pure H_2O fluids. For example, serpentine would also be stable only at relatively low temperatures if $P_{total} > P_{H_2O}$, which might occur if the fluid were migrating through a fissure system open to a shallower depth (Thompson, 1955). Such a situation serves to decrease the maximum dehydration boundary of serpentine from about 500°C to some lower temperature.

However, neither this effect nor the presence of abundant CO_2 would be expected to depress the maximum stability fields of talc, chlorite, or actinolite to the extent that any of these phases would become unstable at the temperatures of peak metamorphism.

It is therefore not unlikely, by a combination of fissure equilibrium and presence of CO_2 in the metamorphic pore fluids, that antigorite did not form during regional metamorphism in the Carlton Quarry area except during the early prograde stages and/or the late retrograde stages in the presence of low-CO_2 waters. Such an origin would be more in line with the anomalously "low" serpentine-magnetite "isotopic temperatures".

Steatitization

Jahns (1967) states that the magnetite of the steatite zone is largely relict from serpentinite. If so, it would appear that the magnetite from the steatite sample was recrystallized during the formation of the talc, because its δO^{18} value is 2.8 per mil heavier than the magnetite in the adjoining serpentinite. This type of change in the magnetite is exactly what would be predicted if steatitization occurred at a higher temperature than the serpentinization.

If we make the not unreasonable assumption that talc and biotite have similar isotopic properties, it is also of interest that the measured Δ talc-magnetite = 6.1 is considerably larger than the range of Δ biotite-magnetite values in kyanite-staurolite zone pelitic schists (3.3 to 4.3, Garlick, 1969). If equilibrium was attained, this might suggest formation and/or re-equilibration of the talc-magnetite pair at temperatures lower than the peak of metamorphism. A very tenuously estimated "isotopic temperature" of this talc-magnetite pair is only slightly higher than that of the adjacent serpentine-magnetite pair (~ 300°C vs. 220°C). Thus, although much more isotope data must be gathered on coexisting talc and magnetite, it is likely that this particular talc-magnetite fractionation does not represent isotopic equilibrium. This might be expected in the light of the geological evidence that the magnetite is relict from the serpentine, because it was probably not completely recrystallized during steatitization.

8.4 Belvedere Mountain Quarry Area

Geological relationships

The Belvedere Mountain Quarry area, described by Cady *et al*. (1963), lies in a schist and amphibolite terrane that has been subjected to a biotite- to garnet-grade metamorphism. Many of the samples in this study were collected along the NE edge of the Lowell Quarry near the contact of the serpentinite and schist of the Hazens Notch formation. Other samples were selected from the C-area quarry about 0.5 miles SW of the Lowell Quarry.

The two principal types of metasomatic zonal relationships that are observed at contacts between the ultramafic bodies and the country rocks are discussed by Cady *et al*. (1963). The most common type, developed primarily at the serpentine-amphibolite contacts, involves the sequence antigorite-chlorite-calc-silicate rock (diopside, clinozoisite, grossularite, and vesuvianite)-amphibolite. However, the principal zonal sequence observed in the NE wall of the Lowell

Quarry is serpentine-talc and carbonate-steatite-chlorite-mica schist. Many of the analyzed talc samples are from this latter type of sequence.

The serpentinite mass itself is generally schistose and highly sheared, particularly at its borders. Some remnant olivine occurs in the central part of the quarry, but most of the ultramafic mass is completely serpentinized. Chrysotile fibres are dispersed throughout the schistose serpentinite on irregular slip planes, and as cross-fibre veins.

There is extensive literature on the development of cross-fibre chrysotile veins. Many workers believe that they are developed by the introduction of new material carried in the aqueous solutions that migrate along fracture openings (Lindgren, 1933, page 395; Riordon, 1962; Stockwell, 1957). However, Gold (1967) suggests that most of the fibre bands were formed within the serpentinite simply by rearrangement of adjacent material.

In the Thetford area in Quebec, Riordon (1955) has studied the development of cross-fibre chrysotile veins, similar in structure to those from the Belvedere Mountain area. He states that the asbestos veins were the latest product of serpentinization, and that asbestos was formed, for the most part, after all of the adjustments associated with the serpentinization had been completed.

Discussion of isotope data

The δD and δO^{18} values of various samples from the Belevedere Mountain Quarry area are given in figure 8-2, Table 8-3, and plate 8-1. Samples 1 and 1b were taken from a small 10 ft. x 20 ft. lens of

Table 8-3. Isotope data of samples from the Belvedere Mtn. Quarry, Vermont.

Sample	Mineralogy*	% serp.	δD_S	δO^{18}_S	δO^{18}_M	T^oC	Calculated $H_2O^{\S}$			Est. Pres. Day H_2O δD†	δO^{18} H_2O Shift‡
							δD	δO^{18} (y/x=∞)	δO^{18} (y/x=1)		
1	A > T	100	-	7.6	-	-	-	-	-	-75	-
1b	T	-	- 62	9.2	-						
5	C (x - f)	100	-100	5.9	-	100	-55	-0.7	-0.3		7.4
	A	100	-	5.9	-2.1	240^+	-	4.5	4.9		-
	brucite vein	-	- 35	1.0	-						
8	C > L	100	- 82	5.8	-	100	-36	-0.8	-0.5		5.0
	A	100	-	5.8	-2.6	230^+	-	4.2	4.5		-
9	A, tr. C	100	- 57	6.1	-2.5	225^+	-25	4.4	5.0		-
	C (x - f)	100	-	5.0	-	100	-	-1.6	-2.1		-
14	T, tr. A	-	- 46	8.3	-	-	-	-	-		-
15	A	100	- 62	6.2	-	$240^{\emptyset}$	-30	4.8	5.5		-
17	T > A	-	- 48	-	-						

Table 8-3 (continued)

Sample	Mineralogy*	% serp.	δD_S	δO^{18}_S	δO^{18}_M	T°C	Calculated H_2O§			Est. Pres. Day H_2O δD†	δO^{18} H_2O Shift‡
							δD	δO^{18} (y/x=∞)	δO^{18} (y/x=1)		
11 a	C (x - f)	100	-114	6.5	-	100	-69	-0.1	0.9	-75	9.8
11 b	C (x - f)	100	-104	-	-	100	-59	-	-		-
11 c	C (x - f)	100	-108	-	-	100	-63	-	-		-
11 d	C (x - f)	100	- 95	6.6	-	100	-50	0.0	1.1		7.5
11 e	C > A	100	- 85	6.1	-	-	-	-	-		-
11 f	C > A	60	- 80	6.1	-	-	-	-	-		-
11 g	C > A	60	-	6.5	-	-	-	-	-		-
11 h	C > A	100	- 80	-	-	-	-	-	-		-
11 i	A, tr. C	100	- 69	6.3	-	240ø	-37	4.9	5.7		-

serpentinite in the albite gneiss unit outside of the main ultramafic body of the Lowell Quarry. The rest of the samples were all collected within or at the contact of the main ultramafic mass. The major isotopic relationships are:

(1) The δD values of chrysotiles (-82 to -114) are consistently much lower than those of pure antigorites (-57 to -69). Where samples contain mixtures of these two types, the δD values usually lie between the two extremes.

(2) The δD of talc (-46 to -62) is similar to that of antigorite.

(3) The brucite vein has a higher δD and lower δO^{18} (-35, +1.0) than the nearby antigorite; (recall that one brucite from SE Pennsylvania has a somewhat lighter δD than much of its adjacent antigorite).

(4) The total O^{18}/O^{16} variation in the serpentinites is small, and essentially independent of the type of serpentine. This is particularly true for all serpentine samples from the main ultramafic body in the Belvedere Mountain area. The small serpentinite lens (Sample 1) is slightly richer in O^{18}.

(5) The δO^{18} values of the talc (+9.2 to +8.3) are generally heavier than those of the antigorite (+5.9 to +6.3).

(6) Both the coarse-grained magnetite veins (samples 5 and 8) and the fine-grained disseminated magnetite in antigorite (sample 9) have very similar δO^{18} values (-2.1, -2.6 and -2.5). The Δ serpentine-magnetite values are also very similar (see figure 4-1).

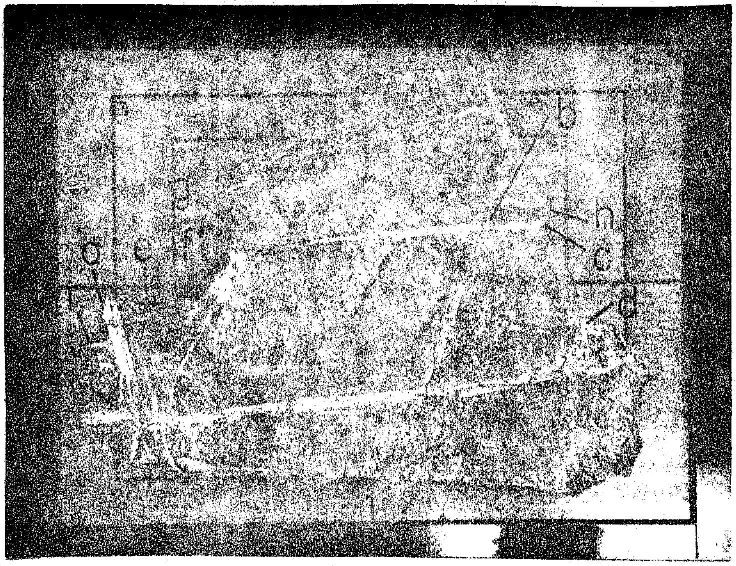

Plate 8-1
(area 3 - 5.2 x 7.0 inches)

Sample 11, Belvedere Mountain, Vermont. Typical mass of serpentinized dunite (light colored zone) altered to antigorite (dark zone) and cut by younger veins of cross-fibre chrysotile. Some platy forms of chrysotile are present adjacent to the cross-fibre veins where they transect antigorite. The cross-fibre chrysotile veins (a,b,c,d) have $\delta D = -95$ to -114, $\delta O^{18} = +6.5$ to $+6.6$. The samples that are dominantly chrysotile with minor antigorite (e.f,g,h) have $\delta D = -85$ to -80, $\delta O^{18} = +6.1$ to $+6.5$ (also, see Table 8-3). A sample largely of antigorite (i) has $\delta D = -69$, $\delta O^{18} = +6.3$.

(7) Analogous to the situation observed in the Carlton Quarry, the "isotopic temperatures" implied by the serpentine-magnetite fractionations also appear to be abnormally low (average of ~230°C) compared to the temperatures estimated for garnet-grade metamorphism (410° to 490°C, Epstein and Taylor, 1967).

In addition to the samples described above, one large sample (#11, plate 8-1) containing cross-fibre chrysotile veins that cut antigorite and partially serpentinized dunite was studied in detail to ascertain the isotopic variations within a single hand specimen. The isotopic relationships observed in this single hand speciman are similar to those observed on a larger scale throughout the entire quarry.

8.5 Other localities

The locations and isotopic data for a variety of other serpentinite bodies from eastern North America are given in figures8-1 and 8-3, and Table 8-4 and 8-5. In general, chrysotile- and lizardite-type serpentines characteristically have light δD values, whereas the antigorite and talc samples are deuterium-rich. For example, even within a single deposit such as the Thetford Quarry, Quebec, both the massive lizardite-chrysotile and a cross-fibre vein of chrysotile have δD of -105 to -111, while a sample of fibrous antigorite (picrolite) has a δD of -49.

The Baie Verte body in Newfoundland contains chrysotile that is about 10 per mil lighter in δD than the Thetford chrysotile. This is compatible with its more northerly occurrence, if one assumes that meteoric ground waters were involved in the formation of the chrysotile.

Table 8-4. Isotope data of samples from miscellaneous localities in Vermont.

							Calculated H_2O§			Est. Pres. Day H_2O	
Sample	Mineralogy*	% serp.	δD_S	δO^{18}_S	δO^{18}_M	T°C	δD	δO^{18} ($y/x=\infty$)	δO^{18} ($y/x=1$)	δD†	δO^{18} H_2O Shift‡
East Dover	L + C	100	-	4.7	-	100	-	-2.1	-2.9	-70	-
Vt. Talc Quarry	A	100	-	6.2	1.4	460+	-	7.8	8.5	-70	-
	T	-	-55	11.3	-						
Rochester Quarry	A	100	-55	-	-	310	-30	-	-	-70	-
Roxbury Quarry	T	-	-59	-	-					-70	
	a Actinolite	-	-91	8.2	-						
	b Actinolite	-	-89	8.1	-						
Missisquoi Valley	A	100	-44	4.7	-	310	-19	4.7	3.9	-80	-

Table 8-5. Isotope data of samples from Quebec and Newfoundland.

							Calculated H2O§			Est. Pres. Day H_2O	δO^{18} H_2O
Sample	Mineralogy*	% serp.	δD_S	δO^{18}_S	δO^{18}_M	T^oC	δD	δO^{18} $(y/x=\infty)$	δO^{18} $(y/x=1)$	δD†	Shift‡
Thetford, Quebec											
N 2-3	L + C	100	-105	-	-	100	-60	-	-	-80	-
N 2-5	C (x - f)	100	-111	-	-	100	-66	-	-		-
N 2-7	A	100	- 49	-	-	310	-24	-	-		-
Baie Verte , Newfoundland											
groundmass	C, tr. B	100	-117	-	-	100	-73	-	-	-80	-
cross-fibre	C	100	-116	-	-	100	-72	-	-		-

It is important to note that antigorite from the Vermont Talc Quarry in a staurolite-kyanite grade metamorphic terrane gives an O^{18} "temperature" of 460 ± 50°C (see Table 5-4), which is the highest temperature antigorite recognized in this work. Even here, however, it would appear that isotopic equilibration (and serpentine formation?) may have taken place at a temperature slightly below the peak metamorphic temperature (510° to 580°C, Epstein and Taylor, 1967).

8.6 General discussion of isotope data on higher-grade alpine serpentinites

The δD values of serpentines from relatively high-grade metamorphic terranes display the *same* pattern as do those from the low-grade areas discussed in the previous chapter. The δD values of lizardite and chrysotile (-82 to -117) are distinct from those of antigorite (-39 to -69) and talc (-46 to -64). Furthermore the average δD values of the lizardite-chrysotile samples decrease in a regular pattern, from -89 in southeastern Pennsylvania (1 sample), to -101 at Belvedere Mountain, Vermont (7 samples), to -108 at Thetford, Quebec (2 samples), to -116 at Baie Verte, Newfoundland (2 samples). In general, samples composed of mixtures of these two different types of serpentine have intermediate δD values compared to end-member samples from the same locality.

Isotopic compositions of waters involved in serpentinization

Estimates of the isotopic compositions of waters assumed to have equilibrated with the Appalachian serpentines are illustrated in figure 8-6. In calculating these waters, the following temperatures are used. (1) For the SE Pennsylvania antigorites, 280°C and 310°C are used for samples 5 and 6 as calculated from measured serpentine-magnetite fractionations; 310°C is assumed for all others. (2) For the Carlton Quarry, Vermont, 220°C is used. (3) For the Belvedere Mountain Quarry, 225° to 240°C is employed for antigorite samples for which serpentine-magnetite fractionations were measured, while 240°C is used for the rest of the antigorites. (4) 310°C is used for all antigorites from other areas. (5) 100°C is used for all chrysotiles.

In addition to the above calculated waters (for $y/x = \infty$), the initial δO^{18} values of waters entering the ultramafic bodies are estimated assuming $y/x = 1$ (see figure 8-6). Both types of calculated waters ($y/x = \infty$ and $y/x = 1$) fall into two discrete groupings; the waters associated with antigorites are enriched in both D/H and O^{18}/O^{16} relative to those associated with chrysotile. The former group strongly suggests metamorphic-type waters, whereas the latter are more suggestive of exchanged meteoric waters. Note that these discrete groupings come about primarily as a result of differences in assumed equilibrium temperatures, because the δO^{18} values of the lizardite-chrysotiles and the antigorites are similar.

Figure 8-6. $\delta D - \delta O^{18}$ plot of analyzed serpentines and corresponding calculated ($y/x = \infty$) waters (connected by dashed tie lines) from the Appalachian alpine ultramafic belt. Calculated ($y/x = 1$) waters are also indicated at the tips of the arrows. Note the completely distinct H_2O isotopic compositions for the chrysotiles and antigorites. Calculated ($y/x = 1$) waters for one Vermont antigorite and all SE Pennsylvania antigorites fall within the range of normal metamorphic waters (see figure 5-1). Those from Belvedere Mountain and from Missisquoi Valley are anomalously depleted in O^{18}, but note that certain pelitic schist country rocks from Vermont are also O^{18}-depleted (see Garlick and Epstein, 1967, samples EV 17, EV 18, EV 20, all from the Moretown formation, the unit in which most of the Vermont ultramafic bodies occur.

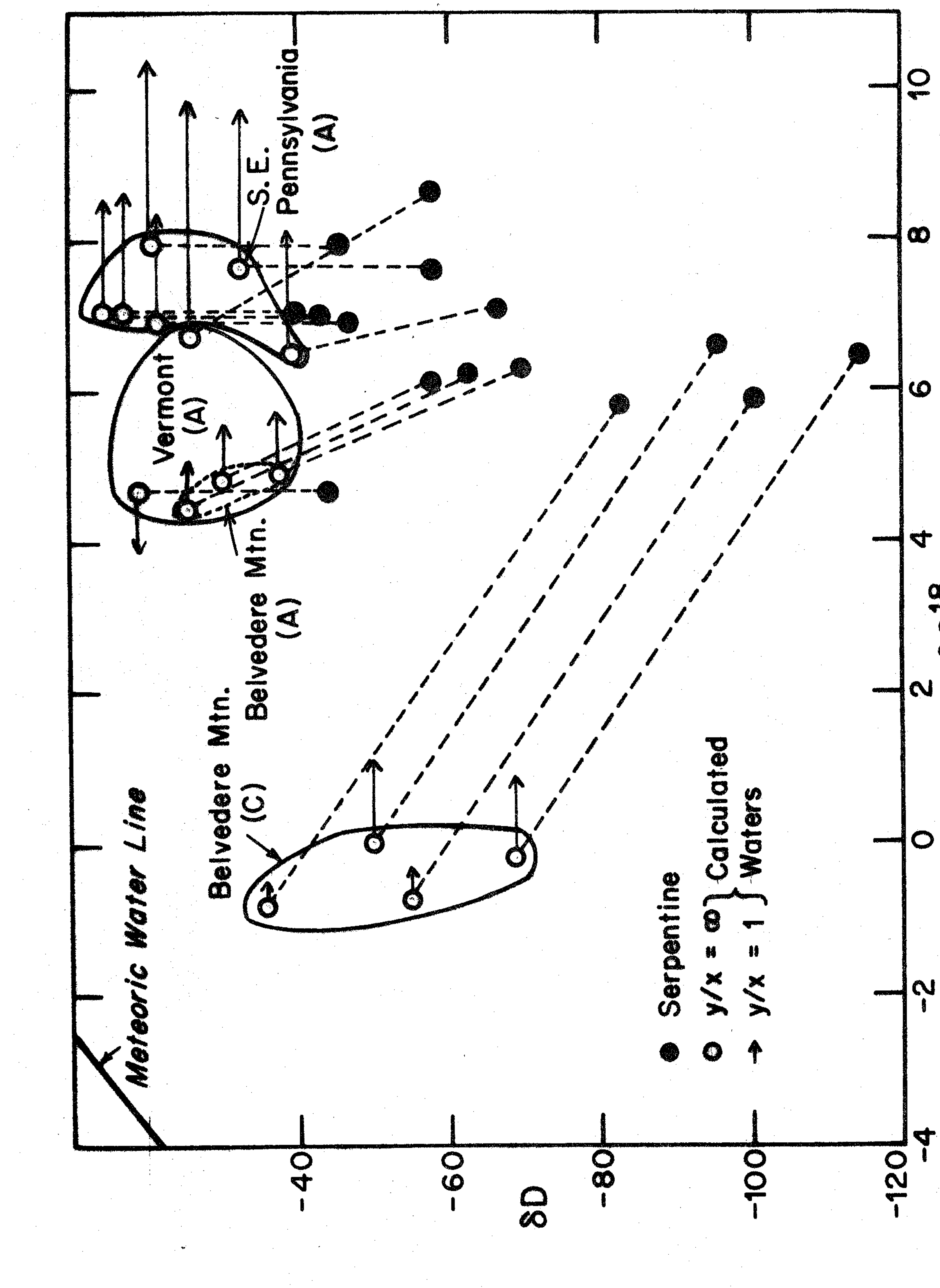
Meteoric Water Line
Belvedere Mtn. (C)
Belvedere Mtn. (A)
Vermont (A)
S.E. Pennsylvania (A)
● Serpentine
○ y/x = ∞
→ y/x = 1
Calculated Waters
δD
-40
-60
-80
-100
-120
δO18
-4
-2
0
2
4
6
8
10

Figure 8-6

It can hardly be a coincidence that the δO^{18} values of both the chrysotile and the adjacent antigorite are similar. In the previous section, it was also noted in the Cassiar serpentinite body that the cross-fibre chrysotile veins and the adjacent massive chrysotile had similar δO^{18} values, but different δD values. However, one would perhaps expect this similarity, if a relatively small amount of exchanged meteoric water enters a fracture zone and simply recrystallizes the antigorite. The δO^{18} might be essentially preserved even though the δD is drastically changed, because the hydrogen/oxygen atom-ratio in serpentine is only 2/9 as large as it is in water. It is difficult to accurately assess this effect quantitatively, however, without knowing the exact isotopic compositions of the water entering the system.

The two groups of calculated waters shown in figure 8-6 further suggest that serpentinization occurred in at least two completely separate events. Similar to the situation described in the previous chapter, antigorite and talc apparently formed during a relatively deep-seated regional metamorphism, whereas the lizardite and chrysotile must have formed at shallower depths during a distinctly later period, perhaps when waters of surficial origin gained access to the ultramafic bodies.

The δO^{18} values of the calculated ($y/x = 1$) waters in equilibrium with antigorites are generally lower in O^{18} than the typical metamorphic waters that would have been present in the nearby pelitic schists during metamorphism. A water coexisting with a typical pelitic schist might have a δO^{18} value of about +12 at 530°C or +9 at 400°C (Taylor, 1967a), decreasing to perhaps +4 or +5 at around 220°C. These lower temperature waters are reasonably consistent with those calculated for many of the antigorite samples. Note also that the H_2O in equilibrium with the blackwall biotite of the Carlton Quarry at about 500°C would have an approximate δO^{18} value of +11 to +12 (Shieh and Taylor, 1969b), consistent with the metamorphic waters in the pelitic schists at this temperature. Furthermore, the δO^{18} differences between the metamorphic waters equilibrated with the antigorite and the nearby blackwall biotite are a further confirmation that these two minerals formed at separate stages.

However, it is important to note that several relatively high temperature metamorphic waters that apparently coexisted with certain pelitic schists in southern Vermont have abnormally light δO^{18} values (+5.6 to +7.9, Taylor, 1967b). Many of the ultramafic bodies in Vermont occur in this particular stratigraphic unit (Moretown formation).

Temperatures of serpentinization

The isotopic "temperatures" (220° to 460°C) deduced from measured antigorite-magnetite fractionations all appear to be abnormally low compared to the maximum estimated temperatures of the adjacent regionally metamorphosed rocks. However, the general consistency of Δ-values and the general chemical purity and homogeneity of the magnetites in several of the serpentinites (see Table 4-1) are consistent with a close approach to equilibrium. Furthermore, many of the antigorites are very fine-grained (< 0.3 mm), whereas adjacent metasomatic "blackwall" minerals (which certainly formed during regional metamorphism) are often coarsely crystalline. This in itself perhaps suggests that antigorites may have formed at lower temperatures than the blackwall-zone minerals, in agreement with the oxygen isotope data.

The "low temperatures" may be due to several different factors, such as (1) isotopic preservation of a pre-existing low-temperature serpentinization event, (2) isotopic retrogradation and recrystallization during cooling of the serpentine body, and/or (3) serpentinization only at low temperatures during the waning stages of metamorphism, after formation of the metasomatic zones at the outer contact of the ultramafic body.

It may be significant that carbonates are abundant in the alteration zones of the Vermont serpentine bodies. Furthermore, abundant metamorphosed carbonate country rocks lie in near proximity to almost all of the Vermont serpentinites examined in this study. Metasomatic carbonates are much less abundant at the Cedar Hill Quarry in Pennsylvania, and the "isotopic temperatures" in these antigorites are generally higher than for most of the Vermont samples. These observations suggest the possibility that during the formation of antigorite in the Cedar Hill area, where the CO_2 content of the fluid was probably very small, antigorite was able to form at relatively high temperatures.

However, in Vermont, where CO_2 was almost certainly present in the fluid phase, antigorite may not have been stable during the period of peak metamorphic temperatures. In fact, the field relationships suggest that it was replaced by talc-magnesite at this stage. Where the CO_2-rich metamorphic pore fluid presumably came into contact with the outer edges of the serpentinite body, talc and magnesite were formed. However, where this fluid phase was unable to completely penetrate the interior portions of the serpentinite body, the serpentine perhaps was able to survive the regional metamorphism.

It seems most likely on the basis of the isotopic evidence that serpentine formed principally during the early stages of prograde metamorphism and/or the late stages of retrograde metamorphism. The geologic field relationships discussed in section 8.3 are more consistent with the former hypothesis. Least likely is the hypothesis that a pervasive isotopic re-equilibration occurred all the way down to relatively low temperatures during the period of cooling following the peak of metamorphism; this is discussed more fully in chapter 12.

IX. VOURINOS OPHIOLITE COMPLEX, GREECE

9.1 Geological relationships

The Vourinos Complex in northern Greece is a type-example of the classic "ophiolite suite", in which the ultramafic rocks form lower portions of pseudostratiform sequences overlain by mafic rocks, lavas, and radiolarian cherts. The Vourinos Complex lies along the western boundary of the Pelagonian Massif, composed dominantly of marbles and the younger Meso-Hellenic sediments (see figure 9-1). Some 50 km to the southwest, a large allochthonous complex, the Pindos Mass, lies at the contact of the Olonos-Pindos Zone flysch and younger Meso-Hellenic Trough sediments.

Several different whole-rock samples from the Pindos Mass were studied by Javoy (1970), who divided the $\delta0^{18}$ values into three groups based on rock type: (a) serpentinized peridotites with $\delta0^{18} = +3.6$ and $+4.8$ per mil, (b) gabbros and dolerites with uniformly low $\delta0^{18}$ values ($+3.6$ to $+3.8$) relative to "normal" basalts, and (c) albitophyres with unusually heavy $\delta0^{18}$ values ($+9.2$ to $+11.8$). According to Montigny et al. (1970), the clearcut distinction between groups (b) and (c) suggests separation of magmas sometime during the magmatic evolution of this complex. The serpentinized peridotites and gabbros, however, are distinctly lower in 0^{18} than "normal" ultramafic and mafic igneous rocks.

Figure 9-1

Legend

⁘	Ionian flysch (Upper Eocene - Lower Miocene
▤	Gavrovo limestone (Jurassic - Middle Eocene)
▦	Pinde flysch (Eocene)
⧇	Meso-Hellenic sediments (Oligocene - Miocene)
▧	Ophiolites
▨	chalky formation (Triassic - Jurassic)
⊞	shelf carbonates (Triassic - Jurassic)
+ +	Pelagonian metamorphic "basement" (Paleozoic - Mesozoic?)
V	Vardar Zone deformed sedimentary and metamorphic rocks (Paleozoic - Mesozoic)

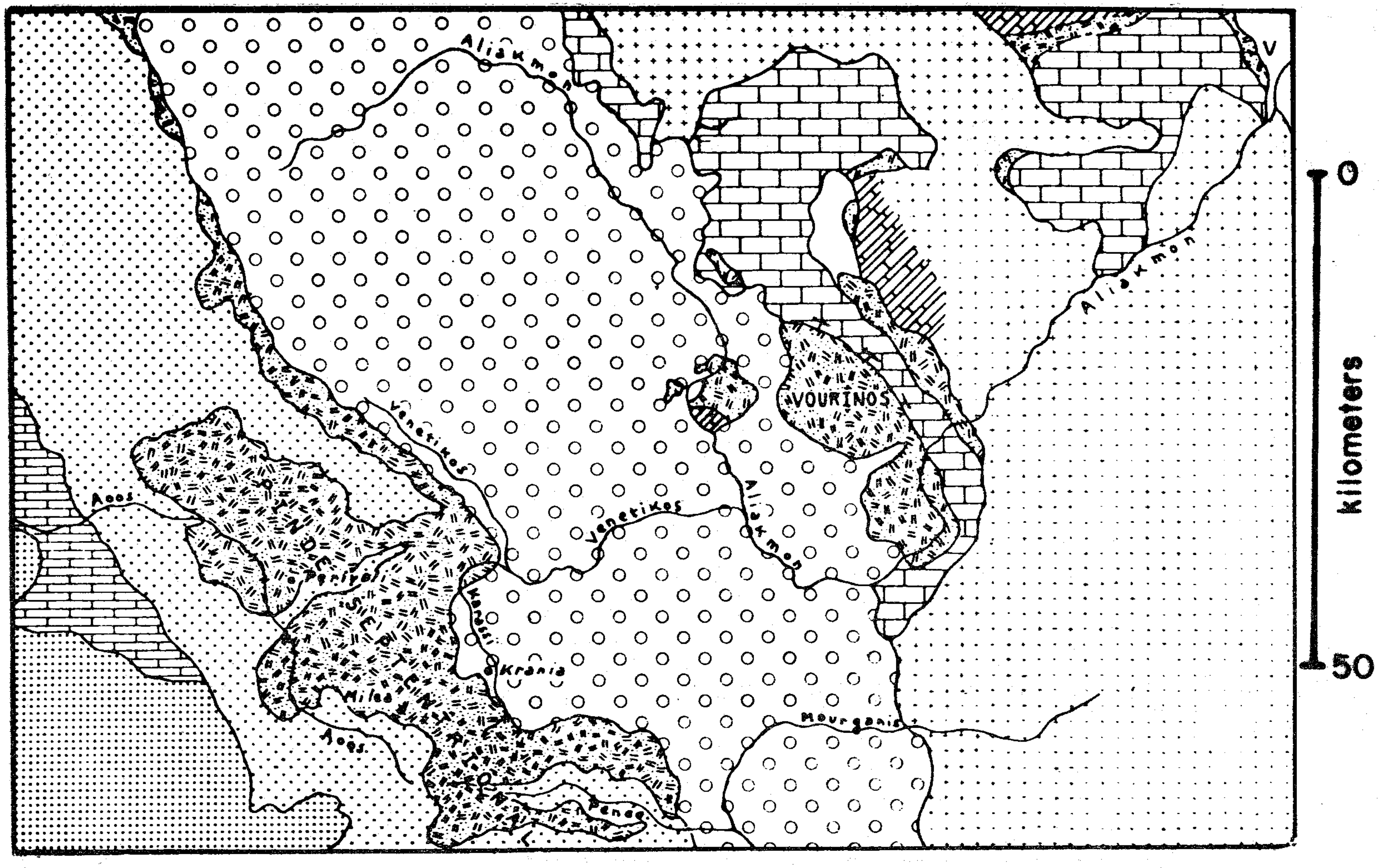

Figure 9-1

Generalized geologic map of the Pinde and Vourinos massifs in Greece (after Parrot, 1967).

According to Moores (1969), the Vourinos Complex was originally emplaced into Lower Jurassic (?) sediments and then covered unconformably by Cretaceous limestone; later the area was involved in a Tertiary (?) regional metamorphism and orogeny.

The complex itself consists of about 75 to 85 per cent dunite, peridotite and pyroxenite, and about 15 to 25 percent gabbro, diorite, quartz diorite, and pillow lavas, all of which represent an integral and consanguineous suite. The ultramafic rocks are layered and complexly folded. The primary mineral chemistry of the dunites and peridotites suggests that the ultramafic rocks are "alpine-type" rather than basaltic differentiates. Moores (1969) suggests that the complex may have originated by partial fusion of lherzolitic mantle material of 80 percent ultramafic residue and 20 percent basaltic liquid. The "ophiolite suites" in general are assumed to represent a submarine outpouring of basaltic and ultramafic magmas in a geosynclinal environment (see Aubouin, 1965).

Serpentine has the following modes of occurrence in the Vourinos Complex, as is illustrated in figure 9-2.

(1) It occurs throughout the complex as a partial alteration of the primary minerals of the ultramafic rocks. Samples of this type were selected from different localities within the ultramafic zone (samples 43a, 70c, 683a, 685a) and from the transition zone, which consists of dunite intruded by and interlayered with pyroxenite and gabbro (sample 590a).

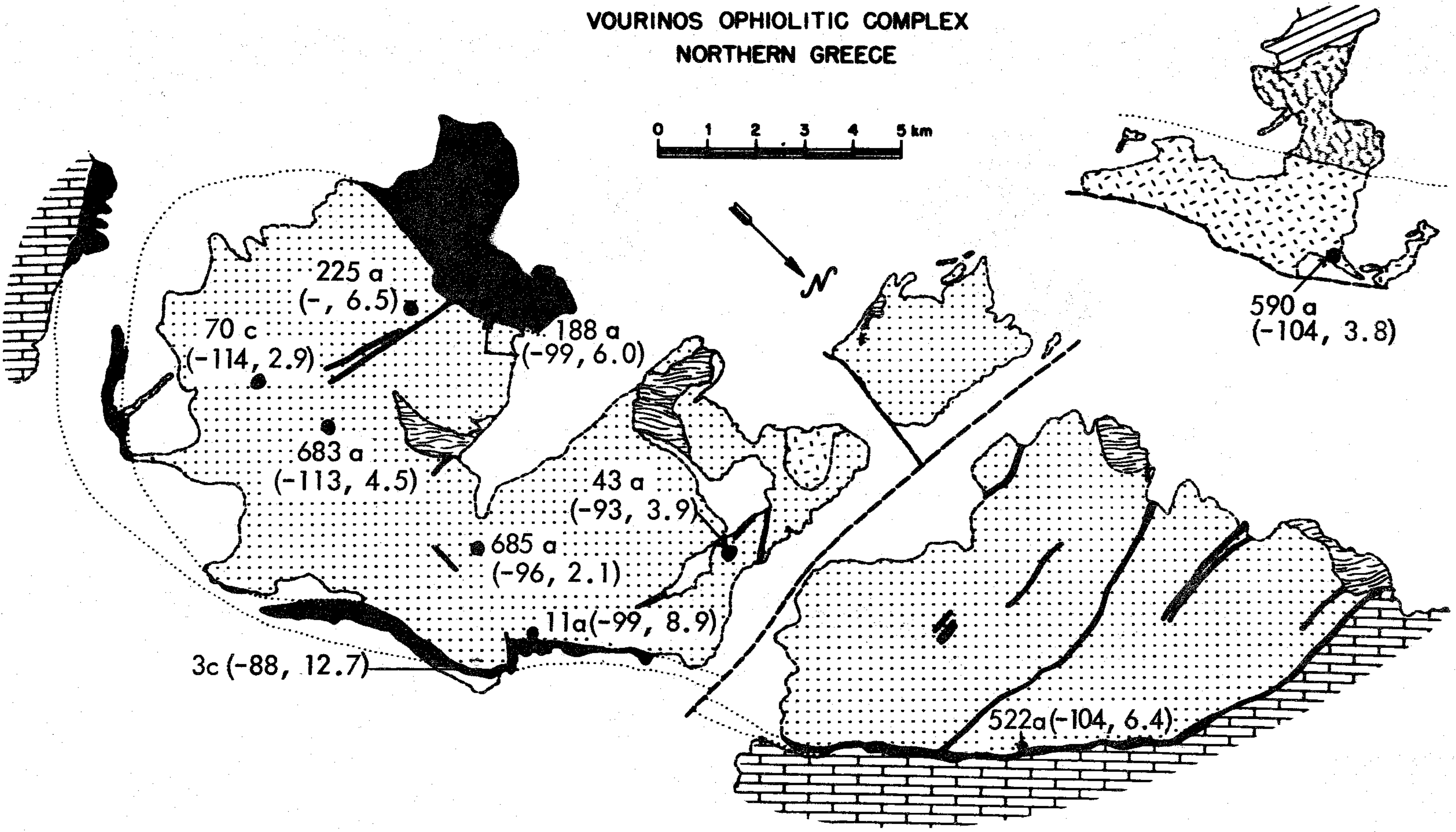

Figure 9-2

Geologic map of the Vourinos Complex, Greece (modified after Moores, 1969) showing sample localities and isotope data.

Vourinos Ophiolite Complex

Legend

Overlying Rocks

Tertiary	□	Sedimentary rocks and Alluvium
	〰	
Cretaceous (Cenomanian?)	▨	Limestone
	〰	

Ophiolite Complex

uppermost Jurrassic lowermost Cretaceous	▩	Sequence of diorite, quartz diorite, lava, with limestone and radiolarian chert along uppermost contact
	⁙	Gabbro and pyroxenite, some serpentine
	░	Ultramafic zone peridotite and dunite.
	■	Serpentine
	▦	Serpentine breccia

Underlying Rocks

Lower Jurassic?	▤	Marble and terriginous rocks

(2) A massive to schistose serpentinite, indicated in figure 9-2 as a separate mappable unit, occurs at the basal contact. This zone is generally 100 to 200 m wide, although in some areas it may be as much as 1 km wide. Inclusions of marble, dunite, peridotite, and rodingite occur in the serpentinite zone. In some areas the marble and serpentinite are intimately interfolded. One sample (3c) from this basal serpentinite unit was examined along with a single pertially serpentinized peridotite inclusion (522b) embedded in the basal serpentinite.

(3) Serpentinite (represented by sample 225a) occurs as relatively narrow east-trending bodies in the ultramafic zone of the complex; some of these grade into the basal serpentinite.

(4) Massive serpentinite (represented by sample 188a) occurs near the upper parts of the ultramafic zone and is shown as a mappable unit in figure 9-2.

(5) Serpentinite (11a) also occurs as a breccia in which about 50 percent of the clasts are derived from the local ultramafic rock.

Moores (1969) suggests the possibility that serpentine may have formed in two distinct episodes. The basal serpentinite is presumed to have formed during emplacement of the complex in Jurassic times, serving to insulate the underlying rocks, which show very minor contact metamorphic effects, from the hot, nearly solid ultramafic body. At a later period, perhaps during Tertiary (?) metamorphism, the breccias may have formed as a result of gas exploxions involving aqueous fluids, perhaps derived from underlying sediments. In fact the breccia, the east-trending serpentine and even a good part of the basal serpentinite may have been produced during this later event. In some areas, all these rock types appear to grade into one another.

9.2 Discussion of the Vourinos isotopic data

All of the serpentines examined in this study are composed solely of lizardite and chrysotile. As is indicated from the isotope data presented in figure 9-2, the δD values vary only from -114 to -88 per mil. Serpentines from the interior portions of the ultramafic zone have slightly lighter δD values than samples that occur near the outer margins of the complex. All of the completely serpentinized rocks fall within the δD range -88 to -99.

In contrast to the relatively small δD distribution, the δO^{18} values exhibit a very wide variation from +2.1 to +12.7 per mil. This δO^{18} variation is greater than that observed within any other ultramafic body studied in the present work.

The following types of samples can be delineated isotopically on figure 9-3.

(1) Serpentines from the partially serpentinized ultramafic rocks have relatively low δO^{18} values (+3.4°/oo, average of 5 samples). However, one serpentinized peridotite (522b) that lies within the O^{18}-enriched basal serpentinite zone has a δO^{18} value of +6.4.

(2) The serpentines from four completely serpentinized ultramafic rocks all have relatively heavy δO^{18} values. Samples from the massive serpentinite zones in the upper part of the complex have an average δO^{18} = +6.2. The highest δO^{18} values (+12.7 and +8.9), however,

Figure 9-3. δD - δO^{18} diagram showing the isotopic compositions of all analyzed serpentine samples from the Vourinos Complex. The partially serpentinized ultramafic rocks form a distinct grouping from the serpentinites; δO^{18} values of the latter appear to be related to distances from the basal carbonate section. One inclusion of partially serpentinized ultramafic rock that lies within the O^{18}-enriched basal serpentinite zone may contain both types of serpentine.

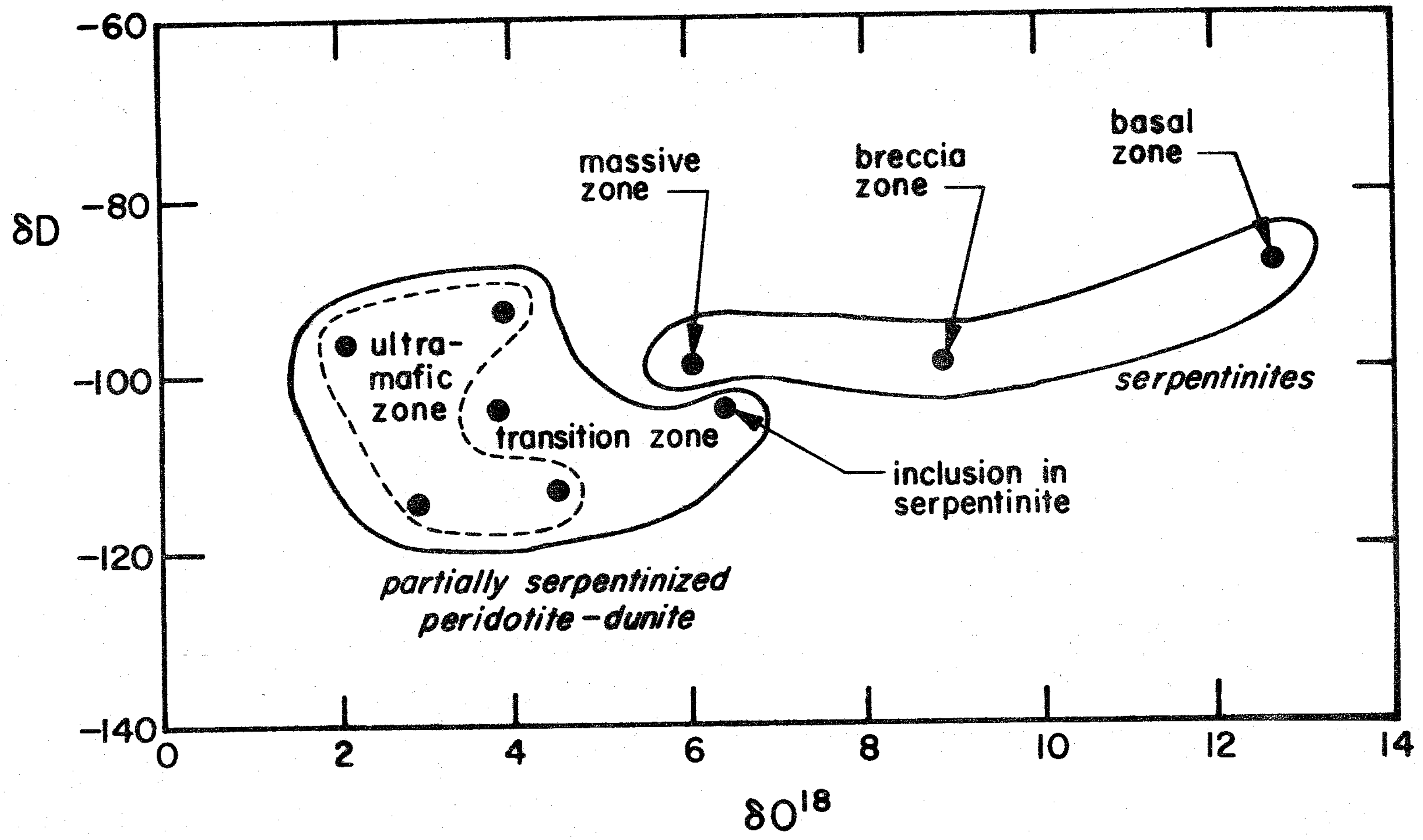
δD
-60
-80
-100
-120
-140
0
2
4
6
8
10
12
14
δO18
ultra-
mafic
zone
transition zone
massive
zone
breccia
zone
basal
zone
inclusion in
serpentinite
serpentinites
partially serpentinized
peridotite-dunite

Figure 9-3

are found in the sheared basal serpentinite zone (3c) and a nearby breccia zone (11a) located in near proximity to the sedimentary carbonate section that underlies the complex. It should be noted that even though the basal serpentinite is both intermixed with carbonates and is itself strongly enriched in 0^{18}, the inclusion of partially serpentinized peridotite in this basal zone has a distinctly lighter $\delta 0^{18}$ value of +6.4.

Calculated waters

If one assumes that all of the lizardite-chrysotile type serpentinization at Vourinos occurred at about 100°C, as suggested by the serpentine-magnetite 0^{18} fractionations in other continental lizardite-chrysotile samples (see chapter 4), then one can estimate the isotopic compositions of the waters that coexisted in equilibrium with the various Vourinos serpentines. The δ values of these calculated waters are given in Table 9-1 and in figure 9-4. The calculated range of δD is -48 to -69 and for $\delta 0^{18}$, -4.5 to +6.1.

Such waters conceivably could be largely of meteoric ground water origin, the high $\delta 0^{18}$ values having resulted from exchange with the adjacent 0^{18}-rich limestones. Inasmuch as the serpentinite and underlying carbonates are intimately interlayered at the basal contact, one might expect that the fluids involved in the serpentinization process would have readily exchanged with the carbonates, even at fairly low temperatures. For example, Clayton _et_ _al_. (1968) suggest that carbonates readily exchange and reach isotopic equilibrium with water at temperatures as low as 100°C.

Table 9-1. Isotope data of samples from the Vourinos Complex, Greece.

							Calculated H_2O§			Est. Pres. Day H_2O	
Sample	Mineralogy*	% serp.	δD_S	δO^{18}_S	δO^{18}_M	T°C	δD	δO^{18} $(y/x=\infty)$	δO^{18} $(y/x=1)$	δD†	δO^{18} H_2O Shift‡
Ultramafic Zone											
43a	L + C	40D	- 93	3.9	-	100	-48	-2.7	-4.3	-40^1	4.5
70c	L + C	40D	-114	2.9	-	100	-69	-3.7	-6.3		6.0
225a	L + C	100	-	6.5	-	100	-	-0.1	0.9		-
683a	L + C	60P	-113	4.5	-	100	-68	-2.1	-3.1		7.8
685a	L + C	50P	- 96	2.1	-	100	-51	-4.5	-7.9		3.1
transition zone											
590a	L + C	30P	-104	3.8	-	100	-59	-2.8	-4.5		5.8
breccia zone											
11a	L + C	100	- 99	8.9	-	100	-54	2.3	5.7		10.3
basal zone											
3c	L + C	100	- 88	12.7	-	100	-43	6.1	13.3		12.7
522b	L + C	45P	-104	6.4	-	100	-59	-0.2	0.7		5.8
massive serpentinite zone											
188a	L + C	100	- 99	6.0	-	100	-54	-0.6	-0.1		7.9

Figure 9-4. δD-δO^{18} diagram of calculated ($y/x = \infty$) waters in equilibrium with the Vourinos serpentines at various temperatures. Tie lines connect all serpentines with their corresponding waters. The solid lines assume equilibration at 100°C. The dashed lines assume that the equilibrated waters everywhere had $\delta D = -55$. Note the overall similarity of this hypothetical single δD-system with the Salton Sea geothermal water system (Craig, 1963), both in terms of temperature distributions and range of δO^{18} values.

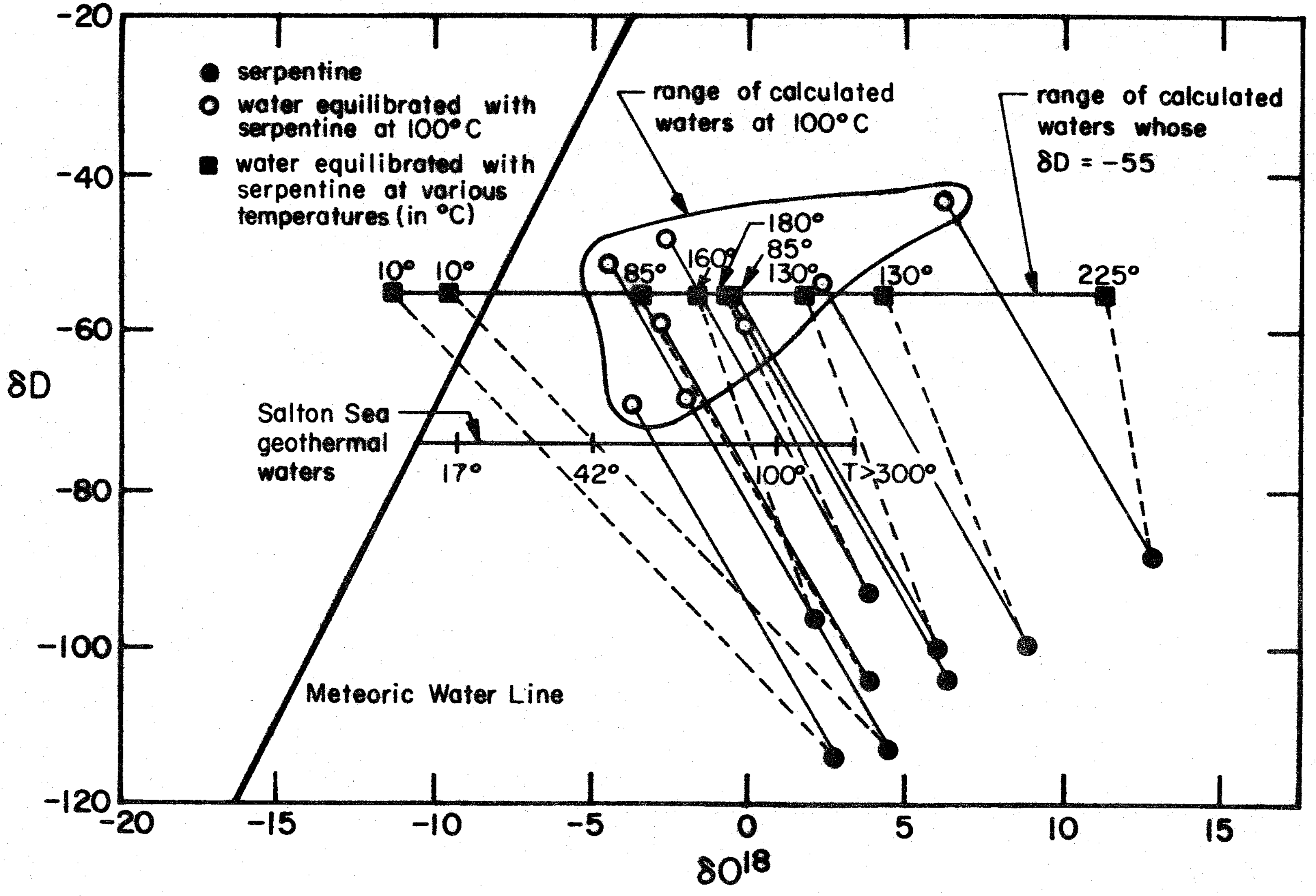

● serpentine
○ water equilibrated with serpentine at 100°C
■ water equilibrated with serpentine at various temperatures (in °C)
range of calculated waters at 100°C
range of calculated waters whose δD = -55
10°
10°
85°
160°
180°
85°
130°
130°
225°
Salton Sea geothermal waters
17°
42°
100°
T>300°
Meteoric Water Line
δD
-20
-40
-60
-80
-100
-120
-20
-15
-10
-5
0
5
10
15
δO18

Figure 9-4

However, extensive isotopic communication with the basement carbonates appears restricted to the basal serpentinite unit and perhaps to the nearby serpentine breccia zones. Much of the serpentinization of the ultramafic mass clearly involved little or no isotopic communication with the 0^{18}-rich carbonates. Even the small, partially serpentinized peridotite (sample 522b) inclusion within the basal serpentinite zone gives only a partial suggestion of such isotopic interaction.

It is noteworthy that the $\delta 0^{18}$ values of serpentinized peridotites from the Pindos Mass (Javoy, 1970) generally fall within the range exhibited by serpentines in analogous rock types of the Vourinos Complex. The relatively light whole-rock $\delta 0^{18}$ values of the Pindos peridotites also are compatible with involvement of meteoric water in their serpentinization.

Even though the wide range of δD values suggests that perhaps several different types of waters (i.e., meteoric-connate, meteoric-metamorphic, or perhaps only exchanged meteoric waters with different δD values) may be involved in the Vourinos serpentinization, it is useful to examine the question of whether a single meteoric water system (exhibiting a wide range in $\delta 0^{18}$ but with a single δD value) can alone be responsible for all serpentinization.

Let us therefore arbitrarily assume that only waters with $\delta D = -55$ were involved in serpentinization at Vourinos. By suitable adjustment of the temperature, we can force the waters in equilibrium with all serpentines to coincide with this δD value, utilizing the D/H geothermometer curve given in figure 4-4. By knowing the temperature and the $\delta 0^{18}$ value of serpentine, we can then calculate the $\delta 0^{18}$ of the water from equation 5, chapter 4. These data are summarized in figure 9-4. Such a model requires that (1) there be a very wide range of temperatures of serpentinization (approximately 10° to 225°C), (2) some of the calculated waters approximately coincide with the meteoric water line (and thus can have suffered little or no change in $\delta 0^{18}$), and (3) some lizardite-chrysotiles must form both at what seem to be abnormally high and abnormally low temperatures. If we select a meteoric water system other than that given above (i.e., one with a different δD value), we encounter other difficulties.

For example, with a lower δD value than -55 for our single meteoric water system, even greater temperatures of serpentinization would be required. If a heavier δD value is assumed, even lower temperatures of serpentinization are necessary, as well as greater 0^{18} shifts to the left of the meteoric water line.

Nevertheless, this overall pattern is not too dissimilar to that displayed by typical geothermal waters such as those of the Salton Sea system shown in figure 9-4. In the latter case, near-neutral, chloride-type geothermal waters exhibit a progressive 0^{18}-enrichment with increasing temperatures, much like the calculated ($\delta D = -55$) waters at Vourinos. Thus, it is conceivable that serpentinization at Vourinos may have been caused by a single geothermal water system.

Figure 9-5. δD - δO^{18} diagram of calculated waters in equilibrium with the Vourinos serpentines at 100°C for different values of y/x. The partially serpentinized ultramafic rocks (excluding the inclusion in serpentinite) exhibit distinctly opposite trends from the serpentinites. Note that the y/x = 0.5 values for the O^{18}-rich serpentinite would lie well to the right of the graph. The band of calculated (y/x = 1) waters for low-grade alpine lizardite-chrysotiles is shown for comparison (see figure 7-17).

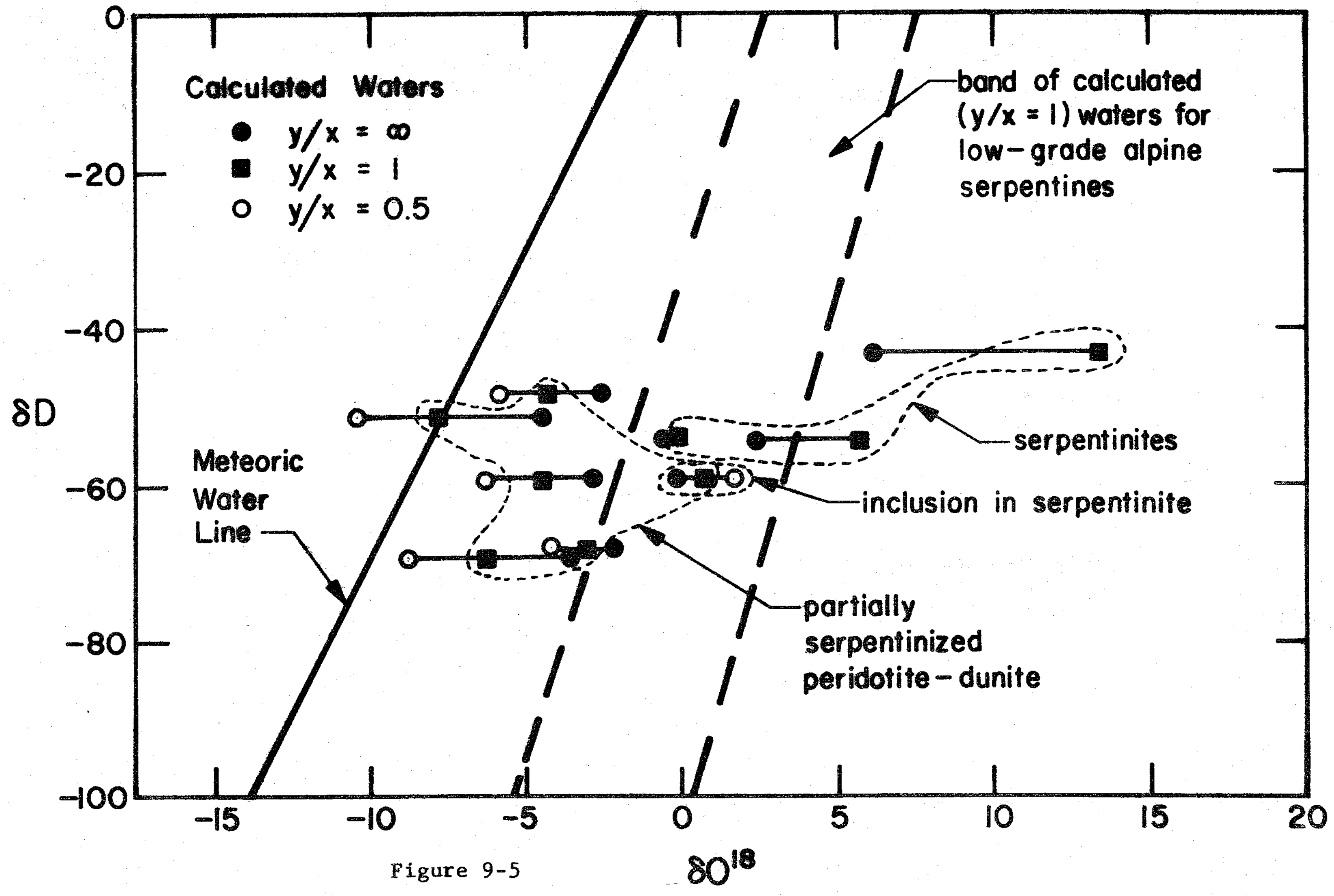
Calculated Waters
● y/x = ∞
■ y/x = 1
○ y/x = 0.5
band of calculated (y/x = 1) waters for low-grade alpine serpentines
serpentinites
inclusion in serpentinite
partially serpentinized peridotite-dunite
Meteoric Water Line
δD
0
-20
-40
-60
-80
-100
-15
-10
-5
0
5
10
15
20
δO18

Figure 9-5

Variations in the water/rock ratio

The effects of variable water/rock ratios on serpentinization are considered in the model outlined in section 7.6. According to this model, the calculated waters illustrated in figure 9-4 will be identical to the initial waters entering the ultramafic system only if a very large reservoir of water passes through and exchanges with the ultramafic rocks. In section 7.6, it was concluded that the ratio of atom percent meteoric water to atom percent exchangeable silicate oxygen (y/x) is not "infinite", but is generally equal to or slightly greater than unity.

Applying this type of model to the Vourinos Complex, calculated waters of different y/x ratios are illustrated in figure 9-5. The waters involved in partial serpentinization of dunite and peridotite in the central ultramafic zone are all uniformly depleted in 0^{18}; this suggests little 0^{18}-exchange with the exterior environment, particularly with the sedimentary carbonates.

In contrast, the $\delta 0^{18}$ values of calculated $(y/x = 1)$ waters for the basal serpentinites are highly 0^{18}-enriched. Such waters could not in any way have produced the ultramafic-zone serpentines unless they somehow became depleted in 0^{18}; this could occur to some degree if an originally high-0^{18} water continued to produce decreasingly 0^{18}-enriched serpentine as it migrated from the outer edges of the complex to the interior. However, by such a process the $\delta 0^{18}$-values could not become as low as the lowest indicated on figure 9-5.

It seems reasonable to expect that the ratio y/x may have been smaller for the partially serpentinized samples than for the serpentinites. However, calculated waters for y/x = 0.5 are even more 0^{18}-depleted than the y/x = 1 calculated waters. These are unrealistically low $\delta 0^{18}$ values for serpentinizing fluids, so that either y/x was considerably larger than 0.5 throughout the Vourinos Complex, or our temperature estimates are too low. These particular serpentine samples are all about 30 to 60 percent serpentinized, hence one might expect that roughly similar water/rock ratios would have been involved in each case.

The partially serpentinized peridotite inclusion in the highly 0^{18}-enriched basal serpentinite has a texture that indicates it may be a composite of two different serpentines. It is plausible that the observed intermediate $\delta 0^{18}$ value (+6.4) is due to a mixture of highly 0^{18}-enriched late-stage serpentine veins and an earlier 0^{18}-depleted serpentine, the latter being the material immediately surrounding the olivine and pyroxene; if similar to the other partially serpentinized samples, its $\delta 0^{18}$ would be about +3.5.

Possible role of ocean water

Finally the possible role of sea water in the Vourinos serpentinization must be examined, since many authors have proposed that ophiolites form in an oceanic or sub-oceanic environment. However, the relatively light δD values, considerably different from those of true oceanic serpentines (see chapter 6), seem to be incompatible with an origin from ocean waters. It is conceivable, nevertheless, that some of the serpentines may have originally formed in the presence of sea water over a wide range of temperatures, and that later these serpentines underwent considerable D/H exchange in the presence of meteoric waters, thereby resulting in a lowering of the δD values.

This latter possibility is made feasible by the fact that many of the δO^{18} values of serpentines in the partially altered peridotites and dunites are similar to those of the oceanic serpentines studied in chapter 6.

Summary

In the previous sections, it was concluded that at least two different serpentinization events probably occurred at Vourinos. One involved low-O^{18} waters, and resulted in a pervasive partial serpentinization of the ultramafic zone of the complex. The other involved relatively O^{18}-rich waters that were probably in isotopic communication with the basal carbonate section. The latter serpentinization event was important in the development of the basal serpentinite zone, the massive serpentinite, the serpentine breccia, and east-trending serpentinite zones. Perhaps this latter serpentinization is related to the proposed gas-explosion events suggested by Moores. There is, however, no isotopic evidence of formation of the basal serpentinite during emplacement of the complex in an oceanic environment, as suggested by Moores (1969).

The textural relations of serpentine in the peridotite inclusion within the basal serpentinite zone suggest that the pervasive partial serpentinization of the ultramafic zone may have predated the formation of the serpentinite zones. Thus the partial serpentinization of the ultramafic zone by low 0^{18}-waters may have occurred during a time when the ultramafic body was not in its present position in near proximity to the basal carbonates. On the other hand, it is probably easier to explain the low D and 0^{18} waters involved in the partial serpentinization if we assume this occurred at relatively low temperatures and/or at shallower depths; under such conditions we would almost certainly be dealing with meteoric waters and there would also probably have been less exchange with the carbonate section.

The low δD of all the Vourinos serpentines, and in particular the low $\delta 0^{18}$ of the partially serpentinized samples, strongly indicate meteoric water involvement in this serpentinization. These meteoric waters probably underwent $\delta 0^{18}$-shifts of as little as 3 and as much as 13 per mil. It is noteworthy that the partially serpentinized samples are lower in 0^{18} than all other alpine serpentines with comparable δD values, except two samples from Costa Rica. Furthermore, the calculated waters for these samples show this same relationship (see figure 9-5).

X. SERPENTINES FROM HIGH-TEMPERATURE ULTRAMAFIC INTRUSIONS

10.1 Zoned Ultramafic Bodies (SE Alaska type)

Geological relationships

The δD and δO^{18} values were measured on serpentines from several zoned ultramafic intrusions in southeastern Alaska and in the Ural Mountains, Soviet Union. The serpentine typically occurs in partially serpentinized dunite or peridotite, but one sample from the Ural Mountains is completely serpentinized. The ultramafic intrusions of both areas are generally small (1 to 5 miles in diameter), cylindrical bodies that show a concentric zoning from a dunite core to outer zones of peridotite and pyroxenite, the entire complex being intruded into a genetically unrelated gabbro (Taylor, 1967).

The rocks can be readily distinguished from those of stratiform or layered gabbro-peridotite complexes, as well as from Alpine-type ultramafic intrusions, on the basis of their structure, mineralogy and chemistry (Thayer, 1967b; Taylor, 1967). The most reasonable interpretation of the origin of the zoned ultramafic bodies is that they were formed by successive intrusions of ultramafic magmas (Taylor, 1967; Irvine, 1967).

The zoned ultramafic complexes in southeastern Alaska occur along an orogenic belt at least 350 miles in length which trends parallel to the major structural features of the region. They were intruded after the folding and metamorphism of the Paleozoic and lower Mesozoic rocks of the orogenic belt during the early middle Cretaceous period between 100 and 110 million years ago (Taylor, 1967). In some of the areas,

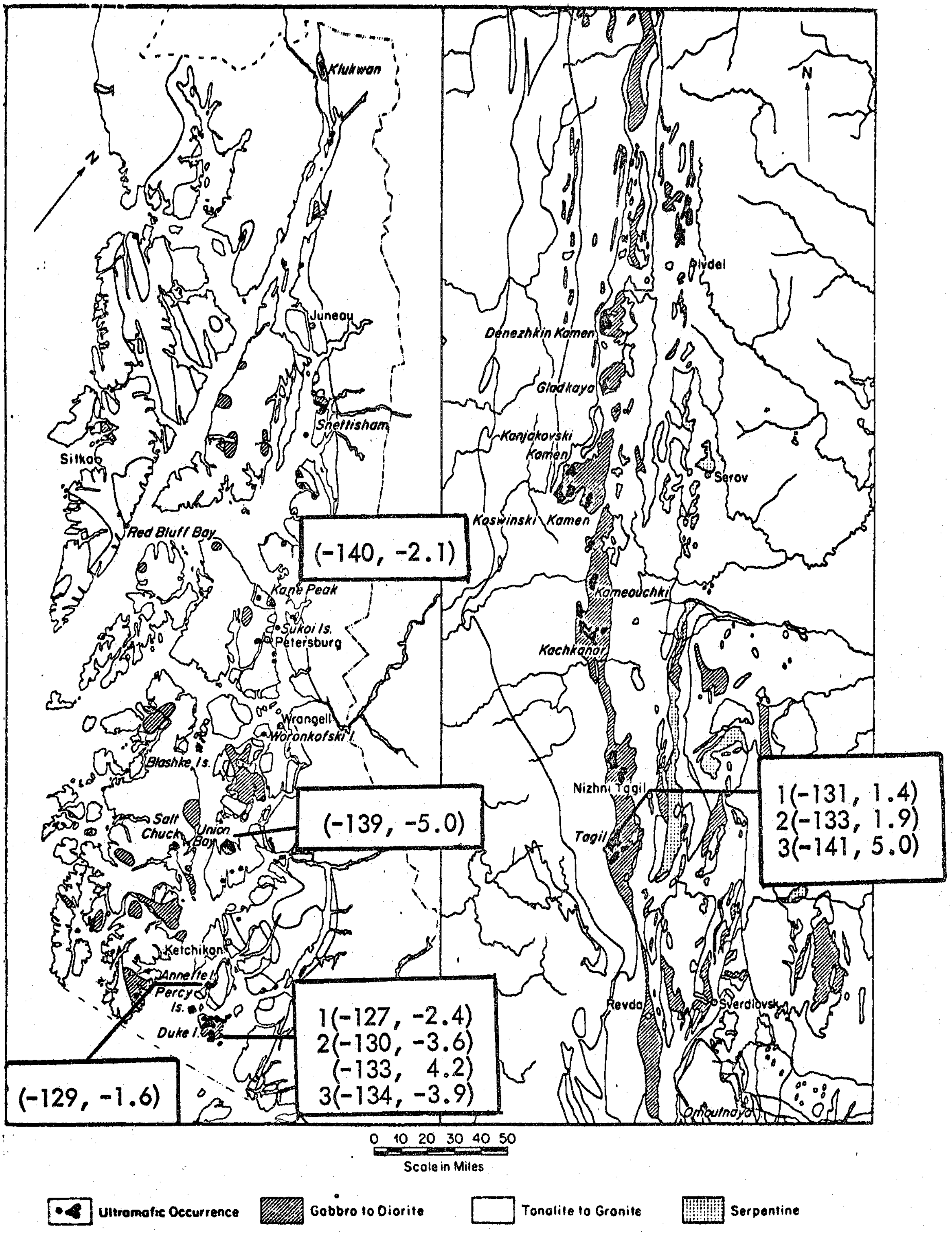

Figure 10-1

Geologic map showing distribution of ultramafic complexes in southeastern Alaska and the Ural Mountains, U.S.S.R. (after Taylor, 1967c). The isotope data obtained on these bodies are also given. All serpentines are composed solely of lizardite and/or chrysotile.

Cretaceous granitic rocks of the Coast Range batholith cut the ultramafic rocks (see map, figure 10-1).

The zoned ultramafic rocks in the Ural Mountains occur within a long, narrow, nearly continuous belt of gabbroic rocks along the north-trending axis of the Ural Mountains. They are Paleozoic in age, probably Devonian, and are more highly sheared and serpentinized than the southeastern Alaska intrusions (Taylor, 1967).

The isotope data and geologic relationships of the various zoned ultramafic bodies in SE Alaska (4 bodies) and the Ural Mountains (one intrusion, Nizhni Tagil) are given in figure 10-1.

Discussion of the isotope data

The δD values of the various SE Alaska samples are relatively light, ranging from -127 to -140 per mil; this is compatible with their northerly occurrence, assuming that meteoric ground waters are involved in their formation. Their δD values are not as light as those directly east in the interior portions of British Columbia (where relatively pure lizardite-chrysotiles from the Nahlin and Cassiar bodies have δD = -162 to -205). Such a pattern is, however, also to be expected if meteoric ground waters are involved, because rainfall and snowfall become depleted in deuterium as one moves inland.

Furthermore, the δD values of serpentines from SE Alaska themselves show a rough correlation between δD and latitude (see figure 10-1). Serpentine from a partially altered dunite sample from Kane Peak, the most northerly occurrence examined, has the lightest δD value (-140), and samples from the southerly occurrences at Annette Island and Duke Island exhibit the heaviest δD (-127 to -134). Also, all five samples from the Duke Island-Annette Island area have nearly identical δD values.

In contrast to all of the alpine-type serpentines previously discussed, the lizardite-chrysotile in these partially serpentinized dunites and peridotites shows considerable depletion in 0^{18}. Typically $\delta 0^{18}$ values of -1.6 to -5.0 are observed, although one cross-cutting veinlet of chrysotile from Duke Island (see sample description in appendix) has a $\delta 0^{18} = +4.2^{o}/_{oo}$. In contrast to the δD results, the $\delta 0^{18}$ values show no overall latitudinal correlation. Greater 0^{18}-depletion is found in serpentinized dunites and peridotites from the SE Alaskan intrusives than in those at Nizhni Tagil, but the hydrogen isotopic compositions from both areas are similar.

A study by Taylor (1967b) of the primary mineral phases from various parts of several zoned ultramafic intrusions from southeastern Alaska shows oxygen isotopic compositions that are 'normal' for deep-seated igneous rocks. Furthermore, a biotite from the Pt. Frederick pyroxenite in southeastern Alaska has a δD value similar to biotites from deep-seated igneous intrusions (δD = -71). Biotite having such a δD value must have formed from waters of deep-seated origin (upper mantle H_20?) with little or no contribution of meteoric waters. Thus, the primary magmatic δD and $\delta 0^{18}$ values in these ultramafic rocks bear no resemblance whatsoever to the corresponding values in the serpentines.

The estimated isotopic compositions of waters that are assumed to have coexisted in equilibrium whith the SE Alaska and Ural Mountain serpentines at 100°C are given in Table 10-1 and figure 10-2. Waters having such isotopic compositions *definitely* must have contained a very large meteoric ground water component.

These calculated waters from SE Alaska are not too dissimilar from completely pristine, unexchanged meteoric waters, as is illustrated figure 10-2. The calculated waters show only a very small 0^{18} shift away from the meteoric water line, indicating that such waters suffered little or no exchange with the surrounding country rocks before entering the ultramafic body. This is in strong contrast to the relationships pointed out previously with regard to the calculated waters in alpine-type serpentines. These differences may be a result of the fact that the country rocks in the SE Alaska occurrences are all igneous and metamorphic rocks in which low-temperature, water-rock 0^{18} exchange is much more difficult than in situations where sedimentary rocks (particularly limestones) are abundant. The contrast with the Cassiar, British Columbia body directly to the east is very apparent in this regard.

No serpentine-magnetite fractionations have been measured in serpentines from any of the zoned ultramafic intrusions; hence all of the calculated waters in Table 10-1 and in figure 10-2 can only be *assumed* to have equilibrated with serpentine at 100°C. If serpentinization actually occurred at temperatures significantly higher than 100°C, the calculated waters would be much more 0^{18}-rich. If a temperature of 185°C is chosen instead, the calculated waters would show a more "normal" type of 0^{18} shift (average of about 6.2 per mil, see figure 10-2), similar to what is observed for some of the alpine-type serpentines.

Table 10-1. Isotope data of samples from zoned ultramafic bodies.

Sample	Mineralogy*	% serp.	δD_S	δO^{18}_S	δO^{18}_M	T^oC	Calculated H_2O§			Est. Pres. Day H_2O δD†	δO^{18} H_2O Shift‡
							δD	δO^{18} $(y/x=\infty)$	δO^{18} $(y/x=1)$		
Alaska											
Duke Island											
1	L + C	50D	-127	-2.4	-	100	-83	- 9.0	-16.9	-90	2.6
2	L + C	40D	-130	-3.6	-	100	-86	-10.2	-19.3		1.8
	C (x - f)	100	-133	4.2	-	100	-89	- 2.4	- 3.7		10.0
3	L + C	40D	-134	-3.9	-	100	-90	-10.5	-19.9		2.0
Annette Island	L + C	50D	-129	-1.6	-	100	-85	- 8.2	-15.3		3.7
Union Bay	L + C	30D	-139	-5.0	-	100	-95	-11.6	-22.1		1.5
Kane Pk.	L + C	30D	-140	-2.1	-	100	-96	- 8.7	-16.3		4.5
U.S.S.R.											
Nizhni Tagil											
1	L + C	60D	-131	1.4	-	100	-87	- 5.2	- 9.3	?	6.9
2	L + C	50D	-133	1.9	-	100	-89	- 4.7	- 8.3		7.7
3	L	100	-141	5.0	-	100	-97	- 1.6	- 2.1		11.8

Figure 10-2. δD-$\delta 0^{18}$ plot of serpentines and calculated (y/x = ∞) waters from the zoned ultramafic bodies of SE Alaska and the Ural Mountains, U.S.S.R. The Salton Sea geothermal water line and the meteoric water line are shown for reference. Symbols: N = Nizhni Tagil, D = Duke Island, A = Annette Island, U = Union Bay, K = Kane Peak, ● = serpentine, ○ = calculated waters at 100°C, x = calculated waters at 185°C, □ = calculated water at 75°C. Solid tie lines connect all serpentines and corresponding calculated waters from SE Alaska, dashed tie lines connect serpentines and calculated waters for U.S.S.R. samples. By assuming an equilibration temperature of 75° for the Duke Island cross-fibre chrysotile and 185°C for the partially serpentinized samples, the calculated waters of the Duke Island samples show similar isotopic compositions.

Figure 10-3. δD - $\delta 0^{18}$ diagram showing calculated waters (for both y/x = 1 and y/x = ∞) that exchanged with serpentines in zoned ultramafic bodies at 100°C. Calculated (y/x = 2) waters would lie roughly intermediate between y/x = 1 and y/x = ∞. The calculated (y/x = 1) waters for the SE Alaska samples all lie well to the left of the meteoric water line, in a region where no known natural waters are known to exist. This suggests that the assumed serpentinization temperature of 100°C is much too low for the SE Alaska samples.

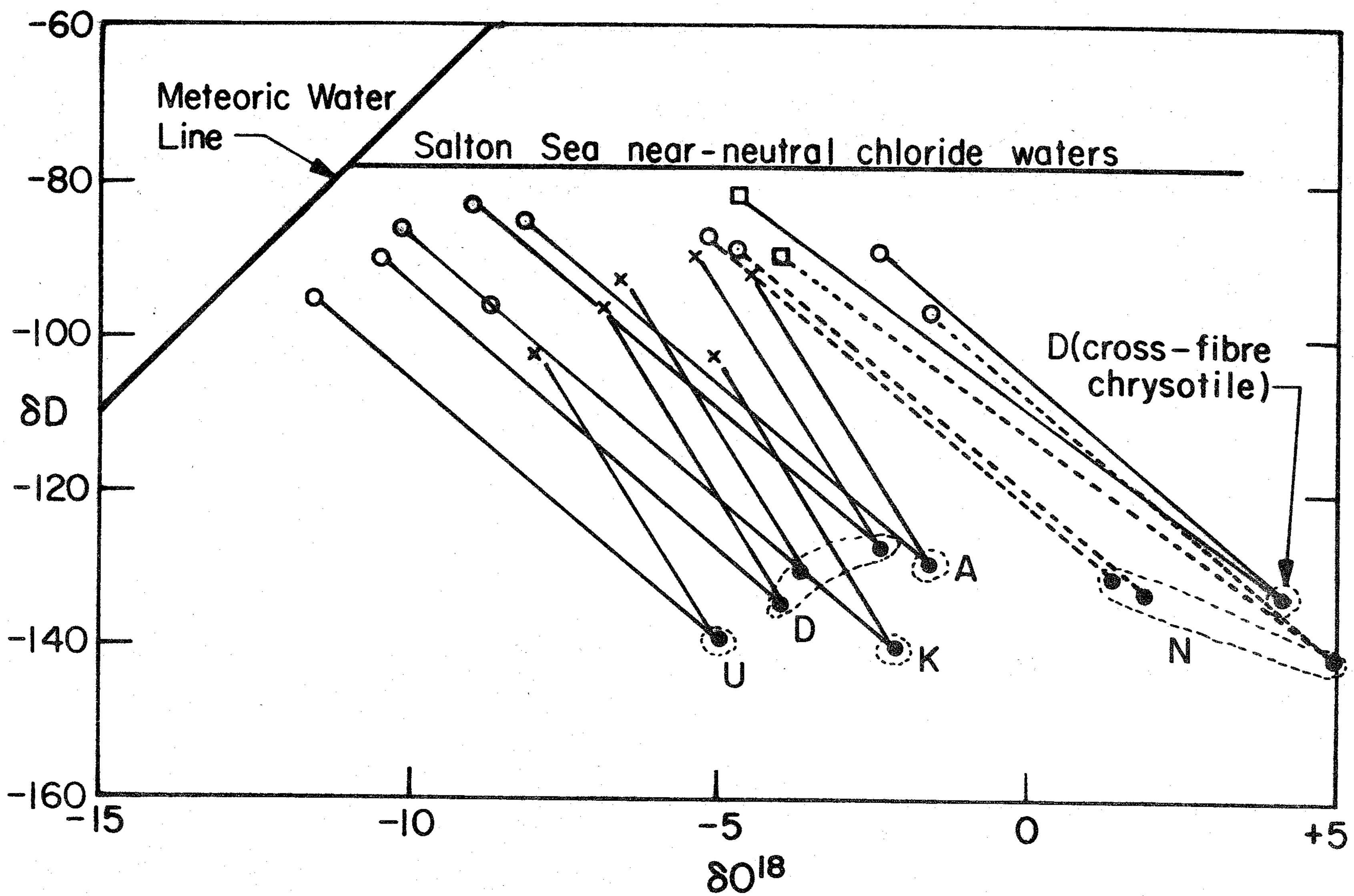
Meteoric Water Line
Salton Sea near-neutral chloride waters
D(cross-fibre chrysotile)
δD
-60
-80
-100
-120
-140
-160
-15
-10
-5
0
+5
δO18
A
D
K
U
N

Figure 10-2

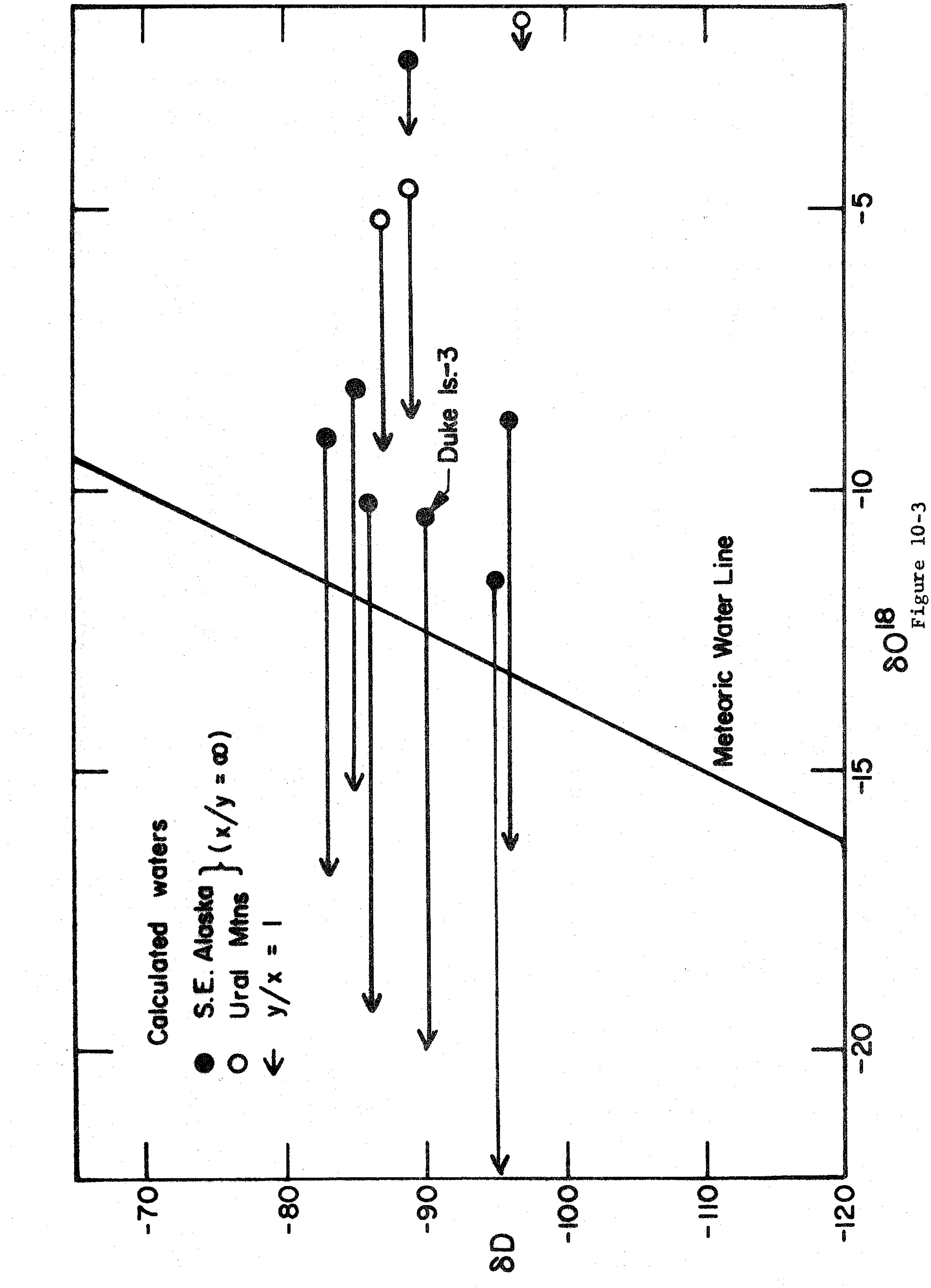
Calculated waters
● S.E. Alaska } (x/y = ∞)
○ Ural Mtns } (x/y = ∞)
↓ y/x = 1
Duke Is.-3
Meteoric Water Line
δD
-70
-80
-90
-100
-110
-120
δO18
-20
-15
-10
-5

Figure 10-3

The relatively 0^{18}-enriched cross-fibre chrysotile vein at Duke Island could be explained in several ways. This vein may, of course, have formed from 0^{18}-enriched waters of unknown derivation at a much later stage of serpentinization. A much simpler explanation is that the vein merely formed from the same type of water, but at a much lower temperature than the earlier serpentine. If it is assumed that serpentinization of the dunites occurred at 185°C (the highest temperature calculated from <u>any</u> measured lizardite-chrysotile-magnetite fractionations), and that the cross-fibre chrysotile vein at Duke Island formed at 75°C, then the estimated isotopic compositions of the waters in equilibrium with all these serpentines are very similar (see figure 10-2).

The serpentines from Nizhni Tagil are heavier in $\delta 0^{18}$ than those from SE Alaska, as are the corresponding calculated waters at 100°C (figure 10-2). Thus, the serpentines at Nizhni Tagil appear to be more analogeous to the typical alpine serpentinites, perhaps because this body is considerably more highly serpentinized than the zoned ultramafic bodies of SE Alaska. Furthermore, the ultramafic body near Nizhni Tagil lies only 3 km east of extensive outcrops of presumably 0^{18}-rich metasediments (schists and carbonates) with which the serpentinizing waters may have exchanged (Duparc and Tikonovich, 1920). Analogeous to the situation at Duke Island, the Nizhni Tagil serpentinite (sample 3) may have formed either at somewhat lower temperatures or from more 0^{18}-rich waters than the serpentine from the dunite (samples 1 and 2).

Further evidence of relatively high temperatures of serpentinization within the SE Alaska bodies is suggested if we consider the initial δO^{18} value of the water (δ_{wi}) that enters an ultramafic body. The calculated waters of figure 10-2 only apply for an 'infinite' water/rock ratio. Because all these samples are only partially serpentinized, we present in figure 10-3 values of δ_{wi} calculated for a lower and more reasonable water/rock ratio ($y/x = 1$). Waters with such low δO^{18} values (well to the left of the meteoric water line) clearly cannot represent the initial serpentinizing fluids; hence our assumptions of serpentinization temperatures are almost certainly in error in this case.

If it is assumed that the minimum reasonable value of δ_{wi} is that of pristine meteoric water, then for Duke Island sample 3 the minimum temperature of isotopic equilibration has to be around 330°C, assuming $y/x = 1$. Water/rock ratios smaller than unity demand temperatures higher than 330°C, as do δ_{wi} values that lie to the right of the meteoric water line. The Duke Island sample suggests a minimum of $y/x \approx 0.9$ for a temperature of 500°C, assuming that δ_{wi} is that of pristine meteoric water. If it were possible to calculate a 'temperature' based on a measured serpentine-magnetite pair (it was found impossible to obtain a magnetite separate for these samples) then one should perhaps be able to place rather definite limits upon y/x.

Although the temperature is higher than any isotopic temperature calculated for serpentine-magnetite pairs from other areas, the fact that these particular ultramafic bodies were originally intruded in the magmatic state at high temperatures certainly makes higher temperatures of serpentinization feasible. All of the temperatures suggested above are compatible with the known stability field of chrysotile. It should be noted that a temperature of 185°C (see above) is compatible with the serpentine having formed from pristine meteoric waters if $y/x = 1.6$, which is not an unreasonably high value for this ratio.

10.2 Layered mafic-ultramafic intrusions

Rocks of the layered gabbro-norite-peridotite association develop in floored magma chambers as cumulates formed during the fractionational crystallization of a parent gabbroic magma of tholeiitic type (Wyllie, 1967). The serpentine occurs as a later replacement of the dunite and peridotite.

Several serpentinites and partially serpentinized ultramafic rocks were studied from two such layered intrusions, the Stillwater Complex in Montana and the Muskox Intrusion, NW Territories, Canada. The hydrogen and oxygen isotopic compositions of these serpentinite samples are given in Table 10-2.

Stillwater Complex, Montana

The Stillwater Complex is of Precambrian age (Jackson, 1967), but the age of serpentinization is unknown. The isotopic compositions of three samples (exact location unknown) are given in Table 10-2. The δD values (-126 to -157) of the serpentines suggest that meteoric waters were involved in the serpentinization. In particular, note that the sample with the lowest δD also has the lowest δO^{18}, a trend roughly parallel to the meteoric water line. The variation in δD suggests that more than one type of water was involved, or that two or more periods of serpentinization occurred.

It is not improbable that much of the serpentinization of the Stillwater Complex occurred during the early Tertiary Laramide orogenic activity which affected this area. The δD values obtained from biotites,

Table 10-2. Isotope data of samples from magmatic ultramafic bodies.

							Calculated $H_2O^§$			Est. Pres. Day H_2O	
Sample	Mineralogy*	% serp.	δD_S	δO^{18}_S	δO^{18}_M	T°C	δD	δO^{18} ($y/x=\infty$)	δO^{18} ($y/x=1$)	δD†	δO^{18} H_2O Shift‡
Stillwater Complex, Mont.											
10	L + C	100	-131	6.1	-	100	-87	-0.5	0.1	-130	11.6
12	L + C	100	-126	6.2	-	100	-82	-0.4	0.3		11.1
45	L + C	50P	-157	4.1	-	100	-114	-2.5	-3.9		13.0
Muskox Intrusion, N.W.T.											
60-416	L + C	10P	-127	-	-	100	- 83	-	-	-160?	-
60-530B	L + C	10P	-105	-	-	100	- 60	-	-		-
Mt. Albert, Quebec											
1	L + C	60P	-123	-	-	100	- 79	-	-	- 90	-
2	L + C	60P	-125	-	-	100	- 81	-	-		-
13	C, tr, brucite	100	- 98	-	-	100	- 53	-	-		-
14	L + C	100	-111	-	-	100	- 66	-	-		-

muscovites, and kaolinites from the early Tertiary Butte ore deposit and Boulder Batholith, about 90 miles to the northwest of the Stillwater complex, range from -160 to -110 (Sheppard and Taylor, 1970). These data clearly indicate the presence of heated meteoric ground waters in the SW Montana area during the early Tertiary, and these waters have the approximate isotopic compositions to explain the Stillwater serpentinization. There is no reason to believe that Precambrian waters would be so low in deuterium.

Estimates of the isotopic compositions of waters in equilibrium with the Stillwater serpentines at 100°C range from -82 to -114 per mil. Such waters are heavier than those of the present day (see Table 10-2), and show a better correspondence with values estimated from data on Tertiary clay deposits by Lawrence (1970, see figure 5-3).

The Muskox Intrusion, Canada

The Precambrian Muskox intrusion of northern Canada was intruded into a basement of schists and gneisses at least 1200 million years ago (Irvine and Smith, 1967). The layered series consists of a variety of ultramafic rocks grading into gabbro and granophyre at the top. Irvine and Smith (1967) conclude that many repeated intrusions of basaltic magma occurred in the magma chamber, with subsequent gravitational settling of the mineral grains. The dunites and peridotites of the layered series are serpentinized to various degrees (Findlay and Smith, 1965).

Aumento (1970) has studied the serpentine minerals from the lower half of the layered series; he reports mostly lizardite alteration of the olivine, and biotite and chlorite alteration of clinopyroxene.

Small amounts of other minerals were reported including brucite and ubiquitous, very fine-grained magnetite.

Taylor (1968), in a study of the δO^{18} values of primary mineral phases of the Muskox intrusion, reports that there is no isotopic evidence that low-O^{18} meteoric ground waters were in any way involved with the Muskox intrusion at the time it was intruded. In fact, just the opposite is argued, as the late-stage red-rock granophyres at the top of the intrusion appear to have exchanged with O^{18}-rich waters ($\delta O^{18} > +8$) at high temperatures. Furthermore, the biotite from the granophyre has a much higher δD value (a typical "normal magmatic" value) than the two serpentines analyzed in the present work (H. P. Taylor, personal communication).

The δD values of two Muskox serpentine samples (-127 and -105 per mil, see Table 10-2) are relatively light. At 100°C, the δD values of waters in isotopic equilibrium with these serpentines are estimated to have been -83 and -60, respectively. Waters of such δD values are much too heavy for this serpentine to have been formed from present-day meteoric waters in the Coppermine River area (estimated to have a δD of -160 or lower, see Table 10-2).

This serpentinization conceivably could have occurred at any time during the late Precambrian, the Paleozoic, or the Mesozoic, as during most of this time climates were overall much warmer than at present. Under such conditions the local meteoric waters would have had considerably higher D/H ratios than they do today. However, the δD values of the calculated waters are also very similar to those of "primary magnatic waters", and inasmuch as no $\delta 0^{18}$ analyses were done we cannot rule out the possibility that such waters were involved in the Muskox serpentinization.

10.3 Mount Albert Intrusion, Quebec

The Mount Albert ultramafic intrusion of Ordovician (?) age occurs in the Gaspe Peninsula of Quebec and consists of partly serpentinized peridotite and dunite. It is surrounded by a high temperature metamorphic aureole, in contrast to most other alpine-type ultramafic intrusions (Smith and MacGregor, 1960). Green (1967) considers this type of peridotite to be genetically distinct from other alpine-type intrusions on the basis of internal stratification and differences in primary mineral chemistry.

The analyzed samples from the Mt. Albert ultramafic intrusion were collected near the northern contact. Samples 1 and 2 are from localities 1 km and 0.5 km, respectively, inward from the contact. Samples 13 and 14 are from a serpentinite zone at the contact. All samples are composed of lizardite and/or chrysotile, with samples 1 and 2 containing remnants of primary minerals.

The δD values of the serpentines are given in Table 10-2 along with estimates of δD values of waters that may have coexisted in equilibrium with these samples at 100°C. These data are compatible with the concept that meteoric waters were involved in the serpentinization. Note that these values are slightly lighter than those of the chrysotile samples from Vermont; this trend is to be expected if meteoric waters are involved, because of the more northerly occurrence of the Mt. Albert intrusion.

There are several possible explanations of the δD differences between the serpentinites at the contact (-98 to -111) and the partially serpentinized samples in the interior of the body (-123 to -125). Among these are: two (or more) periods of serpentinization, mixing of meteoric waters with other types of waters, and/or differences in the amount of exchange of the waters with surrounding rocks.

Samples 13 and 14 themselves differ in δD (-98 and -111, respectively), perhaps due to a small amount of brucite in sample 13. It is to be noted that pure brucite from the Belvedere Mountain area, Vermont (sample 5, Table 8-3) has a higher δD than its coexisting serpentine, although a brucite from Pennsylvania does not show this effect.

XI. MISCELLANEOUS SERPENTINE OCCURRENCES

11.1 Moses Rock Kimberlite Dike, Utah

Kimberlites are uncommon ultramafic rock types that occur in small diatremes, dikes, veins, and sills in stable or fractured continental regions. In this study serpentine samples are examined from the Moses Rock kimberlite dike of the Colorado Plateau (see figure 7-1, Chapter 8).

According to McGetchin (1968), the Moses Rock dike is a breccia, largely composed of locally derived sedimentary rocks, crystalline rock fragments, and kimberlite. The crystalline rock fragments are thought to be derived from the upper and lower parts of the earth's crust, while dense ultramafic fragments such as antigorite-tremolite schist, spinel-lherzolite, and kimberlite are thought to be derived from the upper mantle. The breccias, including kimberlite, are thought to have been emplaced during the Tertiary by a fluidized gas-solid system along a fissure. From hydrodynamic models, McGetchin (1968) suggests that the fluidized, H_2O-rich intrusive material was emplaced at flow velocities of 10 to 50 m/sec at the level of the present surface, and that velocities of about 400 m/sec may have been reached at the earth's surface.

The following samples were analyzed for δD and δO^{18} (see Table 11-1).

MR-1416A is a serpentinized kimberlite containing two types of serpentine. Olivine, which shows various degrees of alteration to mesh-texture serpentine, is set in a fine-grained serpentinite groundmass.

Table 11-1. Isotope data of samples from Moses Rock kimberlite dike, Utah.

							Calculated H20§			Est. Pres. Day H_2O δD†	δO^{18} H_2O Shift‡
Sample	Mineralogy*	% serp.	δD_S	δO^{18}_S	δO^{18}_M	T°C	δD	δO^{18} ($y/x=\infty$)	δO^{18} ($y/x=1$)		
MR-1416 A	C + L	60D	- 97	7.8	-	100	-52	1.2	3.5	-110	10.0
MRX-2	L + C	5P	-102	-	-	100	-57	-	-		-
MRX-51	A, Tr	100	- 65	7.6	-	310	-40	7.6	9.7		-
MRX-1600	A, tr. Ch,Tr	100	- 60	6.7	-	310	-35	6.7	7.9		-

Both serpentine-types are lizardite-chrysotile. Modal analysis of the total rock by McGetchin (1968) suggests about 50% serpentine groundmass and 40% serpentine derived from olivine.

McGetchin (1968) suggests two plausible origins for the serpentine: (1) some alteration of olivine and otrhopyroxene took place during transport, prior to emplacement at the present site, and (2) serpentine was produced *in situ* but from water which was introduced practically simultaneously with the particulate fragments.

MRX-2 is a spinel-lherzolite in which the olivine is incipiently serpentinized. The serpentine is similar to that of sample MR 1416A. The primary mineral assemblage may have crystallized in the mantle at about 48 km depth and 1200°C (McGetchin, 1968).

MRX-51 is an antigorite-tremolite schist and is the most abundant type of ultramafic inclusion in the Moses Rock dike. This particular sample exhibits a matted intergrowth of antigorite and minor tremolite. McGetchin (1968) suggests that the schist may have originated at depth, either in the upper mantle or lower crust, by hydration of a pre-existing ultramafic rock.

MRX-1600, an antigorite schist with minor chlorite and tremolite, is similar to MRX-51.

Discussion of the isotope data

The samples described above and on Table 11-1 can be classified into two groupings on the basis of their δD values. Samples MR-1416A and MRX-2, both consisting predominantly of lizardite-chrysotile, are low in deuterium (δD = -97 to -102). In contrast, the antigorite schist samples (MRX-51, MRX-1600) have very heavy δD values (-60 to -65). The δO^{18} values of both sets of samples are fairly uniform (+6.7 to +7.8).

Based on the model proposed in Chapter 4, the isotopic composition of the waters assumed to have been in equilibrium with these serpentines are presented in Table 11-1. The waters in equilibrium with the lizardite-chrysotile serpentine are isotopically light (δD = -52 to -57, δO^{18} = +1.2) compared with those equilibrated with antigorite (δD = -35 to -40, δO^{18} = +6.7 to +7.6), suggesting different origins. The latter type of water is very close to the values estimated by Sheppard and Epstein (1970) for deep-seated waters that have equilibrated with phlogopites from a variety of mica peridotites and kimberlites. Thus, the antigorites probably also had a deep-seated origin.

In contrast, the waters in equilibrium with the lizardite-chrysotile suggest, but do not necessitate, that meteoric waters were involved in this type of serpentinization. The δD values of these waters can be explained by either a deep-seated or meteoric water source, but the low δO^{18} value suggests the latter. However, a deep-seated water that equilibrated with, for example, a basalt at low temperatures conceivably could generate such δO^{18} values.

If meteoric waters are involved in the formation of the Moses Rock lizardite-chrysotile, then the δD values of these waters are clearly distinct from the present-day meteoric waters in this region. However, this is not unreasonable if emplacement took place in the Tertiary, because Tertiary meteoric waters in the Arizona-New Mexico-Utah area were higher in δD than they are at present (Sheppard et al., 1969).

If meteoric waters were important, the kimberite must have been in large part serpentinized at relatively shallow depths within the range of ground water penetration; this serpentinization may have occurred in situ during or after emplacement. This suggestion is reinforced by the fact that the present-day erosion surface here is only about 5000 feet below the surface at the time of emplacement (McGetchin, 1968).

The antigorite schists show no evidence of any interaction with the postulated meteoric waters. This fact is important in showing that the antigorites preserve their δD values even though surrounded by aqueous fluids that produce abundant serpentinization of adjacent ultramafic rocks.

Even though the isotopic data given in Table 11-1 appear to be most compatible with a meteoric-water origin for the lizardite-chrysotile of the kimberlite, it is conceivable that the major isotopic differences attributed to the calculated waters are due to the assumed low temperatures of serpentinization (i.e., 100°C). If, for example, the lizardite-chrysotile serpentinization of the kimberlite occurred at 220°C, then a water in equilibrium would have an isotopic composition ($\delta D = -64$, $\delta O^{18} = 6.0$) within the range of deep-seated type waters (see figure 5-4).

11.2 Miscellaneous Precambrian serpentinites

The hydrogen isotopic compositions of a series of serpentinites and partially serpentinized Precambrian ultramafic rocks were measured in order to assess the δD values of some Precambrian aqueous fluids possibly involved in serpentinization. Also, it was thought that such data might provide further evidence concerning the preservation of isotopic compositions of serpentine over long periods of time.

The samples were all selected from shield areas which have been geologically relatively stable since the Precambrian. Serpentinites in these terranes appear to be ubiquitous rather than occurring in well-defined belts as do the younger alpine-type ultramafic intrusions (Hess, 1955). The various localities are discussed below and the isotopic data are given in Table 11-2.

Hyland Lake Area

This area is part of the Labrador geosyncline, a sinuous to arcuate belt of sedimentary, volcanic and intrusive rocks more than 750 miles long and up to 60 miles wide, lying unconformably upon granitic and metamorphic rocks of the Superior Province (Stockwell, 1957).

Samples of serpentinite and altered ultramafic rocks were selected from a series of sills in the vicinity of Willbob Lake. According to Frarey (1952), ultramafic sills are intruded into predominantly volcanic units. In general, the marginal zones of these sills contain much tremolite, and the interior portions contain unaltered ultramafic rock and serpentine. The region has been subjected to lower greenschist metamorphism.

Table 11-2. Isotope data of samples from Precambrian terranes.

Sample	Mineralogy*	% serp.	δD_S	δO^{18}_S	δO^{18}_M	T^oC	Calculated H_2O§			Est. Pres. Day H_2O δD†	δO^{18} H_2O Shift‡
							δD	δO^{18} (y/x=∞)	δO^{18} (y/x=1)		
Hyland Lake, Quebec											
154	L + C	60P	-116	-	-	100	-71	-	-	-130	
187	A > C, Tr	50P	- 97	-	-	-					
163	A, tr. C, brucite	100	- 82	-	-	-					
139A	Ch, Tr , tr. brucite	-	- 75	-	-	-					
139c	Tr , Ch., brucite	-	- 77	-	-	-					
Ungava, Quebec	A	100	- 75	-	-	310	-50	-	-	-150	
Manitoba	L	100	-129	-	-	100	-85	-	-	-110	
Barbarton, South Africa											
1	L + C	100	- 61	-	-	100	-14	-	-	- 15[1]	
24	L + C	70P	- 64	-	-	100	-17	-	-		

Sample 139c represents a highly altered ultramafic rock taken near the sill margin. It is completely metamorphosed to a tremolite-chlorite assemblage. Sample 139a, a less altered rock from the sill margin, contains more chlorite than tremolite, while sample 187 is mostly serpentine with a very small quantity of tremolite. Samples 163 and 154 were taken from the interior portions of sills and contain no marginal-zone minerals. However, sample 163 consists predominantly of antigorite, whereas sample 154 contains a large proportion of lizardite-chrysotile. The δD values of various whole-rock samples from several metamorphosed ultramafic sills are presented in Table 11-2.

By analogy with isotopic relationships mentioned previously, the various δD values of the samples can probably best be explained by assuming that all of the hydrous phases except lizardite and chrysotile have relatively heavy δD values ($\delta D \approx -75$ or heavier). It is plausible that all of the chrysotile-lizardite has a δD value similar to that of sample 154 ($\delta D = -116$).

Both the isotope data and the fact that the tremolite and chlorite occur along the outer margins of the sills of antigorite-ultramafic rock suggest that these minerals developed during regional metamorphism. This is analogous to the metasomatic zoning of serpentinites observed in the Appalachian ultramafic belt.

It is almost certain that the formation of lizardite-chrysotile is unrelated to the regional metamorphism. Textural evidence in sample 187 indicates that the chrysotile-lizardite probably formed later than the other phases, and the isotopic data suggest that meteoric waters may have been involved. The model calculation of chapter 4, however, gives a $\delta D \approx -71$ for these waters, indicating that magmatic waters ($\delta D = -50$ to -80) cannot be excluded. This situation is thus similar to that described for the Muskox intrusion; the calculated waters are much heavier than the present-day meteoric waters in this region. Note that neither the antigorite nor the chlorite and tremolite have appreciably exchanged with or been affected by the isotopically lighter waters responsible for the development of the later chrysotile-lizardite.

Povungnituk, Ungava

This area is similar to Hyland Lake where, according to Bergeron (1959), a series of volcanic, ultramafic, and gabbroic rocks unconformably overlie a Lower Precambrian igneous and metamorphic complex. A single sample (see Table 11-2) of antigorite was collected from a highly serpentinized sill from this area. The δD (-75) of this sample suggests that the serpentinization may have occurred during the low-grade metamorphism which affected the uppermost Precambrian rocks. No subsequent exchange with isotopically light meteoric waters has occurred since formation of the antigorite, even though the present-day meteoric waters in this area probably have δD values lighter than -150 (see figure 5-2).

Manitoba

A serpentinite sample was selected in the vicinity of Lynn Lake in the Manitoba Nickel Belt in northern Manitoba. The serpentinite, composed of lizardite, is associated with talc and occurs in the peridotite portion of a gabbroic complex that intrudes volcanic units (Ruttan, 1957). The δD value of this sample (-129$^{o}/_{oo}$) is relatively light, suggesting that meteoric waters may have been involved in the formation of part of the serpentinite. Though specific geologic relationships are unknown, the lizardite is probably much later than the metamorphism. A model calculation of the δD of water that may have coexisted in equilibrium with this sample gives δD = -85. This is only a little bit heavier than the present-day local meteoric ground water (δD ≈ -110). Again, however, magmatic waters cannot necessarily be excluded as being involved in serpentinization, since the calculated water δD value is very close to that of magmatic water (δD = -50 to -80).

Barbarton District, South Africa

Two samples were selected from the ultramafic rocks in the Barbarton district of South Africa (located near Pretoria). The serpentine samples are part of an Archean series of intrusive rocks derived from peridotites intruded into sheet-like diabase bodies (Visser, 1956). The ultramafic rocks are almost completely serpentinized, though small lenses of talc are common within the serpentinite body. The δD values of the two samples, both composed of lizardite and chrysotile, are -61 and -64 per mil.

These isotopic data suggest that this serpentine was formed from peridotite by reaction with waters having an estimated δD = -14 to -17 per mil (see Table 11-2). These serpentinites thus may have originated from connate or heavy meteoric waters, or perhaps from metamorphic-type waters during the Precambrian metamorphism. The δD values suggest that the serpentine has not exchanged with light meteoric water since formation. However, because present-day waters are presumably not very low in δD in this area (see Table 11-2), this is not a favorable area in which to test whether any post-serpentinization isotopic exchange has occurred.

11.3 Deweylites

The hydrogen and oxygen isotopic compositions of a series of 'deweylite' samples were examined in order to determine if such rocks are isotopically distinct from the other types of serpentine samples. According to Lapham (1961), x-ray diffraction patterns of deweylites bear a close resemblance to those of true serpentine, except for the absence of many (hkl) reflections and a characteristic line broadening. Also, the (002)/(020) intensity ratio for serpentine is generally much greater than for deweylite; this intensity ratio is > 1 for serpentine and < 1 for deweylite. The chemistry is distinct, in that for most chrysotiles and antigorites the ratio $Si/(Mg + Fe + Ni) \approx 2/3$ whereas for deweylite it is ≈ 1. Lapham suggests that deweylite may be a dioctahedral modification of antigorite with an undulant character in the ab plane.

Lapham (1961) reports that deweylites are associated with magnesite, brucite, opal and hydromagnesite, and they generally occur as surficial coatings on open fracture surfaces; they appear to be secondary minerals of supergene origin, and they invariably are very fine grained, even compared to serpentine. The particular occurrence at Cedar Hill Quarry, Pennsylvania, suggests that deweylites are of very low temperature origin and are perhaps formed by the alteration of pre-existing serpentine minerals.

Faust and Fahey (1962) state that deweylite is not a true mineral species but is actually a fine-grained mixture of a serpentine-group mineral combined with the mineral stevensite. Stevensite, a montmorillonite-group mineral, exhibits a distinctive 12 - 14 Å basal spacing upon x-ray diffraction analysis; this peak shifts to about 17 Å after treatment with ethylene glycol (Faust et al., 1959).

A series of deweylite samples from several locations (see appendix section) were carefully examined by x-ray diffraction analysis in order to determine the minerals present. Small quantities of stevensite were observed in several samples. A non-crystalline limonite(?) was observed as a brown staining during petrographic examination of one sample.

The hydrogen and oxygen isotopic compositions of the deweylite samples are plotted in figure 11-1. The isotopic compositions of the deweylites are distinct from all other serpentine samples and are clearly different from the host rock antigorite (see Chapter 8). The δD values of deweylites are considerably lighter than the adjacent antigorite at Cedar Hill Quarry, whereas the δO^{18} values are heavier. The oxygen isotopic variations among the deweylite samples can be understood by noting the various amounts of admixed impurities of stevensite or other non-crystalline substances (see figure 11-1). Pure 'deweylites' have the lightest δO^{18} values, whereas mixtures of other components tend to shift the δO^{18} to a heavier value. In the extreme, pure stevensite is clearly displaced to the high O^{18} side of deweylite.

The following conclusions can be drawn from the isotopic data presented in figure 11-1.

Figure 11-1. δD-δO^{18} diagram showing all deweylite-stevensite-(limonite) mixtures examined in this study. Deweylite samples increase in δO^{18} with progressively greater amounts of admixed stevensite or limonite impurities. Tie lines connect typical isotopic values of meteoric ground waters in S.E. Pennsylvania with nearby 'pure' deweylites. A dashed line drawn through the field of 'pure' deweylite roughly parallel to the meteoric water line may define the locus of isotopic compositions of all deweylites formed in equilibrium with meteoric ground waters in a weathering environment. For reference, this 'deweylite line' is compared with the kaolinite line and oceanic montmorillonite band (Savin and Epstein, 1970), and to the gibbsite line and subaerial montmorillonite band (Lawrence, 1970). Note the distinctly different patterns exhibited by deweylites and "normal" serpentines, as shown by the fields of continental antigorites and lizardite-chrysotiles.

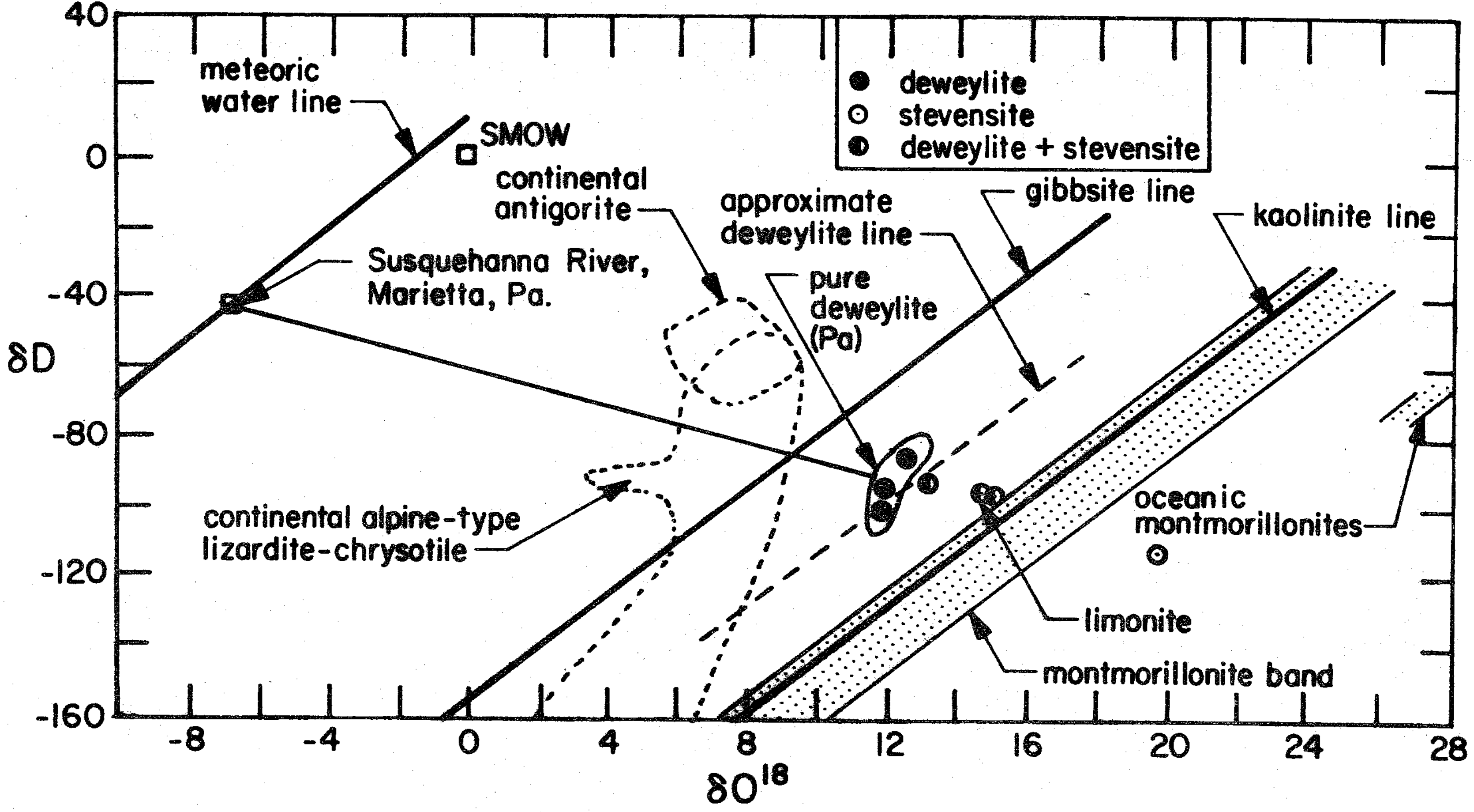
40
0
-40
-80
-120
-160
δD
-8
-4
0
4
8
12
16
20
24
28
δO^{18}
meteoric water line
SMOW
continental antigorite
Susquehanna River, Marietta, Pa.
● deweylite
⊙ stevensite
◐ deweylite + stevensite
approximate deweylite line
pure deweylite (Pa)
gibbsite line
kaolinite line
continental alpine-type lizardite-chrysotile
oceanic montmorillonites
limonite
montmorillonite band

Figure 11-1.

(1) The relatively light δD values of the deweylite and stevensite suggest that meteoric waters were involved in the formation of these minerals. In contrast, antigorite from Cedar Hill Quarry has a relatively heavy δD value (Chapter 7) and probably formed during the regional metamorphism. Clearly the developemnt of deweylite from antigorite involves complete recrystallization and exchange of both hydrogen and oxygen isotopes.

(2) If deweylites are formed in isotopic equilibrium with meteoric water at temperatures similar to those of a weathering environment then it should be possible to draw a 'deweylite' line on a δD - δO^{18} diagram, nearly parallel to the 'kaolinite' line of Savin and Epstein (1970); such a line would define the positions of all such deweylites formed at about 15° to 30°C in the presence of meteoric waters. Note on figure 11-1 that the stevensite, a montmorillonite-type mineral, plots close to the montmorillonite band of Lawrence (1970).

(3) If true serpentine were commonly formed at low temperatures in a weathering-type environment (as suggested, for example, by Barnes and O'Neil, 1969), then all such serpentine samples should lie in close proximity to the 'deweylite' line. However, most serpentines, in fact, lie well to the left of this hypothetical line and do not follow such a pattern, as is illustrated in figure 11-1. The isotopic evidence thus indicates that, except for the deweylites, serpentinization is a process unrelated to weathering at the earth's surface. This is in agreement with much geologic evidence (Turner and Verhoogen, 1960; Mattson, 1964).

It is noteworthy in this regard that one sample (6d, see section 7.3), selected from within the zone of weathering of the sheared serpentinite body at San Luis Obispo, is enriched in 0^{18} by about 0.7 per mil relative to most of the 'fresh' serpentinites. Small amounts of alteration deweylite may account for the increased $\delta 0^{18}$ value of this sample.

The equilibrium isotopic fractionation factors for the pair deweylite-water can be estimated from the data given in figure 11-1. Present-day meteoric waters with $\delta D \cong -42^{o}/oo$, and $\delta 0^{18} \cong -6.5^{o}/oo$ (given by Friedman, et al., 1964, for the Susquehanna River at Marietta, Pennsylvania, which lies 30 miles NW of the deweylite locality) appear to coexist with deweylite having $\delta D = -94^{o}/oo$ and $\delta 0^{18} = +11.9^{o}/oo$ sample 4, Wood Mine, southeastern Pennsylvania). The fractionation factors for deweylite - H_20 at about 15^{o}- $30^{o}C$ are thus $\alpha^{hy} \approx 0.946$ and $\alpha^{ox} \approx 1.0185$. As shown by the data in figure 11-1, these fractionation factors are different from those derived for clay minerals at these temperatures.

XII. PROBLEM OF PRESERVATION OF D/H AND O^{18}/O^{16} RATIOS

The question of whether a given mineral preserves its original isotopic composition subsequent to its formation is of fundamental importance in any stable isotope study. The following arguments can be used to support the idea that the isotopic compositions of minerals studied in this work have been largely preserved since their original formation or recrystallization.

Chlorite, talc, tremolite and biotite

All samples of chlorite, talc, tremolite and biotite, regardless of geographic location have very uniform δD values and thus display no evidence of interaction with meteoric waters. The general consistency of heavy δD values for these minerals, despite the wide range of sample localities and presumed times of formation, implies that essentially no exchange with meteoric ground waters has occurred since their formation. Furthermore, these minerals appear to have preserved their δD and δO^{18} values over long periods of time; examples are the chlorite and tremolite from the Precambrian terrane at Hyland Lake, Canada and the talc, biotite, and actinolite from the Paleozoic Appalachian belt.

Antigorite

All antigorites examined in this study also have relatively heavy δD values suggestive of isotopic preservation since their formation. The δD values of antigorite are invariably similar to those of adjacent talc and chlorite. A large number of samples were studied from regions at high latitudes where, for example in British Columbia, the antigorites may have been in contact with isotopically light meteoric ground waters for millions of years. Antigorites from Hyland Lake and at Ungava in the Canadian shield were probably formed during the Precambrian and have apparently not been "disturbed" at least during the last few tens of millions of years.

At Cedar Hill Quarry in southeastern Pennsylvania, antigorite found in fault zones was probably formed during a Paleozoic metamorphism; the antigorite seems to have preserved its isotopic composition despite being exposed to percolating meteoric ground waters which formed the isotopically distinct deweylites in other parts of the quarry. In the Moses Rock kimberlite dike, antigorite schist fragments have preserved their heavy δD values even though they were probably totally surrounded by low-δD aqueous fluids that produced chrysotile-lizardite serpentinization of adjacent ultramafic material. Even at Belvedere Mountain, Vermont, strong development of cross-cutting chrysotile veins from low-δD waters has apparently not affected the immediately adjacent antigorite.

Lizardite-chrysotile

Inasmuch as most of the continental lizardite-chrysotile samples examined in this work probably originally formed from aqueous fluids containing a significant meteoric water component, the extent of isotopic preservation in these particular serpentine polymorphs is more difficult to prove. Furthermore, a number of the oceanic lizardite-chrysotile samples can be interpreted as having suffered D/H exchange down to relatively low temperatures, if it is legitimate to assume that these samples formed in the presence of pure ocean water. However, the following lines of evidence strongly support the idea that the isotopic compositions of the various lizardite-chrysotile samples studied in this work essentially represent values acquired during formation, and thus are not due to subsequent exchange with waters of the immediate environment at low temperatures:

(1) An exchange experiment utilizing finely-ground (< 0.1 mm) serpentine and water that was isotopically enriched in deuterium was carried out at room temperature for four days. Under these conditions, lizardite-chrysotile type serpentine undergoes D/H exchange to only a negligible extent (< 1%) (see section 3-7).

(2) Many lizardite and chrysotile samples appear to have formed from a meteoric water or a mixed meteoric-connate water whose isotopic composition is quite dissimilar from today's ground waters. Estimates of the isotopic compositions of these waters, according to the model proposed in chapter 4, indicate that the lizardite-chrysotile serpentines from the Muskox Intrusion, for example, were clearly not formed from recent (or probably even from Tertiary) meteoric waters. Other lizardite-chrysotile samples displaying similar discrepancies include those from Manitoba, the Stillwater complex, Montana, the Moses Rock kimberlite dike, and several areas of British Columbia, as for example, the Yalakom ultramafic body.

(3) Several highly fractured and sheared serpentinite bodies, as for example at Cassiar, British Columbia, and at Vourinos, Greece, are very heterogeneous in δD suggesting the possibility that serpentinization occurred over an extended time period in the presence of different types of waters. Cross-fibre chrysotile veins have δD values compatible with formation from present-day meteoric waters in the Cassiar region, but the matrix chrysotile has a heavier δD value, suggesting equilibration with an isotopically heavier water. A highly fractured serpentinite body

that probably has been exposed to light meteoric ground waters for long periods of time would not be expected to exhibit such heterogenous δD values if extensive and rapid isotopic exchange with low-temperature waters can readily take place.

(4) Several samples display textural relationships which suggest that the light δD values of an early generation of lizardite and chrysotile are preserved, having survived development of higher-grade minerals that seem to have formed in the presence of a deep-seated type water. For example, sample 3 from the Nahlin, British Columbia body has a δD value that is apparently a composite of light δD from lizardite and chrysotile (perhaps similar to the pure lizardite-chrysotile samples 1 and 2 from this body) and a much heavier δD characteristic of deep-seated minerals (talc, antigorite, and tremolite).

For this sample, the textural evidence in plate 12-1 strongly suggests that at least some chrysotile veins were formed prior to the talc. This in turn suggests that the chrysotile in this sample was exposed to a higher δD (and temperature?) environment during formation of the talc (and possibly tremolite) without apparently affecting its original light δD. This suggests that extensive isotopic exchange of lizardite and chrysotile probably occurs only if the serpentine undergoes recrystallization.

(5) From structural comparisons of lizardite and chrysotile on the one hand and antigorite on the other, one can make some tentative assertions concerning the ease of isotope exchange.

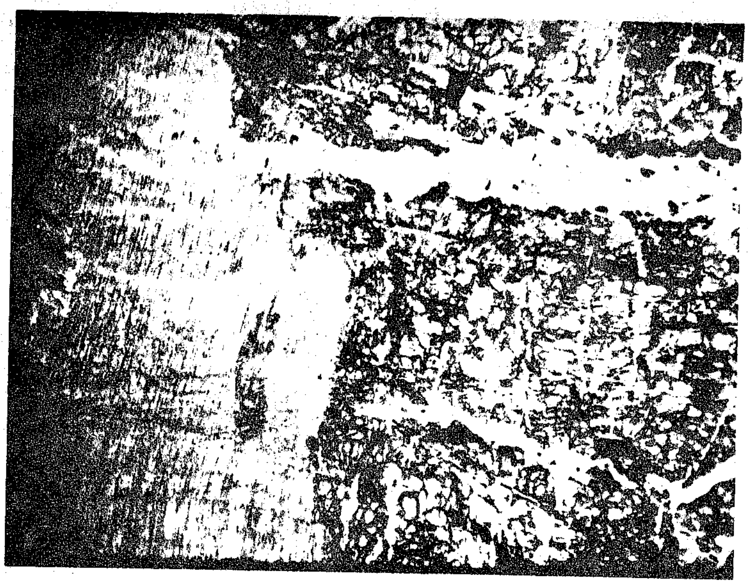

Plate 12-1

(plane light, 1.33 x 0.93 mm)

Sample 3, Nahlin Body, British Columbia. Platy, highly foliated talc (on left) crosscuts the chrysotile veins through olivine on the right. A small remnant mass of tremolite crystals is visible near left of center within the talc. Note also that the talc apparently exhibits a pseudomorphic pattern after the chrysotile vein in the upper part of the photograph, which extends across the talc mass. This talc may be largely pseudomorphic after bastite. The whole rock $\delta D = -143^{\circ}/_{oo}$.

All of the serpentine "polymorphs" have layered-type structures in which a pseudo-hexagonal, tridymite-type network of linked SiO_4 tetrahedra is joined to a brucite layer in which, on one side only, two out of every three hydroxyls are replaced by apical oxygens of the SiO_4 tetrahedra. Such an arrangement is shown in figure 12-1, assuming the approximate parameters a = 5.3, b = 9.2Å , and a perpendicular distance between sheets of about 7.3Å. Due to the joining of the two components, various crystallographic or morphological features occur among the serpentine numerals. This fit, unlike the case of the analogous kaolinite structure in which the gibbsite-like layer and tridymite-like layer match pretty well, is very poor and forces the serpentine layer into a curve; the silica tetrahedral layer is always on the inside of the curve (Bragg and Claringbull, 1968). The fundamental layers in chrysotile are curved about the x axis, forming concentric hollow cylinders elongated parallel to x (Deer, Howie and Zussman, 1966). Lizardite, which has a platy morphology, differs from chrysotile in that crystals are bent about more than one axis (Rucklidge and Zussman, 1965).

Antigorite is structurally distinct, with b dimensions and (001) spacings similar to those of chrysotile and lizardite, but with a large a dimension (generally greater than 40Å). Antigorite displays a corrugated pattern as shown in figure 12-2.

In the absence of recrystallization, the ease or difficulty of isotope exchange is probably dependent primarily upon the strength of the particular atomic bonds that need to be broken, since bond rupture has to occur during such an exchange. For example, hydrogen isotope exchange in

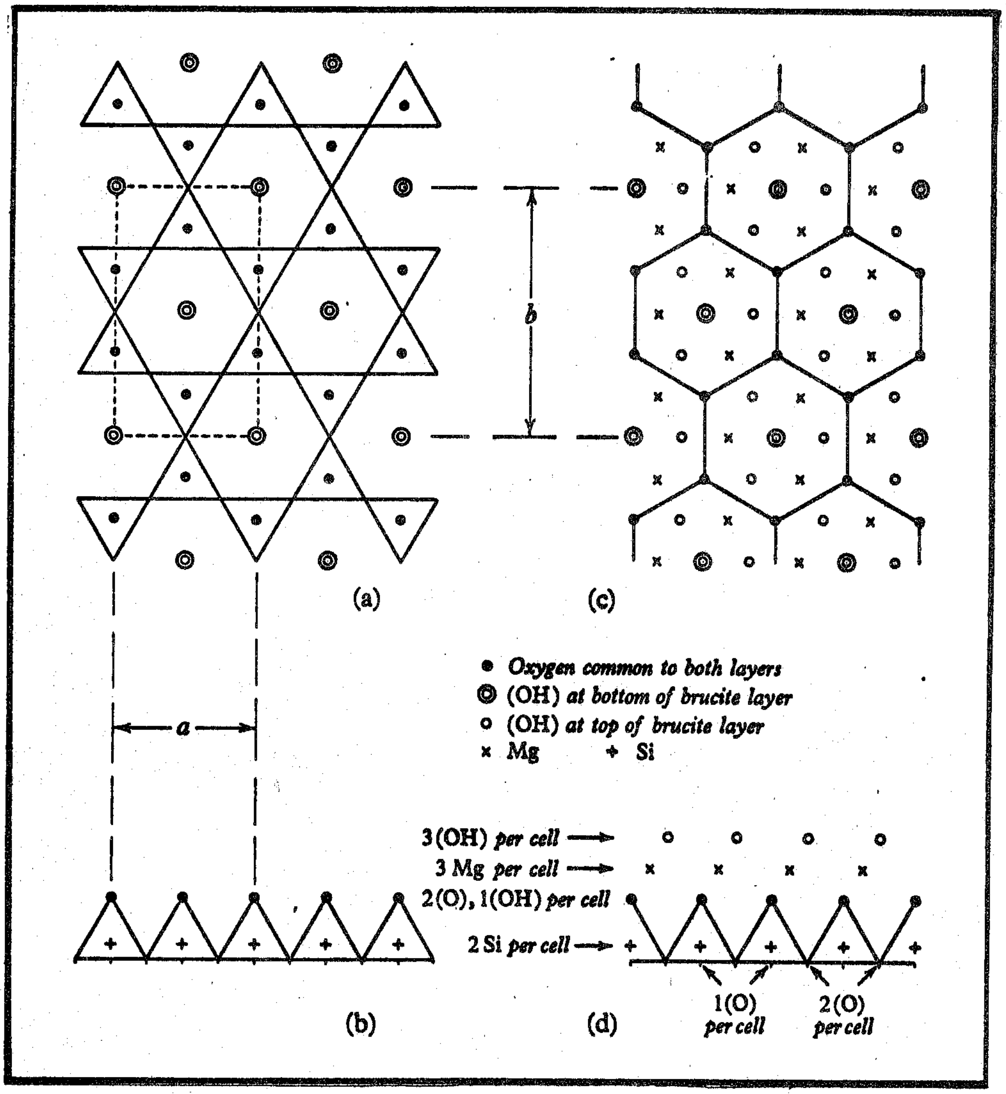

Figure 12-1.

The structure of a serpentine layer (after Deer, Howie and Zussman, 1962):

(a) Tetrahedral Si_2O_5 network in plan.
(b) Tetrahedral network as viewed along y axis.
(c) Tri-octahedral component of serpentine layer (plan).
(d) Serpentine layer as viewed along y axis.

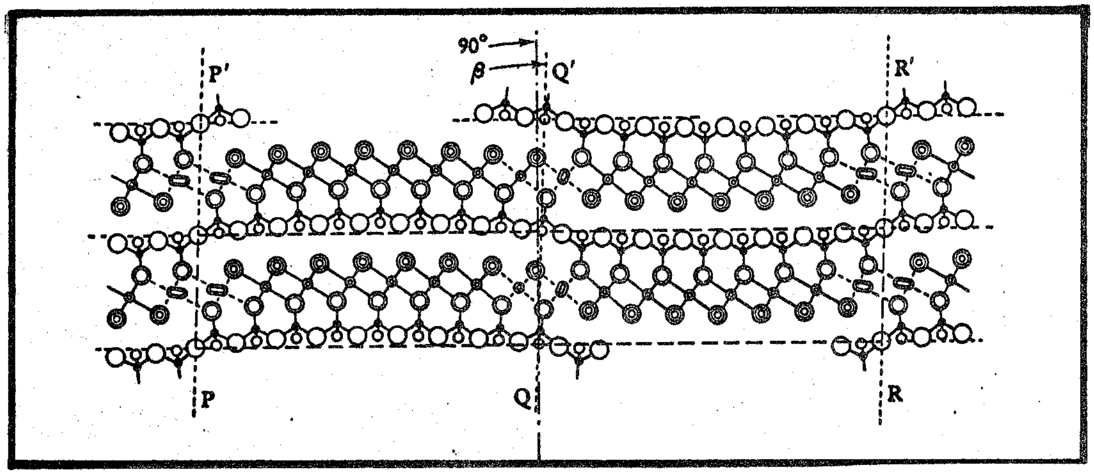

Figure 12-2.

The structure of antigorite as viewed along y axis (after Deer, Howie and Zussman, 1962).

hydrous minerals is known to be much easier than oxygen isotope exchange (Savin and Epstein, 1969; Lawrence, 1970).

The hydroxyl occupies a similar position in all three serpentine polymorphs, and the proportions of various bond-types are also identical in all three. Thus, as a first approximation, the ease of exchangeability for D/H and $0^{18}/0^{16}$ ought to be essentially the same in all serpentine polymorphs. If this assertion is correct, then lizardite and chrysotile should show approximately the same resistance to later isotopic exchange as does antigorite; this is important because the latter polymorph definitely shows no evidence of having undergone any post-formation exchange in the numerous deposits studied.

Lawrence (1970) has shown that in order to have rapid D/H exchange in clay minerals, there must be intimate contact between the water and hydroxyl. This is the case, for example, with interlayer water in halloysite and to a lesser extent with montmorillonite. Both clay minerals have expanding lattices that can accommodate interlayer water, whereas serpentine shows no such characteristics. For example, halloysite undergoes lattice contraction from 10Å to 7.2Å (i.e., the normal d_{001} for kaolinite) upon dehydration. In contrast, although some serpentines do tend to adsorb water in amounts greater than that present as hydroxyl, no lattice contraction is observed upon dehydration.

The exchange experiment mentioned in (1) above clearly differentiates chrysotile-lizardite serpentine from halloysite or montmorillonite, because the latter two minerals both show pronounced D/H exchange under similar experimental conditions (Lawrence, 1970).

The structure of halloysite is thought to be tubular (Bates *et al.*, 1950) and thus might at first glance be considered somewhat analogous to chrysotile. Although kaolinite has a slight tendency to curl due to mismatch between the structural units, this tendency is inhibited by the "stretching" effect that the oxygen ions in the silicon-oxygen sheet of one unit have upon the opposing hydroxyl ions in the gibbsite sheet of the adjoining unit. However, in halloysite, because of the presence of interlayer water, the distance between opposing oxygen and hydroxyl ions of adjacent 1:1 units is appreciably greater, causing reduction of the "stretching" effect and hence allowing curvature (Bates *et al.*, 1950). For the most part, the chrysotile tubes (inner diameter about 100Å) appear to be partially filled by other serpentine material (chrysotile?, Bragg and Claringbull, 1965). Even if water were to diffuse into and along the hollow portions of the tubes, isotopic exchange with the hydroxyl would not be expected to occur, since the hydrogen of the hydroxyl occurs on the outside of the tube, not on the inside, and is thus protected from exchange by the intervening tridymite-type layers.

Preservation of serpentine-magnetite O^{18}/O^{16} fractionations

Several different features strongly suggest that most of the measured serpentine-magnetite O^{18}-fractionations discussed in chapter 4 were "frozen in" under near equilibrium conditions during serpentinization and probably have not undergone significant isotopic retrogradation.

(1) The serpentine-magnetite O^{18} fractionations are exceedingly uniform and consistent within a given class of serpentinized ultramafic bodies. This is particularly true with regard to the 'normal' lizardite-

chrysotile serpentines. The indicated isotopic temperatures for antigorites do seem to be abnormally low when compared to the metamorphic grade of their adjacent country rocks, indicating the possibility of retrogradation. However, if isotopic retrogradation were extensive in a given class of serpentines, one would probably observe a wide spectrum of serpentine-magnetite fractionations, and in fact one does not. The final "temperature", in such instances, would be primarily dependent upon a large number of factors, such as the rate of cooling of a given serpentine body.

(2) The magnetite δO^{18} values within a given class of serpentines are also quite uniform (see figure 4-1). All of the magnetite δO^{18} values in the "normal" continental lizardite-chrysotile type serpentines lie within the remarkably narrow range -6.1 to -4.6, whereas magnetites of continental-type antigorites show a somewhat wider variation, from -2.6 to +1.7. The modal abundances of magnetites in the former serpentines range from 0.5 to 3%, and in the antigorites from 1 to 15%.

If retrogradation were extensive, one should observe widely varying magnetite δO^{18} values, particularly in serpentinites containing very small amounts of magnetite. For example, let us assume that a given serpentinite sample represents a closed system containing a large amount of serpentine and small quantity of magnetite. If this mineral pair is equilibrated at an arbitrary high temperature, then during retrograde exchange, the O^{18}/O^{16} ratio of the serpentine would increase only slightly, whereas the magnetite δO^{18} would decrease by progressively greater amounts, the smaller the abundance of magnetite in the system and/or the lower the "freeze-in" temperature. The O^{18}/O^{16} ratio of the entire system is essentially determined by the serpentine, and this can change significantly only if the entire system is open and in communication with a large exterior reservoir of oxygen.

Within the Belvedere Mountain Quarry of Vermont, all antigorites have δO^{18} values in the range of +5.8 to +6.6, even though many of the samples contain varying proportions of other minerals. For example, sample 9 (+6.1) contains up to about 10 percent magnetite; sample 11j (+6.5) has about 40 percent olivine; and sample 11i (+6.3) is essentially all antigorite. There can have been little or no internal O^{18} exchange among these various minerals during cooling of the ultramafic body.

(3) Although little is known about the resistance of serpentine to isotopic exchange, it is well known that magnetites in other types of rocks commonly preserve their δO^{18} values during cooling, at least at temperatures lower than 600°C (Taylor, 1968). Admittedly, the magnetites in such rocks are commonly much coarser-grained than in most serpentines. Exceedingly fine-grained magnetites (.01 mm) present in only trace amounts in some contact metamorphic schists have been analyzed for O^{18} by Shieh and Taylor (1968), and they do show very large (i.e. retrograded) quartz-magnetite fractionations. Nevertheless, even these assemblages represent much higher temperatures (265-390°C) than do the lizardite-chrysotile serpentines, indicating that retrograde exchange of such fine-grained magnetite does not take place down to temperatures as low as those inferred by the measured serpentine-magnetite fractionations.

The grain size of magnetite in antigorite commonly ranges from 0.001 to 0.5 mm, with a maximum size of 2.0 mm (Jahns, 1967). In the samples examined in this study, the bulk of the analyzed magnetite grains in antigorite are 0.6 to 0.2 mm in size, although some (~ 10 - 20%) are much finer-grained ($\geq$ 0.005 mm). Most of the magnetite in lizardite-chrysotile samples has a grain size 0.05 to 0.01 mm, but in some samples as much as 25% is considerably finer-grained ($<$ 0.001 mm). Thus in the higher temperature serpentinites (antigorite-type), where retrograde exchange would be expected to be the greatest problem, the magnetites are relatively coarse-grained. Even though the magnetites are generally much finer-grained in the lower temperature lizardite-chrysotiles, it is doubtful that retrograde exchange would be important in the 100° - 200°C temperature range.

Summary

The δO^{18} values of serpentinites are almost certainly preserved since their formation or recrystallization because serpentine is essentially the only constituent present. In order to change the O^{18}/O^{16} ratio there would have to be major communication with a large external reservoir of oxygen. Furthermore, the serpentine-magnetite O^{18}-fractionations also seem to be largely preserved, particularly in lizardite-chrysotile samples. In antigorites some very fine-grained magnetites may have retrograded down to temperatures as low as 250° - 300°C, but at least one measured fractionation gives a higher temperature (460°C). The δD values of antigorite, talc, and chlorite seem to be preserved in every case that can be tested, although we cannot yet be quite so certain about chrysotile-lizardite. It is clearly very important to undertake experimental studies on the kinetics of isotopic exchange between the various serpentine polymorphs and water in the temperature range 25° - 500°C.

XIII. SUMMARY AND CONCLUSIONS - IMPLICATIONS OF THE ISOTOPE DATA

13.1 δD-δO^{18} relationships in serpentines

The δD values of almost all continental lizardite-chrysotile type serpentines exhibit a good correlation with the general D/H distribution in present-day meteoric waters. However, none of the antigorites, talcs and chlorites show such a correspondence, even though many samples were selected from high-latitude localities (see figure 13-1). Samples that represent mixtures of antigorite and lizardite-chrysotile generally have δD values intermediate between the values shown by pure end-member samples from the same locality. Some lizardite-chrysotile samples do show exceptions to the general pattern. Two such samples from the Precambrian Muskox intrusion, North-west Territory, Canada (see figure 13-1) are an example of this type of exception; such samples may have been formed at a time when the isotopic patterns of meteoric waters were greatly dissimilar from the present day.

The pronounced geographic pattern shown by δD values in continental lizardite-chrysotile serpentines strongly suggests that meteoric ground waters were involved in a substantial way in the serpentinization of almost all such bodies. On the other hand, it is clear that deep-seated or metamorphic waters must have been largely responsible for the formation of antigorite-type serpentine bodies and their associated magnesian alteration minerals (talc, chlorite, magnesite, etc.).

Figure 13-1. Diagram showing δD values of many of the samples examined in this study as a function of general latitude at which the sample was collected (excluding the oceanic samples). Horizontal tie lines connect all samples from same locality. Only samples composed essentially of pure talc, antigorite, or lizardite-chrysotile are reported.

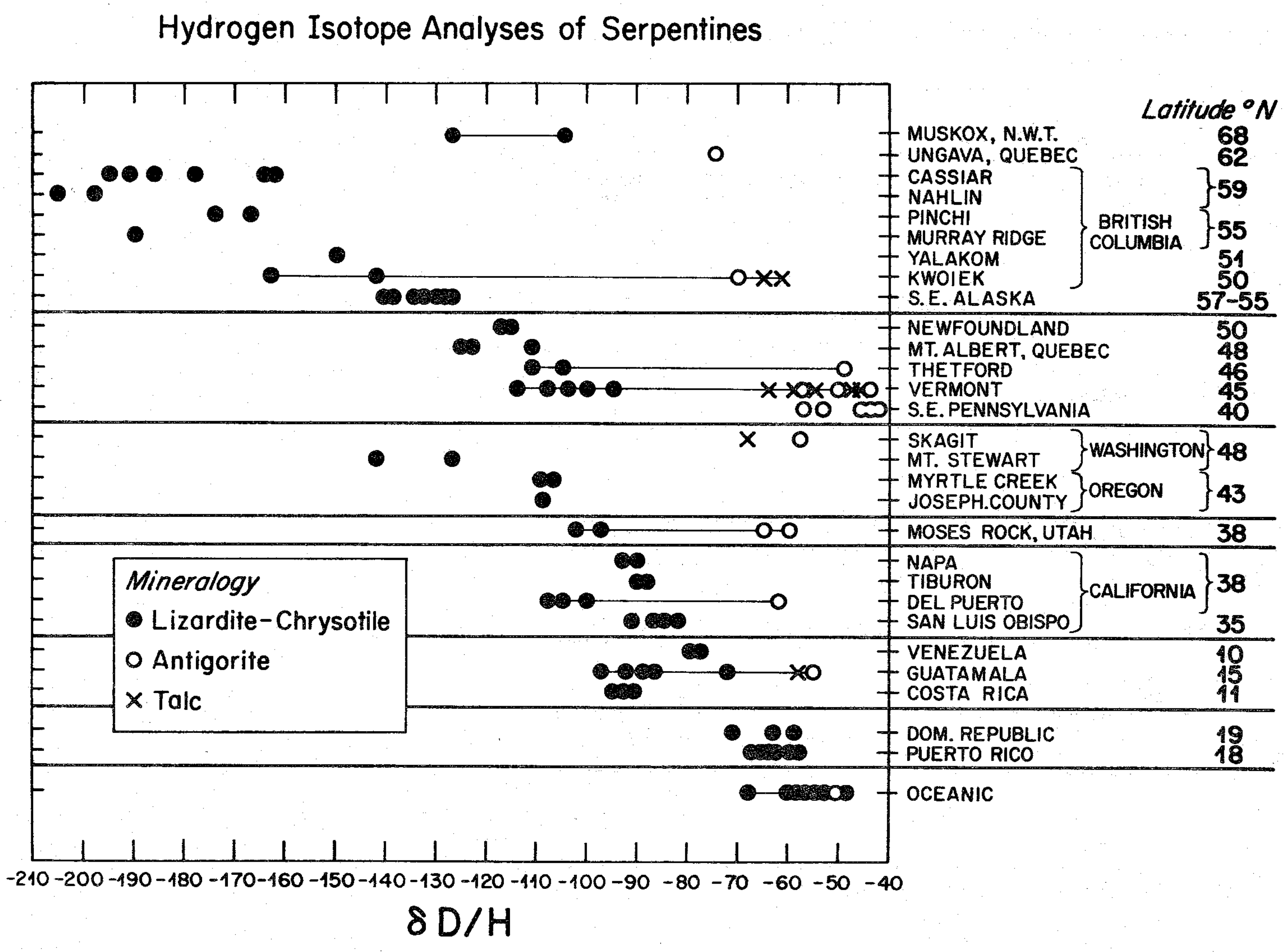
Hydrogen Isotope Analyses of Serpentines
Latitude °N
MUSKOX, N.W.T. 68
UNGAVA, QUEBEC 62
CASSIAR
NAHLIN
59
PINCHI
MURRAY RIDGE
55
BRITISH COLUMBIA
YALAKOM 51
KWOIEK 50
S.E. ALASKA 57-55
NEWFOUNDLAND 50
MT. ALBERT, QUEBEC 48
THETFORD 46
VERMONT 45
S.E. PENNSYLVANIA 40
SKAGIT
MT. STEWART
WASHINGTON 48
MYRTLE CREEK
JOSEPH.COUNTY
OREGON 43
MOSES ROCK, UTAH 38
NAPA
TIBURON
DEL PUERTO
CALIFORNIA 38
SAN LUIS OBISPO 35
VENEZUELA 10
GUATAMALA 15
COSTA RICA 11
DOM. REPUBLIC 19
PUERTO RICO 18
OCEANIC
Mineralogy
● Lizardite-Chrysotile
○ Antigorite
× Talc
-210 -200 -190 -180 -170 -160 -150 -140 -130 -120 -110 -100 -90 -80 -70 -60 -50 -40
δ D/H

Figure 13-1

The isotopic compositions of most of the serpentines examined in this study are shown on figure 13-2. The following different types of serpentine occurrence can be distinguished on such a plot.

Lizardite-chrysotile serpentines from alpine ultramafic rocks in low-grade metamorphic terranes exhibit a wide range in both δD and δO^{18}. Although the δD values are simply correlative with the general D/H distribution of present-day meteoric ground waters, the δO^{18} values appear to be related both to latitude and to the types of country rocks in the immediate environment of the ultramafic bodies. For example, the serpentines from the Cassiar body of Britich Columbia, which lie in a terrane composed of abundant O^{18}-rich carbonates, are O^{18}-enriched compared to serpentines from other bodies in the same general area; the latter serpentinites occur in terranes composed dominantly of relatively low-O^{18} volcanic rocks and graywackes. As an extreme example of this effect, one highly sheared serpentinite sample from the Vourinos Complex (see figure 9-2) that lies next to a series of limestones is exceedingly O^{18}-enriched ($\delta = +12.6$). This general correspondence between serpentine δO^{18} values and type of country rock suggests that the meteoric ground waters involved in serpentinization exchange to various degrees with the country rocks through which they migrate.

Antigorite-type serpentines from high-grade alpine ultramafic rocks show a narrow range in both δD and δO^{18}, -39 to -66 and +5.9 to +8.8, respectively. Samples containing small amounts of lizardite-chrysotile commonly have slightly lighter δD values, as might be expected.

Figure 13-2. $\delta D - \delta O^{18}$ diagram showing isotopic compositions of all the essentially pure serpentines analyzed in the present work. Also reported are the deweylite analyses shown in figure 11-1. The meteoric water line and kaolinite line (Savin and Epstein, 1970) are shown for reference. L - C = lizardite-chrysotile; A = antigorite. It is particularly noteworthy that the continental antigorites fall within the general isotopic range displayed by metamorphic chlorites, (δD = -42 to -71, Taylor and Epstein, 1966; δO^{18} = 6.2 to 8.7, Garlick, 1969).

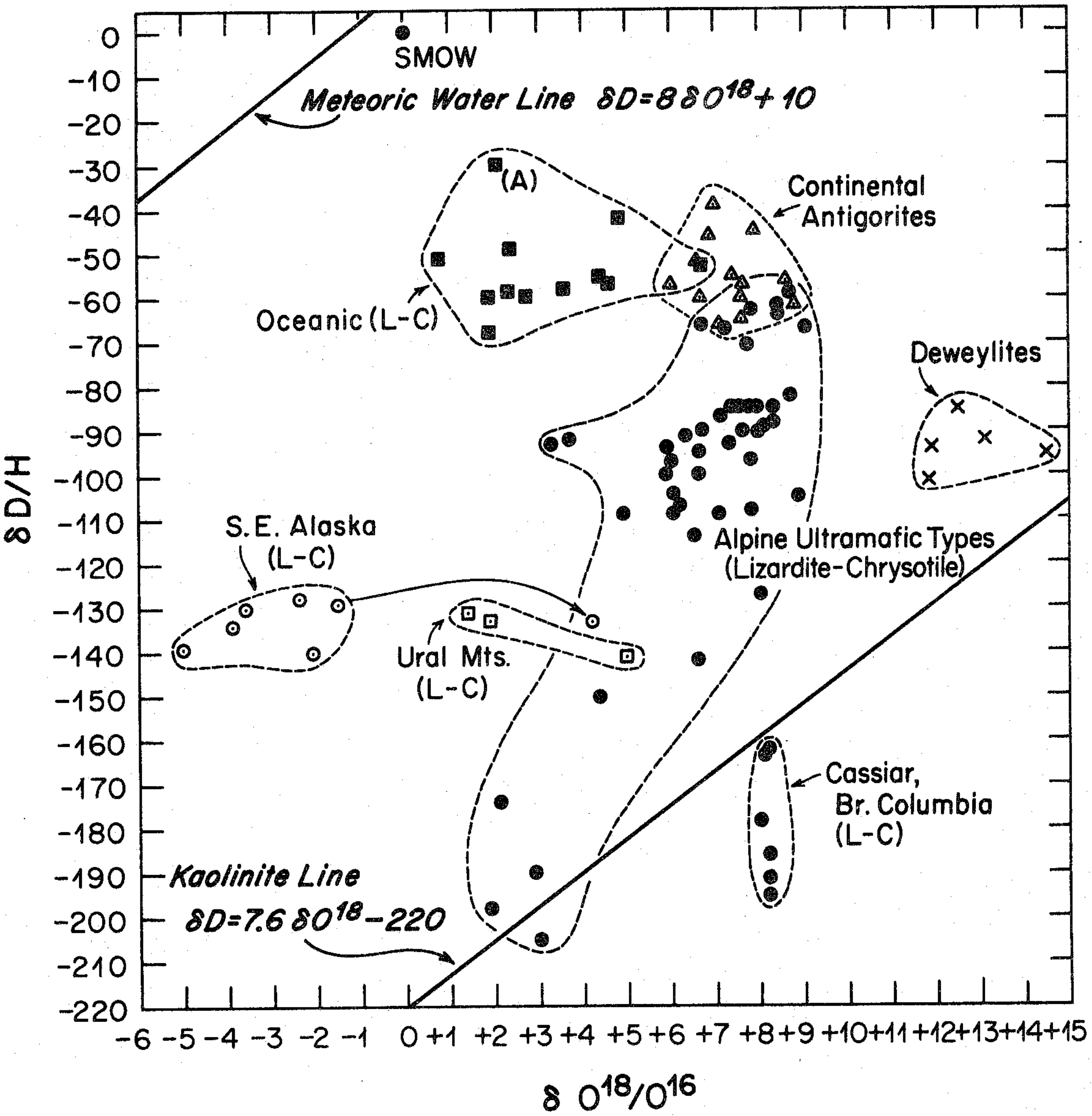
SMOW
Meteoric Water Line δD=8δO18+10
(A)
Continental Antigorites
Oceanic (L-C)
Deweylites
S.E. Alaska (L-C)
Alpine Ultramafic Types (Lizardite-Chrysotile)
Ural Mts. (L-C)
Cassiar, Br. Columbia (L-C)
Kaolinite Line δD=7.6δO18−220
δD/H
δ O18/O16
0
−10
−20
−30
−40
−50
−60
−70
−80
−90
−100
−110
−120
−130
−140
−150
−160
−170
−180
−190
−200
−210
−220
−6 −5 −4 −3 −2 −1 0 +1 +2 +3 +4 +5 +6 +7 +8 +9 +10 +11 +12 +13 +14 +15

Figure 13-2

Lizardite-chrysotile serpentines from zoned ultramafic intrusions are generally depleted in O^{18} relative to most other types of serpentine. Such ultramafic bodies were intruded into gabbro bodies and other crystalline igneous and metamorphic rocks; these rock types are relatively inert to O^{18} exchange with waters at low temperatures. Hence the meteoric waters involved in this type of serpentinization may have been nearly pristine (i.e., unexchanged). The wide δO^{18} variations in these bodies suggest that serpentinization occurred at widely differing temperatures.

Oceanic serpentines are clearly depleted in O^{18} and enriched in D relative to most other serpentines. One oceanic antigorite sample is distinctly heavier in δD than any of the lizardite-chrysotile samples. Although the isotopic compositions of serpentines in both low- and high-grade alpine ultramafic bodies are generally very uniform within a given body (and even uniform for differing textural types of serpentine within the same hand speciman, such as bastite, mesh-textures, or late-stage veins) a single oceanic serpentine specimen commonly will exhibit widely variable isotopic compositions. These isotopic variations also may reflect varying temperatures of serpentinization.

Deweylites are distinctly enriched in O^{18} relative to all other serpentines. On a δD-δO^{18} plot, deweylites from different localities would probably lie along a line nearly parallel to the kaolinite line with $\delta D = 7.6\delta O^{18} - 186$. Any serpentines formed at Earth-surface temperatures in a weathering-type environment ought to lie in the vicinity of such a line.

13.2 Temperatures of serpentinization

Three classifications of serpentine-magnetite O^{18}-fractionations were observed: "normal" lizardite-chrysotile with fractionations of 15.1 to 10.0; antigorites with Δ ranging from 4.8 to 8.7; and "anomalous" lizardite-chrysotiles that exhibit highly irregular fractionations. By way of comparison, chlorite-magnetite fractionations in biotite-grade pelitic schists (~ 400°C) exhibit fractionations in the range 5.3 to 6.7 per mil.

Isotopic equilibrium appears to have been generally attained for serpentine-magnetite pairs in "normal" lizardite-chrysotile and antigorite serpentinites, as evidenced by: (1) the consistency of the O^{18} fractionations in each of the two groups, (2) the similarity of magnetite δO^{18} values within each group, and (3) the chemical homogeneity of the magnetites. The serpentines and magnetites from the "anomalous" lizardite-chrysotile group do not appear to have been formed in either chemical or isotopic equilibrium.

Estimates of the temperatures of serpentinization were obtained by combining these measured serpentine-magnetite fractionations with an "estimated" geothermometer curve. This geothermometer curve was constructed by extrapolation of (1) observed δO^{18}-values of chlorite and Fe-Ti oxides in low-grade pelitic schists whose isotopic temperatures are known from the quartz-muscovite O^{18}-geothermometer, and (2) the conclusion that the O^{18} fractionation between chlorite and serpentine is essentially zero. This hypothetical serpentine-magnetite geothermometer suggests approximate equilibrium temperatures as follows: continental lizardite-chrysotile, 85° to 115°C; oceanic lizardite and chrysotile, 130°C and 185°C, respectively; continental antigorites, 220° to 460°C; and oceanic antigorite, 240°C. Most of the low-grade alpine lizardite-chrysotile serpentinization thus apparently occurs in the approximate temperature range 85° to 115°C. The oceanic lizardite-chrysotile serpentines indicate higher temperatures (up to 185°C), and there is reason to believe that in certain types of ultramafic bodies lizardite-chrysotile serpentinization may occur at even higher temperatures; this type of serpentinization conceivably could occur at any temperature up to the maximum breakdown temperature of chrysotile (about 500°C). In particular, in the zoned ultramafic bodies the temperatures of serpentinization may be as high as 300° - 500°C. This, however, is based on inferences from the calculated δO^{18} values of the water that produced serpentinization, not from actually measured serpentine-magnetite fractionations; no such measurements were made for these samples.

Calculated antigorite-magnetite "temperatures" are invariably low compared to the estimated temperatures at which regional metamorphism occurred in the country rocks surrounding a given ultramafic body. This suggests either preservation of a previously formed serpentinite during the peak metamorphism, serpentinization during the retrograde stages, or retrograde isotopic re-equilibration of serpentine-magnetite pairs down to temperatures lower than that at which serpentinization originally occurred. The very limited stability of serpentine in (1) the presence of CO_2 or in (2) cases of open fissure equilibrium where $P_{H_2O} < P_{total}$, in addition to the geologic evidence that talc-carbonate has marginally replaced many serpentinite bodies at the peak of metamorphism, strongly supports the hypothesis of early serpentinization and preservation through the major metamorphic episode. In such cases, the serpentine body, once formed, appears to be largely shielded from the interstitial fluids prevalent in the country rocks during metamorphism.

13.3 Estimates of the D/H and $0^{18}/0^{16}$ of waters involved in serpentinization

Estimates of the isotopic compositions of waters assumed to have coexisted in equilibrium with various serpentines can be made from (1) calculated temperatures, derived either from measured serpentine-magnetite fractionations or assumed at 100°C for lizardite-chrysotile and 310°C for antigorite and (2) estimates of D/H and $0^{18}/0^{16}$ serpentine-water fractionation curves. The calculated $\delta 0^{18}$ values of such waters will be identical to that of the initial water entering the ultramafic system, if we assume equilibration with an 'infinitely' large reservoir of water.

For any arbitrary water/rock ratio it is also possible, however, to calculate the isotopic compositions of waters initially entering and exchanging with the ultramafic body, because we know the original $\delta 0^{18}$ values of all these ultramafic rocks. The latter are very uniform at $\delta 0^{18} = +5$ to $+6$. Calculated waters for both 'infinite' and 1:1 water/rock (y/x) ratios are illustrated in figure 13-3 for most of the serpentinites examined in this study. In most cases, it is thought that serpentinization involves water/rock ratios that lie between these two extremes. The following points are to be noted from this figure.

(1) The calculated waters associated with lizardite-chrysotile serpentines from low-grade metamorphic terranes define a triangular area that lies to right of the meteoric water line; these waters very likely

Figure 13-3. δD - δO^{18} diagram showing calculated waters for both $y/x = \infty$ and $y/x = 1$ for many of the serpentines examined in this study. All calculated waters for the lizardite-chrysotile serpentines are designated by the lined patterns. The calculated waters associated with continental antigorites are denoted by the open and dotted patterns, and those associated with oceanic serpentines are indicated by the areas enclosed by short dashes; the symbols ∞ and 1 are for $y/x = \infty$ and $y/x = 1$, respectively. The generalized isotopic variations in both magmatic and metamorphic waters are shown for reference (see figure 5-1). Location symbols: C = Caribbean area, Ca + CA = California and Central America (one low - O^{18} sample excluded), O = Oregon, W = Washington, Y = Yalakom, British Columbia; F = Fort St. James, British Columbia, Cs = Cassiar area, British Columbia, N = Nahlin, British Columbia, USSR = Nizhni Tagil, U.S.S.R., V = Vourinos, Greece.

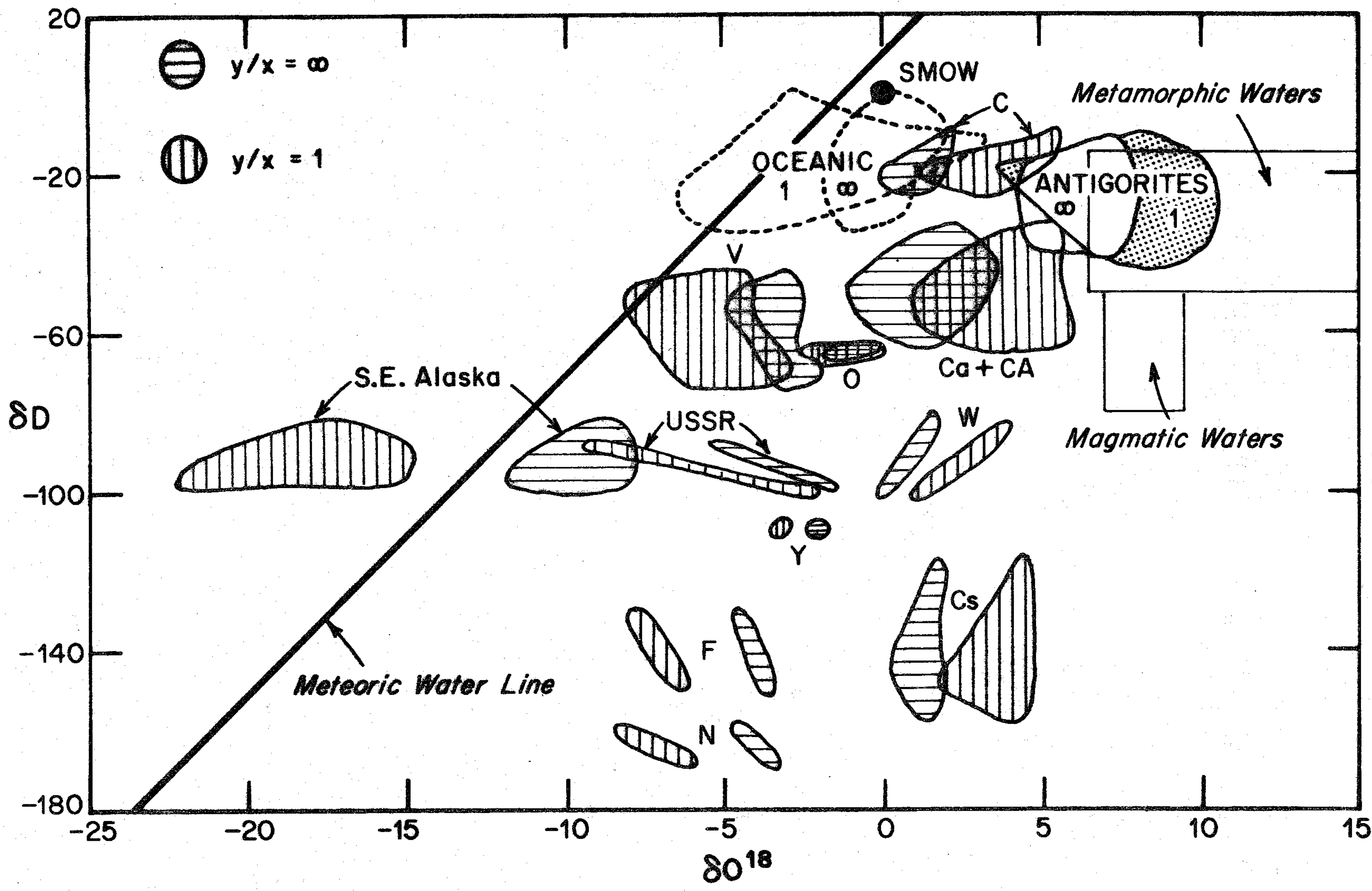
y/x = ∞
y/x = 1
SMOW
C
Metamorphic Waters
OCEANIC
1
∞
ANTIGORITES
∞
1
V
O
Ca + CA
S.E. Alaska
USSR
W
Magmatic Waters
Y
Cs
F
N
Meteoric Water Line
δD
20
-20
-60
-100
-140
-180
-25
-20
-15
-10
-5
0
5
10
15
δO18

Figure 13-3

represent exchanged meteoric waters. Calculated (y/x = 1) waters for serpentines from volcanic- and graywacke-rich terranes (C, Ca-CA, O, Y, F, N in figure 13-3) define a band sub-parallel to the meteoric water line; similarly, calculated (y/x = ∞) waters define another, somewhat steeper band. The calculated waters in Washington (W) and the Cassiar area (Cs) are 0^{18}-enriched, probably due to the presence of 0^{18}-rich country rocks in these localities. Although not indicated on this figure, the calculated waters for both the partially and completely serpentinized samples are similar, suggesting that similar water/rock ratios prevailed in each type of rock during serpentinization.

(2) Most chrysotile samples from high-grade metamorphic terranes also plot within the range of δD and $\delta 0^{18}$ exhibited by the chrysotile-lizardite samples of low-grade regions.

(3) Calculated waters associated with all continental antigorites lie within a narrow zone between $\delta 0^{18} = +4$ to $+10.5$, $\delta D = -12$ to -45. Most of the calculated (y/x = 1) waters lie within the range of normal metamorphic waters, although a few are somewhat 0^{18}-depleted. This suggests that both our temperature estimates and choice of water/rock ratios are probably reasonably accurate for these samples.

(4) Calculated (y/x = ∞) waters for oceanic samples have $\delta 0^{18}$ values that cluster around SMOW (ocean water), although many are depleted in δD. The low δD-values of many of the calculated waters may be partially attributable to ocean water-magmatic water mixing. Many of the calculated (y/x = 1) waters are clearly 0^{18}-depleted relative to ocean water, suggesting that the water/rock ratios for these samples

were very likely higher than 1:1. Water/rock ratios of 2:1 or higher appear to be most likely for oceanic serpentinization.

(5) The calculated (y/x = 1) waters of serpentines from SE Alaska lie to the left of the meteoric water line. For several of the samples, even with water/rock ratios of 3:1 or 4:1, the calculated waters would still lie to the left of the meteoric water line, suggesting that our assumed temperatures (100°C) are probably much too low. Assuming that y/x = 1, several of these samples require serpentinization temperatures of at least 300°C in order to obtain reasonable δO^{18} values for the waters. However, the Ural Mountain serpentines are readily compatible with y/x = 1 and our assumed temperature of 100°C.

(6) The calculated (y/x = 1) waters for the partially serpentinized rocks in the Vourinos Complex (V) are clearly depleted in O^{18} relative to the alpine serpentine band, suggesting that either the meteoric ground waters in this locality underwent very little exchange with the exterior environment, and/or our assumed temperatures (100°C) are too low (probably the latter).

13.4 Oceanic serpentinization

The presence of large amounts of serpentinized ultramafic rocks in oceanic trenches and ridges, together with the geophysical evidence suggesting that the main oceanic crust consists of three different layers, led Hess (1955, 1962, 1964, 1965) to propose an oceanic crustal model consisting of a basal layer (layer 3) composed of serpentinized peridotite, overlain by about 1 km of basalt (layer 2) and a thin layer of sediment (layer 1). In this model, Hess (1965) suggests that the Mohorovicic discontinuity is explicable by the reaction olivine + $H_2O \rightleftarrows$ serpentine. Accordingly, serpentinite is formed by hydration of peridotite above the 500°C isotherm in the crests of the oceanic ridges, and then spreads out laterally away from the ridges due to mantle convection. This model is compatible with the isotopic data in the present work because it is plausible that the serpentinizing fluids in such situations would contain ocean water as the major component.

Other proposals for the layer 3 compositions, however, include basalt or gabbro (Engel, et al., 1965), amphibolite (Cann, 1968; Christensen, 1970), and partially serpentinized plagioclase-chromite peridotite and gabbro (Melson, 1968).

The estimated temperatures of serpentinization of oceanic ultramafic rocks examined in this study are a great deal lower ($< 240^\circ C$) than the maximum temperatures permissible ($\sim 500^\circ C$). There is thus no geothermometric evidence in the present study to suggest that serpentinization occurs at the crust-mantle boundary in the vicinity of oceanic ridges in the manner proposed by Hess. Assuming that serpentinization occurs along the ocean ridges where mantle material may have been brought up from depth by convection, the measured serpentine-magnetite fractionations would suggest that this occurs at depths no greater than about 2 km. Temperatures of about 200°C are probable at this depth underneath oceanic ridges because of the high geothermal gradients known to exist in such areas (see Nicholls, 1965). However, our limited sampling may not be sufficient to provide us with the deeper samples. Also, serpentinization could have occurred in oceanic trenches such as the Puerto Rican trench at the Moho-oceanic crust (layer 3) boundary, because temperatures of about 200°C are reasonable at such depths in these areas (see Nicholls, 1965).

13.5 Conditions of serpentinization in a eugeosynclinal environment

Estimates of the general P-T conditions in which some of the continental serpentines may have formed are given in figure 13-4. In this figure, the general range of temperatures calculated from the serpentine-magnetite fractionations for various alpine serpentinites from both low-grade and high-grade metamorphic areas are shown, along with the appropriate geothermal gradients (Verhoogen, et al., 1970). Only antigorites, with a temperature range of 220° to 460°C, are shown on the Appalachian geothermal gradient, whereas both the lizardite-chrysotile serpentines (85° to 115°C) and a single Franciscan antigorite (225°C) are indicated on the California Coast range geothermal gradient.

Figure 13-4. P - T diagram showing possible conditions of serpentinization of alpine ultramafic rocks in a eugeosynclinal environment based on isotopic temperatures derived in the present study. The geothermal gradients are taken from Verhoogen _et_ _al_., 1970. The dehydration curves for chrysotile + brucite = foresterite + H_2O (Bowen and Tuttle, 1948; King _et_ _al_., 1967) and for chrysotile = forsterite + talc + H_2O (Scarfe and Wyllie, 1967; Pistorius, 1963) represent maximum possible temperatures of stability of these assemblages. The cross-hatch pattern represents uncertainty of pressure due to possible contribution of heat generated during the exothermic serpentinization reactions. Also included are the estimated P - T conditions of formation of Ward Creek type III glaucophane schists (Taylor and Coleman, 1968).

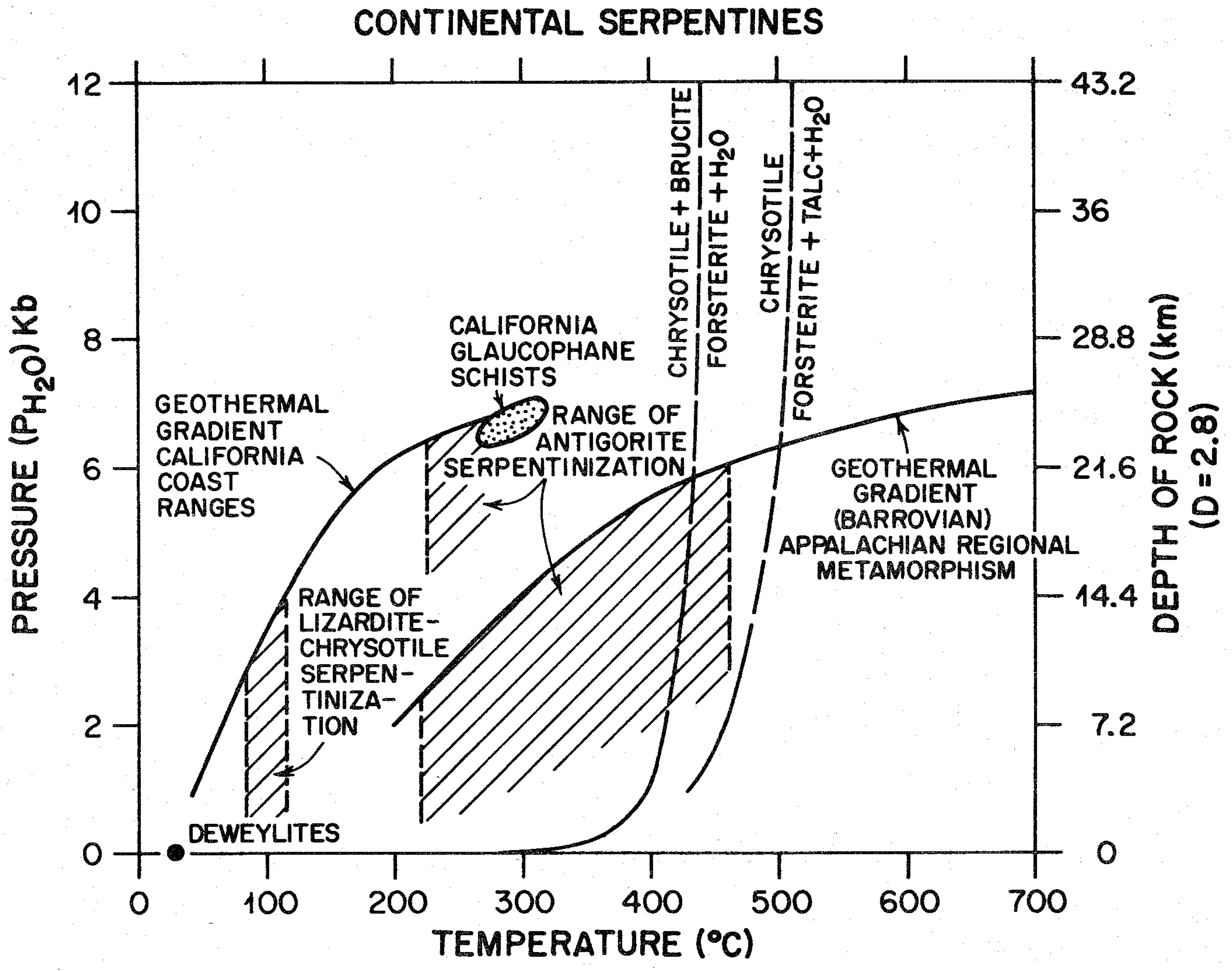
CONTINENTAL SERPENTINES
PRESSURE (P_{H_2O}) Kb
12
10
8
6
4
2
0
DEPTH OF ROCK (km)
(D = 2.8)
43.2
36
28.8
21.6
14.4
7.2
0
TEMPERATURE (°C)
0
100
200
300
400
500
600
700
CHRYSOTILE + BRUCITE
FORSTERITE + H_2O
CHRYSOTILE
FORSTERITE + TALC+H_2O
CALIFORNIA GLAUCOPHANE SCHISTS
GEOTHERMAL GRADIENT CALIFORNIA COAST RANGES
RANGE OF ANTIGORITE SERPENTINIZATION
GEOTHERMAL GRADIENT (BARROVIAN) APPALACHIAN REGIONAL METAMORPHISM
RANGE OF LIZARDITE-CHRYSOTILE SERPENTINIZATION
DEWEYLITES

Figure 13-4

Because serpentinization is an exothermic process (Fyfe, 1967), it might readily take place in shallower environments than might be indicated by the geothermal gradient. The estimated temperatures of serpentinization suggested in the present study could be in part due to this reaction. The general range of pressures shown in figure 13-4 for each of the different serpentine types illustrates the possible consequences of this exothermic reaction, in that the designated geothermal gradient curves would presumably represent the maximum depths at which a given type of serpentinization would occur.

The temperature-rise in an ultramafic body due to such exothermic serpentinization reactions is probably mainly dependent upon the rate of diffusion or flow of water into the body. Martin and Fyfe (1970) suggest that the serpentinization process must be largely diffusion controlled, because the actual reaction rate itself is very rapid. Diffusion rates obviously depend upon many factors such as the degree of fracturing of the ultramafic body, the extent of faulting of the country rock, the availability of a source of water, the size of the body, the amount of water flowing through the body, etc. However, if this diffusion were rapid, one might perhaps expect a sizable heat contribution due to the reaction itself.

Although the above considerations suggest the possibility that lizardite-chrysotile serpentinization could occur at extremely shallow depths (e.g., as proposed by Barnes and O'Neil, 1969), it would appear that most such serpentinization does not occur at the Earth's surface, because the calculated initial waters entering most of the alpine ultramafic bodies in low-temperature terranes apparently are meteoric waters that have to a large extent exchanged with the country rocks. It is noteworthy that the high pH waters that Barnes and O'Neil (1969) suggested were chemically capable of serpentinizing ultramafic rocks at low temperatures are unexchanged meteoric waters nearly identical to local ground waters. They suggest that either small amounts of serpentine is being formed, or that large amounts are formed but at very slow rates. However, the isotopic evidence of this work suggesting that exchanged waters are involved and that serpentinization occurs at about 100°C seems to preclude such high-pH waters having been involved in large amounts of serpentinization. Perhaps these waters are responsible for formation of small amounts of low-temperature deweylite. In any case, the evidence of this work suggests that deweylite is the only type of serpentine that forms in a weathering environment.

Many serpentinites and partially serpentinized alpine ultramafic bodies occur along continental margins in eugeosynclinal environments, and appear to be related to major fault zones. The general tectonic environment and the nature of the primary ultramafic mineral assemblages have led many investigators to suggest that these bodies originally formed in the mantle as peridotite and later were transported up along major fault zones. Such peridotites are envisioned as first invading geosynclinal sediments at considerable depths (10 - 20 km) at low temperatures (300° - 400°), and then being serpentinized during ascent from water derived from the country rocks. Volume expansion during serpentinization is thought to be sufficient to provide a mechanism of upward gravitational transport of the ultramafic rock bodies from great depths to the surface (Coleman, 1967; Hostetler, et al., 1966).

Such concepts of serpentinization of ultramafic rocks have led to various speculations concerning the interactions of oceanic and continental crust that accompany sea floor spreading. For example, the Mesozoic evolution of California can be interpreted by assuming that the oceanic mantle underflowed the continental margin. Accordingly, ocean floor materials, including ultramafic rocks and deep-water sediments (Franciscan Formation), would become juxtaposed next to continental-shelf and continental-slope sediments (Great Valley sequence) separated by a regional thrust fault (fossil Benioff zone?). In this manner, serpentine from the uppermost mantle or lower oceanic crust could have been kneaded tectonically into the Franciscan and injected along the major thrust fault. (Hamilton, 1969, Bailey et al., 1964; Irwin, 1964).

Serpentinites in many localities of the circum-Pacific area are associated with metamorphosed blueschists. Gresens (1969) in fact, attributes much Franciscan blueschist metamorphism to the serpentinization process itself. It is generally thought that such metamorphism occurs at great depths under conditions of abnormally low temperatures (Ernst, et al., 1970; Bailey, et al., 1964). Taylor and Coleman (1968) suggest temperatures of 270° to 315°C at pressures of 6.5 to 7.0 kb (~ 23 to 26 km) for in situ blueschists at Cazadero, California.

Although most of the alpine serpentinite bodies that occur in the low-grade terranes of western North America and the Caribbean area consist of lizardite-chrysotile, minor amounts of antigorite are also present. The results of the present study indicate that the lizardite-chrysotile serpentinization in such terranes must have occurred at relatively shallow levels of the crust. This is suggested by both the low temperatures ($\approx 100^{\circ}C$) and by the dominant role played by meteoric ground waters. There is no evidence that large amounts of serpentine, except perhaps for the much less abundant antigorite, are formed when the ultramafic material first enters the geosynclinal environment at the base of the crust. In fact, these ultramafic bodies may have been transported up to relatively shallow environments in a relatively unserpentinized state.

Massive lizardite-chrysotile serpentinization apparently occurs only after the ultramafic body enters the zone of meteoric ground water penetration. However, this zone probably extends to depths of at least 20,000 feet in a reasonably porous and permeable sandstone-volcanic section. It may even be possible that meteoric ground waters migrate down along the major fault zones that are ubiquitous in such terranes. In any case, it does not seem likely that serpentinization is pervasive enough at great depths to itself provide the mechanism of tectonic transport of the ultramafic rock from the base of the crust up to the surface. However, the present position of most of the serpentinite bodies can readily be ascribed to such a process operating in the upper

5 - 7 km of the crust. Note that many ultramafic bodies must have been serpentinized relatively gradually, since rapid serpentinization in situ is probably not feasible due to the large accompanying volume expansion (Hostetler et al., 1966).

There is no evidence in this study of any relationship between lizardite-chrysotile serpentinization of alpine ultramafic bodies and the formation of blueschists as suggested by Gresens (1969). Blueschist metamorphism probably occurs at much greater depths and at higher temperatures than does most lizardite-chrysotile serpentinization in these terranes. This is suggested in the isotopic evidence that glaucophane schist metamorphism only involves deep-seated metamorphic waters. However, it is conceivable that antigorite formation and blueschist metamorphism may be related.

We must also mention the possibility that antigorite serpentinization may be pervasive at depth, with this serpentine later being almost completely recrystallized to lizardite-chrysotile in the presence of meteoric ground waters at low temperatures. Such a process could explain the isotope data. However, antigorite is very scarce in these low-grade terranes, and there is no geological evidence in support of the large-scale recrystallization that would be required by such a hypothesis.

The general correspondence between present-day meteoric waters and lizardite-chrysotile serpentines also suggests the possibility that much of this serpentinization is entirely unrelated to the Mesozoic orogenies which originally produced these rocks. The isotopic distribution pattern in meteoric waters during the Mesozoic was probably greatly different from the present-day pattern.

The above considerations indicate that much of the alpine serpentinization in low-grade metamorphic terranes may have occurred during the Tertiary or even the Quaternary. The close geologic relationships between serpentinites and low-temperature mercury deposits in California suggest the intriguing possibility that both of these features may be related to the same 'geothermal water systems'. The estimated temperatures of formation of the Hg deposits (around 100°C, White, 1967) are similar to our isotopic estimates of the temperatures of lizardite-chrysotile serpentinization.

Mercury ore commonly occurs with silica-carbonate rock (SiO_2 and Fe-magnesite) as a hydrothermal replacement of highly sheared serpentinite. In the Franciscan formation the silica-carbonate rock is thought to be of late Miocene or younger age (Bailey et al., 1964), although the mercury deposits may even be forming from CO_2-, B-, and NH_4-rich geothermal waters at the present time (White, 1967). These types of waters seem to have a widespread occurrence along the Pacific coast of the United States, and are believed to be products of low-grade metamorphism of marine sediments (Barnes, 1970). Isotopic analyses of these waters from the Sulfer Bank mercury deposit indicate the possibility that exchanged meteoric waters may also be a major component of these waters (see figure 5-1), although it should be pointed out this is in disagreement with the interpretations of White and Roberson (1962).

BIBLIOGRAPHY

Aitken, J. D., Atlin Map-area. British Columbia: Geol. Surv. Can. Mem. 307, 1959.

Albee, A. L., Metamorphic Zones in northern Vermont: in Studies of Appalachian Geology, E-An Zen et al. (ed), Interscience publishers, New York, p. 329-341, 1968.

Armstrong, J. E., Fort St. James Map-Area, Cassiar and Coast Districts, British Columbia: Geol. Surv. Can. Mem. 252, 1949.

Aubouin, J., Geosynclines: Developments in geotectonics I: New York, Elsevier, 335p., 1965.

Aumento, F., Serpentine mineralogy of ultrabasic intrusions in Canada and on the Mid-Atlantic Ridge: Geol. Survey of Canada Paper 69-53, 51p., 1970.

Bailey, E. H., W. P. Irwin, and D. L. Jones, Franciscan and related rocks, and their significance in the geology of western California: Calif. Div. Mines and Geology Bull., 183, 177p., 1964.

Barnes, I., V. C. La Marche, Jr., and G. Himmelberg, Geochemical evidence of present day serpentinization: Science, 156, p. 830-832, 1967.

Barnes, I., and J. R. O'Neil, The relationship between fluids in some fresh alpine-type ultramafics and possible modern serpentinization, western United States: Geol. Soc. Amer. Bull., 80, p. 1947-1960, 1969.

Bates, T. F. and L. B. Sand, J. F. Mink, Tubular crystals of chrysotile asbestos: Science, 111, p. 512-513, 1950.

Bence, A. E. and A. L. Albee, Empirical correction factors for the electron microanalysis of silicates and oxides: Jour. of Geology, 76, p. 382-403, 1968.

Bergeron, R., Preliminary report on Povungnituk Range area, New Quebec: Quebec Dept. of Mines P. R. No. 392, 1959.

Bigeleisen, J. and M. G. Mayer, Calculation of equilibrium constants for isotopic exchange reactions: Jour. Chem. Phys., 15, p. 261, 1947.

Bowen, N. L. and O. F. Tuttle, The system $MgO-SiO_2-H_2O$: Geol. Soc. Amer. Bull., 60, p. 439-460, 1949.

Bowin, C. O., Geology of Central Dominican Republic: in Geol. Soc. Amer. Memoir 98, p. 11-84, 1966.

Bowin, C. O., A. J. Nalwalk, and J. B. Hersey, Serpentinized peridotite from the north wall of the Puerto Rico Trench: Geol. Soc. Amer. Bull., 77, p. 257-270, 1966.

Bragg, L. and Claringbull, G. F., Crystal structures of minerals: in The Crystalline State - Vol. IV, L. Bragg (ed.), Ithica N.Y., Cornell University Press, p. 282-288, 1965.

Cady, W. M., A. L. Albee, and A. H. Chidester, Bedrock geology and asbestos deposits of the upper Missisquoi Valley and vicinity, Vermont: U. S. Geol. Survey Bull., 1122-B, B1-B78, 1963.

Cann, J. R., Geological processes at mid-ocean ridge crests: Jour. Geophys., 15, p. 331-341, 1968.

Chamberlain, J. A., C. R. McLeod, R. J. Traill and G. R. Lachance, Native metals in the Muskox intrusion: Can. Jour. Earth Sciences, 2, p. 188-215, 1965.

Chidester, A. H., Petrology and geochemistry of selected talc-bearing ultramafic rocks and adjacent country rocks in north-central Vermont: U. S. Geol. Survey Prof. Paper 345, 207p., 1962.

Chidester, A. H., M. P. Billings, and W. M. Cady, Talc investigations in Vermont - preliminary report: U. S. Geological Survey Circular 95, 1951.

Christensen, N. I., Composition and evolution of the oceanic crust: Marine Geology, 8, p. 139-154, 1970.

Clayton, R. N., Oxygen isotope fractionation between calcium carbonate and water: Jour. Chem. Phys., 34, p. 724-726, 1961.

Clayton, R. N., and S. Epstein, The use of oxygen isotopes in high-temperature geological thermometry: Jour. Geol., 69, p. 447-452, 1961.

Clayton, R. N., I. Friedman, D. L. Graf, T. K. Mayeda, W. F. Meents and N. F. Shimp, The origin of saline formation waters, 1, isotopic composition: Jour. Geophys. Res., 71, p. 3869-3882, 1966.

Clayton, R. N., L. J. P. Muffler, and D. E. White, Oxygen isotope study of calcite and silicates of the River Ranch No. 1 Well, Salton Sea geothermal field, California: Amer. Jour. Science, 266, p. 968-979, 1968.

Coleman, R. G., Low-temperature reaction zones and alpine ultramafic rocks of California, Oregon and Washington: Geol. Survey Bull. 1247, 49p., 1967.

Craig, H., Isotopic standards for carbon and oxygen and correction factors for mass spectrometric analysis of carbon dioxide: Geochim et Cosmochim Acta, 12, p. 133, 1957.

Craig, H., Isotopic variations in meteoric waters: Science, 133, p. 1702-1703, 1961a.

Craig, H., Standard for reporting concentrations of deuterium and oxygen-18 in natural waters: Science, 133, p. 1833-1844, 1961b.

Craig, H., The isotopic geochemistry of water and carbon in geothermal areas: Conf. on Nuclear Geology in Geothermal Areas, Spoleto, Italy, p. 17-53, 1963.

Craig, H., Isotopic composition and origin of the Red Sea and Salton Sea geothermal brines: Science, 154, p. 1544-1548, 1966.

Craig, H., Geochemistry and origin of the Red Sea brines: in Hot Brines and Recent Heavy Metal Deposits in the Red Sea, Degens (ed.), Springer-Verlag New York Inc., p. 208-242, 1969.

Craig, H., and L. I. Gordon, Deuterium and oxygen-18 variations in the ocean and the marine atmosphere: in Stable isotopes in oceanographic studies and paleotemperatures, Spoleto, Consiglio Nacionale delle Ricerche, Pisa, p. 9-130, 1965.

Dansgaard, W., Stable isotopes in precipitation: Tellus, 16, p. 436-468, 1964.

Deer, W. A., R. A. Howie, and J. Zussman, Serpentines: in Rock-forming minerals, Vol. 3, Sheet Silicates, p. 170-190, 1962.

Dengo, G., Tectonic-igneous sequence in Costa Rica: in Petrologic studies-Buddington Vol., Geol. Soc. Amer., A. E. J. Engel, H. L. James and R. F. Leonard (ed.) p. 133-161, 1962.

Duffel, S. and K. C. McTaggart, Ashcroft Map-area, British Columbia: Geol. Surv. Can. Mem. 262, 1951.

Duparc, L., and M. Tikonovich, Le Platine et les Gites Platiniferes de l'oural et du monde: Geneve, 542p., 1920.

Engel, A. E. J., C. G. Engel, and R. G. Haven, Chemical characteristics of oceanic basalts and the upper mentle: Bull. Geol. Soc. Amer., 76, p. 719, 1965.

Epstein, S., Oxygen and hydrogen isotope studies of serpentine: in preparation, 1966 - reported by Taylor (1967b).

Epstein, S. and T. Mayeda, Variation of 0^{18} content of waters from natural sources: Geochim et Cosmochim, Acta, 4, p. 213-224, 1953.

Epstein, S. and H. P. Taylor, Jr., Variations of $0^{18}/0^{16}$ in minerals and rocks: Researches in Geochemistry, Vol. II, Abelsen (ed.), John Wiley and Sons, New York, p. 29-62, 1967.

Ernst, W. G., Mineral paragenesis in Franciscan metamorphic rocks, Panoche Pass, California: Bull. Geol. Soc. Amer., 76, p. 879-914, 1965.

Ernst, W. G., Y. Seki, H. Onuki, M. C. Gilbert, Comparative study of low-grade metamorphism in the California Coast Ranges and the outer metamorphic belt of Japan, Geological Society of America Memoir 124, 276 p., 1970.

Faust, G. T. and J. J. Fahey, The serpentine-group minerals: U. S. Geol. Survey Prof. Paper 384-A, 92p., 1962.

Faust, George T., J. C. Hathaway, and Georges Millot, A restudy of stevensite and allied minerals: Am. Min., 44, p. 342-370, 1959.

Findlay, D. C., and C. H. Smith, The Muskox drilling project: Geol. Surv. Can., Paper 64-44, p. 1-170, 1965.

Frarey, M. J. Preliminary map Willbob Lake, Quebec and Newfoundland: Geol. Survey Can. Paper 52-16, 1952.

Friedman, I., Deuterium content of natural waters and other substances: Geochim. et Cosmochim. Acta, 4, p. 89-103, 1953.

Friedman, I., A. C. Redfield, B. Schoen, and J. Harris, The variation of the deuterium content of natural waters in the hydrologic cycle: Rev. Geophys., 2, p. 177-224, 1964.

Fyfe, W. S. Metamorphism in mobile belts- the glaucophane schist problem: Trans. Leicester Lit. and Phil. Soc., 61, p. 36-54, 1967.

Gabrielse, H., McDame map-area, Cassiar District, British Columbia: Geol. Survey Can. Mem. 319, 138p., 1963.

Garlick, G. D., Oxygen isotope ratios in coexisting minerals of regionally metamorphosed rocks: Ph.D. Thesis, California Institute of Technology, 1965.

Garlick, D., The stable isotopes of oxygen: in Handbook of Geochemistry, Wedepohl (ed.), Springer-Verlag, New York, p. 1-27, 1969.

Garlick, G. D., and S. Epstein, Oxygen isotope ratios in coexisting minerals of regionally metamorphosed rocks: Geochim. et Cosmochim. Acta, 31, p. 181-214, 1967.

Godfrey, J. D., The deuterium content of hydrous minerals from the east-central Sierra Nevada and Yosemite National Park: Geochim. et Cosmochim. Acta, 26, p. 1215-1245, 1962.

Gold, David P., Local deformation structures in a serpentinite: in Ultramafic and related rocks, P. J. Wyllie (ed.), New York, John Wiley and Sons, Inc., p. 200-202, 1967.

Green, D. H., High temperature peridotite intrusions: in Ultramafic and related rocks, P. J. Wyllie (ed.), New York, John Wiley and Sons, Inc., p. 312-222, 1967.

Greenwood, H. J., Mineral equilibria in the system $MgO-SiO_2-H_2O-CO_2$: in Researches in geochemistry, Vol. II, Abelsen (ed.), John Wiley and Sons, New York, p. 542-567, 1967.

Gresens, R. L., Blueschist alteration during serpentinization: Contr. Mineral. and Petrol., 24, p. 93-113, 1969.

Hamilton, Warren, Mesozoic California and the underflow of Pacific mantle: Bull. Geol. Soc. Amer., 80, p. 2409-2430, 1969.

Harrison, J. V., The geology of the Santa Elena Peninsula in Costa Rica, C. A., 7th Pacific Sci. Cong. Proc., 2 , p. 102-114, 1949.

Hess, H. H., Serpentines, orogeny, and epeirogeny: in Crust of the earth- a symposium, A. Paldervoart (ed.), Geol. Soc. Amer. Spec. Paper 62, p. 391-407, 1955.

Hess, H. H., History of the ocean basins: in Petrologic Studies - Buddington Vol., Geol. Soc. Amer., A. E. J. Engel, H. L. James, and R. F. Leonard (ed.) p. 599-620, 1962.

Hess, H. H., The oceanic crust, the upper mentle and the Mayaguez serpentinized peridotite: in A study of serpentinite, C. A. Burk (ed.), Natl. Res. Council Publ. 1188, p. 169-175, 1964.

Hess, H. H., Mid-ocean ridges and tectonics of the sea-floor: in Submarine geology and geophysics - Proc. 17th Symp. Colston Res. Soc., Butterworths, London, p. 317-332, 1965.

Hess, H. H., and G. Otalora, Mineralogical and chemical composition of the Mayaguez serpentinite cores: in A study of serpentinite, C. A. Burk (ed.), Natl. Acad. Sci.- Natl. Res. Council Publ. 1188, p. 152-168, 1964.

Hitchon, Brian and I. Friedman, Geochemistry and origin of formation waters in the western Canada sedimentary basin - I. Stable isotopes of hydrogen and oxygen: Geochim. et Cosmochim. Acta, 33, p. 1321-1349, 1969.

Hollister, L. S., Contact metamorphism in the Kwoiek Area of British Columbia- an end member of the metamorphic process: Geol. Soc. Amer. Bull. 80, p. 2465-2494, 1969.

Hostetler, P. B., R. G. Coleman, F. A. Mumpton, and B. W. Evans: Brucite in alpine serpentinites: Amer. Min., 51, p. 75-98, 1966.

Irvine, T. N., and C. H. Smith, The ultramafic rocks of the Muskox intrusion, Northwest Territories, Canada: in Ultramafic and Related Rocks, P. J. Wyllie (ed.), New York, John Wiley and Sons, Inc., p. 38-49, 1967.

Irwin, W. P., Late Mesozoic orogenies in the ultramafic belts of northwestern California and southwestern Oregon: in Geological Survey research 1964, U. S. Geol. Survey Prof. Paper 501-C, p. C1-C9, 1964.

Jackson, E. D., Ultramafic cumulates in the Stillwater, Great Dyke, and Bushveld intrusions: in Ultramafic and Related Rocks, P. J. Wyllie (ed.), New York, John Wiley and Sons, Inc., p. 20-38, 1967.

Jahns, Richard H., Serpentinites of the Roxbury district, Vermont: in Ultramafic and Related Rocks, P. J. Wyllie (ed.) New York, John Wiley and Sons, Inc., p. 137-160, 1967.

Javoy, M., Utilisation des isotopes de l'oxygene en magmatologie: Ph.D. thesis. A la Faculte des Sciences de Paris, 1970.

King, E. G., Barany, R., Weller, W. W., and Pankratz, L. B., Thermodynamic properties of forsterite and serpentine: U. S. Bureau of Mines, Rept. Inv. 6962, 1967.

King, P. B., Tectonic map of North America: U. S. Geol. Survey map, 1969.

Lapham, D. M., New data on deweylite: Amer. Min., 46, p. 168-188, 1961.

Lapham, D. M., Spinel-orthopyroxene compositions and their bearing on the origin of the serpentinite near Mayaguez, Puerto Rico: in A study of serpentinite, C. A. Burk (ed.), Natl. Res. Council Publ. 1188, p. 134-144, 1964.

Lapham, D. M., The tectonic history of multiply deformed serpentinite in the piedmont of Pennsylvania: in Ultramafic and related rocks, P. J. Wyllie (ed.), New York, John Wiley and Sons, Inc., p. 174-183, 1967.

Lapham, D. M. and A. R. Geyer, Mineral collecting in Pennsylvania: General Geology Report G33, Pennsylvania Geological Survey, 1965.

Lapham, D. M., and H. L. McKague, Structural patterns associated with the serpentinites of southeastern Pennsylvania: Bull. Geol. Soc. Am., 75, p. 639-660, 1964.

Lawrence, J. R., O^{18}/O^{16} and D/H ratios of soils, weathering zones, and clay deposits: Ph.D. thesis, California Institute of Technology, 1970.

Lindgren, W., Mineral Deposits, 4th ed., McGraw-Hill Book Co., New York, p. 395, 1933.

Little, H. W., Geological Map of British Columbia: Geol. Surv. of Canada Map 932A, 1962.

McBirney, A. R., Geology of a part of the central Guatemalan Cordillera: Univ. of Calif. Publ. in Geol. Sci., 38, p. 177-242, 1963.

McGetchin, T., The Moses Rock Dike: geology, petrology and mode of emplacement of a kimberlite-bearing breccia dike, San Juan County, Utah: Ph.D. thesis, California Institute of Technology, 1968.

McKinney, C. R., J. M. McCrea, S. Epstein, H. A. Allen and H. C. Urey, Improvements in mass spectrometers for the measurement of small differences in isotopic abundance ratios: Rev. Sci. Instr., 21, p. 724-730, 1950.

Maddock, M. E., Geology of the Mount Boardman Quadrangle, Santa Clara and Stanislaus Counties, California: Calif. Div. Mines Geol. Map Sheet 3, 1964.

Martin, B., and W. S. Fyfe, Some experimental and theoretical observations on the kinetics of hydration reactions with particular reference to serpentinization: Chemical Geology, 6, p. 185-202, 1970.

Mattson, P. H., Geology of the Mayaguez area, Puerto Rico: Geol. Soc. Amer. Bull., 71, p. 319-362, 1960.

Mattson, P. H., Petrography and structure of serpentinite from Mayaguez, Puerto Rico: in A Study of Serpentinite, C. A. Burk (ed.), Nat'l. Res. Council Publ. 1188, p. 7-24, 1964.

Melson, W. G., Petrologic model of the earth's crust across the mid-Atlantic ridge: (abstr.), Trans. Am. Geophys. Union, 49, p. 364, 1968.

Melson, W. G., E. Jarosewich, V. T. Bowen, and G. Thompson, St. Peter and St. Paul Rocks: a high-temperature mantle-derived intrusion: Science, 155, p. 1532-1535, 1967a.

Melson, W. G., E. Jarosewich, R. Cifelli, and G. Thompson, Alkali olivine basalt dredged near St. Paul's Rocks, Mid-Atlantic Ridge: Nature, 215 p. 381-382, 1967b.

Misch, P., Tectonic evolution of the northern Cascades of Washington State: in Tectonic History and Mineral Deposits of the Western Cordillera, Can. Inst. Min. Met. Spec. Vol. 8, p. 101-148, 1966.

Montigny, R., M. Javoy, and C. J. Allegre, Sr^{87}/Sr^{86}, K/Rb, and O^{18}/O^{16} ratios in the Pinde Ophiolite Complex: (Abstr.) Geol. Soc. Amer., Milwaukee, p. 627-628, 1970.

Moores, E. M., Petrology and structure of the Vourinos Ophiolite Complex of northern Greece: Geol. Soc. Amer. Special Paper 118, 74p., 1969.

Nicholls, G. D., Petrological and geochemical evidence for convection in the Earth's mantle: in A Symposium on Continental Drift, The Royal Society, London, p. 168-179, 1965.

Nier, A. O., A mass spectrometer for isotope and gas analysis: Rev. Sci. Instr., 18, p. 398-411, 1947.

Ohmoto, H., and R. O. Rye, The Bluebell Mine, British Columbia-I., mineralogy, paragenesis, fluid inclusions and the isotopes of hydrogen, oxygen, and carbon: *Econ. Geol*. *64*, p. 417-437, 1970.

O'Neil, J. R., and R. N. Clayton, Oxygen isotope geothermometry: in *Isotopic and Cosmic Chemistry*, North-Holland Publishing Co., Amsterdam, p. 157, 1964.

O'Neil, J. R. and H. P. Taylor, Jr., The oxygen isotope and cation exchange chemistry of feldspars: *Amer. Mineralogist*, *52*, p. 1414-1437, 1967.

O'Neil, J. R. and H. P. Taylor, Jr., Oxygen isotope fractionation between muscovite and water: *Jour. Geophys. Res*., *74*, p. 6012-6022, 1969.

Page, N. J., Serpentinization at Burro Mountain, California: *Contr. Mineral. and Petrol*., *14*, p. 321-342, 1967.

Page, N. J., Serpentinization in a sheared serpentinite lens, Tiburon Peninsula, California: in *Geological Survey Research 1968*, *U. S. Geol. Survey Prof. Paper 600-B*, p. B21-B28, 1968.

Page, N. J. and R. G. Coleman, Serpentine-mineral analyses and physical properties: in *Geological Survey Research 1967*, *U. S. Geol. Survey Prof. Paper 575-B*, p. B103-107, 1967.

Phillips, A. H., and H. H. Hess, Metamorphic differentiation at contacts between serpentine and siliceous country rocks: *Am. Min*., *21*. p. 333-362, 1936.

Phillips, J. D., G. Thompson, R. P. Von Herzen, and V. T. Bowen, Mid-Atlantic Ridge near 43°N latitude: *Jour. Geophys. Res*., *74*, p. 3069-3081, 1969.

Pistorius, C. W. F. T., Some phase relations in the system $MgO-SiO_2-H_2O$ at high pressures and temperatures: *Neves Jahrb. Mineral. Monats*., *11*, p. 283-293, 1963.

Pundsack, F. L., The properties of asbestos, II. The density and structure of chrysotile: *Jour. of Physical Chem*., *60*, p. 361-364, 1956.

Reuter, J. H., S. Epstein and H. P. Taylor, Jr., O^{18}/O^{16} ratios of some chondritic meteorites and terrestrial ultramafic rocks: *Geochim. et Cosmochim. Acta*, *29*, p. 481-488, 1965.

Riordon, P. H., Geology of the asbestos belt in southeastern Quebec: Bull. Can. Inst. Mining Met., 55, no. 601, p. 311-313, 1962.

Roy, D. M. and R. Roy, Hydrogen-deuterium exchange in clays and problems in the assignment of infrared frequencies in the hydroxyl region: Geochem. et Cosmochim. Acta, 11, p. 72-85, 1957.

Rucklidge, J. C., and J. Zussman, The crystal structure of the serpentine mineral, lizardite. $Mg_3Si_2O_5(OH)_4$: Acta Cryst., 19, p. 381-389, 1965.

Rye, R. O., and J. R. O'Neil, The O^{18} content of water in primary fluid inclusions from Providencia, North-Central Mexico: Econ. Geol., 63, p. 232-238, 1968.

Saad, Afif Hani, Paleomagnetism of Franciscan ultramafic rocks from Red Mountain, California: Jour. of Geophys. Res., 74, p. 6567-6578, 1969.

Savin, S. M. and S. Epstein, The oxygen and hydrogen isotope geochemistry of clay minerals: Geochim. et Cosmochim. Acta, 34, p. 25-42, 1970.

Scarfe, C. M., and P. J. Wyllie, Experimental redetermination of the upper stability limit of serpentine up to 3kbar pressure: Trans. Am. Geophys. Union, 48, p. 225, 1967.

Shagam, R., Geology of Central Aragua, Venezuela: Bull. Geol. Soc. Amer., 71, p. 249-302, 1960.

Sheppard, S. M. F. and S. Epstein, D/H and O^{18}/O^{16} ratios of minerals of possible mantle or lower crustal origin: Earth Planet. Sci. Let. (in press), 1970.

Sheppard, S. M. F., R. L. Nielsen, H. P. Taylor, Jr., Oxygen and hydrogen isotope ratios of clay minerals from porphyry copper deposits: Econ. Geol., 64, p. 755-777, 1969.

Sheppard, S. M. F., R. L. Nielsen, and H. P. Taylor, Jr., Hydrogen and oxygen isotope ratios in minerals from porphyry copper deposits: Econ. Geol. (in press), 1970.

Sheppard, S. M. F. and H. P. Taylor, Jr., Hydrogen and oxygen isotope evidence for the origin of water in the Butte ore deposits and the Boulder batholith, Montana: manuscript in preparation, 1970.

Shieh, Y. N. and H. P. Taylor, Jr., Oxygen and carbon isotope studies of contact metamorphism of carbonate rocks: Jour. Petrology, 10, p. 307-331, 1969a.

Shieh, Y. N. and H. P. Taylor, Jr., Oxygen and hydrogen isotope studies on contact metamorphism in the Santa Rose Range, Nevada and other areas: Contr. Mineral. Petr., 20, p. 306-356, 1969b.

Simons, J. H., Hydrogen fluoride: in Fluorine Chemistry, Vol. 1, J. H. Simons (ed.), Academic Press, Inc., New York, p. 229, 1950.

Simpson, P. R. and J. A. Chamberlain, Nickel distribution in serpentinites from Puddy Lake, Ontario: Proc. Geol. Assoc. Canada, 18, p. 67-91, 1967.

Smith, C. H., and I. D. MacGregor, Ultrabasic intrusive conditions illustrated by the Mount Albert ultrabasic pluton, Gaspe, Quebec: Bull. Geol. Soc. Am., 71, p. 1978 (abstr.), 1960.

Smith, G. O., Description of the Mount Stewart quadrangle (Washington): U. S. Geol. Survey Geol. Atlas, Folio 106, 10p., 1904.

Stockwell, C. H. (ed.), in Geology and Economic Minerals of Canada, Dept. of Mines and Tech. Surveys, Geol. Survey of Canada Econ. Geology series no. 1, 1963.

Suzuoki, T. and S. Epstein, (manuscript in preparation) 1970.

Taylor, H. P., Jr., O^{18}/O^{16} ratios in coexisting minerals of igneous and metamorphic rocks: Ph.D. thesis, California Institute of Technology, 1959.

Taylor, H. P., Jr., Oxygen isotope studies of hydrothermal mineral deposits: in Geochemistry of Hydrothermal Ore Deposits, H. L. Barnes (ed.), New York, Holt, Rinehart and Winston, p. 109-142, 1967a.

Taylor, H. P., Jr., Stable isotope studies of ultramafic rocks and meteorites: in Ultramafic and Related Rocks, P. J. Wyllie (ed.), New York, John Wiley and Sons, Inc., p. 362-372, 1967b.

Taylor, H. P., Jr., The zoned ultramafic complexes of southeastern Alasks: in Ultramafic and Related Rocks, P. J. Wyllie (ed.), New York, John Wiley and Sons, Inc., p. 97-121, 1967c.

Taylor, H. P. Jr., The oxygen isotope geochemistry of igneous rocks: Contrib. Mineral and Petrol., 19, p. 1-71, 1968.

Taylor, H. P., Jr., Oxygen isotope evidence for large-scale interaction between meteoric ground waters and Tertiary diorite intrusions, Western Cascade Range, Oregon: Trans. Am. Geophys. Union, 51, p. 453, 1970.

Taylor, H. P., Jr., A. L. Albee, and S. Epstein, $0^{18}/0^{16}$ ratios of coexisting minerals in three assemblages of kyanite-zone pelitic schist: Jour. Geology, 71, p. 513-522, 1963.

Taylor, H. P., Jr., and R. G. Coleman, $0^{18}/0^{16}$ ratios of coexisting minerals in glaucophane-bearing metamorphic rocks: Geol. Soc. Am. Bull., 79, p. 1727-1756, 1968.

Taylor, H. P., Jr. and S. Epstein, Relationship between $0^{18}/0^{16}$ ratios in coexisting minerals of igneous and metamorphic rocks, Part I, Principles and experimental results: Bull. Geol. Soc. Amer., 73, p. 461-480, 1962a.

Taylor, H. P., Jr. and S. Epstein, Relationship between $0^{18}/0^{16}$ ratios in coexisting minerals of igneous and metamorphic rocks, Part II, Application to petrological problems: Bull. Geol. Soc. Amer., 73, p. 675-693, 1962b.

Taylor, H. P., Jr., and S. Epstein, Deuterium-hydrogen ratios in coexisting minerals of metamorphic and igneous rocks (abstract): Trans. Am. Geophys. Union, 47, p. 213, 1966.

Taylor, H. P., Jr. and S. Epstein, $0^{18}/0^{16}$ ratios of Apollo 11 lunar rocks and minerals: in Proc. of the Apollo 11 Lunar Science Conf., Vol. 2, p. 1613-1626, 1970.

Taylor, H. P., Jr., and J. A. Noble, Origin of magnetite in the zoned ultramafic complexes of southeastern Alaska: Econ. Geology, p. 209-230, 1969.

Thayer, T. P., Mineralogy and geology of chromium: in Chromium, Vol. 1, Chemistry of Chromium and its Compounds, M. J. Udy (ed.), Reinhold Publ. Corp., New York, p. 14-52, 1956.

Thayer, T. P., Serpentinization considered as a constant volume metasomatic process: a reply: Amer. Mineral., 52, p. 549-552, 1967a.

Thayer, T. P., Chemical and structural relations of ultramafic and feldspathic rocks in alpine intrusive complexes: in Ultramafic and Related Rocks, P. J. Wyllie (ed.), New York, John Wiley and Sons, Inc., p. 222-239, 1967b.

Thompson, G. and Wm. G. Melson, Boron contents of serpentinites and metabasalts in the oceanic crust: implications for the boron cycle in the oceans: Earth Planet. Sci. Letters, 8, p. 61-65, 1970.

Thompson, J. B., The thermodynamic basis for the mineral facies concept: Am. Jour. Science, 253, p. 65-103, 1955.

Turner, F. and J. Verhoogen, Igneous and Metamorphic Petrology, 2nd ed. McGraw-Hill Book Co., New York, 1960.

Urey, H. C., The thermodynamic properties of isotopic substances: Jour. Chem. Soc., p. 562-581, 1947.

Vdovykin, G. P. and L. V. Dmitriyev, Organic matter in ultramafic rocks of the mid-Indian ridge: Geochem. Internat. 5, p. 828-831, 1968.

Verhoogen, J., F. J. Turner, L. E. Weiss, C. Wahrhaftig, and W. S. Fyfe, The Earth; an Introduction to Physical Geology, Holt, Rinehart and Winston, Inc., p. 592, 1970.

Visser, D. J. L., The geology of the Barberton area: Geol. Survey So. Africa, Spec. Publ. No. 15, 1956.

White, D. E., Environments of generation of some base-metal ore deposits: Econ. Geology, 63, p. 301-335, 1968.

White, D. E. and C. E. Roberson, Sulfur Bank, California, a major hot spring quicksilver deposit: in Petrologic Studies, Buddington Volume, Geol. Soc. Amer. Publ., p. 397-428, 1962.

White, W. H., Summary of tectonic history: in Tectonic History and Mineral Deposits of the Western Cordillera, Can. Inst. Min. Met. Spec. Vol. 8, p. 185-189, 1966.

Whittaker, E. J. W., and J. Zussman, The characterization of serpentine minerals by x-ray diffraction: Mineral. Mag., 31, p. 107-126, 1956.

Wolfe, W. J., The Blue River ultramafic intrusion, Cassiar district, British Columbia: Geol. Surv. Can. Paper 64-48, 15p., 1965.

Wyllie, P. J., Petrography and petrology: in Ultramafic and Related Rocks, P. J. Wyllie (ed.), New York, John Wiley and Sons, Inc., p. 1-7, 1967.

APPENDIX I

Oxygen Isotopic Reproducibility of the Rose Quartz Standards

The following raw δO^{18} values of the rose quartz standard (+ 8.43 relative to SMOW) were measured against the mass spectrometer reference gas during the course of the research. The averages of five groups were taken as the raw standard value when converting the raw value of the unknown sample to SMOW.

GROUPS

I	II	III	IV	V
1/23/68-3/27/68	4/9/68 4/29/68	5/13/68-10/15/68	11/9/68-6/9/69	7/16/69 5/1/70
-15.69	-15.70	-15.58	-15.72	-15.99
-15.70	-15.87	-15.42	-15.82	-15.98
-15.49	-15.86	-15.42	-15.67	-15.88
-15.50		-15.45	-15.72	-15.93
-15.57		-15.67	-15.77	-16.07
-15.76		-15.49	-15.60	-16.21
-15.44		-15.69	-15.77	-15.80
-15.75			-15.59	-16.05
-15.59			-15.77	-16.21
-15.59			-15.83	-16.06
-15.54			-15.86	-16.00
			-15.82	-15.89
				-15.79
				-15.74
				-16.08
		Average		
-15.60	-15.81	-15.53	-15.74	-16.00
± 0.09	± 0.08	± 0.10	± 0.08	± 0.11

APPENDIX II

Sample locations descriptions, and isotope data

Abbreviations to Appendix II

Sample Collectors	
Au	author
MB	M. Bass
CB	C. Bowin
C	Cal Tech collection
RC	R. Coleman
JD	J. Duncan
GF	G. Faust
RF	R. Forester
HH	H. Hess
LH	L. Hollister
TI	T. N. Irvine
DL	D. Lapham
TM	T. McGetchin
LM	L. McKague
EM	E. Moores
IP	I. Paterson
LR	L. Rogers
RS	R. Shagam
JS	J. Souther
HT	H. Taylor
USNM	U. S. National Museum
WW	W. Wolfe
JR	J. Ruckmick
GT	G. Thompson

Mineral + Textural Terms	
A	antigorite
b	bastite
carb	carbonate
Ch	chlorite
cp	clinopyroxene
cr	chromite
fg	fine-grained
fp	felted pattern
gi	galvanized iron texture (see plate 3-5)
m	mesh texture
Ol	olivine
op	orthopyroxene
opq	opaque
repl.	replace
S	serpentine
T	talc
Tr	tremolite
tr.	trace
xf	cross fibre
C	chrysotile

± indicates average deviation (for two separate analyses if no number in parentheses)

no ± indicates one analysis (number in parentheses indicates number of analyses)

Sample	Collector & Collector's Sample No.	Location	Petrographic Description	δD_s	δO^{18}_s
Venezuela					
1	RS, 756	E of Villa de Cura at fault contact	sheared and brecciated m, b > fg, S	-79	
2	RS, 676	"	m > isotropic S	-78	
Costa Rica					
1	MB	see figure 7-2	m > 01, op > cr	-	6.7±0.1(3)
19b	"	"	fg m?	-93	3.3±0.1
19e	"	"	fg m?	-	3.7±0.1
36J	"	"	fg m, 01, op > cr	-91	6.3±0.2
36R	"	"	fg m > op > cr	-94	5.8±0.2
Guatemala					
1	Au	1 km N of rd. junction Puerto Barrios Hwy. - Cobán Rd.	m, b > late-stage veins	-88± 1	8.3±0.0
2	Au	2 km S of Morazan on Cobán Rd.	fg m? > late-stage veins > cr	-97± 1	6.0±0.1
4	Au	3 km N of Morazan on Cobán Rd.	fg fp replaces breccia	-55± 0	7.4±0.1
5	Au	S side of Puerto Barrios Hwy. at first crossing of Rio Motagua W of Cobán Rd.	fg T, tr. S	-58	

Sample	Collector & Collector's Sample No.	Location	Petrographic Description	δD_s	δO^{18}_s
Guatemala (continued)					
15	RC	see figure 7-2	m > b > op	-92	
21	RC	" "	m > 01 >opq, xf	-78	
Dominican Republic					
1	CB, 47a	8 km SE of Bonao	m(isotropic) > b xf vein	-63 -59	8.4
2	CB, 882	23 km SE of Bonao	sheared m, b > xf	-71±0	7.7±0.5
Puerto Rico					
Mayaguez bore hole					
1	USNM, 110673	10.67 meters	isotropic m >> b	-66±2	7.8
2	"	195.62 meters	m repl. 01 > b partially repl. op > cr	-63±0	7.8
3	"	204.52 meters q	sheared + brecciated m, b > late-stage fg S	-59	8.7±0.1
4	"	303.58 meters	m almost completely repl. 01 > sheared isotropic b?, xf xf	-64 -60±3	8.4

Sample	Collector & Collector's Sample No.	Location	Petrographic Description	δD_s	$\delta^{18}O_s$
Puerto Rico (cont'd)					
5	USNM, 110673	304.7 meters	m repl. 01 > b partially repl. op, tr. cr	$-67\pm1(6)$	$7.2\pm0.0(3)$
California					
San Luis Obispo					
3	Au	see figure 7-4	highly sheared	-82	8.7 ± 0.1
4	"	"	sheared and deformed b > sheared m > late-stage fg S	b -85 m -85 (total) -85	7.9 ± 0.1 7.4 7.5
6a	"	"	brecciated m > b > xf, tr. cr	-85 ± 2	7.4
6b	"	"	brecciated m > b > many generations xf	$-85\pm3(3)$	7.8 ± 0.1
6c	"	"	highly sheared	-91 ± 1	7.5 ± 0.1
6d	"	"	highly sheared, white colored	-85	8.3
Del Puerto					
2	Au	see figure 7-5	-	-62	8.8 ± 0.2
2a	"	"	coarse fp, highly altered b? minor carb, opq		$8.7\pm0.1(3)$

Sample	Collector & Collector's Sample No.	Location	Petrographic Description	δD_s	δO^{18}_s
Del Puerto (cont'd)					
5	Au	see figure 7-5	-	-105	8.9±0.3
6	"	"	m > 01	- 93	-
8	"	breccia in dolomite matrix at spring site	near isotropic fg m? > small fg S blades	- 74	6.8±0.2
8a	"	taken 50' from 8	m > 01 > cr	-100	6.6±0.3
9	"		m repl. 01, little repl. op, several generations xf	-108	7.8±0.2
Tiburon					
1	Au	see figure 7-6	highly sheared	- 90	8.0
2	"	"	m > platey lizardite? > xf	- 89	8.1±0.1
3	"	"	fg m > fg xf	- 90	7.6
Napa County	Au	S side of Knoxville Rd. 0.1 mi. from Cal. Rt. # 128 intersection	fg m > b > xf	- 93	7.3±0.1
Oregon					
Myrtle Creek					
1	Au	see figure 7-7, roadcut along U.S. hwy. 101, 1 mi. N of Myrtle Creek, on S bank of Umpagua River	rodingite, porphyritic	-127	12.1
2	"	"	b both coarse (< 2 mm) and fg > m, carb > cp	-108	7.5

Sample	Collector & Collector's Sample No.	Location	Petrographic Description	δD_s	δO^{18}_s
Myrtle Creek (cont'd)					
3	Au	see location, previous page	-	-109	7.1±0.1
4	"	"	fg m? > sheared b	-107	6.2
Josephine County					
1	Au	see figure 7-8, roadcut exposure 50 ft. from guard station along N side of Illinois River, 12 m W of U.S. hwy. 199 at Selma, Ore.	m > b (≤ 2 mm)	-109±2	4.9±0.3
2	"	"	m > b > xf	-	4.9±0.2
3	"	"	m > deformed b > platy lizardite, Ch at S - rodingite contact	-	4.6
4	"	"	rodingite, porphyritic	- 50	4.1±0.1
<u>Washington</u>					
Mt. Stewart					
1	Au	see figure 7-9	m, b, tr. xf	-142	6.6±0.0
2	"	"	brecciated b > m > carb	-127	8.0±0.1

Sample	Collector & Collector's Sample No.	Location	Petrographic Description	δD_s	δO^{18}_s
Skagit					
1	Au	lens in schist, Cascade River hwy. 8 mi. E of Marblemont, Wash.	fg T	- 68	-
9	"	float at base of Jordan perid. body, 4 mi. SE Marblemont	fp > carb	-58 ± 3	8.7 ± 0.2
10	"		see plate 5-5	- 85	8.7 ± 0.1
British Columbia					
Grand Forks					
1	IP, Ar121	see section 7.5	m > b >xf	-154	8.0
Kwoiek					
95b	LH	see figure 7-10, contact of S country rock	fg ch > opq, tr. carb, tr. apatite	- 62	
95e	"	50 ft. in from S-country rock contact	S repl. by T	- 70	
102b	"	inside edge of ultramafic body	fg ch, tr. opq, apatite	- 56	
109b	"	center of small pod	fg T, scattered carb grains	- 61	
187a	"	at contact of qtz diorite	01 repl. by S, fg T, 01 brecciated	-163	
371a	"	center of S pod 50 ft x 20 ft	S developed along 01 fractures > Tr in Ch matrix	-142	
371b	"	outer edges of S pod	fg T repl. Ch	- 65	

Sample	Collector & Collector's Sample No.	Location	Petrographic Description	δD_s	δO^{18}_s
Yalakom	IP, P 1607	see section 7.5	01, op > deformed b? repl. op, m repl. 01 at grain edges	-150±3	4.4±0.1
Pinchi Mt.					
3	IP, P 70-68	see figure 7-11	isotropic b, m, op > 01	-174	2.1±0.1
4	IP, P 152-68	"	isotropic b? > m, 01 > op	-167	
Murray Ridge					
5	IP, P4-67	"	m > b, 01, op	-190	2.9±0.1(3)
Mt. Sidney Williams					
2	IP, 41F	"	gi > fp	- 84	9.1
Mitchell Mountains					
1	IP, V-43-69	"	fg m > b (brecciated) > fg S	-128	8.5±0.0
Cassiar					
1	LR	see figure 7-12	-	-186	8.2
2	"	"	-	-176	8.0
3	"	"	-	-162	8.2
5a	"	5a and 5b are parallel xf between massive S 5c	-	-191	8.2
5b	"		-	-195	8.2
5c	"		-	-163	8.1
Blue River					
1	WW, WJ 62-108	see figure 7-12	m > b	-187	7.0±0.1

Sample	Collector & Collector's Sample No.	Location	Petrographic Description	δD_s	δO^{18}_s
Nahlin					
1	JS, DH 22a59	see figure 7-13	fg m?, tr. cr	-205	3.0
2	JS, SE-168b59	"	2 forms S both fg > opq, carb	-198	1.9
3	JS, SE-51a60	"	T repl. op?, Tr repl. T, S repl. 01 along grain edges	-143±4	6.3±0.1
4	JS, T-22a-4	"	S along 01 fractures, T repl op	-174	
SE Pennsylvania					
Cedar Hill Quarry					
1	DL, 818	see figure 8-3. "Williamsonite" - recrystallized original texture	-	- 39	7.0±0.0
2	DL, 821	"picrolite" - in faults	-	- 46	6.9±0.0
5	DL	W quarry wall - partially altered	coarse fp > carb, magnetite grains + veins	- 66	7.1±0.1
6	DL	from dump-'least' altered	fg fp, magnetite grains	- 42	7.0±0.0
7	DL	adjacent to fault	-	- 57	7.6±0.2
8	DL, 186	large B xl flakes in fractures of S	-	- 66	
9	LM	W quarry wall	chrysotile (strongly foliated) > A (repl? 01, Chry) > xf	- 89	

Sample	Collector & Collector's Sample No.	Location	Petrographic Description	δD_s	δO_s^{18}
New Texas Pluton					
2	DL	sheared - central portion of fault zone 0.6 mi. W of New Texas, Pa.	-	- 45	7.9±0.1
4	Au	massive 'least' altered 0.3 mi N of New Texas, Pa.	gi > fp	- 53	6.6±0.1
<u>Vermont</u> Carlton Quarry					
1	Au	see figure 8-4. 2.2 mi. N 85° W of Chester Depot	biotite (coarse grained)	- 96	8.0±0.1
			actinolite (coarse grained)	- 79	8.5±0.1
2	"	"	T, (tr. Ch)	- 64	8.6
3	"	"	S (gi, fp)	- 57±0	8.6±0.1
6	"	"	Schist at contact		
			qtz (fg)		12.1±0.2
			qtz (≤ 1mm wide lenses		11.6±0.0
			muscovite		8.5
			biotite	- 84	6.5±0.0
			chlorite (some non-foliated)		7.0
7	"	"	biotite (coarse-grained)	- 84	7.2±0.1

Sample	Collector & Collector's Sample No.	Location	Petrographic Description	δD_s	δO^{18}_s
Belvedere Quarry					
1	AU	10 x 20 ft. lens in gneiss NE end of quarry 1 from center of pod, 1b from edge	S (gi) > T (fg, occurs partly in veins)		7.6
1b	"		fg T, tr. v. fg. magnetite	- 62	9.2
5	"	1175 ft. level 100 yd. from E contact	c(xf)	-100	5.9
			A(matrix)		5.9±0.2
			B(vein)		1.0±0.3
8	"	from dump in quarry	C,L(massive)	- 82	5.8
			A(matrix)		5.8±0.1
9	"	from dump in center of quarry	A(matrix)	- 57	6.1
			C(x-f)		
14	"	1235 ft. level at E contact of S-country rock	fg T, tr. S	- 46	8.3
15	"	1300 ft. level, 0.5 mi. W of #14	-	- 62	6.2
17	"	from 50 ft. wide lens in amphibolite 300 ft. E of main body	-	- 48	

Sample	Collector & Collector's Sample No.	Location	Petrographic Description	δD_s	δO^{18}_s
Belvedere Quarry (cont'd)					
11a	"	dump in center of quarry	v fg S repl 01 in light zones, only gi, fp in dark zones, crosscut by asbestos veins (see plate 8-1)	-114±4	6.5
11b	"	"	"	-104	
11c	"	"	"	-108	
11d	"	"	"	- 95±2	6.6
11e	"	"	"	- 85±0	6.1
11f	"	"	"	- 80	6.1
11g	"	"	"	-	6.5
11h	"	"	"	- 80	
11i	"	"	"	- 69	6.3
East Dover	Au	see figure 8-2 2mi. E Dover	-		4.7±0.1
Vermont Talc Quarry	"	1.2 mi. S 60° E of S. R. 11 & 21	gi > fp A		6.2±0.1
			fg T > Ch T	- 55	11.3±0.1
Rochester Quarry	"	3 mi. N of Rochester	gi > fp A	- 55	
Roxbury Quarry	C	1.1 mi. S 25° W of Roxbury	coarse grained T	- 59	
			2 crystals Tr	- 91	8.2
			from same Tr	- 89	8.1
			speciman		
Missisquoi Valley	Au	1 mi. E of Lowell on S.R. 58	gi > fp > opq. b? after op	- 44	4.7±0.0

Sample	Collector & Collector's Sample No.	Location	Petrographic Description	δD_s	δO^{18}_s
Newfoundland					
Baie Verte	RF		C(x-f)	-117	
			groundmass	-116	
Greece					
Vourinos Complex					
43a	EM	see figure 9-2	m(repl. 01) > fg xf	- 93	3.9±0.2
70c	"	"	m repl. 01	-114±4	2.9±0.1
225a	"	"	m > b		6.5±0.0
683a	"	"	m repl. 01 > b repl op	-113	4.5±0.0
685a	"	"	m repl 01	- 96	2.1±0.0
590a	"	"	op, cp(unaltered) > m	-104±3	3.8±0.2
11a	"	"	b? (brecciated), m?(isotropic)	- 99	8.9
3c	"	"	fg S matrix > platy lizardite > xf, carb (< 1 mm)	- 88	12.7±0.05
522b	"	"	m repl. 01 > b repl op, xf	-104	6.4
188a	"	"	m	- 99	6.0

Sample	Collector & Collector's Sample No.	Location	Petrographic Description	δD_s	δO^{18}_s
Alaska					
Duke Island					
1	TI, H-4-2	see figure 10-1	m repl. 01, cp, op unaltered	-127±2	-2.4±0.2
2	TI, H-9-8	"	m repl 01, c(x-f) 4 mm wide	-130±2 -133±2	-3.6±0.0 4.2±0.4
3	TI, H-2-1	"	m repl. 01	-134	-3.9±0.1
Annette Island	HT	"	m repl. 01 > xf	-129±2	1.6±0.3
Union Bay	JR, 200	"	S along 01 fractures	-139±0	-5.0±0.2
Kane Peak	HT, A139	"		-140±4	-2.1±0.2
U.S.S.R.					
Nizhni Tagil					
1	HH, d	see figure 10-1	m repl. 01	-131	1.4±0.1
2	HH, e	"	m repl. 01	-133	1.9±0.2
3	HH, f	"	m > b > xf	-141	5.0±0.0
Montana					
Stillwater Complex					
10	C	unknown	m > fg isotropic S (repl. op?)	-131	6.1±0.0
12	"	unknown	m > b > fg isotropic S	-126	6.2±0.0
45	"	unknown	highly sheared m?	-157±0	4.1±0.5

Sample	Collector & Collector's Sample No.	Location	Petrographic Description	δD_s	δO^{18}_s
NWT, Canada					
Muskox Complex					
60-416	TI	olivine clinopyroxenite, layer 11, unit 15 of Findlay and Smith (1965)	S repl. 01, tr. Ch	-127±2(3)	
60-530B	"	olivine clinopyroxenite, layer 16, unit 16 of Findlay and Smith (1965)	S repl. 01 in fractures	-105	
Quebec					
Mt. Albert					
1	HH	see section 10.2	-	-123	
2	HH		-	-125	
13	HH		-	- 98	
14	HH		-	-111	
Utah					
Moses Rock kimberlite dike		see McGetchin (1968)	see McGetchin (1968)		
MR-1416A	TM	"	-	- 97	7.8±0.1
MRX-2	"	"	-	-102	
MRX-51	"	"	-	- 65	7.6±0.0
MRX-1600	"	"	-	- 60	6.7

Sample	Collector & Collector's Sample No.	Location	Petrographic Description	δD_s	δO^{18}_s
Quebec					
Hyland Lake					
154	HH	center of ultramafic sill	m repl. 01, b repl. op	-116	
187	"	"	fp, Tr repl. 01 > xf	- 97±2(3)	
163	"	"	fp, gi repl. op, cp	- 82±2	
139A	"	outer edges of ultramafic sill	Tr repl. op, fg S	- 75	
139c	"	contact of ultramafic sill and country rock	-	- 77	
Ungava	-	-	-	- 75	
Manitoba	-	-	-	-129	
South Africa					
Barbarton					
1	HH	-	-	- 61	
24	"	-	-	- 64	

Sample	Collector & Collector's Sample No.	Location	Petrographic Description	δD_s	δO^{18}_s
Deweylites					
1 (tan)	DL, 493	Cedar Hill Quarry, Pa. fracture at S end of quarry	deweylite	-101±2	11.8±0.0
2 (red)	DL, 824	Cedar Hill Quarry, Pa. fault zone at NE end of quarry	deweylite, non-xl limonite?	- 95±3	14.5±0.2(3)
3 (white)	DL	Cedar Hill Quarry, Pa. same fracture as #1	deweylite, some stevensite	- 96±0	15.0±0.5
4 (brown)	Au	Wood Mine, Pa. fracture N end of pit	deweylite	- 94	11.9
5 F-45	GF	Wood Mine, Pa.	deweylite, some stevensite	- 92	13.1±0.1
6 U.S.N.M #79927		Ways Quarry, Delaware	deweylite	- 85	12.5
7 stevensite	USNM #R4719	Springfield, Essex Co., N.J.	stevensite	-112	19.6

Oceanic Samples	Description	δD_s	δO^{18}_s
<u>Puerto Rican Trench</u>			
Ch19-D2-2, CB	serpentinite, v fg. near isotropic grains, unusual texture (see Bowin <u>et al</u>., 1966)	-51±1	0.8±0.1
Ch19-D10-2, CB	serpentinite, m (isotropic) > b > xf (< 0.1 mm) > xf (0.6 - 2.0 mm)	-58	3.6±0.2
<u>Mid Atlantic Ridge (43°N)</u>			
AII32-8-22, GT	serpentinite, m(isotropic) > b (deformed) > xf (≤ 2.0 mm wide) groundmass	-60	1.9±0.1
	xf vein	-68	1.9
AII32-8-54, GT	serpentinite, 'picrolite' veins (< 10 mm) > xf(< 0.1 mm)	-31±2(3)	2.0±0.1
AII32-8-74, GT	serpentinite, massive, m > b (deformed, < 6 mm), xf	-60	2.1±0.0
AII32-8-70, GT	serpentinite, highly fractured, m (isotropic) > xf	-59	3.2±0.1
<u>Mid Atlantic Ridge (1°N)</u>			
AII20-48-1, GT	serpentinite, m > b (< 1 mm) bastite	-53	6.7
	mesh texture	-55±0	4.4±0.0
AII20-26-118, GT	mylonitized serpentine peridotite alternating bands of S + serp. perid.	-44	4.6±0.0
6404-1a, JD	-	-57±0	4.6
6404-1b, JD	-	-49±2	2.4±0.1(3)

Miscellaneous Samples (not discussed in text)	Description	δD_s	δO^{18}_s
New Caledonia			
81-NC-62, RC	lizardite + chrysotile, isotropic m repl. 01, slight alteration of op	-84±1	9.0±0.0
66-NC-62c, RC	m(highly fractured) > b(deformed) > xf	-88	7.3
60-NC-62, RC	banded serpentinite		8.5±0.0
New Zealand			
104-NZ-62, RC			3.3
41-NZ-62(1), RC		-97	4.5
Contact Metamorphic Serpentines			
2- Ship Mountains, California	lizardite	-114±1	3.6±0.1(5)
Sierra Ancha, Arizona	chrysotile (xf)	-138±1	6.0
Luning, Nevada	lizardite talc	-138 - 74	5.1±0.2 12.4
Iron Hat Mine, California		-119	